MicroRNA Dysregulation in Neuropsychiatric Disorders and Cognitive Dysfunction

Pei-Ken Hsu

Submitted in partial fulfillment of the
requirements for the degree of
Doctor of Philosophy
under the Executive Committee
of the Graduate School of Arts and Sciences

COLUMBIA UNIVERSITY

2012

ABSTRACT

MicroRNA Dysregulation in Neuropsychiatric Disorders and Cognitive Dysfunction

Pei-Ken Hsu

MicroRNAs (miRNAs) are evolutionarily-conserved small non-coding RNAs that are important posttranscriptional regulators of gene expression. Genetic Variants may cause microRNA dysregulation and the concomitant aberrant target expression. The dysregulation of one or a few targets may in turn lead to functional consequences ranging from phenotypic variations to disease conditions. In this thesis, I present our studies of mouse models of two human genetic variants – a rare copy number variant (CNV), 22q11.2 microdeletions, and a common single nucleotide polymorphism (SNP), *BDNF Val66Met*. 22q11.2 microdeletions result in specific cognitive deficits and high risk to develop schizophrenia. Analysis of *Df(16)A*$^{+/-}$ mice, which model this microdeletion, revealed abnormalities in the formation of neuronal dendrites and spines as well as microRNA dysregulation in brain. We show a drastic reduction of miR-185, which resides within the 22q11.2 locus, to levels more than expected by a hemizygous deletion and demonstrate that this reduction impairs dendritic and spine development. miR-185 targets and represses, through an evolutionary conserved target site, a previously unknown inhibitor of these processes that resides in the Golgi apparatus. Sustained derepression of this inhibitor after birth represents the most robust transcriptional disturbance in the brains of *Df(16)A*$^{+/-}$ mice and could affect the formation and maintenance of neural circuits. Reduction of miR-185 also has milder effects on the expression of a group of Golgi-related genes. One the other hand, *BNDF Val66Met* results in impaired activity-dependent secretion of BDNF from neuronal terminals and affects episodic memory and affective behaviors. We found a modest reduction of miR-146b which causes derepression of mRNA and/or protein levels of a few targets. Our findings add to the growing evidence of the pivotal involvement of miRNAs in the development of neuropsychiatric disorders and cognitive dysfunction. In addition, the identification of key players in miRNA dysregulation has implications for both basic and translational research in psychiatric disorders and cognitive dysfunction.

Table of Contents

List of Figures

List of Tables

Acknowledgements

"If I have seen further it is by standing on ye shoulders of Giants." – Isaac Newton

During my journey through graduate school, I was lucky enough to have many Giants that saw me through my maturation as a scientist and as a person. I am immensely grateful to all of you that stood by me along the way, offering my love, support and guidance. If I ever achieve anything, it is because of you. So a big "Thank You" to all of you.

I would like to thank Drs. Joseph Gogos, Maria Karayiorgou and Bin Xu, my three wise mentors that are the most "critical" people in my development. I thank Joseph for including me in this diverse and exciting lab to work with so many incredible people, including Karine Fenelone, Heather McKellar, Xander Arguello, Becky Levy, Merilee Teylan, Scarlet Woodrick, Liam Drew, Wei-Sung Lai, Laura Murillo, Kim Stark, Darshini Mahadevia, Yan Sun, Rozanna Yakub, Megan Sribour, Florence Chaverneff, Mirna Kvajo, Alefiya Dhilla Alberts, Ziyi Sun, Sander Markx, Gregg Crabtree, Tim Spellman, Dionne Swor, Aude-Marie Lepagnol-Bestel, Jun Mukai, Constance Zou, Luxiang Cao, Brenda Huang, Naoko Haremaki, Allie Abrams-Downey, Sara Kishinevsky, Ruby Hsu, Talia Atkin, Andrew Rosen, Ken Yagi, Arielle Torres and Ellen Whitwell. It is hard to describe how positive (and negative) impact my dear labmates have shaped me but it is beyond doubt that through the share of love of science (ya, that's right!), we had amazing time together and we will be friends forever.

I would also like to thank members of Amy MacDermott lab, including Amy, Donald Joseph, Damian Williams, Chi-Kun Tong, Claire Daniele, Papiya Choudhury, Tomo Takazawa, Gregory Scherrer. I always feel like a genuine member of the MacDermott lab and it is a privilege to be part of you in all the data and journal clubs andall the fun we shared.

I thank my committee Brian McCabe, Hynek Wichterle and Tao Sun for consistently giving me different prospectives in scientific reasoning. I am also truly grateful of the program director Ron Liem and administrator Zaia Sivo for making sure that I am alright and on the right track from time to time.

My Taiwanese fellows have been my most supportive friends since I started living abroad and you really make it feel like home. I would especially acknowledge Professor Jun-An Chen, Jung-Wei Fan, Chun-The Lee, Wei-Jen Chung, Chin-Hao Chen, Ya-Ting Lei, Chiung-Ying Chang, Wei-Feng Yen, Ting-

Chun Liu, Huan-Yi Shen, JJ & JJ Chen (my unofficial God daughters), Hua-Sheng Chiu, Ming-Chun Lai, Yuan-Ping Huang, Brenden Chen, Wei-Nan Lian, Che-Hung Shen, Ho-Chou Tu, Li-Chung Cheng, Ji-Wu Tsai. I would also like to thank Ian Orozco, Tahilia Rebello, Priscilla Chan, Hideaki Yano, Jon Mandelbaum, Rachid Skouta for the friendship and encouragement along the way.

I would like to thank Wan-Jin Lu for all the love and support you gave me. You are a wonderful person I wish you all the best in your future endeavors.

I can't express my gratitude for Ruei-Ying Tzeng who came with me to United States together and was my greatest friend and supporter in the first 5 years. Sometimes you don't know what you got 'til it is gone. I can only look forward and wish the best for both of us. There will be a rainbow after the rain.

I am who I am for a reason, and the reason is my family. I owe too much to my family for everything I have. I understand it is not easy to care for and support me sometimes because we are miles away but deep down inside I know we are always together wherever we are and whatever we do. So thank you Mom, Dad and Sister. Thank you.

Finally, I would like to dedicate this thesis to all who love me and all I love. Love makes this world a better place.

Chapter I

Tiny Regulators with Profound Impact in Neuropsychiatric Disorders

1.1 MicroRNAs-mediated Regulation

Non-coding RNAs (ncRNAs), transcribed RNAs that are not further translated into proteins, play an important regulatory role in shaping protein production and are an integral part of the epigenetic network (Bian and Sun, 2011; Esteller, 2011). One class of ncRNAs that has been extensively studied in recent years is miRNAs, which are about 22 nucleotides long (Bartel, 2004). MicroRNAs regulate gene expression primarily through post-transcriptional gene silencing by complementary binding to their target mRNAs (Lewis et al., 2003; Pasquinelli, 2012). The interaction of miRNAs with their target mRNAs is largely through a 5' seed region of the miRNA and one or more binding sites in the 3'UTR of the targets, though it is shown that the interaction can be mediated through other features or regions, such as binding sites in the open reading frame (Chi et al., 2012; Pasquinelli, 2012). This interaction directs miRNA-associated complexes to mediate translational repression and/or mRNA degradation (Prosser et al., 2011). Since the interaction of miRNAs and their mRNA targets are primarily determined by the short seed region encompassing only 6-8 nucleotides, one miRNA typically has multiple mRNA targets (Lewis et al., 2005) while several miRNAs can concertedly bind on the same mRNA target. Therefore, miRNAs can act in combinatorial or synergistic fashion by integrating different intracellular signals and/or coordinating several different signaling pathways at once (Krek et al., 2005). Furthermore, the production of miRNAs is regulated at various steps during biogenesis, both at transcription and post-transcriptional levels (Figure 1.1) (Krol et al., 2010b). Importantly, miRNAs can incorporate into different RNA-binding protein complexes, which provide information for subcellular localization and control the accessibility of potential targets at different intracellular locations. Genuine interaction between a miRNA and its targets can be experimentally detected and validated by either indirect methods, such as luciferase assays or by

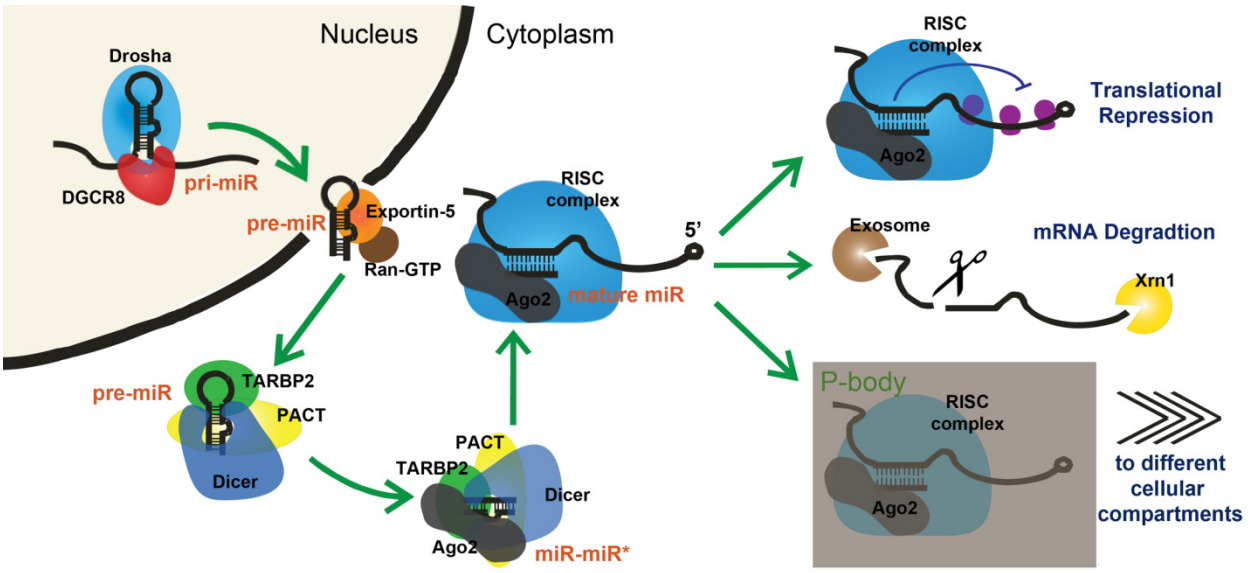

Figure 1.1 MicroRNA Biogenesis. Primary miRNA transcripts (pri-miR) are mostly transcribed by RNA polymerase II. Pri-miR is cleaved by "microprocessor" Drocha–DGCR8 to become precursor (pre-miR) before exiting the nucleus by Exportin-5–Ran-GTP. The hairpin of pre-miR is cleaved by a complex including the RNase III enzyme Dicer, double-strand binding protein TARBP2 and PACT. The miR-miR* duplex recruits Ago2 which help loading the functional strand into the RNA-induced silencing complex (RISC). The complementary binding between miRs and sites at the 3'UTR of target mRNAs will lead to three possible scenarios: (1) Initiation and elongation of mRNA translation is repressed, (2) mRNA is cleaved by Ago2 and degraded by exosome and Xrn1 RNases, (3) the miR-mRNA–RISC complex is translocated to P-bodies. This stored mRNA is later destroyed or translated after releasing from P-body. Notably, P-body and GW182 bodies can be transported to various cellular locations.

more direct approaches such as high-throughput sequencing of RNA isolated by crosslinking and immunoprecipitation (HITS-CLIP) (Chi et al., 2009) or tandem affinity purification of miRNA target mRNA (TAP-Tar) (See reviews by (Takada and Asahara, 2012; Thomson et al., 2011)). More recently a resource of mouse targeted miRNA knockout embryonic stem cells has been generated (Prosser et al., 2011). Studies utilizing such approaches and resources are poised to provide a comprehensive understanding of the role that miRNAs play in animal development and disease.

Overall, miRNA provide great control flexibility by integrating signals from different pathways under a variety of physiological conditions and, therefore, can have a great impact on neuronal function and communication (Cao et al., 2006). Along these lines, it is becoming increasingly clear that miRNAs have a profound impact on cognitive function and are involved in the etiology of several neuropsychiatric disorders, including schizophrenia, mental retardation (or intellectual disability) as well as autism and autism spectrum disorders. In this Chapter, I will summarize the general role of miRNA dysregulation in

neuropsychiatric conditions, based on evidence obtained from human and animal model studies, I will then discuss the potential effect of altered miRNAs on various neural processes that can impact psychiatric disease pathophysiology.

1.2 Altered microRNA Expression and Function in Neuropsychiatric Disorders

Accumulating evidence from human and animal studies strongly suggests that alterations in miRNA regulation or function associate with the genetic architecture of neuropsychiatric disorders including schizophrenia, autism and various forms of intellectual dysfunction. Our understanding the involvement of miRNAs in neuropsychiatric disorders has provided invaluable insights into the etiology and pathophysiology of these mental illnesses and taken us a step forward toward better prognosis and effective treatment.

1.2.1 Schizophrenia

Schizophrenia is one of the most common psychiatric disorders with a prevalence of ~1% in most of the populations studied worldwide (Xu et al., 2011). Schizophrenia is a disabling disease, which is characterized by positive (psychotic) symptoms such as hallucinations, delusions, and disorganized behavior, negative symptoms such as social withdrawal and apathy, as well as increasingly recognized cognitive deficits (Arguello et al., 2010). Classical family, twin, and adoption studies estimating the recurrence risk to relatives have provided direct evidence for a genetic etiology. The risk of developing schizophrenia increases exponentially with the degree of genetic relatedness to a patient and reaches ~50% for a monozygotic twin (Sullivan et al., 2003).

MicroRNA profiling in postmortem brain tissues from individuals with schizophrenia has shown alterations in the levels of many miRNAs (Beveridge et al., 2009; Kim et al., 2010; Moreau et al., 2011; Perkins et al., 2007; Santarelli et al., 2011) (Table 1.1, see also below). However miRNA dyregulation in the disease brain is not specific to schizophrenia and has been described in a variety of other psychiatric, neurodevelopmental and neurological disorders (Abu-Elneel et al., 2008; Kuhn et al., 2008; Talebizadeh et al., 2008). Given the important role that miRNA play in posttranscriptional gene regulation and their potential to regulate a large number of target genes, the majority of the observed changes likely reflect reactive changes due to the disease state or medication. Such changes cannot be interpreted as

indicative of a role of miRNAs in the disease pathogenesis and pathophysiology. Given the strong genetic component of schizophrenia, conclusive evidence that miRNAs are important components of the etiology and pathophysiology of schizophrenia can only be obtained by analyzing the impact that well established mutations or proximal processes affected by them (Kvajo et al., 2010) have on the formation, steady-state levels and function of miRNAs. In that respect, it is notable that the most important insight into the relationship between schizophrenia etiology and miRNAs come from recent studies on a mouse model of the 22q11.2 microdeletion (Stark et al., 2008), a well-established and largest known genetic risk factor for schizophrenia (Karayiorgou et al., 2010; Xu et al., 2010).

The 22q11.2 microdeletion is a major recurrent *de novo* copy number variant (CNV) responsible for introducing new schizophrenia cases in the population (ISC, 2008; Karayiorgou et al., 1995; Stefansson et al., 2008; Xu et al., 2008a; Xu et al., 2009). A 1.5-Mb human 22q11.2 region has been shown to be the critical region for 22q11.2 microdeletion syndrome. Because this 1.5-Mb region is highly conserved in the syntenic region of mouse chromosome 16 and harbors nearly all orthologues of the human genes (except CLTCL1), a mouse model carrying the microdeletion, *Df(16)A*$^{+/-}$, was generated to investigate the abnormalities at different levels (Drew et al., 2011). *Df(16)A*$^{+/-}$ mice exhibit a variety of structural, behavioral, and cognitive alterations that are correlated with neuroanatomical abnormalities and cognitive dysfunction found in individuals with 22q11.2 microdeletions.

Transcript and miRNA profiling indicate that miRNA alterations represent a major changes in *Df(16)A*$^{+/-}$ mice. *Dgcr8* gene, an important component of the miRNA biogenesis, is located within the 1.5-Mb microdeletion region (Stark et al., 2008). Previously in our lab, Stark et al. showed that the hemizygous deletion of the *Dgcr8* gene is the cause of downregulation (by ~20–70%) of 10-20% of all known mature miRNAs, including a number of miRNA clusters involved in neural development (Stark et al., 2008). In addition to *Dgcr8*, the 22q11.2 microdeletion and the equivalent mouse deficiency also remove one copy of a miRNA gene, *mir-185*, located within the minimal 1.5-Mb 22q11.2 critical region, which will be one of the focuses of my thesis work.

It is plausible that there exist convergent pathways which underlie the phenotypic similarity within a genetically heterogeneous disorder like schizophrenia. It is therefore an intriguing idea that the miRNA dysregulateion observed in the 22q11.2 microdeletion animals may have a more general role in

schizophrenia pathogenesis (see also Chapter 2.3.2). In fact, two recent studies provide supporting evidence for this hypothesis. Moreau et al. measured the expression of 435 miRNAs and 18 small nucleolar RNAs in the Brodmann area 9 of the prefrontal cortex using quantitative real-time PCR. After controlling for confounding variables such as sample storage time, brain pH, alcohol at time of death, and postmortem interval, 19% of analyzed miRNAs exhibited altered expression associated with diagnosis of schizophrenia or bipolar disorder and both conditions were associated with reduced miRNA expression levels (Moreau et al., 2011). In a separate study, expression profiling was performed to compare expression of miRNAs in peripheral blood mononuclear cells of 112 patients with schizophrenia and 76 non-psychiatric controls (Gardiner et al., 2011) and showed that a cluster of 17 of the most substantially downregulated miRNAs were located within an imprinted region (*DLK1-DIO3*) on chromosome 14 (14q32). These miRNAs account for 53% of the 30 miRNAs that lie within this locus and are expressed in the peripheral blood mononuclear cells (Gardiner et al., 2011). As we gather more data from miRNA profiling of human samples and mouse models, a consensus of the pattern of miRNA dysregulation in schizophrenia may emerge.

Although targets of the Dgcr8-dependent miRNA dysregulation have not been reported yet, the functional consequences of alterations in miRNA biogenesis have been studied in some detail. Behavioral tests showed that *Dgcr8*-deficient mice show impaired acquisition of the spatial working memory-dependent task (the T-maze delayed non-match to place task) as seen in *Df(16)A*$^{+/-}$ mice, suggestive of altered function of the frontal regions of the mouse neocortex and/or their interaction with the hippocampus. Interestingly, unlike *Df(16)A*$^{+/-}$ mice, *Dgcr8*-deficient mice have normal associative memory (Stark et al., 2008). Thus, *Dgcr8* deficiency and the ensuing abnormality of miRNA biogenesis appears to contribute to some but not all of the cognitive phenotypes observed in the *Df(16)A*$^{+/-}$ mice. Pinpointing the affected miRNAs and their targets will facilitate the identification of the neural substrates underlying these phenotypes. Notably, cognitive deficits, in particular working memory deficits, have become increasingly recognized as key components of schizophrenia and may reflect a more general disruption of neural networks that underlie both sensory perception and cognition. Working memory is thought to be primarily modulated by the prefrontal cortex (PFC) and to depend on persistent and recurrent neuronal excitation even in the absence of continued sensory stimulation. In that respect, the cognitive profile of

Dgcr8 deficiency may reflect a bottom-up impact from defects in neuronal connections and/or synaptic transmission or plasticity to cortical networks. Consistent with this notion, electrophysiological studies of prefrontal pyramidal neurons of *Dgcr8*$^{+/-}$ mutant mice showed that layer 5 (L5) pyramidal neurons from heterozygous mutant mice showed a higher level of short-term synaptic depression (STD) and less potentiation following physiologically relevant persistent high-frequency stimulation, while intrinsic membrane properties and basal synaptic transmission upon activation of superficial layer afferents are normal (Fenelon et al., 2011). These synaptic phenotypes implicate a deficit at the presynaptic level in prefrontal pyramidal neurons of *Dgcr8*$^{+/-}$ mutant mice. On the contrary, unlike the robust deficits observed in the prefrontal cortex, basic synaptic transmission and plasticity at the CA3/CA1 synapse of *Dgcr8*$^{+/-}$ mice appeared normal, suggesting that the effects of *Dgcr8* deficiency on synaptic plasticity are not manifested ubiquitously throughout the brain. *Dgcr8* deficiency caused only modest morphological changes in both prefrontal cortex and hippocampus (Fenelon et al., 2011; Stark et al., 2008). These included changes in the density of layer 2/4 (L2/4) neurons, a modest but significant decrease in the size of spines of basal dendrites of cortical L5 and hippocampal CA1 pyramidal neurons as well as a modest decrease in the complexity of peripheral basal dendritic branches in CA1 pyramidal neurons. Using an independent *Dgcr8*$^{+/-}$ mouse model, Schofield et al. showed that L5 pyramidal neurons in the medial prefrontal cortex of *Dgcr8*-deficient mice have decreased complexity of basal dendrites, and electrical properties were altered including a decrease of frequency but not amplitude of miniature excitatory postsynaptic currents (mEPSC) and spontaneous excitatory postsynaptic currents (sEPSC) of L5 pyramidal cells in slices from P25-30 mice (Schofield et al., 2011). The reason for the discrepancy between this investigation and the Fenelon et al study regarding changes to the basal excitatory transmission and dendritic structures is not clear. Nevertheless, both studies suggested the involvement of miRNA dysregulation in changes to neuronal electrophysiological properties which warrants further investigation.

Recent human genetic studies provide evidence that the contribution of miRNAs and related processing enzymes to the genetic etiology of schizophrenia may extend beyond the 22q11.2 schizophrenia susceptibility locus (Table 1.2). First of all, several large-scale genome-wide scans for structural variants associated with schizophrenia have identified a number of variants within the genes

that control the miRNA biogenesis pathway. For example, Xu et al. identified a *de novo* duplication encompassing the *DICER1* gene in a genome-wide scan for *de novo* CNVs in sporadic schizophrenia (Xu et al., 2008a). *CYFIP1*, another gene within a recurrent CNV regions in a schizophrenia cohort on 15q11.2 (Stefansson et al., 2008), binds two components of miRNA mediated translational control machinery, namely the Fragile X Mental Retardation Protein (FMRP) and the translation initiation factor eIF4E (Jin et al., 2004; Napoli et al., 2008). In addition, genome-wide scans for CNVs have also identified a number of structural variants enriched in patients with schizophrenia that contain miRNAs. For example, *hsa-mir-211* and *hsa-mir-484* are within CNVs at 15q13.1 and 16p13.11 identified by several genome scans in schizophrenia samples (Ingason et al., 2009; ISC, 2008; Kirov et al., 2009; Kirov et al., 2008; Stefansson et al., 2008). Furthermore, Hansen et al. conducted an association study of 101 brain expressed miRNA loci in a Danish and Norwegian schizophrenia cohort using a case-control design. They found evidence suggesting that two miRNA loci, *mir-206* and *mir-198* were associated with schizophrenia in the Danish and Norwegian sample, respectively (Hansen et al., 2007). More recently, a large sample genome-wide association study reported a strong association between schizophrenia and a genetic variant in the vicinity of the *mir-137* gene locus at chromosome 1p21.3 as well as weaker associations with a number of predicted miR-137 targets (Ripke et al., 2011). The effect of the linked variant on the expression of miR-137 remains unknown and, provided that the reported association is not a false finding, it is expected to be rather modest. In addition, although supporting evidence for some of the predicted targets has been obtained using *in vitro* assays (Kwon et al., 2011), whether predicted targets represent genuine targets *in vivo* and more importantly whether they are responsive to the expected modest changes in miR-137 expression remains to be determined. This is an important issue given the rather poor correct prediction rate of available programs (Rajewsky, 2006) and the fact that suppression of downstream targets is miRNA-concentration dependent (Mukherji et al., 2011). As noted elsewhere (Rodriguez-Murillo et al., 2011), interpreting results from GWAS should be done with care and, in the absence of a link between *mir-137* common variants and the function or expression of this miRNA, the possibility that the positive correlation from GWAS reflect disease risk confered by a neighboring gene/locus cannot yet be excluded.

MicroRNA expression-profiling studies have also observed significant changes in miRNA levels in postmortem brains of individuals with schizophrenia (Table 1.1) (Beveridge et al., 2009; Kim et al., 2010; Moreau et al., 2011; Perkins et al., 2007; Santarelli et al., 2011). In the first study of this kind, Perkins et al. studied the expression pattern of 264 human miRNAs using postmortem prefrontal cortex samples from 13 patients with schizophrenia and two with schizoaffective disorder, as well as 21 psychiatrically unaffected controls. The study showed that 14 miRNAs were significant decreased and one was upregulated in schizophrenia patients as compared with controls (Perkins et al., 2007). Although there are discrepancies among the various miRNA expression profiling studies, in aggregate and in the context of accumulating evidence from human genetic studies, they tend to support the view that altered miRNA levels could be a significant factor in the dysregulation of cortical gene expression in schizophrenia at least at the mRNA level. In the same context, the observations that the expression levels of some miRNAs are sensitive to antipsychotics or psychotomimetics drugs can also be interpreted as supportive (but not conclusive) evidence of involvement of miRNA related regulation in schizophrenia etiology. For instance, three miRNAs, miR-128a, miR-128b and miR-199a were upregulated in response to haloperidol treatment in rats as compared to untreated controls (Perkins et al., 2007). In an independent study, miR-219 expression level was reduced in the prefrontal cortex of mice in response to dizocilpine, a selective NMDA receptor antagonist. This dizocilpine-induced effect on miR-219 could be attenuated by pretreating the mice with the antipsychotic drugs haloperidol and clozapine (Kocerha et al., 2009).

1.2.2 Autism Spectrum Disorders

Autism spectrum disorders are a heterogeneous group of neurodevelopmental disorders with impairment in social interaction and repetitive and stereotyped behaviors (as defined in DSM-IV, American Psychiatric Association, 1994). Symptoms start at age three or earlier. The prevalence of autism spectrum disorders in general population is about 1%. Family and twin studies indicate a strong genetic component (Bailey et al., 1995; Folstein and Rutter, 1977; Greenberg et al., 2001; Steffenburg et al., 1989).

Several recent studies have started to explore the possibility of whether dysregulation of miRNAs plays a role in autism spectrum disorders. A number of human genetic studies have provided some

potential connection between miRNA abnormalities and autism spectrum phenotypes due to chromosome structural mutations. One such an example is the 22q11.2 microduplications. In contrast to the enrichment of 22q11.2 microdeletion (but not microduplication) in schizophrenia cohort (Brunet et al., 2008), a higher frequency of 22q11.2 microduplication (but not microdeletion) was observed in unrelated autism spectrum cases according to the results of several genome-wide CNV screenings (Glessner et al., 2009; Marshall et al., 2008). Because the expression level of *DGCR8* gene is upregulation in the 22q11.2 micoduplication, miRNA biogenesis process is likely to be affected. In addition, *miR-185* gene within in the 22q11.2 duplication is also likely altered. Similarly, *hsa-mir-211*, another microRNA gene, is located within a recurrent genomic imbalance region at 15q13.2-q13.3 that has been associated with autism spectrum disorders, intellectual disability, epilepsy, and/or electroencephalogram (EEG) abnormalities (Miller et al., 2009). A number of expression profiling studies examined miRNA dysregulation in autism spectrum disorders patient samples. Talebizadeh et al. checked the expression profile of 470 miRNAs of the lymphoblastoid cell line samples from 6 autism patients and 6 matched controls using microarrays (Talebizadeh et al., 2008). Nine miRNAs were shown to be differential expressed in the autism samples as compared to controls. In an independent study Abu-Elneel et al. probed the expression of 466 miRNAs of the postmortem cerebellar cortex samples from 13 autism spectrum disorders patients and 13 non-autistic controls using multiplex quantitative PCR method. They found that 28 out of 227 miRNAs that could be reliably detected were differentially expressed in at least one of the autism spectrum disorders samples as compared to the mean value observed in non-autistic controls (Abu-Elneel et al., 2008). Three miRNAs, miR-23a, miR-132 and miR-146b overlapped between these two studies. More recently, Sarachana et al. compared miRNA expression in lymphoblastoid cells from three pairs of monozygotic twins discordant for diagnosis of autism spectrum disorders, a normal sibling for two of the twin pairs, two pairs of autistic and unaffected siblings, and a pair of normal monozygotic twins. Forty-three miRNAs were found as significantly changed between autistic and nonautistic individuals. Two miRNAs (miR-23a and miR-106b) overlapped with the ones reported by Abu-Elneel et al. (Abu-Elneel et al., 2008; Sarachana et al., 2010). Ghahramani Seno et al. used a discordant sibling pair design to study mRNA and miRNA expression profiles in lymphoblastoid cells of 20 severe autism patients and 22 unaffected siblings. They identified a subgroup of samples with similar expression patterns using cluster analysis and

determined that 12 miRNAs were differentially expressed in this subset of autism spectrum disorders samples (Ghahramani Seno et al., 2011). Although initial genetic studies at the genomic level suggest that miRNA alterations could contribute to the genetic heterogeneity and phenotypic variation of autism spectrum disorders, miRNA gene profiling studies have not yet produced a convergent picture and additional larger scale systematic investigation will be necessary.

1.2.3 Rett Syndrome

Rett syndrome is a neurodevelopmental disorder with an incidence of 1:10,000–15,000 (Hagberg, 1985). Rett syndrome occurs almost exclusively in girls and 99% of affected girls are sporadic cases. Patients with classic Rett syndrome have an apparently normal development before 6–18 months of age, then gradually exhibit developmental stagnation, stereotypical movements, microcephaly, seizures, autistic features and intellectual disability (Hagberg et al., 1983). Detailed anatomic examination reveals that Rett syndrome patients have a smaller brain and the size and dendritic arborization of individual neurons are also reduced (Armstrong et al., 1995; Leonard and Bower, 1998; Sirianni et al., 1998).

Mutations in the gene encoding methyl-CpG binding protein 2 (*MECP2*) have been associated with many Rett syndrome cases and are thought to be the main cause of Rett syndrome (Amir et al., 1999). Evidence that miRNAs might involve in the etiology and clinical expression of Rett syndrome came from the finding that miR-132 controls the expression a *Mecp2* splice variant in primary cortical neurons through its 3'UTR (Klein et al., 2007). This finding, combined with the observations that miR-132 is a miRNA that regulates neuronal morphogenesis in responding to extrinsic trophic cues such as BDNF and that lack of *Mecp2* decreases BDNF levels in mouse models of Rett syndrome, suggested that miR-132 might exert homeostatic control over *Mecp2* translation (Klein et al., 2007; Vo et al., 2005). More recently, Hansen et al. generated a transgenic mouse strain where miR-132 is over-expressed in forebrain neurons. *mir-132* transgenic mice displayed reduced *Mecp2* levels, a significant increase of dendritic spine density in hippocampal neurons as well as deficits in a novel object test (Hansen et al., 2010). Interestingly, MeCP2 appears to also control miRNAs as well as their downstream targets. Nomura et al. reported that MeCP2 regulated the expression of another brain-specific imprinted miRNA, miR-184, by binding to its promoter region (Nomura et al., 2008). When cultured cortical neurons are depolarized,

MeCP2 is released from the promoter binding site of the paternal allele leading to upregulation of paternal allele-specific expression of miR-184. However, that the authors observed a downregulation of miR-184 expression in the *Mecp2*-deficient mouse brain and no morphological changes were identified when miR-184 was overexpressed in the cultured cortical neurons (Nomura et al., 2008). In addition, Im et al. found that MeCP2 repressed the expression of *mir-212–mir-132* cluster as a part of homeostatic interactions in dorsal striatum that regulate cocaine intake (Im et al., 2010). However, they also confirmed that MeCP2 upregulates BDNF expression. As BDNF enhances miR-132 expression, the net effect on expression of *mir-212–mir-132* cluster is unclear. Perhaps MeCP2 and BDNF cooperatively determine the regional and temporal specific expression pattern of miR-132 and miR-212. More recently, 2 miRNA expression profiling studies of a *Mecp2* knockout mouse model further demonstrated a broader alteration of miRNA expression in response to lack of *Mecp2*. Urdinguio et al. used miRNA microarrays to investigate the miRNA expression profiles of *Mecp2* knockout mice, a mouse model of Rett syndrome. They reported that expression levels in 65 out of 245 miRNAs were altered, with more than 70% of them downregulated (Urdinguio et al., 2010). Wu et al. used massively parallel sequencing methods to identify miRNAs altered in cerebella of *Mecp2*-null mice before and after the onset of severe neurological symptoms. They found that ~17% of all known mature miRNAs were considerably dysregulated (>1.5-fold) in cerebella of knockout mice before the onset of severe neurological symptoms. A further analysis revealed that many upregulated mature miRNAs belong to the miRNA clusters within the *Dlk1-Gtl2* imprinted domain (Wu et al., 2010). Interestingly, dysregulation of miRNAs within this genomic region was also reported in schizophrenia samples, albeit in the opposite direction (see Chapter 1.2.1). Transcription of miRNAs within this cluster has been shown to be regulated by neuronal activity and has been implicated in regulation of dendritic morphology (Fiore et al., 2009). Overall, MeCP2 seems to be an important component of a miRNA-modulated regulatory network: miRNAs such as miR-132 and miR-212 control Mecp2 level and, in turn, Mecp2-regulated miRNAs may serve as critical mechanistic links to the downstream phenotypes. Therefore, deficits in *Mecp2* expression may lead to the disruption of a miRNA regulatory machinery, which may contribute to clinical phenotypes observed in Rett syndrome.

1.2.4 Fragile X Syndrome

Fragile X syndrome is the most common inherited form of mental retardation, affecting about 1:4000 males and 1:8000 females (Turner et al., 1996). It results in a spectrum of cognitive and behavioral manifestation including deficits in speech and language skills similar to the ones seen in autism spectrum disorders patients (Merenstein et al., 1996). Fragile X syndrome is caused by the repeat expansion of a single trinucleotide gene sequence (CGG) in the 5'UTR of *FMRP*, which leads to the failure of *FMRP* gene expression (Penagarikano et al., 2007). FMRP is a RNA binding protein and is thought to act through its translational repression effect. It has been reported that mutations in FMRP affect neuronal morphology as well as electrophysiological properties of neurons such as synaptic plasticity and long term potentiation (Bolduc et al., 2008; Dictenberg et al., 2008; Huber et al., 2002; Jin et al., 2004; Zhang et al., 2001).

FMRP protein was found to associate with Argonaute-2 (Ago2) and Dicer, both of which are critical components of miRNA pathway (Caudy et al., 2002; Ishizuka et al., 2002; Jin et al., 2004). In addition, several studies indicated that the maturation and function of some miRNAs is partially FMRP dependent. Xu et al. showed that ectopic expression of miR-124a precursors *in vivo* decreased dendritic branching of sensory neurons in Drosophila. This effect was partially rescued by the inactivation of *dFMR1*. They further showed that pre-miR-124a (precursor of miR-124a) levels were increased while the level of the mature form was reduced in *dFMR1* mutants (Xu et al., 2008b). More recently, Edbauer et al. showed that several miRNAs, including miR-125b and miR-132, are associated with FMRP in the mouse brain (Edbauer et al., 2010). Alterations of miR-125b and miR-132 expression resulted in spine morphology changes and FMRP was required for the effect of miR-125b and miR-132 on the spine morphology. Furthermore, the expression of the NMDA receptor subunit NR2A was regulated by FMRP partially through miR-125b (Edbauer et al., 2010). This finding is consistent with the several previous results indicating that loss of *FMRP* alters NMDA receptor function in mice (Pfeiffer and Huber, 2007; Pilpel et al., 2009). Muddashetty et al. showed that miR-125a could reversibly control PSD-95 expression, which in turn, alters the dendritic spine morphology (Muddashetty et al., 2011). FMRP phosphorylation status in response to mGluR signaling controls the binding affinity of AGO2-miR-125a complex to PSD-95

mRNA. These studies indicated that *FMRP* gene, at least in part, executes its function via miRNA–modulated regulatory networks.

1.2.5 Tourette's Syndrome

Tourette's syndrome is a neurodevelopmental condition characterized by chronic vocal and motor tics and associated with behavioral abnormalities. Tourette's syndrome has a prevalence of 1% in general population and 3/4 of the patients are male (Staley et al., 1997). The age of onset of the disease ranges from 2 to 14 years old with a peak age of tic onset at 6–7 years of age (Kerbeshian et al., 2009; Robinson, 2010). Tourette's syndrome is often comorbid with other neuropsychiatric disorders such as attention deficit hyperactivity disorder and obsessive-compulsive disorder (Cavanna et al., 2009). Although a strong genetic component is suggested based on family, segregation and twin studies, gene identification via linkage and association studies have been largely unsuccessful indicating it is a complex disease (O'Rourke et al., 2009).

A potential link between miRNA and Tourette's syndrome was first proposed by Abelson et al. based on identification of a sequence variant (var321) in the 3'UTR of *Slit and Trk-like1* (*SLITRK1*) gene (Abelson et al., 2005). The variant was identified when the authors screened the sequence surrounding the breakpoint of a *de novo* chromosomal inversion of a Tourette's syndrome patient. Mutational screening of the resident *SLITRK1* gene in 174 unrelated Tourette's syndrome patients revealed that two patients (but none of the 2,148 controls) carried var321 in the 3'UTR of *SLITRK1*, which affects the binding of a miRNA, miR-189. They further showed that miR-24-1-5p (previous ID: miR-189) has a modest dose-dependent effect on *SLITRK1* expression in an *in vitro* luciferase assay system. In situ hybridization experiments indicated that the expression of *mir-24-1-5p* and *SLITRK1* mRNA are overlapping in many neuroanatomical circuits of postnatal mouse and fetal human brains that are most commonly implicated in Tourette's syndrome (Abelson et al., 2005). Finally, over-expression of *SLITRK1* in cortical neuronal cultures was shown to promote dendritic growth (Abelson et al., 2005). The association between var321 and Tourette's syndrome phenotype was followed up in several independent datasets (Chou et al., 2007; Deng et al., 2006; Keen-Kim et al., 2006; O'Roak et al., 2010; Scharf et al., 2008; Wendland et al., 2006; Zimprich et al., 2008). Although var321 was detected in some of these

studies, it failed to cosegregate with Tourette's syndrome phenotype. Because var321 is a very rare variant in the general population (minor allele frequency of 0.1%), additional studies with larger samples in homogeneous populations are needed to clarify if the original finding was a false positive i.e. due to population stratification, a common problem with the case/control design or the follow-up replication studies were underpowered.

1.2.6 Down Syndrome

The Down syndrome is characterized by mild to moderate mental retardation and its prevalence is estimated to be 1/800 (Carothers et al., 1999). The syndrome is caused by an extra whole or part of chromosome 21, which has a severe impact on the development of nervous system leading to impaired maturation of neurons including atrophic dendritic structure, decreased neuronal numbers and abnormal neuronal differentiation in the brain of Down syndrome patient. Some patients show early appearance of senile plaques (Mrak and Griffin, 2004; Wisniewski et al., 1985). A potential connection between miRNAs and Down syndrome phenotypes was recently explored (Kuhn et al., 2008). Five miRNA genes (*mir-9*9a, *let-7c*, *mir-125b*-2, *mir-155*, and *mir-802*) located on human chromosome 21 were found upregulated in the fetal brain tissue of Down syndrome patients compared to age- and sex-matched controls (Kuhn et al., 2008). The same group further demonstrated that a common target of miR-155 and miR-802 is MeCP2 (see Chapter 1.2.3). In brain samples from patients and mouse models, the expression of MeCP2 and its downstream targets, CREB1 and Mef2c, were all altered. In a Down syndrome mouse model, the expression level of MeCP2, CREB1 and Mef2c was restored when endogenous miR-155 or miR-802 were knocked down by intra-ventricular injections of corresponding antagomirs (Kuhn et al., 2010). These results suggest that over-expression of the miRNAs on chromosome 21 may repress the expression of MeCP2, which in turn contributes, at least in part, to the neural deficits observed in the brains of Down syndrome individuals. An important unresolved issue in these studies is that none of analyzed miRNAs are located within the Down syndrome critical region, which was previously identified to be associated with many of the Down syndrome phenotypes (Delabar et al., 1993). Therefore, how these miRNAs contribute to the DS phenotypes, especially intellectual disability requires further analysis.

1.3 Potential Mechanistic Connections between microRNA Dysregulation and Neuro-psychiatric Disorders

Although genetic and miRNA expression profiling studies described above provide strong evidence that miRNAs are involved in various psychiatric and neurodevelopmental disorders, the details on how miRNA dysregulation contributes to specific clinical pictures remains to be elucidated. A collective role of miRNAs in modulating normal neural morphology and function as well as various behavioral phenotypes is supported by many recent studies (see recent reviews in (Fineberg et al., 2009; Siegel et al., 2011)) and the impact of altered expression of individual miRNAs has been assessed using a variety of strategies. Below, I present a few relevant examples that offer potential mechanistic insight that illuminates the connection between miRNA dysfunction and neuropsychiatric disorders.

1.3.1 Insights from Global Disruption of miRNA Biogenesis and Action

The majority of miRNAs identified so far are transcribed by RNA polymerase II as long primary transcripts called pri-miRNA. Pri-miRNAs are then processed into stem-loop precursor miRNAs (pre-miRNAs) by the microprocessor (a complex containing type-III RNase Drosha and its partner protein

Dgcr8) in the nucleus. Pre-miRNAs are then exported to the cytoplasm and further cleaved into mature miRNA duplexes by Dicer, another type-III RNase (Figure 1.1). The final mature miRNAs have one strand incorporated into the RNA-induced silencing complex (RISC) with the help of Dicer and several other RNA binding proteins including Ago2, PACT and TARBP2. The miRNA-associated RISC binds to the target mRNA to inhibit its translation or cause the degradation of the target mRNA (Kim, 2005). Disruptions of the components in miRNA biogenesis pathway have been shown to have a critical impact on neuronal survival, development, differentiation and function in the central nervous system. For example, knockout of the *Dicer* gene led to severe defects in neural tube morphogenesis arising from abnormal neuronal differentiation in zebrafish and embryonic lethality in mouse (Giraldez et al., 2005; Murchison et al., 2005). Conditional knockout of *Dicer* in mouse further demonstrated that morphogenesis of the neurons in the cortex and hippocampus was disrupted (Davis et al., 2008) and postnatal progressive neuron death was observed in the cerebellum and forebrain (Kim et al., 2007; Schaefer et al., 2007). In addition, *Dicer* ablation in hippocampus at different developmental time points revealed stage-

dependent, region-specific requirement for miRNAs in proper hippocampal development (Li et al., 2011). Mutation of *dAgo1*, one of the Argonaute proteins that facilitate the loading of miRNAs into the RISC, results in global developmental defects in *Drosophila*. The most prominent malformation is seen in the nervous system (Kataoka et al., 2001). Similarly *Ago2*-null mice have severe defects in neural tube formation and die early in development (Mukai et al., 2004). Deficiency of *Dgcr8* gene, which is disrupted by the 22q11.2 microdeletion, was the first example of a clinically relevant disruption of a component of miRNA biogenesis pathway. Similar to the situation of *Dicer* knockout, homozygous *Dgcr8* knockout mice die at embryonic day 6.5 (Stark et al., 2008; Wang et al., 2007), while *Dgcr8* heterozygous mice ($Dgcr8^{+/-}$) show partially impaired miRNA biogenesis and a number of neuronal and behavioral deficits similar to what have been observed in human disease conditions (Fenelon et al., 2011; Schofield et al., 2011; Stark et al., 2008) (see Chapter 1.2.1). Recently, the development of high throughput sequencing technologies and advanced bioinformatics tools, afforded the identification of many small RNAs with characteristics of miRNAs. Interestingly, these putative miRNAs are generated by alternative miRNA biogenesis pathways that bypass one or more key steps of the canonical pathway (Yang and Lai, 2011). It will be interesting to see whether anomalies in any components of these alternative pathways contribute to the various neuropsychiatric disorders.

1.3.2 Individual miRNAs Modulate Dendritic Complexity and Spine Morphology in Neurons

Alterations in dendritic complexity and spine morphology of neurons have been reported frequently in various neuropsychiatric disorders and cognitive dysfunctions. Understanding the molecular underpinnings of these changes may provide insights into the etiologies of these conditions and may reveal new drug targets. miR-134 is the first miRNA shown to contribute to dendritic complexity and spine morphology of neurons. Overexpression of miR-134 significantly decreases spine volume while overexpression of a 2′-*O*-methylated anti-miR-134 oligonucleotide increases spine width (Schratt et al., 2006). Schratt et al. proposed that BDNF treatment relieves miR-134-dependent translational inhibition of its target, Limk1 (a kinase that regulates actin and microtubule polymerization), which in turn results in higher Limk1 protein levels and morphological changes of dendritic spines. Further investigation indicated that Myocyte enhancing factor 2 (MEF2) was necessary and sufficient to induce expression of miR-134 in

response to external stimuli, such as neurotrophic factors and neuronal activity. High level of miR-134 inhibits translation of Pumilio2, a translational repressor, and promotes neurite outgrowth (Fiore et al., 2009).

miR-132 is another extensively studied miRNA that has been shown to modulate neuronal morphology. Vo et al. identified neuronal-enriched miR-132 as a target of the transcription factor cAMP-response element binding protein (CREB) through a genome-wide screen. There is a CRE (cAMP response element) in the promoter of *mir-132* that allows CREB binding downstream of neurotrophin signaling. Overexpression of this miRNA in primary cortical neurons dramatically increases neurite outgrowth. Conversely, inhibition of *miR-132* blunts neurite outgrowth under basal conditions and blocks the response to BDNF (Vo et al., 2005). Magill et al. further demonstrated that ablation of the *mir-212–mir-132* locus dramatically reduces dendritic length, branching, and spine density in newborn hippocampal neurons in young adult mice. Because miR-132 was shown to be the predominantly product of the *mir-212–mir-132* locus in hippocampal neurons, the authors concluded that miR-132 was required for normal dendrite maturation of newborn neurons in the adult hippocampus (Magill et al., 2010). In an independent study, Hansen et al. employed a transgenic mouse strain that expresses miR-132 in forebrain neurons. Morphometric analysis of hippocampal neurons indicated a dramatic increase in dendritic spine density in miR-132 overexpressing mice (Hansen et al., 2010). As mentioned previously (in Chapter 1.2.4), Edbauer et al. demonstrated that miR-132 and miR-125b interacts with FMRP in mouse brain and regulates dendritic spine morphology of hippocampal neurons in largely opposite directions. Downregulation of FMRP gene affects the impact of these miRNAs on spine morphology (Edbauer et al., 2010).

Overall, these studies suggest that a group of miRNAs play multiple regulatory roles in controlling neuronal morphology in response to external stimuli, such as neurotrophic factors or neuronal activity. Given that miR-134 is altered in the brain of the 22q11.2 microdeletion model (Stark et al 2008) and alteration of miR-132 expression is associated with FMRP expression (Edbauer et al., 2010), it is tempting to speculate that dysregulation of these 2 miRNAs is part of the pathophysiological processes underlying the corresponding clinical conditions (see also Chapter 1.2.1 and 1.2.4). Along these lines, observations from independent studies suggest that miRNAs may regulate dendritic morphology in

concert with other disease-related signaling pathways. For example, two independent studies demonstrated that miR-138 controls the depalmitoylating enzyme lysophospholipase1 (Lypla1)/acyl protein thioesterase 1 (APT1), which modulates palmitoylation states of neuronal proteins (Banerjee et al., 2009; Siegel et al., 2009). In this respect, it is noteworthy that in 22q11 microdeletion, deficits in both miRNA biogenesis and palmitoylation (due to the hemizygous deletion of *ZDHHC8* gene that encodes for a palmitoyltranferase) contribute to the abnormalities in dendritic and spine morphogenesis (Mukai et al., 2008; Stark et al., 2008). Chapter 3.1.1 and 3.1.2 will further detail the roles of miRNAs in dendritic and spine morphogenesis.

1.3.3 Individual miRNAs Modulate Neurogenesis, Neuronal Proliferation, Migration and Integration

Neuropsychiatric disorders such as schizophrenia, autism spectrum disorders and mental retardation have been associated with an array of abnormalities in neurodevelopmental processes from neurogenesis, neuronal proliferation to neuron migration and integration (Hsieh and Eisch, 2010; Wegiel et al., 2010; Yang et al., 2011). Recent studies demonstrated that miRNAs participate in many aspects of these processes. Therefore, elucidating the regulatory mechanisms involving individual miRNAs might provide important insights into the pathogenesis of neuropsychiatric disorders. Below, I present a few examples that miRNAs play important roles in neurodevelopmental processes.

miR-124a is one of the most abundant miRNAs in mammalian brain and mainly expressed in differentiating and mature neurons, accounting for 25%–48% of all mouse brain miRNAs (Deo et al., 2006; Lagos-Quintana et al., 2002). Ectopic expression of miR-124a in HeLa cells leads to a shift of expression profile from non-neuronal pattern to neuronal-like pattern (Lim et al., 2005), indicating this miRNA might specify neuronal identity. Several studies showed that miR-124a promote neuronal progenitor differentiation by de-repression of RE1-Silencing Transcription Factor (REST). The corresponding downregulation of REST target mRNAs such as PTBP1, a RNA-binding protein that globally represses neuronal-specific alternative pre-mRNA splicing, results in neuronal identity (Conaco et al., 2006; Makeyev et al., 2007; Wu and Xie, 2006). Subsequently, Cheng et al. showed that miR-124 regulated neurogenesis in the subventricular zone stem cell niche by repressing the SRY-box transcription factor Sox9 in the adult mammalian brain (Cheng et al., 2009). Yu et al. showed that miR-

124 controls neurite outgrowth in differentiating neurons of P19 mouse and in primary cortical neurons (Yu et al., 2008). Besides its roles in neuronal development, Rajasethupathy et al. provided evidence that miR-124 also plays a role in serotonin mediated long-term plasticity of synapses in the nervous system of mature *Aplysia californica* (Rajasethupathy et al., 2009).

miR-9 is another miRNA abundantly expressed in vertebrate brains (Griffiths-Jones, 2006; Lagos-Quintana et al., 2002). Several studies suggested that miR-9 and miR-9* target Nr2e1, REST, Corepressor of REST (CoREST) and BAF53a to suppress progenitor proliferation and promotes neural differentiation (Packer et al., 2008; Yoo et al., 2009; Zhao et al., 2009). miR-9 also promotes proliferation of human embryonic stem cell-derived neural progenitors by targeting *STMN1* mRNA (Delaloy et al., 2010). Mutant mice lacking *mir-9*-2 and *mir-9*-3 (referred to as *mir-9*-2/3 double mutants) was generated to examine the function of miR-9 and miR-9* in telencephalic development. These mice exhibited aberrant proliferation and/or differentiation of pallial and subpallial progenitors, and displayed multiple defects in telencephalic structures (Shibata et al., 2011).

Luikart et al. provided evidence that the temporal expression pattern of miR-132 is correlated with time course of newborn neurons integration into mature circuits in dentate gyrus. When a retroviral vector containing a "sponge" consisting of multiple miR-132 binding sites is introduced into the newborn neurons, miR-132 expression is downregulated. As a result, integration of newborn neurons into the excitatory synaptic circuitry in adult brain was disrupted (Luikart et al., 2011). Interestingly, the mice also exhibited a decrease in MeCP2 levels and impairment in novel object recognition memory (Hansen et al., 2010). More recently, Gaughwin et al. showed that miR-134 modulates cortical development in a stage-specific fashion. Through interaction with Doublecortin and/or Chordin-like 1, miR-134 promotes cell proliferation and counteracts Chrdl-1–induced apoptosis and Dcx-induced differentiation in neural progenitors. miR-134 also affected neuronal migration *in vitro* and *in vivo* in a Dcx-dependent manner. When overexpressed in differentiating cortical neurons, miR-134 leads to several subtle alterations in neurites, including reductions of number, length and overall complexity. Exogenous BMP-4 treatment can significantly reverse the effect of miR-134 overexpression, resulting in more complex processes. The author concluded that miR-134 might be a modulator of BMP-4 signals on neurite outgrowth in a noggin-reversible manner (Gaughwin et al., 2011).

1.3.4 Individual miRNAs Modulate Neuronal Electrophysiological Properties in Response to Neuronal Activity

MicroRNA expression is modulated by neuronal activity (Krol et al., 2010a). Studies from *Dgcr8* mutant mice demonstrated that miRNAs alterations in neuropsychiatric conditions lead to the changes of the electrical and synaptic properties of neurons (Fenelon et al., 2011; Schofield et al., 2011). Lambert et al. tested the effects of miR-132 expression on synaptic function. Their results indicated that features of short term synaptic plasticity of cultured mouse hippocampal neurons is altered when miR-132 is overexpressed, including an increased paired-pulse ratio and decreased synaptic depression. However, the presynaptic vesicular release properties such as the initial probability of neurotransmitter release, the size of the readily releasable pool of synaptic vesicles and the rate of refilling of the pool are unchanged (Lambert et al., 2010). The direct impact of other miRNAs on electrophysiological properties of neurons is still largely unexplored and thus warrants further investigation.

1.4 Summary

The evidence reviewed here strongly suggests that miRNAs play an important role in the pathogenesis and pathophysiology of neuropsychiatric disorders (Kvajo et al., 2011) as well as cognitive dysfunction. Although the exact mode of action of individual miRNAs affected in various psychiatric conditions remains largely unclear, our understanding is rapidly improving by the convergence of findings from various recent studies, including ones involving carefully designed animal models.

In the following chapters, I will present our study of miRNA dysregulation in animal models of two human genetic variants, 22q11.2 microdeletions and *BDNF Val66Met* SNP. Given that these genetic variants are associated with psychiatric disorders and cognitive dysfunction, our finding further strengthen the comprehension that miRNAs play central roles in pathophysiology of neuropsychiatric disorders. In addition, the identification of physiological relevant targets that mediate the influence of miRNA dysregulation helps us elucidate the disease mechanism. In the 22q11.2DS model, we demonstrate that the elevation of a major downstream effector of miRNA dysregulation, Mirta22 (2310044H10Rik) and the concerted mild dysregulation of Golgi related genes contribute to the morphological phenotype. Thus miRNAs and Mirta22 represent novel targets for therapeutic intervention for these devastating conditions.

Table 1.1 MicroRNA Dysregulation in Psychiatric Disorders from Profiling Data

Schizophrenia			
Sample (n=patient, control)	**MicroRNA coverage**	**Dysregulated MicroRNA**	**Reference**
Postmortem DLPFC (BA9) (n=15, 21)	custom array w/ 264 miRNAs	[Upregulated] miR-106b [Downregulated] miR-26b, miR-30b, miR-29b, miR-195, miR-92, miR-30a, miR-30d, miR-20b, miR-29c, miR-29a, miR-212, miR-24, miR-30e, miR-9*	Perkin et al., 2007
Postmortem STG (BA22) (n=21, 21)	miRBase v7.1	[Upregulated] let-7e, miR-107, miR-125b, miR-128a, miR-128b, miR-129, miR-130a, miR-133b, miR-138, miR-146b, miR-148a, miR-150, miR-152, miR-155, miR-15a, miR-15b, miR-16, miR-17-3p, miR-17-5p, miR-181b, miR-195, miR-197, miR-199a*, miR-19a, miR-20a, miR-222, miR-23a, miR-24, miR-26b, miR-27b, miR-28, miR-296, miR-328, miR-330, miR-335, miR-338, miR-339, miR-340, miR-373*, miR-381, miR-409-5p, miR-432*, miR-452*, miR-455, miR-484, miR-485-5p, miR-486, miR-487a, miR-489, miR-494, miR-499, miR-502, miR-517a, miR-517c, miR-518b, miR-519d, miR-520*, miR-520g, miR-9*, miR-99a	Beveridge et al., 2010
Postmortem DLPFC (BA9) (n=15, 15)	miRBase v7.1	[Upregulated] let-7d, miR-101, miR-105, miR-107, miR-126*, miR-128a, miR-153, miR-15a, miR-15b, miR-16, miR-181a, miR-181b, miR-181d, miR-184, miR-195, miR-199a, miR-20a, miR-219, miR-223, miR-26b, miR-27a, miR-29c, miR-302a*, miR-302b*, miR-31, miR-33, miR-338, miR-409-3p, miR-512-3p, miR-519b, miR-7	Beveridge et al., 2010
Postmortem DLPFC (BA46) (n=69, 35; Stanley Samples)	miRBase v13	[Upregulated] miR-132, miR-132*, miR-154*, miR-212, miR-34a, miR-544, miR-7	Kim et al., 2010
Postmortem DLPFC (BA9) (n=35, 35)	miRBase v9.2	[Upregulated] miR-148b, miR-151, miR-27b, miR-301, miR-545, miR-639 [Downregulated] miR-106b, miR-138, miR-193b, miR-210, miR-22, miR-324-3p, miR-338, miR-339, miR-425	Moreau et al., 2011
Postmortem DLPFC (BA46) (n=37, 37)	miRBase v9.1	[Upregulated] miR-105, miR-134, miR-148b, miR-150, miR-152, miR-154, miR-17-5p, miR-187, miR-193a, miR-199a*, miR-199b, miR-222, miR-25, miR-328, miR-382, miR-409-3p, miR-423, miR-425-5p, miR-433, miR-452*, miR-487a, miR-495, miR-502, miR-512-3p, miR-519c, miR-532, miR-542-3p, miR-548b, miR-590, miR-592, miR-652, miR-767-5p, miR-92b	Santarelli et al., 2011
Peripheral blood monoclear cells (PBMC) (n=112, 76)	miRBase v9.1	[Downregulated] miR-107, miR-1275, miR-128, miR-130b*, miR-134, miR-148b, miR-150*, miR-151-3p, miR-16-2*, miR-181a, miR-200c, miR-224, miR-28-3p, miR-28-5p, miR-29b-1*, miR-30e*, miR-31, miR-329, miR-335*, miR-342-5p, miR-409-3p, miR-431, miR-432, miR-486-3p, miR-487b, miR-544, miR-574-3p, miR-576-5p, miR-584, miR-625*, miR-664, miR-877, miR-99b	Gardiner et al., 2011
Overlapped miRNA (reported in at least 2 references)		**[Upregulated] miR-105, miR-107, miR-148b, miR-150, miR-152, miR-15a, miR-15b, miR-16, miR-17-5p, miR-181b, miR-195, miR-199a*, miR-20a, miR-222, miR-26b, miR-27b, miR-328, miR-338, miR-409-3p, miR-452*, miR-487a, miR-502, miR-512-3p, miR-7**	

Table 1.1 (cont.) MicroRNA Dysregulation in Psychiatric Disorders from Profiling Data

Autism Spectrum Disorders			
Sample (n=patient, control)	**MicroRNA coverage**	**Dysregulated MicroRNA**	**Reference**
Lymphoblastoid cell lines (n=6, 6)	miRBase v9.0	[Upregulated] miR-23a, miR-23b, miR-132, miR-146a, miR-146b, miR-663 [Downregulated] miR-92, miR-320, miR-363	Talebizadeh et al., 2008
Postmortem cerebellum cortex (n=13, 13)	466 miRNAs	[Upregulated] miR-106a, miR-539, miR-652, miR-550, miR-432, miR-193b, miR-181d, miR-146b, miR-140, miR-381, miR-320a, miR-106b [Downregulated] miR-484, miR-21, miR-212, miR-23a, miR-598, miR-95, miR-129, miR-431, miR-7, miR-15a, miR-27a, miR-15b, miR-148b, miR-132, miR-128	Abu-Elneel et al., 2008
Lymphoblastoid cell lines (n=5, 9)	Custom array w/ 1237 miRNA clones	[Upregulated] miR-185, miR-103, miR-107, miR-29b, miR-194, miR-524, miR-191, miR-376a*, miR-451, miR-23b, miR-342, miR-23a, miR-186, miR-25, miR-519c, miR-346, miR-205, miR-30c, miR-93, miR-186, miR-106b [Downregulated] miR-182*, miR-136, miR-518a, miR-153-1, miR-520b, miR-455, miR-326, miR-199b, miR-211, miR-132, miR-495, miR-16-2, miR-190, miR-219, miR-148b, miR-189, miR-133b, miR-106b, miR-367, miR-139	Sarachana et al., 2010
Lymphoblastoid cell lines (n=20, 22)	Illumina Universal-12 BeadChips	[Upregulated] miR-486-5p, miR-181c, miR-486-3p, miR-181a, miR-30a*, miR-181b, miR-181a*, miR-548o, miR-10a, miR-10a*, miR-199b-5p, miR-502-3p, miR-500*	Ghahramani Seno et al., 2011
Overlapped miRNA (reported in at least 2 references)		**[Upregulated] miR-146b, miR23a, miR-23b** **[Downregulated] miR-132, miR-148b**	

DLPFC: dorsolateral prefrontal cortex, BA: Brodmann's Area, STG: superior temporal gyrus.

Table 1.2 Psychiatric Disorders-associated Genetic Variants at MicroRNA or MicroRNA-biogenesis Gene Loci

Schizophrenia			
Populations (case-control, n=patient, control)	**Type of Study** (# of CNV or SNP tested)	**miRNA or miRNA biogenesis gene** (CNV or associated SNP)	**Reference**
Danish (n=420, 1006) Norwegian (n=163, 177)	Case-control SNP association study (18 miRNAs)	miR-198 (rs17578796, with Danish samples), miR-206 (rs1700, with Norwegian samples)	Hansen et al., 2007
Mixed European population (n=1433, 33250)	Case-control (66 *de novo* CNVs found in the same studies)	*DGCR8*, *has-mir-185* (22q11.2 deletion), *CYFIP1* (15q11.2 deletion and duplication), *has-mir-211* (15q13.2 deletion), *has-mir-484* (16p13.11 deletion)	Stefansson et al., 2008
Afrikaner (152 trios w/ proband, 159 trios w/o proband)	Family-based CNV scan	*DICER1* (14q32.12-q32.2 dupicatation)	Xu et al., 2008a
Mixed worldwide population (n=17836, 33859)	Case-control GWAS	*hsa-mir-137* (rs1625579)	Ripke et al., 2011
Autism Spectrum Disorders			
Populations (case-control, n=patient, control)	**Type of Study** (# of CNV or SNP tested)	**miRNA or miRNA biogenesis gene** (CNV or associated SNP)	**Reference**
American of European ancestry (n=859, 1409)	Case-control CNV scan	*DGCR8* , *has-mir-185* (22q11.2 duplication)	Glessner et al., 2009
1445 patients from Children's Hospital Boston	CNV scan	*has-mir-211* (15q13.2-q13.3 deletion, duplication)	Miller et al., 2009

CNV: copy-number variant, GWAS: genome-wide association study.

1.5 References

Abelson, J.F., Kwan, K.Y., O'Roak, B.J., Baek, D.Y., Stillman, A.A., Morgan, T.M., Mathews, C.A., Pauls, D.L., Rasin, M.R., Gunel, M.*, et al.* (2005). Sequence variants in SLITRK1 are associated with Tourette's syndrome. Science (New York, NY *310*, 317-320.

Abu-Elneel, K., Liu, T., Gazzaniga, F.S., Nishimura, Y., Wall, D.P., Geschwind, D.H., Lao, K., and Kosik, K.S. (2008). Heterogeneous dysregulation of microRNAs across the autism spectrum. Neurogenetics *9*, 153-161.

Amir, R.E., Van den Veyver, I.B., Wan, M., Tran, C.Q., Francke, U., and Zoghbi, H.Y. (1999). Rett syndrome is caused by mutations in X-linked MECP2, encoding methyl-CpG-binding protein 2. Nat Genet *23*, 185-188.

Arguello, P.A., Markx, S., Gogos, J.A., and Karayiorgou, M. (2010). Development of animal models for schizophrenia. Dis Model Mech *3*, 22-26.

Armstrong, D., Dunn, J.K., Antalffy, B., and Trivedi, R. (1995). Selective dendritic alterations in the cortex of Rett syndrome. Journal of neuropathology and experimental neurology *54*, 195-201.

Bailey, A., Le Couteur, A., Gottesman, I., Bolton, P., Simonoff, E., Yuzda, E., and Rutter, M. (1995). Autism as a strongly genetic disorder: evidence from a British twin study. Psychological medicine *25*, 63-77.

Banerjee, S., Neveu, P., and Kosik, K.S. (2009). A coordinated local translational control point at the synapse involving relief from silencing and MOV10 degradation. Neuron *64*, 871-884.

Bartel, D.P. (2004). MicroRNAs: genomics, biogenesis, mechanism, and function. Cell *116*, 281-297.

Beveridge, N.J., Gardiner, E., Carroll, A.P., Tooney, P.A., and Cairns, M.J. (2009). Schizophrenia is associated with an increase in cortical microRNA biogenesis. Molecular psychiatry.

Bian, S., and Sun, T. (2011). Functions of noncoding RNAs in neural development and neurological diseases. Molecular neurobiology *44*, 359-373.

Bolduc, F.V., Bell, K., Cox, H., Broadie, K.S., and Tully, T. (2008). Excess protein synthesis in Drosophila fragile X mutants impairs long-term memory. Nature neuroscience *11*, 1143-1145.

Brunet, A., Armengol, L., Pelaez, T., Guillamat, R., Valles, V., Gabau, E., Estivill, X., and Guitart, M. (2008). Failure to detect the 22q11.2 duplication syndrome rearrangement among patients with schizophrenia. Behav Brain Funct *4*, 10.

Cao, X., Yeo, G., Muotri, A.R., Kuwabara, T., and Gage, F.H. (2006). Noncoding RNAs in the mammalian central nervous system. Annual review of neuroscience *29*, 77-103.

Carothers, A.D., Hecht, C.A., and Hook, E.B. (1999). International variation in reported livebirth prevalence rates of Down syndrome, adjusted for maternal age. Journal of medical genetics *36*, 386-393.

Caudy, A.A., Myers, M., Hannon, G.J., and Hammond, S.M. (2002). Fragile X-related protein and VIG associate with the RNA interference machinery. Genes & development *16*, 2491-2496.

Cavanna, A.E., Servo, S., Monaco, F., and Robertson, M.M. (2009). The behavioral spectrum of Gilles de la Tourette syndrome. The Journal of neuropsychiatry and clinical neurosciences *21*, 13-23.

Cheng, L.C., Pastrana, E., Tavazoie, M., and Doetsch, F. (2009). miR-124 regulates adult neurogenesis in the subventricular zone stem cell niche. Nature neuroscience *12*, 399-408.

Chi, S.W., Hannon, G.J., and Darnell, R.B. (2012). An alternative mode of microRNA target recognition. Nature structural & molecular biology *19*, 321-327.

Chi, S.W., Zang, J.B., Mele, A., and Darnell, R.B. (2009). Argonaute HITS-CLIP decodes microRNA-mRNA interaction maps. Nature *460*, 479-486.

Chou, I.C., Wan, L., Liu, S.C., Tsai, C.H., and Tsai, F.J. (2007). Association of the Slit and Trk-like 1 gene in Taiwanese patients with Tourette syndrome. Pediatric neurology *37*, 404-406.

Conaco, C., Otto, S., Han, J.J., and Mandel, G. (2006). Reciprocal actions of REST and a microRNA promote neuronal identity. Proceedings of the National Academy of Sciences of the United States of America *103*, 2422-2427.

Davis, T.H., Cuellar, T.L., Koch, S.M., Barker, A.J., Harfe, B.D., McManus, M.T., and Ullian, E.M. (2008). Conditional loss of Dicer disrupts cellular and tissue morphogenesis in the cortex and hippocampus. J Neurosci *28*, 4322-4330.

Delabar, J.M., Theophile, D., Rahmani, Z., Chettouh, Z., Blouin, J.L., Prieur, M., Noel, B., and Sinet, P.M. (1993). Molecular mapping of twenty-four features of Down syndrome on chromosome 21. Eur J Hum Genet *1*, 114-124.

Delaloy, C., Liu, L., Lee, J.A., Su, H., Shen, F., Yang, G.Y., Young, W.L., Ivey, K.N., and Gao, F.B. (2010). MicroRNA-9 coordinates proliferation and migration of human embryonic stem cell-derived neural progenitors. Cell Stem Cell *6*, 323-335.

Deng, H., Le, W.D., Xie, W.J., and Jankovic, J. (2006). Examination of the SLITRK1 gene in Caucasian patients with Tourette syndrome. Acta neurologica Scandinavica *114*, 400-402.

Deo, M., Yu, J.Y., Chung, K.H., Tippens, M., and Turner, D.L. (2006). Detection of mammalian microRNA expression by in situ hybridization with RNA oligonucleotides. Dev Dyn *235*, 2538-2548.

Dictenberg, J.B., Swanger, S.A., Antar, L.N., Singer, R.H., and Bassell, G.J. (2008). A direct role for FMRP in activity-dependent dendritic mRNA transport links filopodial-spine morphogenesis to fragile X syndrome. Developmental cell *14*, 926-939.

Drew, L.J., Crabtree, G.W., Markx, S., Stark, K.L., Chaverneff, F., Xu, B., Mukai, J., Fenelon, K., Hsu, P.K., Gogos, J.A*., et al.* (2011). The 22q11.2 microdeletion: fifteen years of insights into the genetic and neural complexity of psychiatric disorders. International journal of developmental neuroscience : the official journal of the International Society for Developmental Neuroscience *29*, 259-281.

Edbauer, D., Neilson, J.R., Foster, K.A., Wang, C.F., Seeburg, D.P., Batterton, M.N., Tada, T., Dolan, B.M., Sharp, P.A., and Sheng, M. (2010). Regulation of synaptic structure and function by FMRP-associated microRNAs miR-125b and miR-132. Neuron *65*, 373-384.

Esteller, M. (2011). Non-coding RNAs in human disease. Nat Rev Genet *12*, 861-874.

Fenelon, K., Mukai, J., Xu, B., Hsu, P.K., Drew, L.J., Karayiorgou, M., Fischbach, G.D., Macdermott, A.B., and Gogos, J.A. (2011). Deficiency of Dgcr8, a gene disrupted by the 22q11.2 microdeletion, results in altered short-term plasticity in the prefrontal cortex. Proceedings of the National Academy of Sciences of the United States of America *108*, 4447-4452.

Fineberg, S.K., Kosik, K.S., and Davidson, B.L. (2009). MicroRNAs potentiate neural development. Neuron *64*, 303-309.

Fiore, R., Khudayberdiev, S., Christensen, M., Siegel, G., Flavell, S.W., Kim, T.K., Greenberg, M.E., and Schratt, G. (2009). MEF2-mediated transcription of the miR379-410 cluster regulates activity-dependent dendritogenesis by fine-tuning Pumilio2 protein levels. EMBO J *28*, 697-710.

Folstein, S., and Rutter, M. (1977). Infantile autism: a genetic study of 21 twin pairs. Journal of child psychology and psychiatry, and allied disciplines *18*, 297-321.

Gardiner, E., Beveridge, N.J., Wu, J.Q., Carr, V., Scott, R.J., Tooney, P.A., and Cairns, M.J. (2011). Imprinted DLK1-DIO3 region of 14q32 defines a schizophrenia-associated miRNA signature in peripheral blood mononuclear cells. Molecular psychiatry.

Gaughwin, P., Ciesla, M., Yang, H., Lim, B., and Brundin, P. (2011). Stage-specific modulation of cortical neuronal development by Mmu-miR-134. Cerebral cortex (New York, NY : 1991) *21*, 1857-1869.

Ghahramani Seno, M.M., Hu, P., Gwadry, F.G., Pinto, D., Marshall, C.R., Casallo, G., and Scherer, S.W. (2011). Gene and miRNA expression profiles in autism spectrum disorders. Brain Res *1380*, 85-97.

Giraldez, A.J., Cinalli, R.M., Glasner, M.E., Enright, A.J., Thomson, J.M., Baskerville, S., Hammond, S.M., Bartel, D.P., and Schier, A.F. (2005). MicroRNAs regulate brain morphogenesis in zebrafish. Science (New York, NY *308*, 833-838.

Glessner, J.T., Wang, K., Cai, G., Korvatska, O., Kim, C.E., Wood, S., Zhang, H., Estes, A., Brune, C.W., Bradfield, J.P.*, et al.* (2009). Autism genome-wide copy number variation reveals ubiquitin and neuronal genes. Nature *459*, 569-573.

Greenberg, D.A., Hodge, S.E., Sowinski, J., and Nicoll, D. (2001). Excess of twins among affected sibling pairs with autism: implications for the etiology of autism. Am J Hum Genet *69*, 1062-1067.

Griffiths-Jones, S. (2006). miRBase: the microRNA sequence database. Methods Mol Biol *342*, 129-138.

Hagberg, B. (1985). Rett syndrome: Swedish approach to analysis of prevalence and cause. Brain & development *7*, 276-280.

Hagberg, B., Aicardi, J., Dias, K., and Ramos, O. (1983). A progressive syndrome of autism, dementia, ataxia, and loss of purposeful hand use in girls: Rett's syndrome: report of 35 cases. Annals of neurology *14*, 471-479.

Hansen, K.F., Sakamoto, K., Wayman, G.A., Impey, S., and Obrietan, K. (2010). Transgenic miR132 alters neuronal spine density and impairs novel object recognition memory. PLoS ONE *5*, e15497.

Hansen, T., Olsen, L., Lindow, M., Jakobsen, K.D., Ullum, H., Jonsson, E., Andreassen, O.A., Djurovic, S., Melle, I., Agartz, I.*, et al.* (2007). Brain expressed microRNAs implicated in schizophrenia etiology. PLoS ONE *2*, e873.

Hsieh, J., and Eisch, A.J. (2010). Epigenetics, hippocampal neurogenesis, and neuropsychiatric disorders: unraveling the genome to understand the mind. Neurobiol Dis *39*, 73-84.

Huber, K.M., Gallagher, S.M., Warren, S.T., and Bear, M.F. (2002). Altered synaptic plasticity in a mouse model of fragile X mental retardation. Proceedings of the National Academy of Sciences of the United States of America *99*, 7746-7750.

Im, H.I., Hollander, J.A., Bali, P., and Kenny, P.J. (2010). MeCP2 controls BDNF expression and cocaine intake through homeostatic interactions with microRNA-212. Nature neuroscience *13*, 1120-1127.

Ingason, A., Rujescu, D., Cichon, S., Sigurdsson, E., Sigmundsson, T., Pietilainen, O.P., Buizer-Voskamp, J.E., Strengman, E., Francks, C., Muglia, P.*, et al.* (2009). Copy number variations of chromosome 16p13.1 region associated with schizophrenia. Molecular psychiatry.

ISC (2008). Rare chromosomal deletions and duplications increase risk of schizophrenia. Nature *455*, 237-241.

Ishizuka, A., Siomi, M.C., and Siomi, H. (2002). A Drosophila fragile X protein interacts with components of RNAi and ribosomal proteins. Genes & development *16*, 2497-2508.

Jin, P., Zarnescu, D.C., Ceman, S., Nakamoto, M., Mowrey, J., Jongens, T.A., Nelson, D.L., Moses, K., and Warren, S.T. (2004). Biochemical and genetic interaction between the fragile X mental retardation protein and the microRNA pathway. Nature neuroscience *7*, 113-117.

Karayiorgou, M., Morris, M.A., Morrow, B., Shprintzen, R.J., Goldberg, R., Borrow, J., Gos, A., Nestadt, G., Wolyniec, P.S., Lasseter, V.K.*, et al.* (1995). Schizophrenia susceptibility associated with interstitial deletions of chromosome 22q11. Proceedings of the National Academy of Sciences of the United States of America *92*, 7612-7616.

Karayiorgou, M., Simon, T.J., and Gogos, J.A. (2010). 22q11.2 microdeletions: linking DNA structural variation to brain dysfunction and schizophrenia. Nat Rev Neurosci *11*, 402-416.

Kataoka, Y., Takeichi, M., and Uemura, T. (2001). Developmental roles and molecular characterization of a Drosophila homologue of Arabidopsis Argonaute1, the founder of a novel gene superfamily. Genes Cells *6*, 313-325.

Keen-Kim, D., Mathews, C.A., Reus, V.I., Lowe, T.L., Herrera, L.D., Budman, C.L., Gross-Tsur, V., Pulver, A.E., Bruun, R.D., Erenberg, G.*, et al.* (2006). Overrepresentation of rare variants in a specific ethnic group may confuse interpretation of association analyses. Hum Mol Genet *15*, 3324-3328.

Kerbeshian, J., Peng, C.Z., and Burd, L. (2009). Tourette syndrome and comorbid early-onset schizophrenia. Journal of psychosomatic research *67*, 515-523.

Kim, A.H., Reimers, M., Maher, B., Williamson, V., McMichael, O., McClay, J.L., van den Oord, E.J., Riley, B.P., Kendler, K.S., and Vladimirov, V.I. (2010). MicroRNA expression profiling in the prefrontal cortex of individuals affected with schizophrenia and bipolar disorders. Schizophrenia research *124*, 183-191.

Kim, J., Inoue, K., Ishii, J., Vanti, W.B., Voronov, S.V., Murchison, E., Hannon, G., and Abeliovich, A. (2007). A MicroRNA feedback circuit in midbrain dopamine neurons. Science (New York, NY *317*, 1220-1224.

Kim, V.N. (2005). MicroRNA biogenesis: coordinated cropping and dicing. Nat Rev Mol Cell Biol *6*, 376-385.

Kirov, G., Grozeva, D., Norton, N., Ivanov, D., Mantripragada, K.K., Holmans, P., Craddock, N., Owen, M.J., and O'Donovan, M.C. (2009). Support for the involvement of large copy number variants in the pathogenesis of schizophrenia. Hum Mol Genet *18*, 1497-1503.

Kirov, G., Gumus, D., Chen, W., Norton, N., Georgieva, L., Sari, M., O'Donovan, M.C., Erdogan, F., Owen, M.J., Ropers, H.H.*, et al.* (2008). Comparative genome hybridization suggests a role for NRXN1 and APBA2 in schizophrenia. Hum Mol Genet *17*, 458-465.

Klein, M.E., Lioy, D.T., Ma, L., Impey, S., Mandel, G., and Goodman, R.H. (2007). Homeostatic regulation of MeCP2 expression by a CREB-induced microRNA. Nature neuroscience *10*, 1513-1514.

Kocerha, J., Faghihi, M.A., Lopez-Toledano, M.A., Huang, J., Ramsey, A.J., Caron, M.G., Sales, N., Willoughby, D., Elmen, J., Hansen, H.F.*, et al.* (2009). MicroRNA-219 modulates NMDA receptor-mediated neurobehavioral dysfunction. Proceedings of the National Academy of Sciences of the United States of America *106*, 3507-3512.

Krek, A., Grun, D., Poy, M.N., Wolf, R., Rosenberg, L., Epstein, E.J., MacMenamin, P., da Piedade, I., Gunsalus, K.C., Stoffel, M.*, et al.* (2005). Combinatorial microRNA target predictions. Nat Genet *37*, 495-500.

Krol, J., Busskamp, V., Markiewicz, I., Stadler, M.B., Ribi, S., Richter, J., Duebel, J., Bicker, S., Fehling, H.J., Schubeler, D.*, et al.* (2010a). Characterizing light-regulated retinal microRNAs reveals rapid turnover as a common property of neuronal microRNAs. Cell *141*, 618-631.

Krol, J., Loedige, I., and Filipowicz, W. (2010b). The widespread regulation of microRNA biogenesis, function and decay. Nat Rev Genet *11*, 597-610.

Kuhn, D.E., Nuovo, G.J., Martin, M.M., Malana, G.E., Pleister, A.P., Jiang, J., Schmittgen, T.D., Terry, A.V., Jr., Gardiner, K., Head, E.*, et al.* (2008). Human chromosome 21-derived miRNAs are overexpressed in down syndrome brains and hearts. Biochem Biophys Res Commun *370*, 473-477.

Kuhn, D.E., Nuovo, G.J., Terry, A.V., Jr., Martin, M.M., Malana, G.E., Sansom, S.E., Pleister, A.P., Beck, W.D., Head, E., Feldman, D.S.*, et al.* (2010). Chromosome 21-derived microRNAs provide an etiological basis for aberrant protein expression in human Down syndrome brains. J Biol Chem *285*, 1529-1543.

Kvajo, M., McKellar, H., and Gogos, J.A. (2010). Molecules, signaling, and schizophrenia. Curr Top Behav Neurosci *4*, 629-656.

Kvajo, M., McKellar, H., and Gogos, J.A. (2011). Avoiding mouse traps in schizophrenia genetics: lessons and promises from current and emerging mouse models. Neuroscience.

Kwon, E., Wang, W., and Tsai, L.H. (2011). Validation of schizophrenia-associated genes CSMD1, C10orf26, CACNA1C and TCF4 as miR-137 targets. Mol Psychiatry.

Lagos-Quintana, M., Rauhut, R., Yalcin, A., Meyer, J., Lendeckel, W., and Tuschl, T. (2002). Identification of tissue-specific microRNAs from mouse. Curr Biol *12*, 735-739.

Lambert, T.J., Storm, D.R., and Sullivan, J.M. (2010). MicroRNA132 modulates short-term synaptic plasticity but not basal release probability in hippocampal neurons. PLoS ONE *5*, e15182.

Leonard, H., and Bower, C. (1998). Is the girl with Rett syndrome normal at birth? Developmental medicine and child neurology *40*, 115-121.

Lewis, B.P., Burge, C.B., and Bartel, D.P. (2005). Conserved seed pairing, often flanked by adenosines, indicates that thousands of human genes are microRNA targets. Cell *120*, 15-20.

Lewis, B.P., Shih, I.H., Jones-Rhoades, M.W., Bartel, D.P., and Burge, C.B. (2003). Prediction of mammalian microRNA targets. Cell *115*, 787-798.

Li, Q., Bian, S., Hong, J., Kawase-Koga, Y., Zhu, E., Zheng, Y., Yang, L., and Sun, T. (2011). Timing specific requirement of microRNA function is essential for embryonic and postnatal hippocampal development. PLoS ONE *6*, e26000.

Lim, L.P., Lau, N.C., Garrett-Engele, P., Grimson, A., Schelter, J.M., Castle, J., Bartel, D.P., Linsley, P.S., and Johnson, J.M. (2005). Microarray analysis shows that some microRNAs downregulate large numbers of target mRNAs. Nature *433*, 769-773.

Luikart, B.W., Bensen, A.L., Washburn, E.K., Perederiy, J.V., Su, K.G., Li, Y., Kernie, S.G., Parada, L.F., and Westbrook, G.L. (2011). miR-132 mediates the integration of newborn neurons into the adult dentate gyrus. PLoS ONE *6*, e19077.

Magill, S.T., Cambronne, X.A., Luikart, B.W., Lioy, D.T., Leighton, B.H., Westbrook, G.L., Mandel, G., and Goodman, R.H. (2010). microRNA-132 regulates dendritic growth and arborization of newborn neurons in the adult hippocampus. Proceedings of the National Academy of Sciences of the United States of America *107*, 20382-20387.

Makeyev, E.V., Zhang, J., Carrasco, M.A., and Maniatis, T. (2007). The MicroRNA miR-124 promotes neuronal differentiation by triggering brain-specific alternative pre-mRNA splicing. Molecular cell *27*, 435-448.

Marshall, C.R., Noor, A., Vincent, J.B., Lionel, A.C., Feuk, L., Skaug, J., Shago, M., Moessner, R., Pinto, D., Ren, Y.*, et al.* (2008). Structural variation of chromosomes in autism spectrum disorder. Am J Hum Genet *82*, 477-488.

Merenstein, S.A., Sobesky, W.E., Taylor, A.K., Riddle, J.E., Tran, H.X., and Hagerman, R.J. (1996). Molecular-clinical correlations in males with an expanded FMR1 mutation. Am J Med Genet *64*, 388-394.

Miller, D.T., Shen, Y., Weiss, L.A., Korn, J., Anselm, I., Bridgemohan, C., Cox, G.F., Dickinson, H., Gentile, J., Harris, D.J.*, et al.* (2009). Microdeletion/duplication at 15q13.2q13.3 among individuals with features of autism and other neuropsychiatric disorders. Journal of medical genetics *46*, 242-248.

Moreau, M.P., Bruse, S.E., David-Rus, R., Buyske, S., and Brzustowicz, L.M. (2011). Altered microRNA expression profiles in postmortem brain samples from individuals with schizophrenia and bipolar disorder. Biol Psychiatry *69*, 188-193.

Mrak, R.E., and Griffin, W.S. (2004). Trisomy 21 and the brain. Journal of neuropathology and experimental neurology *63*, 679-685.

Muddashetty, R.S., Nalavadi, V.C., Gross, C., Yao, X., Xing, L., Laur, O., Warren, S.T., and Bassell, G.J. (2011). Reversible inhibition of PSD-95 mRNA translation by miR-125a, FMRP phosphorylation, and mGluR signaling. Molecular cell *42*, 673-688.

Mukai, J., Dhilla, A., Drew, L.J., Stark, K.L., Cao, L., MacDermott, A.B., Karayiorgou, M., and Gogos, J.A. (2008). Palmitoylation-dependent neurodevelopmental deficits in a mouse model of 22q11 microdeletion. Nature neuroscience *11*, 1302-1310.

Mukai, J., Liu, H., Burt, R.A., Swor, D.E., Lai, W.S., Karayiorgou, M., and Gogos, J.A. (2004). Evidence that the gene encoding ZDHHC8 contributes to the risk of schizophrenia. Nat Genet *36*, 725-731.

Mukherji, S., Ebert, M.S., Zheng, G.X., Tsang, J.S., Sharp, P.A., and van Oudenaarden, A. (2011). MicroRNAs can generate thresholds in target gene expression. Nat Genet *43*, 854-859.

Murchison, E.P., Partridge, J.F., Tam, O.H., Cheloufi, S., and Hannon, G.J. (2005). Characterization of Dicer-deficient murine embryonic stem cells. Proceedings of the National Academy of Sciences of the United States of America *102*, 12135-12140.

Napoli, I., Mercaldo, V., Boyl, P.P., Eleuteri, B., Zalfa, F., De Rubeis, S., Di Marino, D., Mohr, E., Massimi, M., Falconi, M.*, et al.* (2008). The fragile X syndrome protein represses activity-dependent translation through CYFIP1, a new 4E-BP. Cell *134*, 1042-1054.

Nomura, T., Kimura, M., Horii, T., Morita, S., Soejima, H., Kudo, S., and Hatada, I. (2008). MeCP2-dependent repression of an imprinted miR-184 released by depolarization. Hum Mol Genet *17*, 1192-1199.

O'Roak, B.J., Morgan, T.M., Fishman, D.O., Saus, E., Alonso, P., Gratacos, M., Estivill, X., Teltsh, O., Kohn, Y., Kidd, K.K.*, et al.* (2010). Additional support for the association of SLITRK1 var321 and Tourette syndrome. Molecular psychiatry *15*, 447-450.

O'Rourke, J.A., Scharf, J.M., Yu, D., and Pauls, D.L. (2009). The genetics of Tourette syndrome: a review. Journal of psychosomatic research *67*, 533-545.

Packer, A.N., Xing, Y., Harper, S.Q., Jones, L., and Davidson, B.L. (2008). The bifunctional microRNA miR-9/miR-9* regulates REST and CoREST and is downregulated in Huntington's disease. J Neurosci *28*, 14341-14346.

Pasquinelli, A.E. (2012). MicroRNAs and their targets: recognition, regulation and an emerging reciprocal relationship. Nat Rev Genet *13*, 271-282.

Penagarikano, O., Mulle, J.G., and Warren, S.T. (2007). The pathophysiology of fragile x syndrome. Annu Rev Genomics Hum Genet *8*, 109-129.

Perkins, D.O., Jeffries, C.D., Jarskog, L.F., Thomson, J.M., Woods, K., Newman, M.A., Parker, J.S., Jin, J., and Hammond, S.M. (2007). microRNA expression in the prefrontal cortex of individuals with schizophrenia and schizoaffective disorder. Genome biology *8*, R27.

Pfeiffer, B.E., and Huber, K.M. (2007). Fragile X mental retardation protein induces synapse loss through acute postsynaptic translational regulation. J Neurosci *27*, 3120-3130.

Pilpel, Y., Kolleker, A., Berberich, S., Ginger, M., Frick, A., Mientjes, E., Oostra, B.A., and Seeburg, P.H. (2009). Synaptic ionotropic glutamate receptors and plasticity are developmentally altered in the CA1 field of Fmr1 knockout mice. The Journal of physiology *587*, 787-804.

Prosser, H.M., Koike-Yusa, H., Cooper, J.D., Law, F.C., and Bradley, A. (2011). A resource of vectors and ES cells for targeted deletion of microRNAs in mice. Nat Biotechnol *29*, 840-845.

Rajasethupathy, P., Fiumara, F., Sheridan, R., Betel, D., Puthanveettil, S.V., Russo, J.J., Sander, C., Tuschl, T., and Kandel, E. (2009). Characterization of small RNAs in aplysia reveals a role for miR-124 in constraining synaptic plasticity through CREB. Neuron *63*, 803-817.

Rajewsky, N. (2006). microRNA target predictions in animals. Nat Genet *38 Suppl*, S8-13.

Ripke, S., Sanders, A.R., Kendler, K.S., Levinson, D.F., Sklar, P., Holmans, P.A., Lin, D.Y., Duan, J., Ophoff, R.A., Andreassen, O.A.*, et al.* (2011). Genome-wide association study identifies five new schizophrenia loci. Nat Genet.

Robinson, P.N. (2010). Whole-exome sequencing for finding de novo mutations in sporadic mental retardation. Genome Biol *11*, 144.

Rodriguez-Murillo, L., Gogos, J.A., and Karayiorgou, M. (2011). The Genetic Architecture of Schizophrenia: New Mutations and Emerging Paradigms. Annu Rev Med.

Santarelli, D.M., Beveridge, N.J., Tooney, P.A., and Cairns, M.J. (2011). Upregulation of dicer and microRNA expression in the dorsolateral prefrontal cortex Brodmann area 46 in schizophrenia. Biol Psychiatry *69*, 180-187.

Sarachana, T., Zhou, R., Chen, G., Manji, H.K., and Hu, V.W. (2010). Investigation of post-transcriptional gene regulatory networks associated with autism spectrum disorders by microRNA expression profiling of lymphoblastoid cell lines. Genome medicine *2*, 23.

Schaefer, A., O'Carroll, D., Tan, C.L., Hillman, D., Sugimori, M., Llinas, R., and Greengard, P. (2007). Cerebellar neurodegeneration in the absence of microRNAs. The Journal of experimental medicine *204*, 1553-1558.

Scharf, J.M., Moorjani, P., Fagerness, J., Platko, J.V., Illmann, C., Galloway, B., Jenike, E., Stewart, S.E., and Pauls, D.L. (2008). Lack of association between SLITRK1var321 and Tourette syndrome in a large family-based sample. Neurology *70*, 1495-1496.

Schofield, C.M., Hsu, R., Barker, A.J., Gertz, C.C., Blelloch, R., and Ullian, E.M. (2011). Monoallelic deletion of the microRNA biogenesis gene Dgcr8 produces deficits in the development of excitatory synaptic transmission in the prefrontal cortex. Neural development *6*, 11.

Schratt, G.M., Tuebing, F., Nigh, E.A., Kane, C.G., Sabatini, M.E., Kiebler, M., and Greenberg, M.E. (2006). A brain-specific microRNA regulates dendritic spine development. Nature *439*, 283-289.

Shibata, M., Nakao, H., Kiyonari, H., Abe, T., and Aizawa, S. (2011). MicroRNA-9 regulates neurogenesis in mouse telencephalon by targeting multiple transcription factors. J Neurosci *31*, 3407-3422.

Siegel, G., Obernosterer, G., Fiore, R., Oehmen, M., Bicker, S., Christensen, M., Khudayberdiev, S., Leuschner, P.F., Busch, C.J., Kane, C.*, et al.* (2009). A functional screen implicates microRNA-138-dependent regulation of the depalmitoylation enzyme APT1 in dendritic spine morphogenesis. Nat Cell Biol *11*, 705-716.

Siegel, G., Saba, R., and Schratt, G. (2011). microRNAs in neurons: manifold regulatory roles at the synapse. Current opinion in genetics & development *21*, 491-497.

Sirianni, N., Naidu, S., Pereira, J., Pillotto, R.F., and Hoffman, E.P. (1998). Rett syndrome: confirmation of X-linked dominant inheritance, and localization of the gene to Xq28. Am J Hum Genet *63*, 1552-1558.

Staley, D., Wand, R., and Shady, G. (1997). Tourette disorder: a cross-cultural review. Comprehensive psychiatry *38*, 6-16.

Stark, K.L., Xu, B., Bagchi, A., Lai, W.S., Liu, H., Hsu, R., Wan, X., Pavlidis, P., Mills, A.A., Karayiorgou, M.*, et al.* (2008). Altered brain microRNA biogenesis contributes to phenotypic deficits in a 22q11-deletion mouse model. Nat Genet *40*, 751-760.

Stefansson, H., Rujescu, D., Cichon, S., Pietilainen, O.P., Ingason, A., Steinberg, S., Fossdal, R., Sigurdsson, E., Sigmundsson, T., Buizer-Voskamp, J.E.*, et al.* (2008). Large recurrent microdeletions associated with schizophrenia. Nature *455*, 232-236.

Steffenburg, S., Gillberg, C., Hellgren, L., Andersson, L., Gillberg, I.C., Jakobsson, G., and Bohman, M. (1989). A twin study of autism in Denmark, Finland, Iceland, Norway and Sweden. Journal of child psychology and psychiatry, and allied disciplines *30*, 405-416.

Sullivan, P.F., Kendler, K.S., and Neale, M.C. (2003). Schizophrenia as a complex trait: evidence from a meta-analysis of twin studies. Arch Gen Psychiatry *60*, 1187-1192.

Takada, S., and Asahara, H. (2012). Current strategies for microRNA research. Modern rheumatology / the Japan Rheumatism Association.

Talebizadeh, Z., Butler, M.G., and Theodoro, M.F. (2008). Feasibility and relevance of examining lymphoblastoid cell lines to study role of microRNAs in autism. Autism Res *1*, 307.

Thomson, D.W., Bracken, C.P., and Goodall, G.J. (2011). Experimental strategies for microRNA target identification. Nucleic Acids Res *39*, 6845-6853.

Turner, G., Webb, T., Wake, S., and Robinson, H. (1996). Prevalence of fragile X syndrome. Am J Med Genet *64*, 196-197.

Urdinguio, R.G., Fernandez, A.F., Lopez-Nieva, P., Rossi, S., Huertas, D., Kulis, M., Liu, C.G., Croce, C.M., Calin, G.A., and Esteller, M. (2010). Disrupted microRNA expression caused by Mecp2 loss in a mouse model of Rett syndrome. Epigenetics : official journal of the DNA Methylation Society *5*, 656-663.

Vo, N., Klein, M.E., Varlamova, O., Keller, D.M., Yamamoto, T., Goodman, R.H., and Impey, S. (2005). A cAMP-response element binding protein-induced microRNA regulates neuronal morphogenesis. Proceedings of the National Academy of Sciences of the United States of America *102*, 16426-16431.

Wegiel, J., Kuchna, I., Nowicki, K., Imaki, H., Marchi, E., Ma, S.Y., Chauhan, A., Chauhan, V., Bobrowicz, T.W., de Leon, M.*, et al.* (2010). The neuropathology of autism: defects of neurogenesis and neuronal migration, and dysplastic changes. Acta Neuropathol *119*, 755-770.

Wendland, J.R., Kruse, M.R., and Murphy, D.L. (2006). Functional SLITRK1 var321, varCDfs and SLC6A4 G56A variants and susceptibility to obsessive-compulsive disorder. Molecular psychiatry *11*, 802-804.

Wisniewski, K.E., Wisniewski, H.M., and Wen, G.Y. (1985). Occurrence of neuropathological changes and dementia of Alzheimer's disease in Down's syndrome. Annals of neurology *17*, 278-282.

Wu, H., Tao, J., Chen, P.J., Shahab, A., Ge, W., Hart, R.P., Ruan, X., Ruan, Y., and Sun, Y.E. (2010). Genome-wide analysis reveals methyl-CpG-binding protein 2-dependent regulation of microRNAs in a mouse model of Rett syndrome. Proceedings of the National Academy of Sciences of the United States of America *107*, 18161-18166.

Wu, J., and Xie, X. (2006). Comparative sequence analysis reveals an intricate network among REST, CREB and miRNA in mediating neuronal gene expression. Genome biology *7*, R85.

Xu, B., Karayiorgou, M., and Gogos, J.A. (2010). MicroRNAs in psychiatric and neurodevelopmental disorders. Brain Res *1338*, 78-88.

Xu, B., Roos, J.L., Dexheimer, P., Boone, B., Plummer, B., Levy, S., Gogos, J.A., and Karayiorgou, M. (2011). Exome sequencing supports a de novo mutational paradigm for schizophrenia. Nat Genet *43*, 864-868.

Xu, B., Roos, J.L., Levy, S., van Rensburg, E.J., Gogos, J.A., and Karayiorgou, M. (2008a). Strong association of de novo copy number mutations with sporadic schizophrenia. Nat Genet *40*, 880-885.

Xu, B., Woodroffe, A., Rodriguez-Murillo, L., Roos, J.L., van Rensburg, E.J., Abecasis, G.R., Gogos, J.A., and Karayiorgou, M. (2009). Elucidating the genetic architecture of familial schizophrenia using rare copy number variant and linkage scans. Proc Natl Acad Sci U S A *106*, 16746-16751.

Xu, X.L., Li, Y., Wang, F., and Gao, F.B. (2008b). The steady-state level of the nervous-system-specific microRNA-124a is regulated by dFMR1 in Drosophila. J Neurosci *28*, 11883-11889.

Yang, J.S., and Lai, E.C. (2011). Alternative miRNA Biogenesis Pathways and the Interpretation of Core miRNA Pathway Mutants. Mol Cell *43*, 892-903.

Yang, Y., Fung, S.J., Rothwell, A., Tianmei, S., and Weickert, C.S. (2011). Increased interstitial white matter neuron density in the dorsolateral prefrontal cortex of people with schizophrenia. Biol Psychiatry *69*, 63-70.

Yoo, A.S., Staahl, B.T., Chen, L., and Crabtree, G.R. (2009). MicroRNA-mediated switching of chromatin-remodelling complexes in neural development. Nature *460*, 642-646.

Yu, J.Y., Chung, K.H., Deo, M., Thompson, R.C., and Turner, D.L. (2008). MicroRNA miR-124 regulates neurite outgrowth during neuronal differentiation. Exp Cell Res *314*, 2618-2633.

Zhang, Y.Q., Bailey, A.M., Matthies, H.J., Renden, R.B., Smith, M.A., Speese, S.D., Rubin, G.M., and Broadie, K. (2001). Drosophila fragile X-related gene regulates the MAP1B homolog Futsch to control synaptic structure and function. Cell *107*, 591-603.

Zhao, C., Sun, G., Li, S., and Shi, Y. (2009). A feedback regulatory loop involving microRNA-9 and nuclear receptor TLX in neural stem cell fate determination. Nat Struct Mol Biol *16*, 365-371.

Zimprich, A., Hatala, K., Riederer, F., Stogmann, E., Aschauer, H.N., and Stamenkovic, M. (2008). Sequence analysis of the complete SLITRK1 gene in Austrian patients with Tourette's disorder. Psychiatric genetics *18*, 308-309.

Chapter II

A Major Downstream Effector of MicroRNA Dysregulation in 22q11.2 Genomic Losses

2.1 Introduction

22q11.2 microdeletion was identified in 1995 (Karayiorgou et al., 1995) as a causative genetic factor for schizophrenia with high penetrance (~30%) and was the first example that chromosomal microdeletions and microduplications (copy-number variants or CNVs) play in the etiology of human diseases. In recent years, discovery of a widespread role of CNVs in determining susceptibility to psychiatric disorders such as schizophrenia, as well as neurodevelopmental disorders such as autism and intellectual disability, further represents a shift in our understanding of the genetic architecture of these disorders and highlights the pervasive contribution of rare and highly penetrant structural mutations (ISC, 2008; Karayiorgou et al., 1995; Levy et al., 2011; Sanders et al., 2011; Stefansson et al., 2008; Xu et al., 2008). However, 22q11.2 microdeletions remain the only confirmed recurrent chromosomal structural alteration responsible for the introduction of sporadic (*de novo*) cases of schizophrenia into human population (Karayiorgou et al., 2010). Due to the clear association with schizophrenia, this mutation allows the generation of an etiologically valid animal model of schizophrenia. A 22q11.2 microdeletion model we generated, *Df(16)A*$^{+/-}$ mice, thus presents unprecedented opportunities to determine key pathophysiological alterations which may underlies schizophrenia in general.

2.1.1 22q11.2 Microdeletions and Schizophrenia

It has long been known that an individual's genetic composition is a stro ng determinant of susceptibility to mental illness (Shields, 1982). With the increasing genetic similarity to a schizophrenia patient, an individual's risk of developing schizophrenia also increases, from 1% risk of totally genetically unrelated to ~50% risk of identical twins. Unfortunately, characterization of the genetic underpinning of schizophrenia proved to be a hard task, as schizophrenia is a genetically complex and heterogeneous disorder. Nevertheless, after years of research since the discovery of 22q11.2, a strong link has been

established between 22q11.2 microdeletion, cognitive dysfunction and schizophrenia (Karayiorgou et al., 2010). Up to one third of individuals with 22q11.2 microdeletion develop schizophrenia or schizoaffective disorder in adolescence or early adulthood, accounting for 1–2% of sporadic schizophrenia cases (Karayiorgou et al., 1995; Karayiorgou et al., 2010). Importantly, the symptoms observed in 22q11.2 microdeletion carriers affected by schizophrenia are indistinguishable from other schizophrenia patients (Bassett et al., 2003; Bassett et al., 1998). Moreover, children carrying the microdeletion have specific behavioral impairments and exhibit a spectrum of deficits in cognitive abilities linked to activity in the hippocampus and prefrontal cortex, such as measures of attention, working memory and executive function (Karayiorgou et al., 2010). Understanding how the genes disrupted by this deletion contribute to the emergence of the psychiatric and cognitive phenotypes associated with this genomic imbalance will provide important mechanistic insights and can guide analysis of other CNVs that cause psychiatric disorders and cognitive dysfunction (Arguello and Gogos, 2006, 2010; ISC, 2008; Karayiorgou et al., 2010).

2.1.2 A Mouse Model of 22q11.2 Microdeletion

Since 22q11.2 microdeletion is a defined genetic variant with a clear and strong association with schizophrenia, a mouse line that faithfully models this genetic variant offers an opportunity to study the etiology and pathophysiology of 22q11.2-associated schizophrenia. Using chromosomal engineering, our lab generated a mouse model carrying a hemizygous 1.3-Mb chromosomal deficiency on mouse chromosome 16 [*Df(16)A*], which is syntenic to the 22q11.2 1.5-Mb microdeletion (Figure 2.1) (Stark et al., 2008). Although mouse models of psychiatric disorders can never fully recapitulate the entire spectrum of symptoms and behavioral abnormalities of human patients, careful characterization has shown that *Df(16)A*$^{+/-}$ mice have alterations at behavioral, cognitive and cellular levels that are correlated with neuroanatomical abnormalities and cognitive dysfunction found in individuals with 22q11.2 microdeletions (Table 2.1; Figure 2.2). For example, disruption of prepulse inhibition (PPI), a measure of sensorimotor gating and preattentive processing, is observed in both *Df(16)A*$^{+/-}$ mice (Stark et al., 2008) and individuals with 22q11.2 microdeletions (Ornitz et al., 1986; Sobin et al., 2005). In addition, aspects of cognitive dysfunction in 22q11.2 microdeletion carriers (Casey et al., 1995; Lajiness-O'Neill et al., 2005; Shprintzen et al., 1978) are also observed in *Df(16)A*$^{+/-}$ mice, as demonstrated by decreased accuracy in delayed-

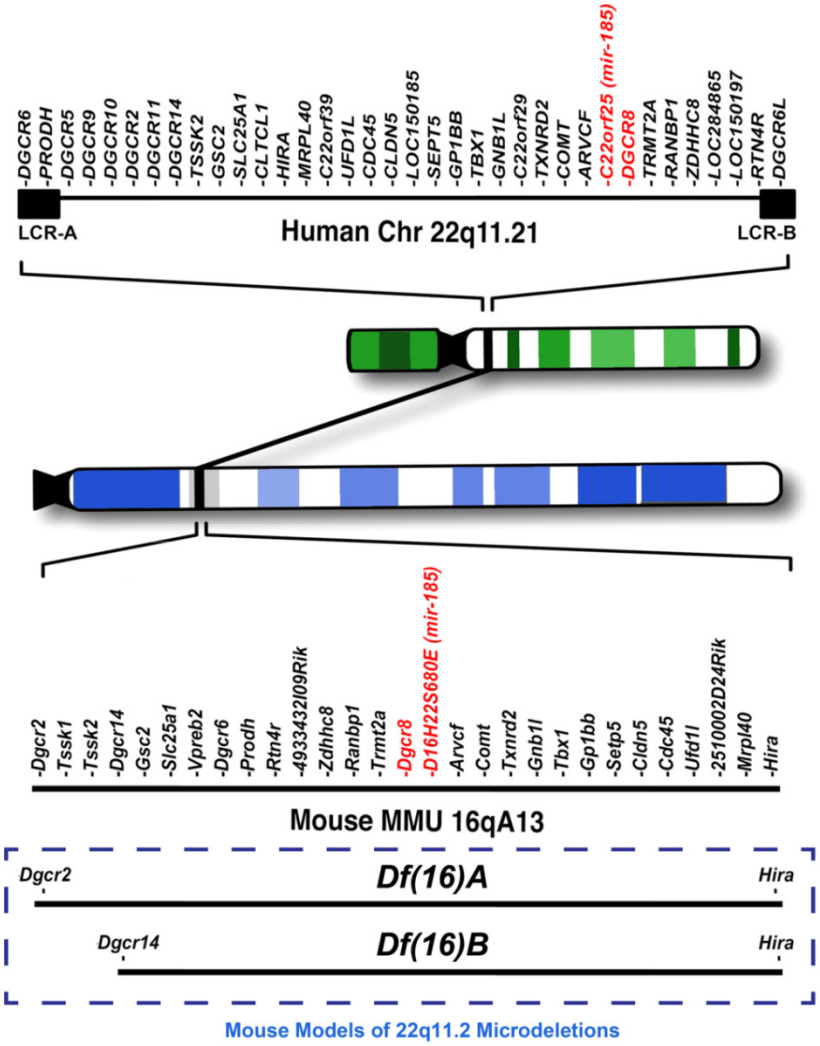

Figure 2.1 Mouse Models of 22q11.2 Microdeletions. Human 22q11.2 locus and syntenic mouse locus 16qA13 are shown, and genes in the loci are listed. The human 1.5 Mb region is flanked by low-copy-repeat seq-uences (blak boxs). The non-homologues re-combineation between these sequences results in deletion or duplication. *DGCR8* and *C22orf25* that harbors *mir-185*) orthologues are in red. We generated 2 mouse models of 22q11.2 micro-deletions. Using chromosomal engineering, regions spanning *Dgcr2–Hira* and *Dgcr14–Hira* are deleted to generate *Df(16)A* and *Df(16)B* allele, respectively. An *Dp(16)B* allele with a duplicated *Dgcr14–Hira* are also generated. Most experiments are done with *Df(16)A*$^{+/-}$ mice. The expression profilings comparing the effect genomic dosage were performed in *Df(16)B*$^{+/-}$ and *Dp(16)B*$^{+/-}$ mice (see Chapter 2.2.2).

non-match to place (DNMP) task of spatial working memory and deficits in both cued and contextual fear conditioning (Stark et al., 2008). Morphological analysis reveals that the CA1 neurons of *Df(16)A*$^{+/-}$ animals have simplified dendritic trees and decreased spine density(Mukai et al., 2008), which may partially account for the reduction in hippocampal volume (Campbell et al., 2006; Eliez et al., 2000b; Simon et al., 2005) in individuals with 22q11.2 microdeletions. Moreover, altered neural synchrony between dorsal hippocampus (HPC) and medial prefrontal cortex (PFC) as compared to WT mice (Sigurdsson et al., 2010) is consistent with PFC-HPC coupling abnormalities observed in schizophrenia patients (Ford et al., 2002; Lawrie et al., 2002; Meyer-Lindenberg et al., 2005). Although additional comparative analysis is necessary, results so far outline a number of conserved anomalies in

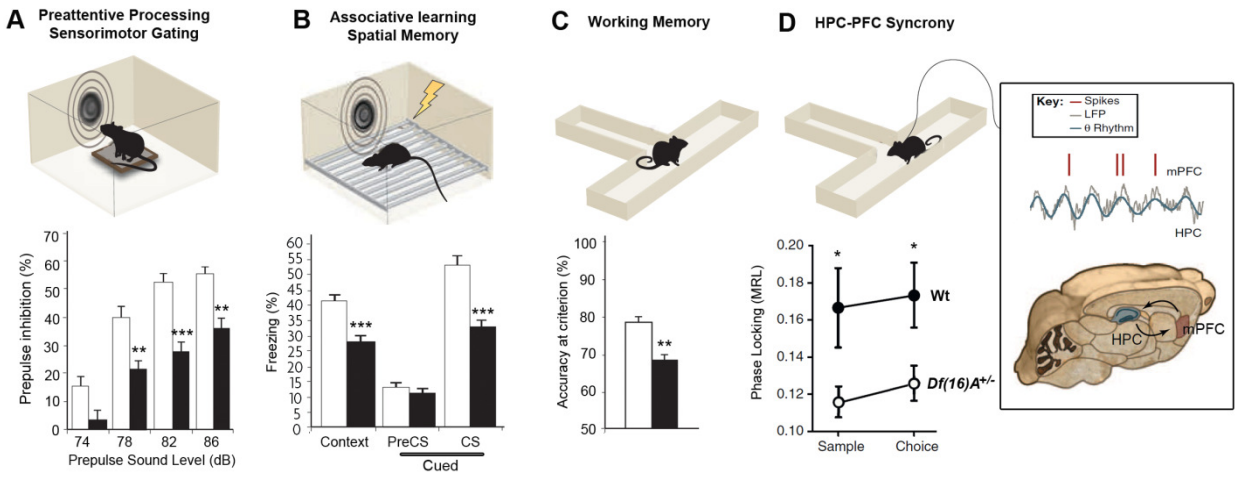

Figure 2.2 Behavioral and Cognitive Phenotypes of *Df(16)A*$^{+/-}$ Mice. A battery of tests showed the behavioral and cognitive deficits in *Df(16)A*$^{+/-}$ Mice. The results from Wt and *Df(16)A*$^{+/-}$ mice are shown in white and black columns, respectively. (A) Prepulse inhibition was used to measure preattentive processing and sensorimotor. The inhibition of startle response is impaired in *Df(16)A*$^{+/-}$ mice when primed with non-startling prepulses of various levels (78, 82 or 86 dB). (B) Associative learning and spatial memory are impaired as shown by reduced freezing response in cued and contextual fear conditioning. The mice were trained to associate the context (contextual conditioning) or a condition stimulus (CS, a tone) (cued conditioning) to an aversive electric shock (uncondition stimulus). In contrast, in cued conditioning, there is no difference in time spent in freezing before CS was presented. The deficits indicate deficits in hippocampal and amygdala circuitries. (C) Impaired working memory was revealed by a delayed non-match to place (DNMP) task. In this task, food-deprived mice were trained to use location information held by frontal cortex (working memory) to retrieve food pellets. Accuracy of successful retrieval was lower in *Df(16)A*$^{+/-}$ mice, as compared to Wt mice. (D) Phase locking between the spike timing in a medial prefrontal cortex (mPFC) neuron and the θ rhythm of hippocampus (HPC) field potential was computed as a measure of HPC–PFC connectivity (see box at the right). In *Df(16)A*$^{+/-}$ mice HPC–PFC synchrony is reduced during both sample and choice phase of a DNMP task, as compared to Wt mice. See text and Stark et al., 2008; Sigersson et al., 2010 for details. Figures adapted from Karayiorgou et al., 2010).

hippocampal and frontal circuitry in 22q11.2 microdeletion carriers and the *Df(16)A*$^{+/-}$ mouse model (Drew et al., 2011; Karayiorgou et al., 2010).

2.1.3 miRNA Dysregulation in of 22q11.2 Microdeletion Mouse Model

The *Df(16)A*$^{+/-}$ mice also provided compelling evidence that the 22q11.2 deletion results in abnormal processing of brain microRNAs (miRNAs), a class of small, noncoding RNAs that regulate the stability and translation of mRNAs (Fineberg et al., 2009; Kosik, 2006; Schratt, 2009; Xu et al., 2010). One gene disrupted by the 22q11.2 microdeletion is *DGCR8*, a component of the "microprocessor" complex that is essential for miRNA production (Tomari and Zamore, 2005). Extensive miRNA alterations are found in *Df(16)A*$^{+/-}$ mice (Figure 2.3) (Stark et al., 2008). Specifically, primary transcripts (pri-forms) of

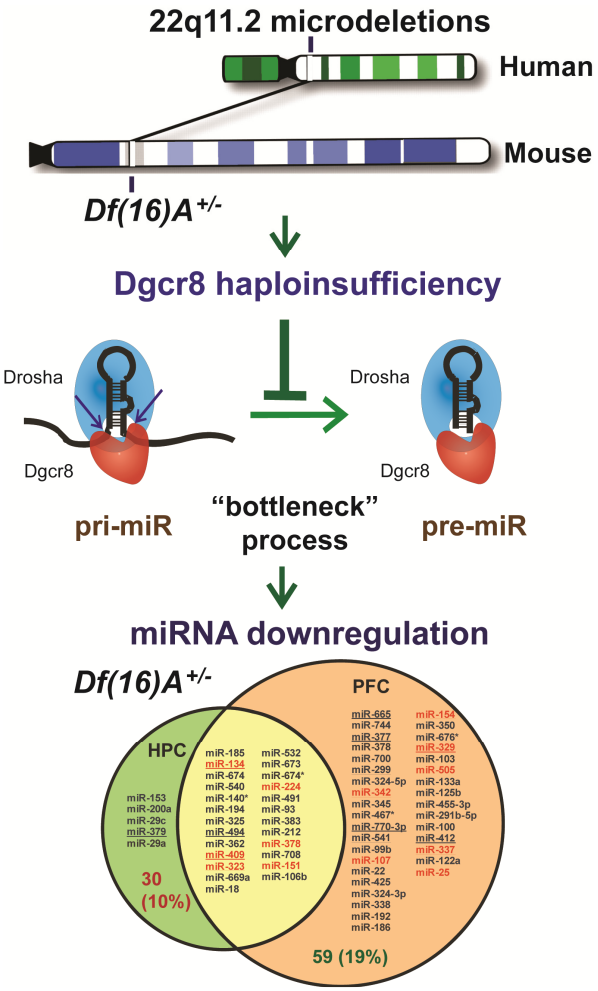

Figure 2.3 MicroRNA Dysregulation due to *Dgcr8* Deficiency in *Df(16)A*$^{+/-}$ Mice. Individuals with 22q11.2 microdeletions and the *Df(16)A*$^{+/-}$ mice lose one couple of the *Dgcr8* gene. The cleavage of pri-miRNAs by the microprocessor, Drosha-Dgcr8 complex, to become pre-miRNAs is the "bottleneck" process that limits the biogenesis of miRNAs. Therefore, Dgcr8 haploinsufficiency results in the downregulation of a subset of miRNAs in *Df(16)A*$^{+/-}$ mice, as compared to Wt mice. 30 and 59 miRNAs are downregulated in hippocampus and prefrontal cortex of *Df(16)A*$^{+/-}$ mice, respectively. The 25 overlapped miRNAs include miRNAs known to express in brain and have brain-specific functions, such as miR-134. Due to sampling limitations, large-scale miRNA profiling has not been conducted in human samples.

many miRNAs are upregulated while the mature forms of a specific subset of those upregulated pri-miRNAs are downregulated, as one would expect in a miRNA processing bottleneck. *Dgcr8* haploinsufficiency likely contributes a large part of these miRNA alterations. The pri-forms of miRNAs accumulate due to limited microprocessors available as well as compensatory upregulation of miRNA transcription. Indeed, dysregulation of pri-forms and mature forms of the same set of miRNAs is observed in *Dgcr8*$^{+/-}$ mice (Stark et al., 2008). A comprehensive picture of miRNA dysregulation in *Df(16)A*$^{+/-}$ mice was provided by miRNA microarray studies whereby 30 and 59 mature miRNAs were found to be downregulated in HPC and PFC, respectively. There are 25 miRNAs that are downregulated in both HPC and PFC, including miR-185, which is encoded in the 22q11.2 locus. Several of these miRNAs are found to be enriched in synaptic compartment and have important roles in the brain (see Chapter 2.3.3). Moreover, a higher proportion of upregulated PFC and HPC transcripts contained one or more potential seed sites for the affected miRNAs, as compared to downregulated transcripts (TargetScan: PFC, 39% versus 14%, P = 1.5 X 10^{-8}; HPC, 40% versus 6%, P = 1.5 X 10^{-5}). Among the transcripts significantly

altered and possessing at least one seed site, upregulated transcripts are enriched in transcripts with 2 or more seed sites, indicating possible convergent effects of the affected miRNAs in regulating targets with more than 2 target sites (Stark et al., 2008). These results suggest that the miRNA dysregulation in *Df(16)A*$^{+/-}$ mice likely accounts for at least part of the transcript dysregulation in this mouse line. Thus *Df(16)A*$^{+/-}$ mice provide a reliable model to interrogate the effects of miRNA dysregulation on neural circuit structure and function in a disease context.

2.1.4 In this Chapter

As mentioned above, miRNA dysregulation likely accounts for a fraction of the transcript misexpression observed in the brains of *Df(16)A*$^{+/-}$ mice(Stark et al., 2008) but direct targets have not been reported. Moreover, the impact of copy number change of individual miRNA genes due to CNV has not been investigated. In this chapter, I describe the discovery of a drastic reduction of mir-185 levels as an important component of miRNA dysregulation due to genomic loss at 22q11.2 and the identification of a previously uncharacterized gene as a major target affected by this miRNA dysregulation.

2.2 Results

2.2.1 A Drastic Reduction of miR-185 Levels in Df(16)A$^{+/-}$ *Mice*

Studies of the *Df(16)A*$^{+/-}$ mouse strain have shown that the 22q11.2 microdeletion results in abnormal processing of a specific subset of brain miRNAs due to the removal of one copy of the *Dgcr8* gene causing a decrease in Dgcr8 expression in the adult brain (Stark et al., 2008) as well as earlier in development (Figure 2.4). It is noteworthy that, in addition to *Dgcr8*, the 22q11.2 microdeletion and the equivalent mouse deficiency remove one copy of a miRNA gene (*mir-185*) located within the minimal 1.5-Mb 22q11.2 critical region (Figure 2.1). *In situ* hybridization assays indicated that miR-185 is expressed in several brain regions such as hippocampus (HPC) and cortex (Figure 2.5A). Quantitative real-time PCR (qRT-PCR) analysis showed that expression of mature miR-185 is dramatically reduced by ~70-80% in both HPC ($P < 10^{-6}$) and prefrontal cortex (PFC, $P < 10^{-11}$) of adult *Df(16)A*$^{+/-}$ mice as compared to their wild type (Wt) littermates (Figure 2.5B, C). This reduction was also observed at earlier developmental stages (E17 and P6) (Figure 2.5D). miR-185 also showed a more modest decrease in *Dgcr8*$^{+/-}$ mice

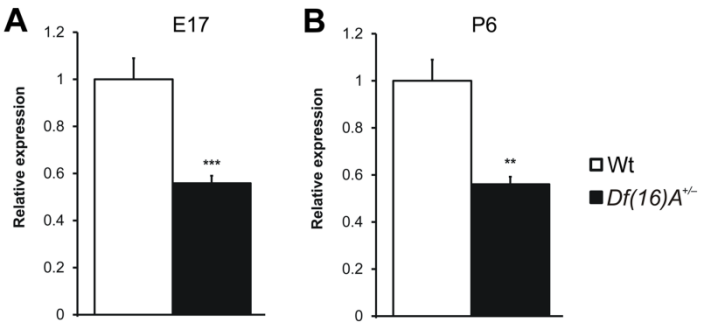

Figure 2.4 *Dgcr8* Levels in *Df(16)A*$^{+/-}$ Mice during Brain Development. *Dgcr8* expression levels in hippocampus of E17 (A) and P6 (B) *Df(16)A*$^{+/-}$mice (n = 10) and their respective wild type (Wt) littermates (n = 10), as assayed by qRT-PCR.

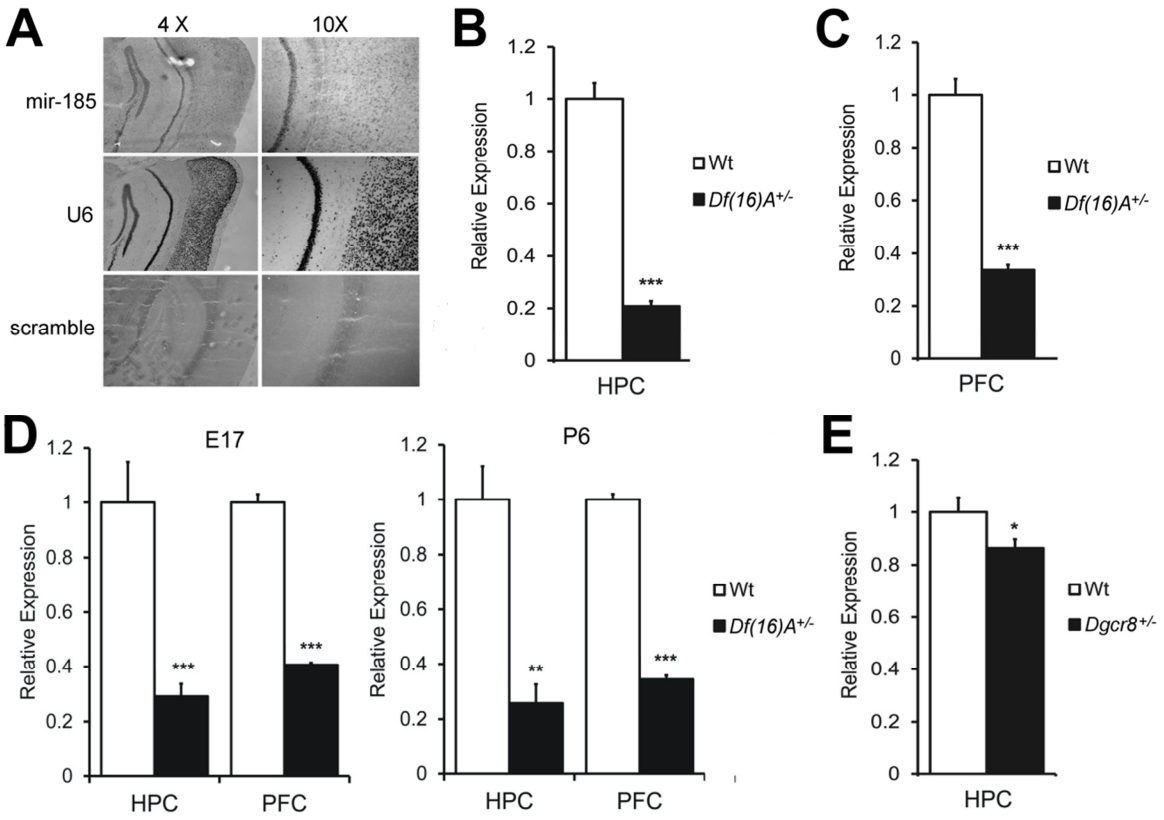

Figure 2.5 Drastic Reduction of miR-185 Expression in *Df(16)A*$^{+/-}$ Mice. (A) Expression of *mir-185* mRNA in HPC and cortex as shown by *in situ* hybridization in coronal brain sections using an antisense *mir-185* probe. An antisense U6 probe and a scramble probe were used as positive and negative controls, respectively. Images were taken at either × 4 (left panels) or × 10 (right panels) magnification. (B-E) miR-185 expression levels in adult hippocampus (HPC) (B) or prefrontal cortex (PFC) (C) (n = 7 for mutant, n = 9 for Wt littermates), in E17 and P6 (D) (n = 10 for HPC or PFC, each genotype) of *Df(16)A*$^{+/-}$ and in HPC (E) (n = 10, each genotype) of *Dgcr8*$^{+/-}$ as assayed by qRT-PCR. Expression levels in mutant animals were normalized to their respective Wt littermates. Results are expressed as mean ± SEM. *p < 0.05, **p < 0.01, ***p < 0.001 (Student's *t*-test).

(~20% in HPC, $P < 0.05$; Figure 2.5E) suggesting that the severe reduction of mature miR-185 expression in *Df(16)A*$^{+/-}$ mice is due to a combined effect of hemizygosity of the *mir-185* gene and impaired maturation of the pri-miR-185 transcript produced from the remaining copy due to the reduction

in Dgcr8 levels. This represents a genuine gene X gene interaction within a pathogenic CNV that results in a considerably greater reduction of the expression of a resident gene than expected by the 50% decrease in gene dosage. Such a large reduction in relative expression is unique among genes affected by the microdeletion and may represent an important and previously unappreciated component of 22q11.2-associated miRNA dysregulation. As such, drastically diminished miR-185 activity may lead either on its own or in combination with other miRNAs affected due to the *Dgcr8* deficiency, to altered developmental regulation of one or more targets and thereby impact a number of neural processes. However, direct targets for this miRNA as well as for other affected miRNAs have not been reported to date.

2.2.2 A Primary Transcriptional Consequence of 22q11.2 Genomic Losses

Previous microarray analysis of adult *Df(16)A*$^{+/-}$ mice revealed that a genomic loss in the 22q11.2 region results in genome-wide alterations of transcriptional programs in the HPC and PFC (Stark et al., 2008). We extended expression profile analysis of these two brain regions to two earlier developmental stages, embryonic day 17 (E17) and postnatal day 6 (P6). Only one gene, *2310044H10Rik*, was consistently found to be significantly upregulated in at least two of the three developmental stages examined and in at least one of the two brain areas tested. Indeed, *2310044H10Rik* was among the top upregulated genes in both postnatal stages examined and the top upregulated transcript in the frontal cortex of P6 mutant mice (Figure 2.6A, B). Notably, no significant difference in *2310044H10Rik* expression was found in either frontal cortex or HPC at E17 (Figure 2.6A, B). Importantly, there is not any known miRNA within or surrounding this genomic locus suggesting that the upregulation is not due to impaired processing of overlapping pri-miRNA transcripts.

In independent experiments, we attempted to distinguish primary versus secondary gene targets of the 22q11.2 microdeletion by looking for genes which expression changes in the opposite direction as a result of genomic losses or gains in this locus. Such genes are likely to represent primary targets and direct transcriptional readouts of the underlying copy number imbalances. By contrast, expression changes specific to genomic losses or in the same direction independent of genomic dosage are more likely to be secondary reflections of affected physiological process or malfunctioning brain regions (Chahrour et al., 2008). We compared the PFC and HPC gene expression profiles in mice carrying a

A

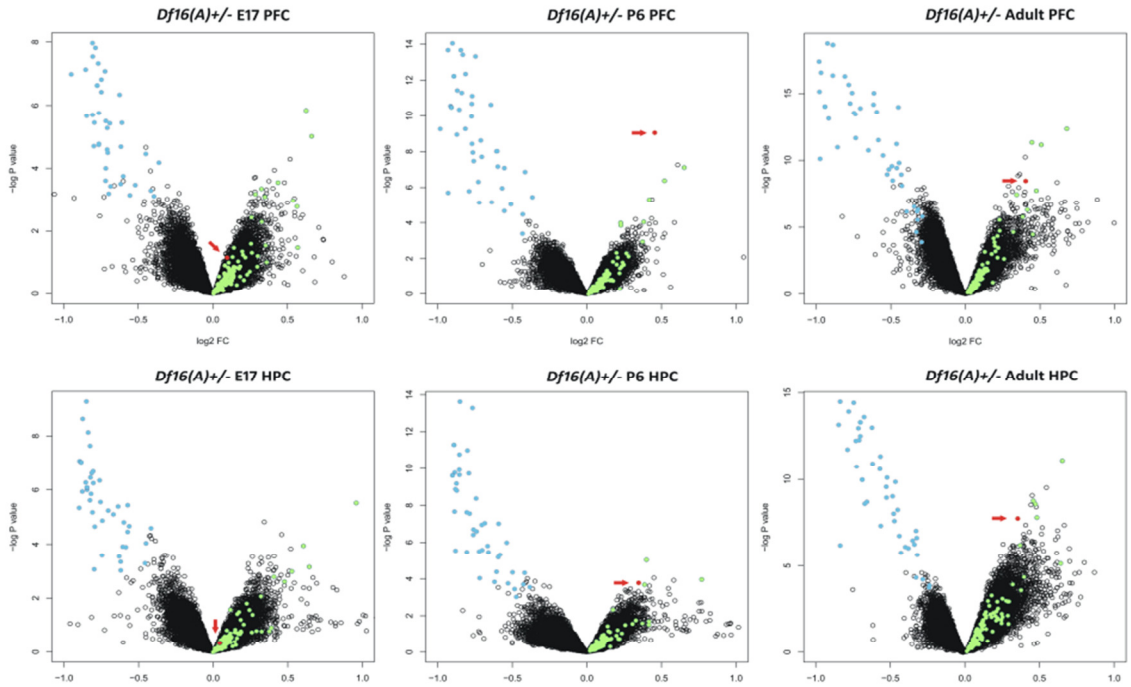

B

E17 PFC		
AffyID	Symbols	P.Value
1450625_at	Col5a2	1.15E-04
1430644_at	Wbscr25	1.92E-04
1419147_at	Rec8	4.30E-04
1419028_at	Arpp21	4.49E-04
1427083_a_at	Map4k5	4.79E-04
1440240_at	Npb	6.16E-04
1421648_at	Nlgn1	6.30E-04
1424659_at	Slit2	8.03E-04
1458119_at	Slc25a27	8.84E-04
1449914_at	Ribc1	9.42E-04

P6 PFC		
AffyID	Symbols	P.Value
1424038_a_at	2310044H10Rik	9.08E-10
1428021_at	Mccc2	5.82E-05
1430976_a_at	Mrpl9	6.26E-05
1438967_x_at	Amhr2	9.71E-05
1427962_at	Ccdc102a	1.03E-04
1437236_a_at	Zfp110	1.49E-04
1451688_s_at	Cant1	1.76E-04
1453380_a_at	Xrcc6bp1	1.77E-04
1420117_at	Golph3	2.04E-04
1431678_at	4930556N08Rik	2.32E-04

Adult PFC		
AffyID	Symbols	P.Value
1455326_at	Clec16a	1.38E-09
1424038_a_at	2310044H10Rik	3.40E-09
1456488_at	Wdr33	4.36E-09
1428208_at	Bcl7a	1.06E-08
1437125_at	Camk2a	3.73E-08
1439661_at	Slc16a14	3.76E-08
1426446_at	6430548M08Rik	6.03E-08
1458870_x_at	Mycbp2	1.04E-07
1452322_a_at	Brwd1	1.32E-07
1450661_x_at	Nfic	1.61E-07

E17 HPC		
AffyID	Symbols	P.Value
1450625_at	Col5a2	4.40E-05
1460245_at	Klrd1	2.84E-04
1460451_at	Tmem52	2.96E-04
1453816_at	Nsa2	4.81E-04
1420170_at	Myh9	5.38E-04
1434423_at	Gulp1	5.72E-04
1442160_at	Fam19a3	5.73E-04
1422263_at	Bdkrb2	8.09E-04
1416529_at	Emp1	8.99E-04
1418710_at	Cd59a	9.23E-04

P6 HPC		
AffyID	Symbols	P.Value
1460613_x_at	Gh	8.98E-05
1424038_a_at	2310044H10Rik	1.68E-04
1418547_at	Tfpi2	2.42E-04
1460471_at	Ooep	3.33E-04
1418541_at	Cenpo	3.44E-04
1427202_at	4833442J19Rik	4.12E-04
1438624_x_at	Hs3st2	4.66E-04
1421298_a_at	Hipk1	4.75E-04
1449191_at	Wfdc12	4.87E-04
1454576_at	A230102O21Rik	5.02E-04

Adult HPC		
AffyID	Symbols	P.Value
1455326_at	Clec16a	8.58E-10
1423125_at	Dclk1	2.98E-09
1425690_at	B3gat1	3.94E-09
1424038_a_at	2310044H10Rik	1.81E-08
1441312_at	Cnnm1	4.33E-08
1449931_at	Cpeb4	4.44E-08
1421200_at	Dlg2	9.01E-08
1421339_at	Extl3	1.10E-07
1431254_at	Kbtbd11	1.40E-07
1452742_at	Trak1	1.45E-07

C

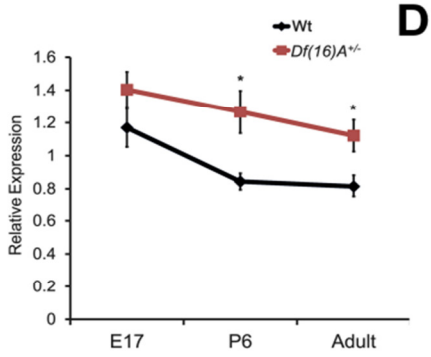

D

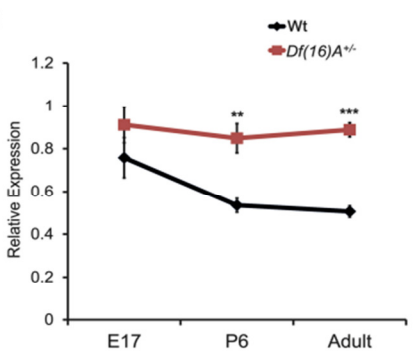

E

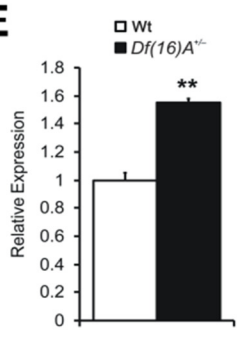

Figure 2.6 [previous page] *2310044H10Rik* (*Mirta22*) is Robustly Upregulated in the Brain of *Df(16)A*$^{+/-}$ Mice. (A) Changes in gene expression in the prefrontal cortex (PFC, upper panel) or hippocampus (HPC, lower panel) of *Df(16)A*$^{+/-}$ and Wt littermate control mice at E16, P6 and adulthood (n = 10 each group): Volcano plot of the *P*-values and the corresponding relative expression of each gene. Light blue dots indicate genes within *Df(16)A* deficiency; light green dots indicate upregulated miRNA-containing transcripts; red dots indicate probe sets representing *Mirta22*. (B) Top 10 protein encoding genes that show significant upregulation in the PFC (upper panel) or HPC (lower panel) of *Df(16)A*$^{+/-}$ and Wt littermate mice at E16, P6 and adulthood. *Mirta22* is highlighted in red. (C-D) Temporal expression of *2310044H10Rik (Mirta22)* in the PFC (C) and HPC (D) of *Df(16)A*$^{+/-}$ and Wt littermate mice as monitored by qRT-PCR. n = 9–10 for each group. (E) Increased expression of endogenous *2310044H10Rik (Mirta22)* in DIV9 hippocampal neurons isolated from *Df(16)A*$^{+/-}$ animals as assayed by qRT-PCR (n = 3 each genotype). Expression levels in mutant neurons were normalized to Wt neurons. Results are expressed as mean ± SEM. *p < 0.05, **p < 0.01, ***p < 0.001 (Student's *t*-test).

deletion or duplication at the syntenic mouse locus using as a reference compound heterozygous mice balanced for copy number (see Chapter 2.5.1 and Figure 2.7). We identified a number of inversely altered transcripts in either PFC or HPC (*P*-value <0.001, Table 2.2), in addition to the transcripts from the 22q11.2 region. As expected the majority of the identified transcripts are pri-miRNA forms. Only twelve transcripts were significantly misregulated in a reciprocal manner in both PFC and HPC (Table 2.3). Among them, *2310044H10Rik* is the only gene with protein coding potential.

Taken together, our expression profiling highlighted the misregulation of *2310044H10Rik* as a major consequence of the 22q11.2 genomic imbalances at the transcriptome level. We confirmed the pattern of *2310044H10Rik* upregulation in both PFC and HPC by TaqMan qRT-PCR (PFC: E17, 20%, $P = 0.24$; P6, 59%, $P < 0.01$; Adult, 76%, $P < 10^{-6}$; HPC: E17, 20%, $P = 0.16$; P6, 50%, $P < 0.05$; Adult, 38%, $P < 0.05$; Figure 2.6C, D). This analysis revealed a profile of temporal regulation where levels of *2310044H10Rik* rapidly decline during the first week after birth (between E17 and P6) and remain constantly low thereafter, as well as a corresponding pattern of misregulation in *Df(16)A*$^{+/-}$ mice where elevated expression of *2310044H10Rik* persists throughout postnatal and adult life. Increased brain expression of *2310044H10Rik* is recapitulated in primary neurons from *Df(16)A*$^{+/-}$ mice (Figure 2.6E).

2.2.3 2310044H10Rik as a Major Downstream Target of miRNAs Dysregulated in Df(16)A$^{+/-}$ *Mice*

Notably, *2310044H10Rik* mRNA levels were also elevated in *Dgcr8*$^{+/-}$ mice (HPC: 30%, $P < 0.05$; PFC: 24%, $P < 0.05$; Figure 2.8A), suggesting that upregulation may be due to miRNA dysregulation. Indeed, two miRNA target site prediction programs, TargetScan (Grimson et al., 2007) and mirDB (Wang,

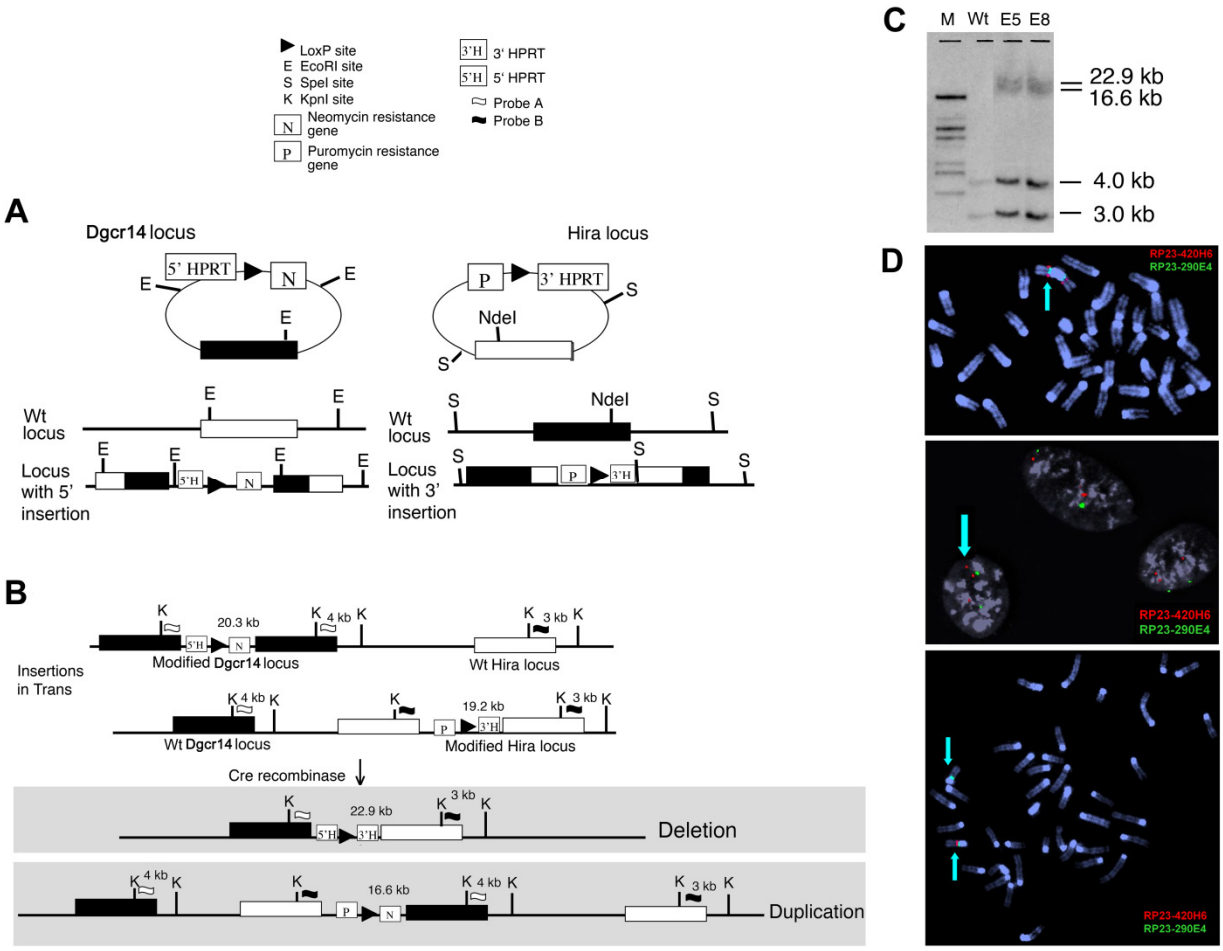

Figure 2.7 Generation of *Df(16)B* and *Dp(16)B*. (A) *Dgcr14* and *Hira* loci and the corresponding targeted loci following the introduction of 5' *HPRT* and 3' *HPRT* mini-cassettes, respectively. (B) Upon exposure to Cre recombinase, recombination between the Lox P sites of modified loci positioned in the trans orientation, led to the generation of a deletion between *Dgcr14* and *Hira,* as well as a duplication of the region. (C) Southern blot of 2 ES cell clones, using probes A and B (positions of probes, as well as expected sizes upon digestion with *Kpn*I, indicated in panel B. E5 and E8 possess both the deletion (indicated by a 22.9 kb band) as well as the duplication (indicated by a 16.6 kb band). Wt indicates lane with DNA from wild type ES cells. M indicates the marker lane, *Bst*EII cut λ DNA. (D) FISH verification. Top panel: metaphase chromosome spread of MEFs possessing the duplication. A slightly brighter red signal (arrow) indicates the duplicated region. Middle panel: Interphase FISH of the duplication. The duplication is demonstrated by a third separate red signal. Bottom panel: Metaphase chromosome spread of MEFs possessing the deletion. The red signal indicates the deleted region, and the green signal is from the control probe, located outside of the deleted region. MEF: mouse embryonic fibroblast. FISH: fluorescent *in situ* hybridization. RP23-420H6: mouse BAC probe located within the deleted and duplicated regions. RP23-290E4: mouse BAC probe located outside of the deleted and duplicated regions.

2008), report that the 3′UTR of *2310044H10Rik* contains binding sites of miRNAs that were shown to be affected in *Df(16)A*$^{+/-}$ mice by microarray profiling (Stark et al., 2008). Specifically, mirDB predicted 5 such miRNAs with binding sites in the 3′UTR of *2310044H10Rik* including miR-185 and miR-485, whereas

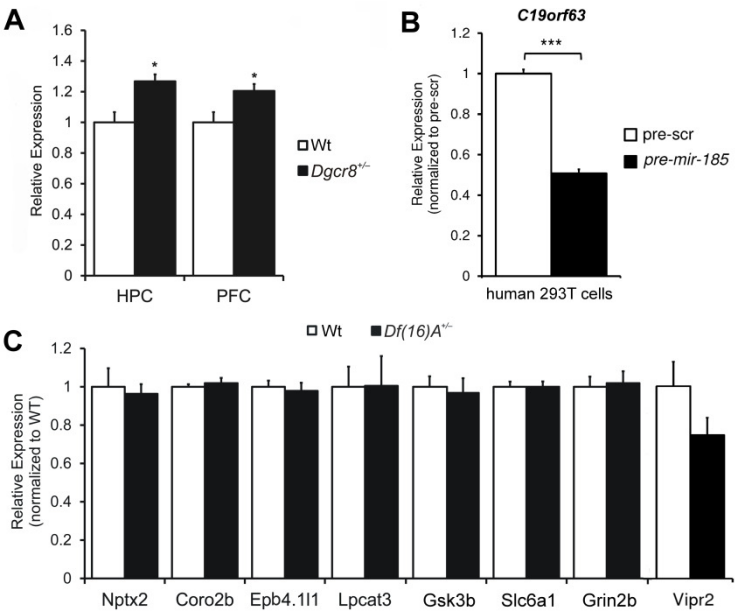

Figure 2.8 *2310044H10Rik* (*Mirta22*) is the Major Downstream Target of the miRNA Dysregulation.

(A) *2310044H10Rik (Mirta22) e*xpression levels in hippocampus (HPC) and prefrontal cortex (PFC) of adult *Dgcr8*$^{+/-}$mice (n = 7 for HPC; n = 10 for PFC) and their respective Wt littermate controls (n = 8 for HPC; n = 10 for PFC), as assayed by qRT-PCR. Expression levels in mutant animals were normalized to their respective Wt littermates. (B) 293T cells transfected with pre-miR-185 mimic or pre-scramble (pre-scr) oligo. Expression levels of *C19orf63,* the human homolog of *2310044H10Rik (Mirta22),* were assayed by qRT-PCR. Expression levels of *C19orf63* in cells transfected with pre-miR-185 (n = 3) were normalized to the pre-scr controls (n = 3). (C) Expression levels of a sample of putative miR-185 targets predicted by both TargetScan and miRanda (*Nptx2*, *Coro2b*, *Epb4.1l1*, *Lpcat3*, *Gsk3b*, *Slc6a1,Grin2b* and *Vipr2*) in the HPC of adult *Df(16)A*$^{+/-}$mice (n= 10) and their respective Wt littermate mice (n = 10), as assayed by qRT-PCR. Expression levels in mutant animals were normalized to their respective Wt littermates. For all genes tested, expression levels were not significantly altered in mutant animals. Expression levels in mutant animals were normalized to their respective Wt littermates

TargetScan predicted 13 miRNA sites, including sites for miR-185, miR-485, miR-491 and miR-224. Notably, both programs predicted sites for miR-185 and miR-485 (Figure 2.9A, red rectangles).

Because increased brain expression of *2310044H10Rik* is recapitulated in primary neurons from *Df(16)A*$^{+/-}$ mice (Figure 2.6E), we first used primary neurons to determine if endogenous *2310044H10Rik* expression is actually under the control of miR-185. To examine the effect of miR-185 overexpression on *2310044H10Rik* level, we introduced into primary neuronal cultures a miRNA precursor mimic ("pre-miR-185"), which is processed into mature miRNA, or a scramble precursor ("pre-scramble") with no homology to the mouse genome, which serves as a control for nonspecific effects of small RNA expression. 24 hours post-transfection there was a decrease in the levels of *2310044H10Rik* in pre-miR-185 transfected neurons when compared to pre-scramble transfected neurons ($P < 0.01$; Figure 2.9B). In a complementary experiment, introduction of an anti-miR-185 LNA oligonucleotide or a scramble control oligonucleotide resulted in an increase of *2310044H10Rik* mRNA levels in anti-miR-185 transfected cells when compared to scramble transfected cells ($P< 0.05$; Figure 2.9C). Taken together, these results

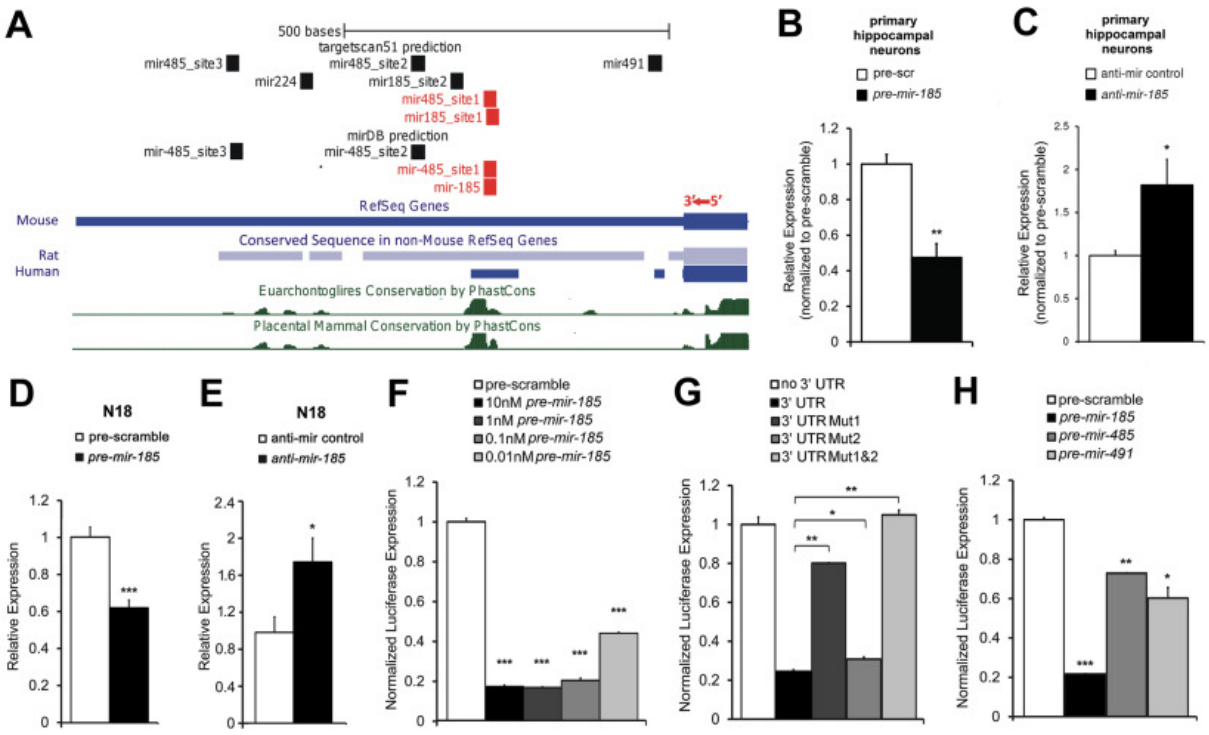

Figure 2.9 miR-185 Directly Targets and Represses *2310044H10Rik (Mirta22).* (A) Structure of the 3′UTR of *2310044H10Rik (Mirta22)* showing miRNA binding sites predicted by TargetScan or mirDB. Blocks in mouse *2310044H10Rik* 3′UTR that are highly conserved in rat and human orthologues are shown below the mouse 3′UTR. Evolutionary conservation is also assessed by the "30-way multiz alignment and conservation analysis" in the USCS browser, with conserved blocks indicated by green peaks. miR-185 and miR-485 binding sites located within the conserved blocks are shown in red. (B-C) qRT-PCR quantification of endogenous *Mirta22* in DIV7 hippocampal neurons. Expression levels in anti-miR-185-treated and pre-miR-185-treated neurons were normalized to expression levels under respective controls. (B) Increased expression levels of *Mirta22* in neurons transfected with anti-miR-185 at DIV5 (*n* = 5, each treatment). (C) Reduced expression levels of *Mirta22* in DIV9 hippocampal neurons transfected with pre-miR-185 mimic at DIV7 (*n* = 3, each treatment). (D-E) qRT-PCR quantification of endogenous *Mirta22* in N18 cells. Expression levels in pre-miR-185-treated and anti-miR-185-treated cells were normalized to expression levels under respective controls. (D) Reduced expression levels of *Mirta22* in cells transfected with pre-miR-185 mimic (n = 3, each treatment). (E) Up-regulation of *Mirta22* in cells transfected with an anti-miR-185 LNA oligo (n = 3, each treatment). (F-H) Repression effects of pre-miR-185, pre-miR-485 and pre-miR-491 on *Mirta22* 3′UTR were examined by a dual-luciferase reporter assay. psiCHECK2 plasmids containing a *Renilla* luciferase gene under the control of either Wt or one of the mutant *2310044H10Rik* 3′UTRs were co-transfected with pre-miRNA or pre-scramble mimic into the N18 neuroblastoma cell line (n = 3 for each condition). Firefly luciferase expressed from the same plasmid was used as internal control. Values are *Renilla* luciferase levels relative to firefly luciferase levels and normalized to the relative expression levels under pre-scramble treatment (F, H) or to the relative expression levels from plasmid with no 3′UTR (G). Pre-miR-185 significantly decreases the *2310044H10Rik 3*′UTR reporter expression over a concentration range of 10nM to 0.01nM (F). pre-miR-185 mediated repression on *2310044H10Rik (Mirta22)* 3′UTR reporter expression depends on conserved miRNA binding sites (G). *2310044H10Rik* 3′UTR luciferase reporters with mutations at Site 1 (Mut1) or Site 2 (Mut2) or both sites (Mut1&2) were analyzed. Mutated *2310044H10Rik (Mirta22)* 3′UTR reporters express significantly higher luciferase activities than Wt *Mirta22* 3′UTR reporters. Pre-miR-485 and pre-miR-491 significantly decreases the *2310044H10Rik (Mirta22)* 3′UTR reporter expression (H). Results are expressed as mean ± SEM. *p < 0.05, **p < 0.01, ***p < 0.001 (Student's *t*-test).

confirm that *2310044H10Rik* expression in primary neurons is under the repressive control of miR-185. Essentially identical results were obtained when *2310044H10Rik* expression was assayed in N18 cells (Figure 2.9D, E). Therefore we used this cell line in order to facilitate further molecular characterization of the inhibition of miR-185 on *2310044H10Rik* expression.

To test if the inhibition of miR-185 on *2310044H10Rik* expression is 3′UTR-dependent as predicted by TargetScan and mirDB (see above), *2310044H10Rik* 3′UTR-fused luciferase reporter genes (see Chapter 2.5.7 and Figure legend for details) were cotransfected with either “pre-miR-185” mimic or a scramble precursor (“pre-scramble”) into N18 cells. While pre-scramble did not affect the reporter activity, introduction of *pre-miR-185* mimic led to a dramatic decrease of luciferase activity as compared to the pre-scramble control ($P < 0.001$ for all pre-*miR-185* concentrations used, compared to pre-scramble control; Figure 3F). Repression by *miR-185* occurs over a 10^3-fold concentration range and more than 55% repression was still observed at a pre-*miR-185* mimic concentration of 0.01 nM (Figure 2.9F). To investigate if miR-185-mediated repression is specific and operates directly via the two binding sites predicted by TargetScan (Figure 3A), we engineered luciferase reporters carrying mutated versions of *2310044H10Rik* 3′UTR with either individual or both miR-185 binding sites mutated (Mut1: Site 1 mutant; Mut2: Site 2 mutant; Mut1&2: Site 1 and 2 mutants, see Supplementary Methods). The pre-miR-185 mimic significantly reduced the luciferase activity of the Wt reporter to ~25% relative to a control reporter without 3′UTR, while it reduced the luciferase activities of the Mut1 and Mut2 reporters to 80% ($P < 0.01$) and 33% ($P < 0.05$) respectively (Figure 2.9G). Notably, the pre-miR-185 mimic could not repress luciferase activity driven from a mutant reporter where both binding sites are simultaneously disrupted (Figure 3G). Thus, both miR-185 cognate binding sites have an impact on the 3′UTR-mediated regulation of *2310044H10Rik* expression, although the site disrupted in the Mut1 reporter (Site 1) seems to be the major target site via which miR-185 directly exerts its repressive effect.

We further addressed the dependence of *2310044H10Rik* 3′UTR reporter repression on the levels of miR-485 or miR-491, which are also predicted to target binding sites in the 3′UTR of *2310044H10Rik*. Neither of these two miRNAs is located within the 22q11.2 microdeletion, but both are modestly down-regulated in HPC of *Df(16)A*$^{+/-}$ mice due to the *Dgcr8* hemizygosity (Figure 2.10). The pre-miRNA mimics of either miRNA modestly but significantly reduced the luciferase activity of the 3′UTR fused reporter compared to the pre-scramble control (pre-*miR-485*: 27%, $P < 0.05$; pre-miR-491: 35%, *P*

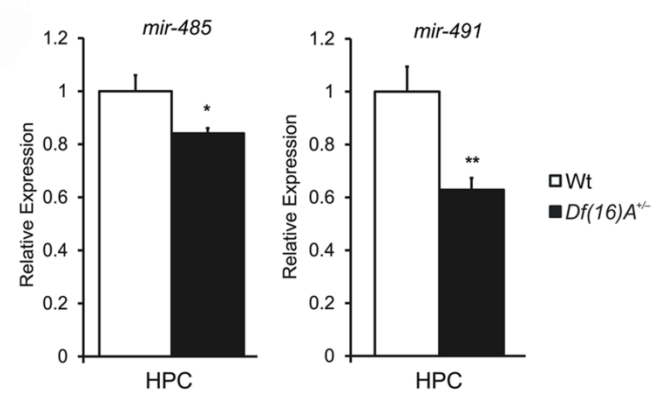

Figure 2.10 Reduction of miR-485 and miR-491 Expression in *Df(16)A*$^{+/-}$ Mice. Expression levels of miR-485 and miR-491 in hippocampus of adult *Df(16)A*$^{+/-}$mice (n = 7) and their respective Wt littermate mice (n = 9), as assayed by qRT-PCR. Expression levels in mutant animals were normalized to their respective Wt littermates

< 0.05; Figure 2.9H). A three factor ANOVA analysis indicated that all three miRNAs (miR-185, miR-485 and miR-491) and their interactions have significant impact on the luciferase activity with the exception of the interaction between miR-485 and miR-491 (Table 2.4).

Taken together, these findings suggest that the persistent elevation of *2310044H10Rik* levels observed *in Df(16)A*$^{+/-}$ mice is likely the result of the combined hemizygosity at *mir-185* and *Dgcr8* loci. Although more than one miRNA contributes, the major effect is due to the dramatic downregulation of miR-185. Consistent with this notion and the less profound reduction of miR-185 in *Dgcr8*$^{+/-}$ mice (Figure 2.5E), *2310044H10Rik* is only modestly upregulated in this strain (Figure 2.8A). Interestingly, a comparison between the 3′UTR of human and mouse orthologues (Figure 2.9A) reveals that miR-185 cognate Site 1 as well as one miR-485 binding site are located within a highly conserved region, suggesting that these sites are critical in regulating the levels of the human orthologue (*C19orf63*). Consistent with this expectation, introduction of pre-miR-185 into human 293T cells resulted in a significant decrease of endogenous *C19orf63* levels (Figure 2.8B). In addition, similar to the pattern observed in the mouse brain, expression of *C19orf63* decreases in infant brain (see also Chapter 3.3.2) (Colantuoni et al., 2011).

It is noteworthy that inspection of our gene expression database as well as qRT-PCR analysis of a sample of eight high-likelihood miR-185 targets identified by more than one prediction program did not reveal any additional significant transcript level changes in the brains of *Df(16)A*$^{+/-}$ mice (Figure 2.8C). Furthermore, unlike 2310044H10Rik, none of the top upregulated genes shown in Figure 2.6 are consistently altered in the HPC and frontal cortex of E17, P6 and adult *Df(16)A*$^{+/-}$ mice and only one of them contains miR-185 seed sites in its 3′UTR. Overall, although additional downstream targets of miR-

185 likely exist (see Chapter 3.2.3), our analysis suggests that *2310044H10Rik* represents the major downstream effector of miR-185 and a major hub target of miRNA dysregulation due to the 22q11.2 microdeletion. Due to confirmed miRNA-mediated regulation, we renamed the gene *Mirta22* (*miRNA target of the 22q11.2 microdeletion*). In the Chapter 3, I will discuss the efforts to characterize the localization and function of Mirta22 protein.

2.3 Discussion

2.3.1 CNV-associated miRNA Dysregulation

In our 22q11.2 microdeletion mouse model, *Df(16)A*$^{+/-}$, downregulation of a subset of mature miRNA due to *Dcgr8* haploinsufficiency was described previously (Stark et al., 2008). Dgcr8 is the RNA-binding moiety of the microprocessor complex and its deficiency impedes the processing of pri-miRNAs to pre-miRNAs. Proper miRNA function involves the delicate pathways controlling miRNA biogenesis and targeting, including transcription, enzymatic processing and formation of miRNA-containing complexes and their intracellular tracking. Gain or loss of any of the gene involved in these processes generally leads to modest dysregulation of a group of miRNAs. How much impact the collective changes of a subset of miRNA can make is discussed next in Chapter 2.3.3, but it is conceivable that this kind of extensive miRNA dysregulation could be a more general phenomenon underlying the etiology of pathogenic CNVs associated with neuropsychiatric disorders. Indeed, as mentioned in Chapter 1.2.1, a CNV encompassing *DICER1* and recurrent CNVs encompassing *CYFIP1* (encoding a protein interacting with components of miRNA-silencing machinery) were identified in large-scale genome-wide studies for CNV associated with schizophrenia (Napoli et al., 2008; Xu et al., 2008). As there are increasing genome-wide efforts to identify structural variants associated with neuropsychiatric disorders, it seems promising that other CNVs containing genes involved in miRNA processing will be uncovered. In fact, CNVs were found to encompass *DROSHA*, *XPO5* (*Exportin 5*), *GEMIN4* and *PIWIL1* loci (Duan et al., 2009). The understanding of the resulting abnormalities of miRNA biogenesis and function will greatly increase our understanding of the pathophysiology of neuropsychiatric disorders and even the normal function of the genes involved.

Instead of a more widespread dysregulation of miRNAs, CNVs that encompass individual miRNA

genes lead to aberrant expression of specific miRNAs. Besides *hsa-mir-185*, *hsa-mir-1306* and *hsa-mir-1286* (without mouse orthologues) are also located in the 1.5 Mb 22q11.2 microdeletion region (ISC, 2008; Karayiorgou et al., 1995; Stefansson et al., 2008; Xu et al., 2008). These 2 miRNAs were experimental identified relatively recently and are likely to be expressed at much lower levels than *hsa-mir-185* as suggested by the accumulated deep sequencing reads so far (see their respective entries at miRBase). Whether mir-1306 is downregulated in *Df(16)A*$^{+/-}$ mouse and the potential functional impact remains to be investigated. Furthermore, other miRNA genes located in recurrent CNVs identified in schizophrenia and autism spectrum disorder include *hsa-mir-211* in the 15q13 (ISC, 2008; Kirov et al., 2009; Kirov et al., 2008; Miller et al., 2009; Stefansson et al., 2008) and *hsa-mir-484* in 16p13.11 (Ingason et al., 2009; Kirov et al., 2009). Since miRNA genes are dispersed in the genome, many CNVs likely include miRNA genes. As the genome of any individual contains a number of inherited and *de novo* CNVs that likely encompass miRNA genes (Freeman et al., 2006; MacArthur et al., 2012; Pinto et al., 2007), dysregulation of individual miRNAs due to CNVs is possibly more prevalent than was previously appreciated. In support of this hypothesis, an analysis focusing on 380 miRNA genes at gene loci enriched in biological processes found that more than 50% (193 out of 380) of these genes are located in regions covered by 385 CNVs in public databases. However, it is conceivable that most of the resulting miRNA expression change is mild and likely due to compensation by downregulation (in the case of duplication) or upregulation (in the case of deletion) of the existing miRNA copies. More substantial alterations in miRNA levels are likely to occur when there is gene X gene or variant X variant interaction.

In this regard, in this chapter I present our finding that a drastic reduction in miR-185, which resides in the 22q11.2 locus, is a previously unappreciated component of the miRNA dysregulation in 22q11.2 microdeletion syndrome. This discovery is particularly interesting as it represents an example of a gene X gene interaction within a CNV that leads to more severe dysregulation of a miRNA encoded within the CNV locus. Other CNVs that include a miRNA gene and a gene involved in processing of that miRNA can result in larger alterations than changing the copy number of the miRNA alone. Gene X gene or variant X variant interaction likely contributes to drastic alteration of miRNA expression. In cases where a chromosomal deletion causes a loss of a miRNA gene is coupled with a variant in the remaining copy of the miRNA gene, a greater alteration than expected by the change of copy number itself results.

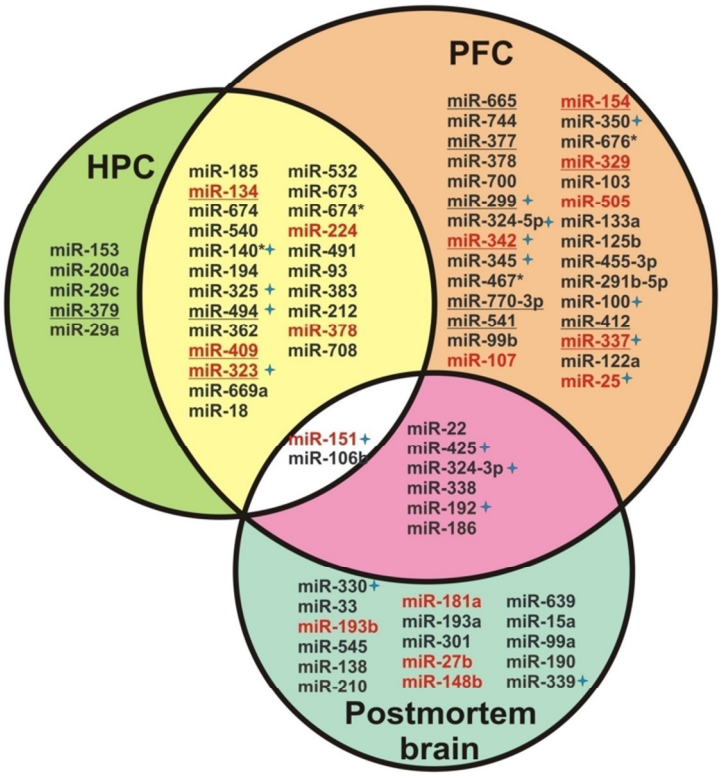

Figure 2.11 Convergent down-regulation of miRNAs in schizophrenia patients and *Df(16)A*$^{+/-}$ mice. In *Df(16)A*$^{+/-}$ mice, expression of 30 miRNAs in hippocampus (HPC) and 60 miRNAs in prefrontal cortex (PFC) is reduced due to hemizygosity of *Dgcr8* gene. Among them 25 miRNAs are downregulated in both HPC and PFC. In a study of postmortem brain samples from patients with SCZ or bipolar disorder (BP), Moreau et al identified 24 dysregulated miRNAs (having > 95% posterior probability of nonzero effect of psychiatric diagnosis). Among those, 8 are underexpressed in the PFC of *Df(16)A*$^{+/-}$ mice, including miR-151 and miR-106b that are downregulated in the HPC as well (Moreau et al 2011). In addition, miRNA profiling in PBMC of patients with SCZ found 83 miRNAs down-regulated with a false discovery rate (FDR) < 5% (Gardiner et al., 2011). Interestingly, 17 miRNAs, including miR-134, are transcribed and possibly co-regulated from the maternally expressed *DLK1-DIO3* locus on chromosome 14q32 (a homologous locus on mouse chromosome 12qF1), suggesting that fine control of miRNA expression from this locus may be critical for normal brain development and function. MicroRNAs identified as downregulated in both the Gardiner et al study and the *Df(16)A*$^{+/-}$mice are shown in RED. Overalapping miRNAs located in the *DLK1-DIO3* locus are underlined. It is important to note that many of these convergent miRNAs are synaptically enriched, suggesting they may function at synaptic sites. Those miRNAs with a synaptic enrichment ratio (synaptic fraction/total homogenate) > 2 are marked with a blue star (Lugli et al 2008).

2.3.2 Convergent Downregulation of miRNAs in Schizophrenia Patients and Df(16)A$^{+/-}$ *Mice*

Compelling evidence for miRNA dysregulation due to 22q11.2 microdeletion provides a useful etiological context to interpret results obtained from ongoing studies monitoring miRNA expression changes in the brains and peripheral blood cells in schizophrenia. As mentioned in Chapter 1.2.1, two recent studies provide supporting evidence suggesting that miRNAs dysregulated as a result of the 22q11.2 microdeletion may have a more general role in schizophrenia pathogenesis (Figure 2.11). A postmortem study found that reduction in a subset of miRNAs in Brodmann area is associated with schizophrenia and bipolar disorder (Moreau et al., 2011). Interestingly, when the 24 misexpressed miRNAs with posterior probabilities of a nonzero diagnostic effect > 95% were compared with 22

identified in the mouse model of 22q11.2 microdeletion, 8 of them overlapped. Another line of evidence came from an expression profiling study of miRNAs in peripheral blood mononuclear cells of 112 patients with schizophrenia and 76 non-psychiatric controls (Gardiner et al., 2011). Gardiner et al. showed that a cluster of 17 of the most substantially downregulated miRNAs were located within an imprinted region (*DLK1-DIO3*) on chromosome 14q32. These miRNAs account for 53% of the 30 miRNAs that lie within this locus and are expressed in the peripheral blood mononuclear cells (Gardiner et al., 2011). Notably, the expression levels of many miRNAs within this cluster including miR-134 were also downregulated in *Df(16)A*$^{+/-}$ and *Dgcr8*$^{+/-}$ mice. It is interesting to note that many of these convergent miRNAs have been shown to be synaptically enriched (Lugli et al., 2008) and may function at synaptic sites (Figure 2.11). It is an intriguing idea that there exist a "core group" of miRNAs which play important roles in brain function that are collectively downregulated in schizophrenia or certain subtypes of schizophrenia. This hypothesis remains to be tested by future miRNA expression profiling studies in patients as well as in etiologically valid animal models.

2.3.3 Impact of Modest Dysregulation of miRNAs

Although the observed fold change of individual miRNAs in studies of the *Df(16)A*$^{+/-}$ mouse model (Stark et al., 2008) as well as in human postmortem studies (Beveridge et al., 2010; Gardiner et al., 2011; Kim et al., 2010; Moreau et al., 2011; Perkins et al., 2007; Santarelli et al., 2011) is generally small (typically <0.70, i.e. <30% decrease), it is conceivable (although not yet unequivocally established) that even relatively small changes in specific miRNA levels can disrupt the fine-tuning of target protein expression. Many of the miRNAs found altered in the aforementioned studies are not among the most highly expressed miRNAs in the brain, suggesting that they may not be able to stoichiometrically saturate their target mRNAs under physiological condition. Fluctuation in the levels of such miRNAs may result in changes of expression levels of target proteins, especially those targets that have multiple binding sites for the dysregulated miRNAs. Indeed, it has been recently shown that alterations in the levels of at least some miRNAs have a low magnitude but widespread impact on proteome, suggesting that individual miRNAs can act as "rheostats" to adjust the fine-scale control of protein output (Selbach et al., 2008). In that context, modest dysregulation of many miRNAs can, in principle, interact additively and cooperatively resulting in an even more prevalent impact on proteome. More studies are certainly required to validate if

additive or synergistic miRNA dysregulation is indeed at play in individuals with 22q11.2 microdeletions.

2.3.4 Not all miRNA Targets are Created Equal?

Our analysis suggests that *Mirta22* is the major downstream target affected by drastically dysregulated miR-185 starting at postnatal development. We began by speculating that any major target with expression critically regulated by miR-185 during normally brain maturation would be derepressed and significantly upregulated in brains of *Df(16)A*$^{+/-}$ mice. We thus searched for the top upregulated genes in the transciptome that harbor miR-185 binding sites in the 3'UTR and found *Mirta22* as the only gene consistently altered in both hippocampus and frontal cortex and possessing a miR-185 binding site.

This finding may seem surprising considering the many possible targets predicted by various in silico programs to be regulated by miR-185. Furthermore, microarray and proteomic studies generally show a large number of targets simultaneously repressed by individual miRNAs (Baek et al., 2008; Chi et al., 2009; Guo et al., 2010; Lim et al., 2005; Selbach et al., 2008). It was also reported that at least 16% of the proteins from mRNAs with single 7-8mer 3'UTR sites responded to miRNAs overexpression (Baek et al., 2008). However, in these studies, only a very small percentage of altered targets changed by at least 0.5 on $\log_2$ scale (~>30% downregulation or ~>40% upregulation) when miRNAs levels were drastically manipulated (Baek et al., 2008; Chi et al., 2009; Selbach et al., 2008). It is also relevant to note that although CNVs clearly contribute to human diseases, many CNVs and the resulting heterozygosities or gene duplications are likely well-tolerated and only have limited contribution to phenotypic variation (Freeman et al., 2006; MacArthur et al., 2012). In similar fashion, it is conceivable that the majority of the mildly dysregulated targets can be neutralized by compensatory regulation. Effects of collective modest dysregulation of a group of targets only become noticeable when those targets are involved in specific functional pathways (see Chapter 5.2.1). Although we also observed a coordinated dysregulation of targets with Golgi-related function due to reduced miR-185 levels (results present in Chapter 3.2.3), in studies mentioned above, the functional impact of the dysregulation of a cohort of targets due to miRNA manipulations is largely unexplored.

On the other hand, ever since the discovery of miRNA, it is well-documented that in certain contexts, especially during development, repression of a few targets or even one single target, among the large cohort of targets of a single miRNA, is the primary role of that particular miRNA (Lee et al., 1993;

Reinhart et al., 2000; Wightman et al., 1993). In nematode *C. elegans* the phenotype of the loss of function (lf) mutant of *lin-4*, the first identified miRNA gene, is the reiteration of early fates and cell division at inappropriate late developmental stages (Chalfie et al., 1981; Lee et al., 1993). The phenotype is largely accounted for by the loss of repression of only 2 targets, *lin-14* and *lin-28 (Lee et al., 1993; Moss et al., 1997; Wightman et al., 1993)*. Later, similar regulatory interactions with major phenotypic importance were discovered for let-7 miRNA and its targets HBL-1 and LIN-41 in L4-adult transition in worm (Abbott et al., 2005; Reinhart et al., 2000) and for miR-223 and Mef2c in myeloid-lineage differentiation in mouse (Johnnidis et al., 2008). To date, numerous miRNAs have been demonstrated to regulate important key targets at least in certain contexts (see also review by Alex Flynt and Eric Lai (Flynt and Lai, 2008)). A future challenge is to determine the extent of situations where miRNAs regulate only a few of key targets versus where miRNAs concurrently control a large number of targets to exert effects on phenotypes. Of course, these two possibilities are not necessarily mutually exclusive and I argue that miRNAs can simultaneously regulate key targets that have decisive impacts as well as other secondary targets that can collectively modulate the functional consequences. As shown in this and the next chapter, such a complicated scenario is likely the case for miR-185.

2.4 Summary

While extensive miRNA dysregulation in *Df(16)A*$^{+/-}$ mice was previously observed, we investigate a miRNA gene (*mir-185*) located in the 22q11.2 locus and discover a drastic downregulation of mir-185 in hippocampus (HPC) and prefrontal cortex (PFC) of *Df(16)A*$^{+/-}$ mice. This effect is due to the gene X gene interaction in which Dgcr8 haploinsufficiency is coupled with the loss of one copy of the *mir-185*. Since a miRNA exerts its function by repressing its target genes, we looked for downstream targets of miRNA dysregulation in *Df(16)A*$^{+/-}$ mice. We identified *2310044H10Rik* (later renamed *Mirta22*) from the top upregulated genes in the transcriptome analysis and showed that 3 miRNAs dysregulated in *Df(16)A*$^{+/-}$ mice, miR-185, miR-491 and miR-485, regulate *Mirta22* expression by targeting the 3'UTR of *Mirta22*. We conclude *Mirta22* is a major effector of miRNA dysregulation in *Df(16)A*$^{+/-}$ mice and will describe the functional characterization of Mirta22 in the next Chapter.

Table 2.1 Examples of Phenotypic Correlation between 22q11.2DS and *Df(16)A*$^{+/-}$

Cognitive Function			
22q11.2 DS Patients	**Functional correlates**	***Df(16)A*$^{+/-}$**	**Refs**
Impaired suppression in prepulse inhibition (PPI) test	**Preattentive processing Sensorimotor gating**	Impaired suppression in prepulse inhibition (PPI) test	1, 2, 3
Decreased accuracy in *N*-back task	**Working memory**	Decreased accuracy in delayed non-match to place (DNMP) task	4, 3
Visual-spatial memory in CMS dot location task	**Spatial memory**	Reduced fear response in contextual fear conditioning	5, 3
Learning disability	**Learning and memory**	Reduced fear response in contextual and cued fear conditioning; longer time to reach criteria in DNMP task	6, 7, 3
Brain Morphology			
22q11.2 DS Patients	**Structural correlates**	***Df(16)A*$^{+/-}$**	**Refs**
Decreased hippocampal volume	**Structural complexity in Hippocampus**	Reduced dendritic complexity, spine number and spine size of CA1 neurons	8, 9, 10, 3
Decreased cortical thickness	**Structural complexity in prefrontal cortex**	Reduced basal dendritic complexity and spine number of layer V PFC neurons	11, 12, 13
Attenuated concomitant activation of DLPFC and HPC in *N*-back task	**HPC-PFC circuitry**	Reduced neural synchrony and phase locking between HPC and PFC	14, 15

CMS: Children's Memory Scale, DLPFC: dorsolateral prefrontal cortex, PFC: prefrontal cortex, HPC: hippocampus.

References: 1. (Ornitz et al., 1986), 2. (Sobin et al., 2005), 3. (Stark et al., 2008), 4. (Casey et al., 1995), 5. (Bearden et al., 2001), 6. (Shprintzen et al., 1978), 7. (Lajiness-O'Neill et al., 2005), 8. (Simon et al., 2005), 9. (Campbell et al., 2006), 10. (Eliez et al., 2000a), 11. (Schaer et al., 2006), 12. (Schaer et al., 2009), 13. (Kim Stark & Joseph Gogos, unpublished data), 14. (Meyer-Lindenberg et al., 2005), 15, (Sigurdsson et al., 2010).

Table 2.2 Transcripts outside the 22q11.2 Syntenic Region Misregulated in a Reciprocal Manner

Brain region	AffyID	Chr	Chr_start	Chr_end	Fold change (Del/Bal)*	Fold change (Dup/Bal)*	F	P Value	Symbols
PFC	**1424038_a_at**	**7**	**51745308**	**51751883**	**1.43**	**0.86**	**73**	**2.60E-11**	***2310044H10Rik***
PFC	1435179_at	13	83867710	83875274	1.46	0.89	52.6	8.50E-10	*C130071C03Rik (miR-9-2)*
PFC	1460033_at	1	196850302	196864096	1.76	0.85	44.49	4.60E-09	*A330023F24Rik (miR-29c)*
PFC	1435089_at	13	63116293	63400964	1.77	0.78	43.72	5.50E-09	*2010111I01Rik (miR-23b)*
PFC	1428562_at	11	75275040	75280192	1.33	0.85	42.88	6.70E-09	*2210403K04Rik (miR-22)*
PFC	1440357_at	15	85537748	85537832	2.07	0.87	32.51	9.40E-08	*(let-7b)*
PFC	1438838_at	X	100764843	100819093	1.3	0.88	18.77	9.60E-06	*B230206F22Rik (miR-374)*
PFC	1431094_at	12	110833610	110835408	1.2	0.91	17.13	1.90E-05	*1110006E14Rik (miR-136)*
PFC	1439305_at	X	100772966	100773671	1.4	0.97	15.3	4.20E-05	*(miR-374)*
PFC	1430959_at	17	17967938	17976035	1.46	0.88	14.93	5.00E-05	*Ncrna00085*
PFC	1456904_at	11	97049276	97050652	0.82	1.08	14.92	5.10E-05	*NA*
PFC	1457030_at	12	110973190	110987665	1.29	0.91	14.82	5.30E-05	*Mirg*
PFC	1434730_at	7	86676773	86677477	1.42	0.96	14.75	5.50E-05	*AI854517 (miR-9-3)*
PFC	1427410_at	14	62221673	62301210	1.27	0.9	13.75	8.80E-05	*Dleu2 (miR-15a)*
PFC	1419161_a_at	7	94395304	94547116	1.17	0.97	13.66	9.20E-05	*Nox4*
PFC	1441666_at	1	148274740	148342171	0.81	1.02	13.48	1.00E-04	*AK162963*
PFC	1453713_s_at	17	17967938	17976035	1.8	0.89	13.18	1.20E-04	*Ncrna00085*
PFC	1457181_at	15	81822952	81846570	0.84	1.16	12.67	1.50E-04	*Pppde2*
PFC	1438053_at	16	56690444	56717467	0.71	1.06	11.63	2.60E-04	*Tfg*
PFC	1431343_at	14	8603700	8625033	1.16	0.91	11.59	2.60E-04	*Gm10044*
PFC	1430603_at	9	98462878	98464030	0.93	1.25	11.14	3.30E-04	*4930579K19Rik*
PFC	1459704_at	11	100447804	100448219	0.85	1.05	10.91	3.70E-04	*Dnajc7*
PFC	1457760_at	4	131435283	131436411	0.7	1.04	10.8	4.00E-04	*A930004J17Rik*
PFC	1425173_s_at	3	95392880	95423164	1.03	0.82	10.4	4.90E-04	*Golph3l*
PFC	1419586_at	X	19941733	19977475	0.78	1.03	10.36	5.00E-04	*Rp2h*
PFC	1453087_at	5	139475528	139476533	0.91	1.08	10.35	5.10E-04	*6330403L08Rik*
PFC	1420483_at	1	36568720	36585082	1.23	0.94	10.07	5.90E-04	*Cnnm3*
PFC	1436503_at	6	128489839	128531624	1.1	0.87	9.98	6.20E-04	*BC048546*
PFC	1417272_at	5	65361313	65433140	0.82	1.1	9.97	6.30E-04	*Fam114a1*

PFC	1442913_at	3	118242789	118243450	1.31	0.92	9.92	6.40E-04	*NA*
PFC	1437686_x_at	5	136750114	137043301	1.2	0.95	9.79	6.90E-04	*Cux1*
PFC	1429599_a_at	5	91360221	91450395	1.26	0.98	9.79	6.90E-04	*Mthfd2l*
PFC	1424291_at	8	96738500	96838966	1.23	0.97	9.77	7.00E-04	*Nup93*
PFC	1427587_at	7	6336027	6349347	0.98	1.22	9.48	8.30E-04	*Zfp28*
PFC	1446835_at	17	6109658	6110258	0.96	1.31	9.48	8.30E-04	*Tulp4*
PFC	1429647_at	1	89083240	89084978	0.93	1.25	9.38	8.80E-04	*1700027L20Rik*
PFC	1452817_at	1	180885169	181448134	0.94	1.3	9.37	8.80E-04	*Smyd3*
PFC	1446932_at	4	108470038	108470615	0.98	1.34	9.2	9.70E-04	*NA*
HPC	**1424038_a_at**	**7**	**51745308**	**51751883**	**1.29**	**0.88**	**68.49**	**1.10E-10**	***2310044H10Rik***
HPC	1440357_at	15	85537748	85537832	1.68	0.81	48.73	3.30E-09	*(let-7b)*
HPC	1435179_at	13	83867710	83875274	1.42	0.95	45.42	6.40E-09	*C130071C03Rik (miR-9-2)*
HPC	1435089_at	13	63116293	63400964	1.41	0.82	43.86	8.90E-09	*2010111I01Rik (miR-23b)*
HPC	1460033_at	1	196850302	196864096	1.71	0.86	42.71	1.10E-08	*A330023F24Rik (miR-29c)*
HPC	1427410_at	14	62221673	62301210	1.49	0.95	33.16	1.20E-07	*Dleu2 (miR-15a)*
HPC	1428562_at	11	75275040	75280192	1.33	0.92	30.51	2.40E-07	*2210403K04Rik (miR-22)*
HPC	1431094_at	12	110833610	110835408	1.2	0.87	25.24	1.20E-06	*1110006E14Rik (miR-136)*
HPC	1442913_at	3	118242789	118243450	1.39	0.84	22.06	3.50E-06	*AK141880*
HPC	1438838_at	X	100764843	100819093	1.3	0.93	19.9	7.70E-06	*B230206F22Rik (miR-374)*
HPC	1447298_at	13	83879857	83880314	1.29	0.98	19.9	7.70E-06	*(miR-9-2)*
HPC	1436467_at	9	41422406	41423268	1.2	0.83	15.31	5.10E-05	*D230004N17Rik (miR-125b-1)*
HPC	1424525_at	18	66033147	66046233	1.06	0.83	14.34	7.80E-05	*Grp*
HPC	1434730_at	7	86676773	86677477	1.4	0.95	13.99	9.20E-05	*AI854517 (miR-9-3)*
HPC	1460695_a_at	13	63116293	63400964	1.11	0.89	13.92	9.40E-05	*2010111I01Rik*
HPC	1455965_at	1	173180552	173190053	0.75	1.02	13.5	1.20E-04	*Adamts4*
HPC	1428792_at	2	170172490	170253345	0.8	1.03	13.37	1.20E-04	*Bcas1*
HPC	1458783_at	11	22753661	22754585	1.19	0.97	13.05	1.40E-04	*B3gnt2*
HPC	1459340_at	3	94771437	94772099	1.25	1	12.96	1.50E-04	*NA*
HPC	1453184_at	11	61497911	61523452	1.22	0.97	11.96	2.40E-04	*Fam83g*
HPC	1419148_at	10	126437764	126458050	1.15	0.87	11.45	3.20E-04	*Avil*
HPC	1430600_at	14	55555306	55558114	0.81	1.02	11.27	3.50E-04	*Cmtm5*
HPC	1445039_at	1	120955632	120956425	0.9	1.09	11.21	3.60E-04	*NA*
HPC	1426852_x_at	15	54577482	54585316	1.11	0.92	11.15	3.70E-04	*Nov*
HPC	1440109_at	7	54261880	54262492	0.88	1.07	10.94	4.10E-04	*D7Ertd413e*
HPC	1436796_at	18	35721811	35751699	0.88	1.06	10.91	4.20E-04	*Matr3*
HPC	1454212_x_at	15	63712281	63720628	0.86	1.01	10.71	4.60E-04	*Gsdmcl2*
HPC	1432862_at	2	146909611	146911081	0.89	1.15	10.37	5.60E-04	*Nkx2-4*
HPC	1439943_at	11	21138891	21221136	0.8	1.01	10.27	5.90E-04	*Vps54*
HPC	1426851_a_at	15	54577482	54585316	1.12	0.92	9.98	6.90E-04	*Nov*

HPC	1449465_at	5	21390271	21850523	1.14	0.93	9.95	7.00E-04	*Reln*
HPC	1415951_at	11	100277007	100286153	0.95	1.2	9.84	7.50E-04	*Fkbp10*
HPC	1459493_at	18	79083283	79083877	1.21	0.95	9.83	7.50E-04	*Setbp1*
HPC	1419411_at	10	127162447	127168824	1.2	0.84	9.76	7.80E-04	*Tac2*
HPC	1435047_at	13	110844396	111070414	1.03	0.9	9.74	7.90E-04	*Rab3c*
HPC	1457030_at	12	110973190	110987665	1.22	0.8	9.73	7.90E-04	*Mirg*
HPC	1438748_at	19	60600598	60656926	1.06	0.85	9.62	8.40E-04	*2700078E11Rik*
HPC	1422703_at	X	82947275	83022158	0.98	1.15	9.39	9.60E-04	*Gyk*

***** Bal = mouse strain balanced for copy number; Del = mouse model of the 22q11.2 microdeletion; Dup = mouse model of the 22q11.2 microduplication

Table 2.3 Transcripts outside the 22q11.2 Syntenic Region Misregulated in a Reciprocal Manner in both PFC and HPC

		PFC				HPC				
AffyID	Chr	Fold change (Del/Bal)*	Fold change (Dup/Bal)*	F	P Value	Fold change (Del/Bal)	Fold change (Dup/Bal)	F	P Value	Symbols
1424038_a_at	**7**	**1.43**	**0.86**	**73.00**	**2.6E-11**	**1.29**	**0.88**	**68.49**	**1.1E-10**	***2310044H10Rik***
1435179_at	13	1.46	0.89	52.60	8.5E-10	1.42	0.95	45.42	6.4E-09	*C130071C03Rik (mir-9-2)*
1460033_at	1	1.76	0.85	44.49	4.6E-09	1.71	0.86	42.71	1.1E-08	*A330023F24Rik (mir-29c)*
1435089_at	13	1.77	0.78	43.72	5.5E-09	1.41	0.82	43.86	8.9E-09	*2010111I01Rik (mir-23b)*
1428562_at	11	1.33	0.85	42.88	6.7E-09	1.33	0.92	30.51	2.4E-07	*2210403K04Rik (mir-22)*
1440357_at	15	2.07	0.87	32.51	9.4E-08	1.68	0.81	48.73	3.3E-09	*(let-7b)*
1438838_at	X	1.30	0.88	18.77	9.6E-06	1.30	0.93	19.90	7.7E-06	*B230206F22Rik (mir-374)*
1431094_at	12	1.20	0.91	17.13	1.9E-05	1.20	0.87	25.24	1.2E-06	*1110006E14Rik (mir-136)*
1457030_at	12	1.29	0.91	14.82	5.3E-05	1.22	0.80	9.73	7.9E-04	*Mirg*
1434730_at	7	1.42	0.96	14.75	5.5E-05	1.40	0.95	13.99	9.2E-05	*AI854517 (mir-9-3)*
1427410_at	14	1.27	0.90	13.75	8.8E-05	1.49	0.95	33.16	1.2E-07	*Dleu2 (mir-15a)*
1442913_at	3	1.31	0.92	9.92	6.4E-04	1.39	0.84	22.06	3.5E-06	*AK141880*

* Bal: mouse strain balanced for copy number, Del: mouse model of the 22q11.2 microdeletion, Dup: mouse model of the 22q11.2 microduplication

Table 2.4 Three Factor ANOVA of the Impact of miR-185, miR-485 and miR-491 on Luciferase Activity

FACTOR	DF	SS	MS	F	Pr > F
pre-miR-185	1	0.582	0.582	6554	0
pre-miR-491	1	0.0307	0.0307	346.3	0
pre-miR-185 X pre-miR-491	1	0.0062	0.0062	70.27	0
pre-miR-485	1	0.0011	0.0011	12.86	0.0059
pre-miR-185 X pre-miR-485	1	0.0008	0.0008	9.069	0.0147
pre-miR-485 X pre-miR-491	1	2.50E-05	2.50E-05	0.282	0.6084

2.5 Methods

2.5.1 Generation of Df(16)A$^{+/-}$, Df(16)B$^{+/-}$, Dp(16)B$^{+/-}$ and Dgcr8$^{+/-}$ Mice

Df(16)A$^{+/-}$: By using a chromosomal engineering approach (Zheng et al., 1999), we generated a mouse model carrying a 1.3-Mb deficiency on chromosome 16 syntenic to the human 22q11.2 region ranging from the *Dgcr2* gene to the *Hira* gene and encompassing 27 genes (*Df(16)A$^{+/-}$*, Figure 2.1). The 5' and 3' ends of the deficiency were introduced into *HPRT* deficient AB2.2 ES cells through homologous recombination. Exposure to Cre recombinase *in vitro* led to the generation of ES cells with the expected deficiency. Chimeric mice were generated and germline transmission of the deficiency was achieved. Southern blot, PCR analysis and Fluorescent in situ hybridization (FISH) analysis of mice confirmed that the deficiency was present and stable. Mice harboring the deficiency appeared normal by gross observation, although, we obtained fewer *Df(16)A$^{+/-}$* adult mice (37.3%, *n* = 300) than the 50% transmission rate expected from heterozygote (HET) X wild-type (WT) crosses. *Df(16)A$^{+/-}$* mice do not show any gross anatomical brain abnormalities. For more details, please see previous work by Stark et al. (Stark et al., 2008).

Df(16)B$^{+/-}$, Dp(16)B$^{+/-}$: Because we did not observe germline transmission for the ES clones positive for *Dp(16)A* duplication [reciprocal of *Df(16)A* deficiency], in order to compare the PFC and HPC gene expression profiles in mice carrying genomic losses or gains in the 22q11.2 syntenic locus we took advantage of a different pair of deficiency/reciprocal duplication (*Df(16)B* and *Dp(16)B*), which is slightly smaller than *Df(16)A/Dp(16)A* (extending from *Dgcr14* to *Hira,* see Figure 2.1) but includes both *Dgcr8* and *mmu-mir-185*. The corresponding mouse lines were created using a chromosomal engineering approach (Figure 2.7). ES cell clones were screened by Southern blot, using a *Kpn*I digest of ES cell DNA. A16.6 kb band, indicating the presence of the duplication, was detected. A 22.9 kb band, indicating an expected change in the location of the *Kpn*I sites when the reciprocal deletion is obtained, was also seen. Clones positive for the duplication and a reciprocal heterozygous deletion were amplified and injected into C57BL/6J blastocysts. Resulting chimeric males were bred to C57BL/6J females in order to obtain F1 mice. PCR screening was used in order to detect the duplication and/or the deletion in tail DNA samples. To screen for the duplication, PCR primers were used to detect the puromycin resistance gene. 5'-ATGACCGAGTACAAGCCCAC-3' and 5'-GCGTGAGGAAGAGTTCTTGC-3' primers led to the

generation of a 166-bp PCR product. A second set of primers: 5'-CTAGGCCACAGAATTGAAAGATCT-3' and 5' GTAGGTGGAAATTCTAGCATCATCC-3' was included in these assays in order to detect a 324-bp *IL-2* internal control band The PCR cycling conditions we used were: 94℃ for 3 min; 35 cycles of 94℃ for 30 s, 65℃ for 30 s, and 72℃ for 90 s; then 72℃ for 10 min. To screen for the deletion, primers were selected such that an 829-bp band would be detected when the 5' and 3' insertions were directly abutted, due to the recombination of *loxP* sites, as previously described (Zheng et al., 1999). Only mice containing the duplication were obtained using this approach. Germline transmission of the deficiency was not observed. We therefore used an alternative approach to obtain these mice. ES cell clones where the 5' and 3' insertions were found to be in a cis configuration were injected into C57BL/6J blastocysts. Resulting chimeric males were bred to C57BL/6J females in order to obtain F1 mice. PCR was used to detect the puromycin resistance gene in the offspring. Puromycin positive mice were further screened by Southern blot. Probes external to the 5' *Dgcr14* insertion, as well as external to the 3' *Hira* insertion, were used to verify the 5' and 3' insertions. Mouse genomic DNA was prepared from tail clips, and digested with *EcoR*I (to check for the *Dgcr14* insertion) or *Spe*I (to check for the 3' *Hira* insert). Southern blot analysis detected a 14.0 kb band, demonstrating the proper positioning of the 5' insertion, as well as a 16.2 kb WT band. For the 3' insert, probing of *Spe*I cut DNA revealed a 14.5 kb band indicating proper positioning of the 3' construct, in addition to an expected 17.7 kb Wt band. These mice were then bred with mice expressing Cre recombinase in their germline using the *HPRT-Cre* line (stock # 004302, The Jackson Laboratory, Bar Harbor, ME). Offspring that were positive by PCR for both the puromycin resistance gene (see PCR conditions above) and *Cre recombinase* (using primers 5'-GCGGTCTGGCAGTAAAAACTATC-3' and 5'-GTGAAACAGCATTGCTGTCACTT-3', and cycling conditions 94℃ for 3 min; 35 cycles of 94℃ for 30 s, 51℃ for 1 min, and 72℃ for 1 min; then 72℃ for 10 min) were bred with C57BL/6J Wt mice. The resulting offspring from these crosses were screened for the presence of the deletion by using the primers and PCR conditions described (Stark et al., 2008). Once the duplication and deletion mouse lines were established, maintenance of the lines was performed by PCR-based genotyping. Both lines have been backcrossed to C57BL/6J background for at least 10 generations.

Dgcr8$^{+/-}$: We generated *Dgcr8*-deficient mice using an ES cell line (XH157 ES, BayGenomics) carrying a β-geo gene trap inserted into intron 8 of the *Dgcr8* gene. A transcriptional fusion, expected to

be generated as a result of splicing between the splice donor site at *Dgcr8* exon 8 and the splice acceptor site located at the gene trap, was detected in Northern blots in brain samples of HET mice. As expected, by using qRT-PCR we showed that the full-length *Dgcr8* mRNA levels are reduced by approximately half in *Dgcr8*-deficient mice (P = 0.0001). At the protein level, we can also readily detect by Western blots, using total brain protein extracts, a chimeric protein produced as a result of the translational fusion between the N-terminal part of Dgcr8 and the β-geo moiety (expected size ~220-kD) and the reduced WT 120-kD product. As a result of the translational fusion, two functional double-stranded RNA binding domains (DRBs) of Dgcr8 are either truncated or lost, resulting in a chimeric protein predicted to have severely impaired activity. Consistent with this prediction, homozygous mice die before birth. For more details, please see previous work by Stark et al. (Stark et al., 2008).

2.5.2 Fluorescent in situ Hybridization (FISH)

Further confirmation of the deletion and reciprocal duplication was obtained using FISH. A mouse chromosome 16 BAC clone located within both the duplicated and deleted regions (BAC RP23-420H6), as well a BAC clone from outside of these regions (BAC RP23-290E4), were differentially labeled with SpectrumRed and SpectrumGreen, respectively, and used as fluorescent probes. All BAC clones were purchased from Invitrogen. Metaphase and interphase chromosome spreads were prepared from E13.5 mouse embryonic fibroblast (MEF) cultures, from embryos carrying either the duplication or the deletion, as determined by PCR screening. A minimum of 10 metaphases was examined for each sample. For the duplication, MEFs were observed from 4 individual embryos, from the N7 backcross generation (to C57BL/6J). For the deletion, MEFs from 2 individual embryos of an N6 backcross generation (to C57BL/6J) were observed.

2.5.3 In situ Hybridization

Digoxigenin tail labeled anti-mir-185 locked nucleic acid (LNA) and scramble LNA oligo-nucleotides were obtained from Exiqon. *In situ* hybridization was conducted as described previously (Nuovo et al., 2009).

2.5.4 Quantitative RT-PCR

Total RNA samples were extracted from 8-wk old male mice or cultured cell using miRNeasy mini kit (QIAGEN) according to manufacturer's protocol. We treated 3 µg of total RNA from each sample with DNA-free kit (Ambion/Applied Biosystems). For qRT-PCR of mature miRNA, 100 ng of treatment RNA each sample was reverse transcribed and qPCR was performed using TaqMan MicroRNA PCR kit and individual Mouse TaqMan MicroRNA Assays according to the company's protocol (Applied Biosystems). A *glyceraldehyde-3-phosphate dehydrogenase (GAPDH)* gene-specific RT primer was also included RT reaction and expression of endogenous control *GAPDH* was measured in a duplex reaction that included the miRNA primer and probe set and *GAPD*H primer and probe set was used in qPCR reactions. For qRT-PCR of other genes, the remaining DNase-treated RNA each sample was reverse transcribed using random primers and SuperScript II Reverse Transcriptase (Invirtogen). For each gene, a duplex qPCR was performed using TaqMan Universal PCR Master Mix, no AmpErase UNG (Applied Biosystems) and custom designed primer and probe set, as well as primer and probe set for *GAPDH*.

TaqMan expression assays are purchased from Applied Biosystems. MicroRNA assay name and ID: hsa-miR-185: 002271; mmu-miR-491: 001630; hsa-miR-485-5p: 001036. These assays are able to detect mature miRNAs in both human or mouse samples. Gene assays name and ID: C19orf63: Hs00382250_m1; Nptx2: Mm00479438_m1; Vipr2: Mm01238618_g1; Slc6a1: Mm01183568_m1; Grin2b: Mm00433820_m1. For other genes, PCR primers and probes were designed at Primer3 web site (http://frodo.wi.mit.edu/) and purchased from Sigma Genosys (Sigma-Aldrich) and the sequences can be found in Appendix 1). All target gene probes were 5' FAM and 3' BHQ™-1 Dual labeled. Mouse or human *GAPDH* was measured as endogenous control. *GAPDH* Control Reagents was purchased from Applied Biosystems (mouse: #4352339E, #4308313; human: #402869).

The reactions were incubated in a 96-well plate at 95℃ for 10 min, followed by 45 cycles of 95℃ for 10 sec and 58℃ for 1 min on a 7900 Sequence Detection System (Applied Biosystems). All reactions were repeated 5 times. Relative qualification was based on a standard curve method. The highest concentrated cDNA template was drew from a cDNA pool mixing portion of cDNA from each sample in equal amount and other standards were made from a series of 1:4 dilution of the highest concentrated templates. cDNA samples were then diluted 1:3 relative to the highest concentrated standard before qPCR was performed. Quantity of amplified Gene (or miRNA) and *GAPDH* product from the highest

concentrated template was arbitrarily set to 256 and the quantity of amplified signals from other standards were set according to the dilution. A standard curve is then made and the relative quantity of each sample was determined.

2.5.5 Expression Profiling

For development-dependent expression profiles of *Df(16)A*$^{+/-}$ mice: A total of 48 PFC and 48 HPC from 12 *Df(16)A*$^{+/-}$ mutants and 12 Wt littermate control mice at E17 and P6 were dissected and processed using standard protocols recommended by Affymetrix. RNA quality was assessed with Bioanalyzer (Agilent Technologies) and all RNAs had a RIN > 7.0. For hybridization, cRNA was exposed to the Affymetrix Mouse genome 430 2.0 array, which includes 45,000 probe sets from > 34,000 well characterized mouse genes, and then scanned (Agilent). Sequence clusters were created and refined from the UniGene and the Whitehead Institute Center for Genome Research databases. Initial intensity files (CEL files) were obtained from microarray images using GeneChip (Affymetrix) Analysis Software Microarray Suite version 5 (Affymetrix). Data analysis of *Df(16)A*$^{+/-}$ and Wt littermate expression profiling at E17 and P6 was performed using limma package in the bioconductor project (www.bioconductor.org) as previously described (Stark et al., 2008).

For expression profiles of *Df(16)B*$^{+/-}$ and *Dp(16)B*$^{+/-}$ mice: Expression profiling was conducted on 8 mice carrying a deletion (*Df(16)B*$^{+/-}$), 8 carrying a duplication (*Dp(16)B*$^{+/-}$) and 8 reference compound heterozygous mice balanced for copy number (*Df(16)B*/*Dp(16)B*). The experimental procedure is as described above. Data analysis of the *Df(16)B*$^{+/-}$, *Dp(16)B*$^{+/-}$, *Df(16)B*/*Dp(16)B* expression profiling was also performed as previously described (Stark et al., 2008), with the exception that an ANOVA F-test was used because three groups were compared with the limma package.

2.5.6 Neuronal Culture and Transfection

Dissociated hippocampal neurons were isolated from E17 mouse embryos and plated at 2 x 10^5 cells/ml in 6-well plates containing glass coverslips coated with poly-D-lysine. Neurons were cultured for 9 – 19 days, depending on the experiments. Pre-miR-185 mimic and pre-scramble control (Ambion) were used for high efficiency calcium-phosphate mediated transfections as described previously (Jiang and Chen, 2006). For all experiments, 100 pmol of pre-miRNA mimics were used per well.

2.5.7 Luciferase Assay

Mirta22 3′UTR was cloned into psiCHECK2. Binding site mutant clones were generated by PCR-based mutagenesis (see Supplementary Methods for details). N18 neuroblastoma cells were transfected with various psiCHECK2 reporter constructs together with *pre-miR-185* mimic or pre-scramble control unless mentioned otherwise and luciferase assays were performed using the Promega Dual-Luciferase Reporter Assay System. All experiments were performed at least 2 times and all data presented is the average of 3 technical repeats. *Mirta22* 3′UTR was cloned into *Xho*I and *Not*I sites of psiCHECK2 (Promega). Binding site mutant clones were generated by PCR-based mutagenesis. Site Mut1 sequence (starting from position 289 in 3′UTR): GGAgtTTGCCAAGCTCggTaaA (lower case letters denote altered nucleotide). Site Mut2 sequence (starting from position 350): AtTGTCACgCTaaA. Mutations are predicted by RNAhybrid (Rehmsmeier et al., 2004) to disrupt the binding of *miR-185* at the seeds and secondary binding sites. N18 neuroblastoma cells were transfected with various psiCHECK2 reporter constructs (100 ng per well of a 24-well plate) together with pre-miR-185 mimic or pre-scramble control (1 nM = 0.5 pmol), unless mentioned otherwise, and luciferase assays were performed 24 hrs post-transfection using the Dual-Luciferase Reporter Assay System (Promega) according to the manufacturer's instructions. All experiments were performed at least 2 times and all data presented is the average of 3 technical repeats.

2.6 References

Abbott, A.L., Alvarez-Saavedra, E., Miska, E.A., Lau, N.C., Bartel, D.P., Horvitz, H.R., and Ambros, V. (2005). The let-7 MicroRNA family members mir-48, mir-84, and mir-241 function together to regulate developmental timing in Caenorhabditis elegans. Developmental cell *9*, 403-414.

Arguello, P.A., and Gogos, J.A. (2006). Modeling madness in mice: one piece at a time. Neuron *52*, 179-196.

Arguello, P.A., and Gogos, J.A. (2010). Cognition in mouse models of schizophrenia susceptibility genes. Schizophrenia bulletin *36*, 289-300.

Baek, D., Villen, J., Shin, C., Camargo, F.D., Gygi, S.P., and Bartel, D.P. (2008). The impact of microRNAs on protein output. Nature *455*, 64-71.

Bassett, A.S., Chow, E.W., AbdelMalik, P., Gheorghiu, M., Husted, J., and Weksberg, R. (2003). The schizophrenia phenotype in 22q11 deletion syndrome. The American journal of psychiatry *160*, 1580-1586.

Bassett, A.S., Hodgkinson, K., Chow, E.W., Correia, S., Scutt, L.E., and Weksberg, R. (1998). 22q11 deletion syndrome in adults with schizophrenia. Am J Med Genet *81*, 328-337.

Bearden, C.E., Woodin, M.F., Wang, P.P., Moss, E., McDonald-McGinn, D., Zackai, E., Emannuel, B., and Cannon, T.D. (2001). The neurocognitive phenotype of the 22q11.2 deletion syndrome: selective deficit in visual-spatial memory. J Clin Exp Neuropsychol *23*, 447-464.

Beveridge, N.J., Gardiner, E., Carroll, A.P., Tooney, P.A., and Cairns, M.J. (2010). Schizophrenia is associated with an increase in cortical microRNA biogenesis. Molecular psychiatry *15*, 1176-1189.

Campbell, L.E., Daly, E., Toal, F., Stevens, A., Azuma, R., Catani, M., Ng, V., van Amelsvoort, T., Chitnis, X., Cutter, W.*, et al.* (2006). Brain and behaviour in children with 22q11.2 deletion syndrome: a volumetric and voxel-based morphometry MRI study. Brain : a journal of neurology *129*, 1218-1228.

Casey, B.J., Cohen, J.D., Jezzard, P., Turner, R., Noll, D.C., Trainor, R.J., Giedd, J., Kaysen, D., Hertz-Pannier, L., and Rapoport, J.L. (1995). Activation of prefrontal cortex in children during a nonspatial working memory task with functional MRI. NeuroImage *2*, 221-229.

Chahrour, M., Jung, S.Y., Shaw, C., Zhou, X., Wong, S.T., Qin, J., and Zoghbi, H.Y. (2008). MeCP2, a key contributor to neurological disease, activates and represses transcription. Science (New York, NY *320*, 1224-1229.

Chalfie, M., Horvitz, H.R., and Sulston, J.E. (1981). Mutations that lead to reiterations in the cell lineages of C. elegans. Cell *24*, 59-69.

Chi, S.W., Zang, J.B., Mele, A., and Darnell, R.B. (2009). Argonaute HITS-CLIP decodes microRNA-mRNA interaction maps. Nature *460*, 479-486.

Colantuoni, C., Lipska, B.K., Ye, T., Hyde, T.M., Tao, R., Leek, J.T., Colantuoni, E.A., Elkahloun, A.G., Herman, M.M., Weinberger, D.R.*, et al.* (2011). Temporal dynamics and genetic control of transcription in the human prefrontal cortex. Nature *478*, 519-523.

Drew, L.J., Crabtree, G.W., Markx, S., Stark, K.L., Chaverneff, F., Xu, B., Mukai, J., Fenelon, K., Hsu, P.K., Gogos, J.A.*, et al.* (2011). The 22q11.2 microdeletion: fifteen years of insights into the genetic and neural complexity of psychiatric disorders. International journal of developmental neuroscience : the official journal of the International Society for Developmental Neuroscience *29*, 259-281.

Duan, S., Mi, S., Zhang, W., and Dolan, M.E. (2009). Comprehensive analysis of the impact of SNPs and CNVs on human microRNAs and their regulatory genes. RNA biology *6*, 412-425.

Eliez, S., Schmitt, J.E., White, C.D., and Reiss, A.L. (2000a). Children and adolescents with velocardiofacial syndrome: a volumetric MRI study. American Journal of Psychiatry *157*, 409-415.

Eliez, S., Schmitt, J.E., White, C.D., and Reiss, A.L. (2000b). Children and adolescents with velocardiofacial syndrome: a volumetric MRI study. Am J Psychiatry *157*, 409-415.

Fineberg, S.K., Kosik, K.S., and Davidson, B.L. (2009). MicroRNAs potentiate neural development. Neuron *64*, 303-309.

Flynt, A.S., and Lai, E.C. (2008). Biological principles of microRNA-mediated regulation: shared themes amid diversity. Nat Rev Genet *9*, 831-842.

Ford, J.M., Mathalon, D.H., Whitfield, S., Faustman, W.O., and Roth, W.T. (2002). Reduced communication between frontal and temporal lobes during talking in schizophrenia. Biol Psychiatry *51*, 485-492.

Freeman, J.L., Perry, G.H., Feuk, L., Redon, R., McCarroll, S.A., Altshuler, D.M., Aburatani, H., Jones, K.W., Tyler-Smith, C., Hurles, M.E.*, et al.* (2006). Copy number variation: new insights in genome diversity. Genome research *16*, 949-961.

Gardiner, E., Beveridge, N.J., Wu, J.Q., Carr, V., Scott, R.J., Tooney, P.A., and Cairns, M.J. (2011). Imprinted DLK1-DIO3 region of 14q32 defines a schizophrenia-associated miRNA signature in peripheral blood mononuclear cells. Molecular psychiatry.

Grimson, A., Farh, K.K., Johnston, W.K., Garrett-Engele, P., Lim, L.P., and Bartel, D.P. (2007). MicroRNA targeting specificity in mammals: determinants beyond seed pairing. Molecular cell *27*, 91-105.

Guo, H., Ingolia, N.T., Weissman, J.S., and Bartel, D.P. (2010). Mammalian microRNAs predominantly act to decrease target mRNA levels. Nature *466*, 835-840.

Ingason, A., Rujescu, D., Cichon, S., Sigurdsson, E., Sigmundsson, T., Pietilainen, O.P., Buizer-Voskamp, J.E., Strengman, E., Francks, C., Muglia, P.*, et al.* (2009). Copy number variations of chromosome 16p13.1 region associated with schizophrenia. Molecular psychiatry.

ISC (2008). Rare chromosomal deletions and duplications increase risk of schizophrenia. Nature *455*, 237-241.

Jiang, M., and Chen, G. (2006). High Ca2+-phosphate transfection efficiency in low-density neuronal cultures. Nat Protoc *1*, 695-700.

Johnnidis, J.B., Harris, M.H., Wheeler, R.T., Stehling-Sun, S., Lam, M.H., Kirak, O., Brummelkamp, T.R., Fleming, M.D., and Camargo, F.D. (2008). Regulation of progenitor cell proliferation and granulocyte function by microRNA-223. Nature *451*, 1125-1129.

Karayiorgou, M., Morris, M.A., Morrow, B., Shprintzen, R.J., Goldberg, R., Borrow, J., Gos, A., Nestadt, G., Wolyniec, P.S., Lasseter, V.K.*, et al.* (1995). Schizophrenia susceptibility associated with interstitial deletions of chromosome 22q11. Proceedings of the National Academy of Sciences of the United States of America *92*, 7612-7616.

Karayiorgou, M., Simon, T.J., and Gogos, J.A. (2010). 22q11.2 microdeletions: linking DNA structural variation to brain dysfunction and schizophrenia. Nat Rev Neurosci *11*, 402-416.

Kim, A.H., Reimers, M., Maher, B., Williamson, V., McMichael, O., McClay, J.L., van den Oord, E.J., Riley, B.P., Kendler, K.S., and Vladimirov, V.I. (2010). MicroRNA expression profiling in the prefrontal cortex of individuals affected with schizophrenia and bipolar disorders. Schizophrenia research *124*, 183-191.

Kirov, G., Grozeva, D., Norton, N., Ivanov, D., Mantripragada, K.K., Holmans, P., Craddock, N., Owen, M.J., and O'Donovan, M.C. (2009). Support for the involvement of large copy number variants in the pathogenesis of schizophrenia. Hum Mol Genet *18*, 1497-1503.

Kirov, G., Gumus, D., Chen, W., Norton, N., Georgieva, L., Sari, M., O'Donovan, M.C., Erdogan, F., Owen, M.J., Ropers, H.H.*, et al.* (2008). Comparative genome hybridization suggests a role for NRXN1 and APBA2 in schizophrenia. Hum Mol Genet *17*, 458-465.

Kosik, K.S. (2006). The neuronal microRNA system. Nat Rev Neurosci *7*, 911-920.

Lajiness-O'Neill, R.R., Beaulieu, I., Titus, J.B., Asamoah, A., Bigler, E.D., Bawle, E.V., and Pollack, R. (2005). Memory and learning in children with 22q11.2 deletion syndrome: evidence for ventral and dorsal stream disruption? Child Neuropsychol *11*, 55-71.

Lawrie, S.M., Buechel, C., Whalley, H.C., Frith, C.D., Friston, K.J., and Johnstone, E.C. (2002). Reduced frontotemporal functional connectivity in schizophrenia associated with auditory hallucinations. Biol Psychiatry *51*, 1008-1011.

Lee, R.C., Feinbaum, R.L., and Ambros, V. (1993). The C. elegans heterochronic gene lin-4 encodes small RNAs with antisense complementarity to lin-14. Cell *75*, 843-854.

Levy, D., Ronemus, M., Yamrom, B., Lee, Y.H., Leotta, A., Kendall, J., Marks, S., Lakshmi, B., Pai, D., Ye, K.*, et al.* (2011). Rare de novo and transmitted copy-number variation in autistic spectrum disorders. Neuron *70*, 886-897.

Lim, L.P., Lau, N.C., Garrett-Engele, P., Grimson, A., Schelter, J.M., Castle, J., Bartel, D.P., Linsley, P.S., and Johnson, J.M. (2005). Microarray analysis shows that some microRNAs downregulate large numbers of target mRNAs. Nature *433*, 769-773.

Lugli, G., Torvik, V.I., Larson, J., and Smalheiser, N.R. (2008). Expression of microRNAs and their precursors in synaptic fractions of adult mouse forebrain. J Neurochem *106*, 650-661.

MacArthur, D.G., Balasubramanian, S., Frankish, A., Huang, N., Morris, J., Walter, K., Jostins, L., Habegger, L., Pickrell, J.K., Montgomery, S.B.*, et al.* (2012). A systematic survey of loss-of-function variants in human protein-coding genes. Science (New York, NY *335*, 823-828.

Meyer-Lindenberg, A.S., Olsen, R.K., Kohn, P.D., Brown, T., Egan, M.F., Weinberger, D.R., and Berman, K.F. (2005). Regionally specific disturbance of dorsolateral prefrontal-hippocampal functional connectivity in schizophrenia. Arch Gen Psychiatry *62*, 379-386.

Miller, D.T., Shen, Y., Weiss, L.A., Korn, J., Anselm, I., Bridgemohan, C., Cox, G.F., Dickinson, H., Gentile, J., Harris, D.J.*, et al.* (2009). Microdeletion/duplication at 15q13.2q13.3 among individuals with features of autism and other neuropsychiatric disorders. Journal of medical genetics *46*, 242-248.

Moreau, M.P., Bruse, S.E., David-Rus, R., Buyske, S., and Brzustowicz, L.M. (2011). Altered microRNA expression profiles in postmortem brain samples from individuals with schizophrenia and bipolar disorder. Biol Psychiatry *69*, 188-193.

Moss, E.G., Lee, R.C., and Ambros, V. (1997). The cold shock domain protein LIN-28 controls developmental timing in C. elegans and is regulated by the lin-4 RNA. Cell *88*, 637-646.

Mukai, J., Dhilla, A., Drew, L.J., Stark, K.L., Cao, L., MacDermott, A.B., Karayiorgou, M., and Gogos, J.A. (2008). Palmitoylation-dependent neurodevelopmental deficits in a mouse model of 22q11 microdeletion. Nature neuroscience *11*, 1302-1310.

Napoli, I., Mercaldo, V., Boyl, P.P., Eleuteri, B., Zalfa, F., De Rubeis, S., Di Marino, D., Mohr, E., Massimi, M., Falconi, M.*, et al.* (2008). The fragile X syndrome protein represses activity-dependent translation through CYFIP1, a new 4E-BP. Cell *134*, 1042-1054.

Nuovo, G.J., Elton, T.S., Nana-Sinkam, P., Volinia, S., Croce, C.M., and Schmittgen, T.D. (2009). A methodology for the combined in situ analyses of the precursor and mature forms of microRNAs and correlation with their putative targets. Nature protocols *4*, 107-115.

Ornitz, E.M., Guthrie, D., Kaplan, A.R., Lane, S.J., and Norman, R.J. (1986). Maturation of startle modulation. Psychophysiology *23*, 624-634.

Perkins, D.O., Jeffries, C.D., Jarskog, L.F., Thomson, J.M., Woods, K., Newman, M.A., Parker, J.S., Jin, J., and Hammond, S.M. (2007). microRNA expression in the prefrontal cortex of individuals with schizophrenia and schizoaffective disorder. Genome biology *8*, R27.

Pinto, D., Marshall, C., Feuk, L., and Scherer, S.W. (2007). Copy-number variation in control population cohorts. Hum Mol Genet *16 Spec No. 2*, R168-173.

Rehmsmeier, M., Steffen, P., Hochsmann, M., and Giegerich, R. (2004). Fast and effective prediction of microRNA/target duplexes. RNA *10*, 1507-1517.

Reinhart, B.J., Slack, F.J., Basson, M., Pasquinelli, A.E., Bettinger, J.C., Rougvie, A.E., Horvitz, H.R., and Ruvkun, G. (2000). The 21-nucleotide let-7 RNA regulates developmental timing in Caenorhabditis elegans. Nature *403*, 901-906.

Sanders, S.J., Ercan-Sencicek, A.G., Hus, V., Luo, R., Murtha, M.T., Moreno-De-Luca, D., Chu, S.H., Moreau, M.P., Gupta, A.R., Thomson, S.A*., et al.* (2011). Multiple recurrent de novo CNVs, including duplications of the 7q11.23 Williams syndrome region, are strongly associated with autism. Neuron *70*, 863-885.

Santarelli, D.M., Beveridge, N.J., Tooney, P.A., and Cairns, M.J. (2011). Upregulation of dicer and microRNA expression in the dorsolateral prefrontal cortex Brodmann area 46 in schizophrenia. Biol Psychiatry *69*, 180-187.

Schaer, M., Debbane, M., Bach Cuadra, M., Ottet, M.C., Glaser, B., Thiran, J.P., and Eliez, S. (2009). Deviant trajectories of cortical maturation in 22q11.2 deletion syndrome (22q11DS): a cross-sectional and longitudinal study. Schizophrenia research *115*, 182-190.

Schaer, M., Schmitt, J.E., Glaser, B., Lazeyras, F., Delavelle, J., and Eliez, S. (2006). Abnormal patterns of cortical gyrification in velo-cardio-facial syndrome (deletion 22q11.2): an MRI study. Psychiatry research *146*, 1-11.

Schratt, G. (2009). microRNAs at the synapse. Nat Rev Neurosci *10*, 842-849.

Selbach, M., Schwanhausser, B., Thierfelder, N., Fang, Z., Khanin, R., and Rajewsky, N. (2008). Widespread changes in protein synthesis induced by microRNAs. Nature *455*, 58-63.

Shields, I.I.G.A.J. (1982). Schizophrenia: The Epigenetic Puzzle (Cambridge, UK: Cambridge University Press).

Shprintzen, R.J., Goldberg, R.B., Lewin, M.L., Sidoti, E.J., Berkman, M.D., Argamaso, R.V., and Young, D. (1978). A new syndrome involving cleft palate, cardiac anomalies, typical facies, and learning disabilities: velo-cardio-facial syndrome. The Cleft palate journal *15*, 56-62.

Sigurdsson, T., Stark, K.L., Karayiorgou, M., Gogos, J.A., and Gordon, J.A. (2010). Impaired hippocampal-prefrontal synchrony in a genetic mouse model of schizophrenia. Nature *464*, 763-767.

Simon, T.J., Ding, L., Bish, J.P., McDonald-McGinn, D.M., Zackai, E.H., and Gee, J. (2005). Volumetric, connective, and morphologic changes in the brains of children with chromosome 22q11.2 deletion syndrome: an integrative study. NeuroImage *25*, 169-180.

Sobin, C., Kiley-Brabeck, K., and Karayiorgou, M. (2005). Lower prepulse inhibition in children with the 22q11 deletion syndrome. The American journal of psychiatry *162*, 1090-1099.

Stark, K.L., Xu, B., Bagchi, A., Lai, W.S., Liu, H., Hsu, R., Wan, X., Pavlidis, P., Mills, A.A., Karayiorgou, M.*, et al.* (2008). Altered brain microRNA biogenesis contributes to phenotypic deficits in a 22q11-deletion mouse model. Nat Genet *40*, 751-760.

Stefansson, H., Rujescu, D., Cichon, S., Pietilainen, O.P., Ingason, A., Steinberg, S., Fossdal, R., Sigurdsson, E., Sigmundsson, T., Buizer-Voskamp, J.E.*, et al.* (2008). Large recurrent microdeletions associated with schizophrenia. Nature *455*, 232-236.

Tomari, Y., and Zamore, P.D. (2005). MicroRNA biogenesis: drosha can't cut it without a partner. Curr Biol *15*, R61-64.

Wang, X. (2008). miRDB: a microRNA target prediction and functional annotation database with a wiki interface. RNA *14*, 1012-1017.

Wightman, B., Ha, I., and Ruvkun, G. (1993). Posttranscriptional regulation of the heterochronic gene lin-14 by lin-4 mediates temporal pattern formation in C. elegans. Cell *75*, 855-862.

Xu, B., Karayiorgou, M., and Gogos, J.A. (2010). MicroRNAs in psychiatric and neurodevelopmental disorders. Brain research *1338*, 78-88.

Xu, B., Roos, J.L., Levy, S., van Rensburg, E.J., Gogos, J.A., and Karayiorgou, M. (2008). Strong association of de novo copy number mutations with sporadic schizophrenia. Nat Genet *40*, 880-885.

Zheng, B., Mills, A.A., and Bradley, A. (1999). A system for rapid generation of coat color-tagged knockouts and defined chromosomal rearrangements in mice. Nucleic acids research *27*, 2354-2360.

Chapter III

Dysregulation of A Novel Inhibitor of Dendritic and Spine Morphogenesis In *Df(16)A*$^{+/-}$ Mice

3.1 Introduction

Since the discovery of dendritic spines by Ramon y Cajal in 1888 (Garcia-Lopez et al., 2007), it gradually became clear that dendritic spines are the synaptic sites between neurons. It has also become evident that spine morphology is intimately linked to synaptic strength and it is the dynamics of these synaptic contacts that ultimately underlie learning and cognitive function (Kasai et al., 2010; Segal, 2002). In addition, activation of individual spines at different dendritic segments is integrated spatially and temporally before the information reaches the soma to generate a specific output pattern (Henny et al., 2012; Kim et al., 2012). Therefore the structure of dendritic arbors is critical in controlling the source of synaptic inputs a neuron receives and in determining the computational ability of a given neuron (Magee, 2000; Piskorowski and Chevaleyre, 2012). It is not surprising that dysfunction in neuronal communication due to aberrant pattern of dendritic arborization or spine morphology is an important underlying cause of neuropsychiatric disorders (Kasai et al., 2010; van Spronsen and Hoogenraad, 2010).

Analysis of *Df(16)A*$^{+/-}$ mice provided evidence for abnormalities in dendritic morphogenesis and formation of dendritic spines of hippocampal pyramidal neurons both in culture and *in vivo* (Mukai et al., 2008; Stark et al., 2008). Such changes may account, at least in part, for the regional decreases in grey matter volumes observed in human 22q11.2 deletion carriers (Chow et al., 2002). Even modest alterations in dendritic and spine formation may result in a suboptimal number of synapses, formation of inappropriate connections or changes in the integration of synaptic inputs, and may ultimately lead to altered information processing (Henny et al., 2012; Mainen and Sejnowski, 1996; Yuste and Tank, 1996). However, how miRNA dysregulation contribute to the structural anomaly in *Df(16)A*$^{+/-}$ mice was not previously determined.

3.1.1 miRNA Regulation of Dendritic Arborization

As described briefly in Chapter 1.3, miRNAs regulate various aspects of neuronal function and morphology, including the growth and maintenance of dendritic structures. *De novo* dendritic growth and arborization of cultured neurons and newborn neurons in the brain is regulated by miRNAs including miR-132 and miR-134 (Table 3.1).

miR-132 was the first miRNA found to promote neurite sprouting in cultured cortical neurons by decreasing levels of p250GAP, a CNS-enriched Rac/Rho GTPase-activating protein (Vo et al., 2005). In morphogeneis of newborn neurons in dentate gyrus (DG), miR-132 begins to be expressed as the neurons mature and maintains high levels of expression in fully mature neurons (Luikart et al., 2011). Correlating with the time course of miR-132 expression, deletion of the *mir-212–mir-132* locus in adult DG was shown to cause a dramatic decrease in dendritic arborization in newborn neurons (Magill et al., 2010). As miR-132 is the predominant miRNA expressed from this locus in hippocampal neurons, this effect was thought to be mainly due to the loss of mir-132 expression. Furthermore, miR-134, which is from a large miRNA cluster at the *Dlk1-Gtl2* region in mouse (*Dlk1-Dio3* in human), is expressed during neuron differentiation (Tay et al., 2008). Postembryonic virus-mediated miR-134 overexpression results in reduction in length and complexity of layer V cortical pyramidal neurons (Christensen et al., 2010). In cultured cortical neurons, miR-134 overexpression also causes decreased arborization (Fiore et al., 2009; Gaughwin et al., 2011). However, miR-134 sensitizes neurons to BMP-induced dendritogenesis, resulting in more complex dendrite trees (Gaughwin et al., 2011). It seems the effects of miR-134 on neuronal morphogenesis are complex and mir-134 levels need to be critically controlled in neurons (Fiore et al., 2009). Other miRNAs that are implicated in regulating dendrite outgrowth include miR-375, which reduces dendrite density in adult mouse hippocampus (Abdelmohsen et al., 2010), and miR-124, which promotes neurite outgrowth in primary cortical neurons (Yu et al., 2008).

Activity induces the growth of dendrites through transcription factors like CREB and Mef2 (Fiore et al., 2009; Vo et al., 2005). The activation of these transcription factors in turn induces the transcription of miRNAs important for dendritic morphogenesis. This process is exemplified by the induction of miR-132 by BDNF (Vo et al., 2005) or by bicuculline or KCl which increase spontaneous synaptic activity (Wayman et al., 2008). Binding of CREB to CRE motifs in the *mir-212–mir-132* locus results in rapid (in a transcriptional sense) and long lasting (at least 24 hours) miR-132 expression within 2 hours after

sustained activity (Vo et al., 2005). As during neuronal maturation, elevated miR-132 levels promote dendrite growth through inhibition of p250GAP (Wayman et al., 2008). The induction of mir-132 by activity is also observed in organotypic hippocampal slices. Increased activity due to BDNF or KCl also induces MEF2-mediated transcription of the *mir-379–mir-410* cluster that includes more than 50 miRNA genes. These miRNAs expressed from the *mir-379–mir-410* cluster are co-expressed and many of them are brain-enriched (Tierling et al., 2006). At least 3 miRNAs from this cluster, miR-134, miR-381 and miR-329, are required for activity-dependent dendritic growth. This effect of miR-134 is at least partly through inhibition of translational repressor Pumilio2 (Pum2). However, miR-134 overexpression or Pum2 knockdown also disrupts activity-induced dendritic growth. As mentioned earlier, it seems that miR-134 is required for fine-tuning expression of proteins like Pum2 whose levels need to be maintained in a specific range. This fine-tuning relationship is especially desirable for controlling dynamic processes in response to rapid changes in neuron activity.

3.1.2 miRNA Regulation of Spine Morphogenesis

It was known for many years that activity regulates local protein translation in dendrites and especially near or at the site of synapses (Liu-Yesucevitz et al., 2011; Swanger and Bassell, 2011). Accumulating evidences suggests that synaptic miRNAs are integral parts of the local translation machinery and regulate the protein production locally in a rapid fashion. Several miRNAs are enriched in synaptic fractions (Lugli et al., 2008; Siegel et al., 2009) and some of these miRNAs were already shown to regulate spinogenesis in response to neuronal activity (Table 3.2) (Impey et al., 2010; Schratt et al., 2006).

It was also reported that both protein degradation and synthesis are required for synaptic plasticity (Ashraf et al., 2006; Fonseca et al., 2006). Activity-induced NMDA receptor signaling triggers proteasome-mediated MOV10 degradation at about half of the synaptic sites (Banerjee et al., 2009). MOV10, mammalian homologue of *Drosophila* helicase Armitage, is a component of the RISC complex. Interestingly, MOV10 degradation is correlated with translation of several proteins that normally associate with the RISC complex. Thus, activity-induced degradation of MOV10 (and possibly other components of the RISC complex) possibly relieves miRNA-repressed local protein translation that is required for

synaptic plasticity. Protein candidates that are controlled in this fashion include Limk1 (a miR-134 target), Lypla1/APT1 (a miR-138 target) and CaMKIIa (a miR-219 target) (see below).

As described in Chapter 1.3, the first miRNA shown to regulate spine development is miR-134 (Schratt et al., 2006). Although miR-134 is transcriptionally upregulated by activity, it is immediately inhibited upon BDNF treatment and results in derepression of Limk1 which regulates actin filament dynamic. The loss of miR-134 repression leads to increased spine volume. Similarly, miR-138, another synaptically enriched miRNA, targets depalmitoylation enzyme Lypla1/APT1 and negatively regulates spine size (Siegel et al., 2009). By reducing Lypla1 expression, miR-138 results in membrane-localization of $G\alpha_{13}$ which in turn elevates Rho activity and spine shrinkage. Calcium influx reduces pre-miR-138 levels rapidly and progressively, suggesting miR-138 regulation of spine size is also activity-controlled. Furthermore, it is noteworthy that FMRP-associated miRNAs miR-125b and miR-132 have largely opposite effects on spine morphology (Edbauer et al., 2010). miR-125b promotes the formation of immature spines (long and thin) while mir-132 promotes an increase in spine width. In addition, the effect of miR-125b and miR-132 on spine morphology is FMRP-dependent, suggesting the possible loss of miRNA-mediated spine morphogenesis in Fragile X syndrome.

As spine formation and elimination are consistent and dynamic processes under the control of neural activity, the number of spines may reflects the strength of neural circuits. Not surprisingly, miRNAs play important roles in controlling the number of spines of neurons under normal condition and when excited. Besides regulating spine size, activity-induced miR-132 controls spine formation. The time course of miR-132 upregulation during postnatal development in rodent hippocampus correlates with the time course of active spine formation (Impey et al., 2010). *In vitro* and *in vivo* manipulations of miR-132 levels show that miR-132 promotes mushroom spine formation (Hansen et al., 2010; Impey et al., 2010; Luikart et al., 2011; Mellios et al., 2011). In cultured hippocampal neurons, this effect is due to the inhibition of p250GAP, which also mediates the effect of miR-132 on dendritic growth, and the subsequent activation of Rac1–PAK pathway by Rac GEF, Kakirin-7 (Impey et al., 2010). In contrast to miR-132, miRNAs like miR-34a and miR-485 negatively affect spine number (Agostini et al., 2011; Cohen et al., 2011).

Importantly, miRNA-regulated spine formation is emerging as one of the underlying mechanisms of neural plasticity. Homeostatic synaptic plasticity in response to persistent activity is mediated through miR-485-mediated decrease in spine density, PSD-95 clustering and surface expression of GluR2. miR-

132 is rapidly upregulated in visual cortex after eye opening and regulates spine maturation of pyramidal neurons. Inhibition of miR-132 in visual cortex results in more immature spines (thin and filopodia) and fewer mature spines (mushroom and stubby) as well as an impairment of ocular dominance (Mellios et al., 2011). On the other hand, miR-29a/b, which was identified in a screen for miRNAs involved in neuroadaptations induced by psychostimulants, decreases mushroom spines while increasing filopodias through downregulation of Arpc3, a component of ARP2/3 actin nucleation complex (Lippi et al., 2011). These results strongly suggest miRNAs regulate behavior-associated plasticity by regulating spine formation and maturation.

3.1.3 Structural Alterations in Df(16)A$^{+/-}$ Neurons

As mentioned briefly in Chapter 2.1.2, individuals with 22q11.2DS exhibit morphological deficits such as reduced hippocampal volume (Campbell et al., 2006; Eliez et al., 2000; Simon et al., 2005) and enlarged lateral ventricles (Campbell et al., 2006; Machado et al., 2007; Simon et al., 2005) which suggest a decrease in neuron density or reduced dendritic complexity in hippocampal areas. More importantly, these morphological deficits are consistent with structural alterations found in general schizophrenia patients (Chow et al., 2002; van Amelsvoort et al., 2001) and may contribute to the cognitive dysfunction in schizophrenia.

Although the morphological features of neurons in the affected brain area of 22q11.2DS patients have been not examined, studies of a 22q11.2DS mouse model, *Df(16)A*$^{+/-}$,reveal that genomic loss of the 22q11.2 locus leads to several structural deficits in hippocampal neurons (Mukai et al., 2008). Basal dendritic branching of CA1 hippocampal neurons is significantly simplified (Drew et al., 2011a). Sholl analysis indicated that the decrease in dendritic complexity is especially prominent in the proximal part. The impaired dendritic arborization is recapitulated in cultured hippocampal neurons, as indicated by a 45% decrease in the number of branch points and a 38% decrease in the number of primary dendrites. Besides deficits in dendritic trees, spine growth and maturation appear to be compromised in *Df(16)A*$^{+/-}$ mice. Both spine density and spine width are reduced in CA1 hippocampal neurons. These deficits are also recapitulated in cultured hippocampal neurons. *Df(16)A*$^{+/-}$ neurons have 45% less mushroom spines which are on average 23% smaller in diameter as compared to Wt neurons. Additionally, there are 30-50% decreases in the number of PSD95, VGLUT1, Homer1 and GluR2 puncta on dendrites of *Df(16)A*$^{+/-}$

neurons, indicating a reduced density of excitatory postsynaptic complexes correlating with decreased spine density. In a parallel analysis of prefrontal cortical pyramidal neurons, deficits in complexity of basal dendritic trees and in spine density on basal dendrites are found (Kim Stark and Joseph Gogos, unpublished data). Therefore, 22q11.2 microdeletion appears to affect morphogenesis of excitatory neurons in multiple brain areas which may together result in reduced connectivity in neural circuits across the brain.

Notably, part of these structural abnormalities in dendrites and spines of hippocampal neurons are also observed in *Zdhhc8*-deficent and *Dgcr8*$^{+/-}$ neurons (Mukai et al., 2008; Stark et al., 2008). *Dgcr8*$^{+/-}$ CA1 neurons show lower dendritic complexity and a 8.5% decrease in average spine width, while CA1 neurons in *Zdhhc8*-deficent mice have reduced dendritic arborization and spine density, as compared to neurons in Wt littermates. These results suggest that the loss of a copy of *Zdhhc8* or *Dgcr8* (both located in 22q11.2 locus) and the subsequent dysregulation of palmitoylation or miRNA biogenesis, respectively, contribute to aberrant morphogenesis of hippocampal neurons. It remains to be examined how deficiency of additional individual genes in 22q11.2 locus affect the neuronal structures.

3.1.4 In this Chapter

Since a novel gene *Mirta22* (*miRNA target of the 22q11.2 microdeletion*, or *2310044H10Rik*) appears to be the major downstream target of miRNA dysregulated in *Df(16)A*$^{+/-}$ mice, including miR-185 (see Chapter 2), we try to characterize the gene and its protein product. We generated a specific anti-Mirta22 antibody and used it to probe the distribution of Mirta22 in neurons. We show that Mirta22 is expressed in neurons but not glial cells and is localized to the Golgi apparatus intracellularly. Besides the characterization of miRNA and target dysregulation in *Df(16)A*$^{+/-}$ mice, we examined the functional consequences of this dysregulation. We demonstrate that the drastic decrease of miR-185, one of the most prominent miRNA dysregulation in *Df(16)A*$^{+/-}$ mice, contributes to the structural deficits in *Df(16)A*$^{+/-}$ neurons. Furthermore, we speculated that the persistent elevation of *Mirta22* downstream of miRNA dysregulation partly mediated the effect of mir-185 reduction on these deficits. We manipulated Mirta22 levels in neurons and show that Mirta22 is an inhibitor of dendritic and spine development.

3.2 Results

3.2.1 Generation of Mirta22 Specific Antibody

Mirta22 encodes a 28 kD protein without any known sequence homology or functional domain (http://www.uniprot.org/uniprot/Q3TAS6). The murine orthologue is located on mouse chromosome 7 and contains seven coding exons. The human ortholog (*C19orf63*) is located on chromosome 19q13.33 and encodes a protein with 92.3% identity to the murine protein (Figure 3.1A). One mouse reference sequence (isoform 1) is reported in GeneBank, while two *C19orf63* isoforms (isoform 1 and 2) are reported in GeneBank and in the literature (Junes-Gill et al., 2011). The protein encoded by isoform 1 is predicted to contain an N-terminal signal peptide, as well as a transmembrane segment (Figure 3.1A, red rectangles), which separates a long N-terminal region from a short C-terminal segment that contains a polyglycine tail with unknown function. Isoform 2 differs from isoform 1 by an alternatively spliced exon located after exon 6. The protein encoded by isoform 2 is shorter by 8 amino acids, contains the N-terminal signal peptide but not the transmembrane segment, and is predicted to be secreted (Figure 3.1A). We raised a polyclonal antibody against a segment of the protein (amino acids 207–226, Figure 3.1A, green rectangle; see Methods). The specificity of the antibody was validated by Western blot analysis on protein extracts from 293T cells transfected with a plasmid expressing full length *Mirta22* cDNA with a C-terminal FLAG tag (Figure 3.2A) or a mouse neuroblastoma cell line (N18), transfected with either a *Mirta22* shRNA (Figure 3.2B) or a full length cDNA plasmid (Figure 3.2C) . Western blot assays of protein extracts from the brain of *Df(16)A*$^{+/-}$ mice and their Wt littermates showed the expected increase (25%) in the levels of Mirta22 in mutant mice (Figure 3.1B). An increase of similar magnitude of the Mirta22 immunocytochemical signal was observed in *Df(16)A*$^{+/-}$ cultured neurons, as compared to Wt neurons (Figure 3.1C). These results provided independent confirmation of the specificity of the antibody.

3.2.2 Mirta22 is a Neuronal Protein Residing in the Golgi Apparatus

Immunostaining of neuronal cultures showed that Mirta22 is colocalized with neuron-specific marker NeuN, but not astrocyte-specific marker GFAP, indicating that Mirta22 is primarily a neuronal protein (Figure 3.1D, upper panel). At the subcellular level, Mirta22 is found primarily in the soma, where

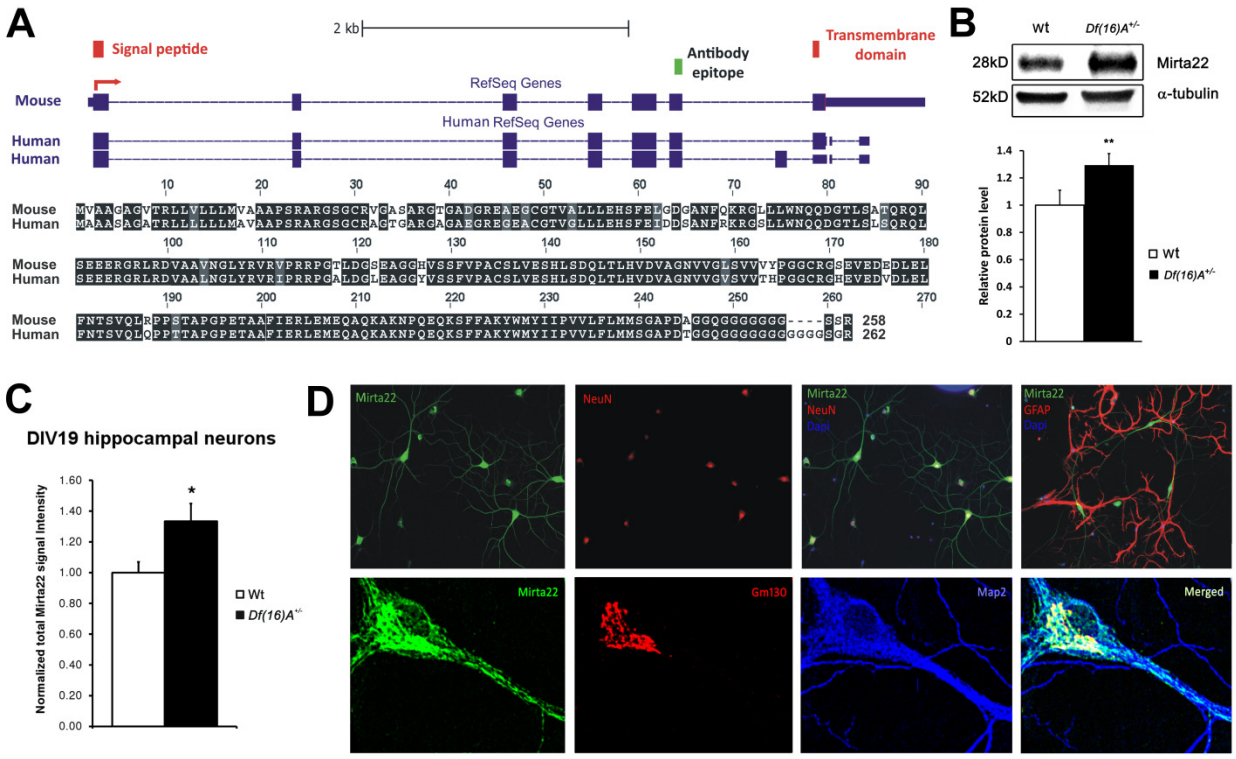

Figure 3.1 Genomic Structure, Neuronal Expression and Subcellular Localization of 2310044H10Rik (Mirta22). (A) *Top:* Structure of mRNA transcripts of *2310044H10Rik (Mirta22)* and its human orthologue, *C19orf63*. RefSeq reports a *2310044H10Rik (Mirta22)* transcript with 7 exons (blue rectangles), which is predicted to encode a signal peptide and a transmembrane domain (red rectangles). The peptide epitope used to generate a polyclonal antibody is marked by green rectangle. For *C19orf63*, RefSeq reports 2 alternatively spliced transcripts: one that encodes a predicted transmembrane protein and one with an additional exon that encodes a predicted secreted protein. *Bottom:* Protein sequence alignment of predicted transmembrane isoforms encoded by *2310044H10Rik* and its human orthologue. Black blocks indicate completely conserved residues; grey blocks indicate similar residues (defined by Boxshade default similarities); white blocks indicate different residues. (B) *Upper:* Representative western blot assays of 2310044H10Rik (Mirta22) in prefrontal cortex (PFC) lysates prepared from *Df(16)A*$^{+/-}$ animals and Wt littermates. Alpha-tubulin is used as loading control. *Lower:* Quantification of 2310044H10Rik protein level in PFC of Wt and *Df(16)A*$^{+/-}$ animals (n = 9 each genotype). Expression levels in mutant mice were normalized to Wt littermates. Results are expressed as mean ± SEM. **p < 0.01 (Student's *t*-test). (C) Quantification 2310044H10Rik (Mirta22) immunocytochemical signals in Wt and *Df(16)A*$^{+/-}$ cultured neurons (n = 34 for Wt; n = 31 for *Df(16)A*$^{+/-}$). Expression levels in mutant neurons were normalized to Wt neurons. Results are expressed as mean ± SEM. *p < 0.05 (Student's *t*-test). (D) *Upper panel:* 2310044H10Rik (Mirta22) co-localizes with neuron specific marker NeuN, but not with glia specific marker GFAP, in cultured hippocampal neurons at DIV20. *Lower panel:* 2310044H10Rik (green) co-localizes with Golgi specific marker GM130 (red) in the soma. 2310044H10Rik is also found in vesicles and tubular-like clusters in the dendrites, which are highlighted by the dendritic marker MAP2 (blue).

it colocalizes with the Golgi apparatus marker GM130 (Nakamura et al., 1995) and as neurons mature it is also found in vesicles and tubular-like clusters within the dendritic shafts (Figure 3.1D, lower panel).

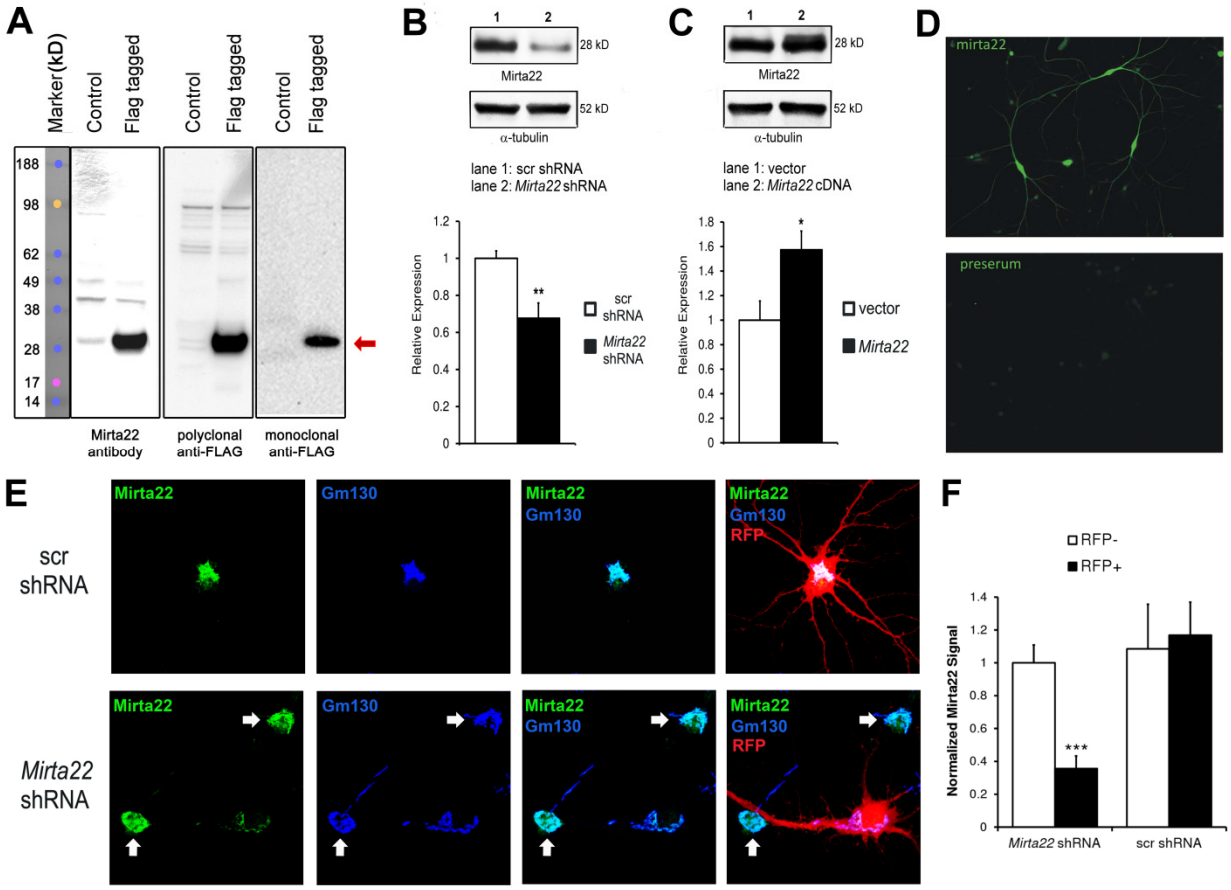

Figure 3.2 Specificity of Mirta22 (2310044H10Rik) Antibody. (A) Anti-2310044H10Rik (anti-Mirta22) antibody, as well as polyclonal and monoclonal anti-FLAG antibodies, recognize a 28 kD band in western blots on lysates of 293T cells transfected with a plasmid expressing full length Mirta22 cDNA with a C-terminal FLAG tag ("Flag tagged" lanes). Lysates of cells transfected with empty vector were used as control ("control" lanes). Note that there is a 28 kD band recognized by anti-Mirta22 antibody, but not by anti-FLAG antibodies, in control lysates. This likely represents the endogenous human Mirta22 orthologous protein (C19orf63). (B-C) *Upper panel:* Representative western blot showing the endogenous Mirta22 protein in N18 cells transfected with *Mirta22* shRNA (B, lane 2) or *Mirta22* cDNA (C, lane 2) compared to contol cells (lane 1). Alpha-tubulin is the loading control. *Lower panel:* Quantification of western blots showing a 32% reduction ($p < 0.01$; $n = 6$ each condition) in Mirta22 signal in *Mirta22* shRNA-transfected cells, compared to scramble shRNA-transfected cells (B). Quantification of western blots showing a 57% increase ($p < 0.05$; $n = 6$ each condition) in Mirta22 signal in *Mirta22* cDNA-transfected cells. Expression levels in *Mirta22* shRNA or cDNA-manipulated neurons were normalized to their respective controls. (D) Anti-Mirta22 antiserum, but not pre-immune serum, recognizes endogenous Mirta22 protein (green signal) in DIV20 Wt hippocampal neurons, as assayed by immunocytochemistry. (E) Representative immunocytochemistry images showing that Mirta22 signal (green) as compared to Golgi marker GM130 (blue), is largely reduced in *Mirta22* shRNA-transfected (RFP+) DIV14 Wt hippocampal neurons (lower panel) but not in scramble shRNA-transfected (RFP+) neurons (upper panel). Note that in *Mirta22* shRNA-treated culture (lower panel), Mirta22 signal (green) in un-transfected neurons (marked by white arrows) is not reduced, as compared to scramble shRNA-transfected (RFP+) neurons (shown in upper panel). Transfection was performed at DIV12. (F) Quantification of Mirta 22 immunocytochemical signal shown in (E). Note that in *Mirta22* shRNA-treated neuronal cultures, there is a 64% decrease ($p < 0.001$) in Mirta22 signal in transfected neurons (RFP+, $n = 20$), compared to un-transfected neurons in (RFP-, $n = 20$). In scramble

[Figure 3.2, continued from p84] shRNA-treated cultures, there is no difference in Mirta22 signal between transfected (RFP+, n = 10) and un-transfected (RFP-, n = 10) neurons. Mirta22 signal measurements in transfected (RFP+) and un-transfected (RFP-) neurons in scramble shRNA treated culture and *Mirta22* shRNA-tranfected neurons (RFP+) were normalized to un-tranfected neurons (RFP-) in *2310044H10Rik (Mirta22)* shRNA treated culture. Results are expressed as mean ± SEM. *p < 0.05, **p < 0.01, ***p < 0.001 (Student's *t*-test).

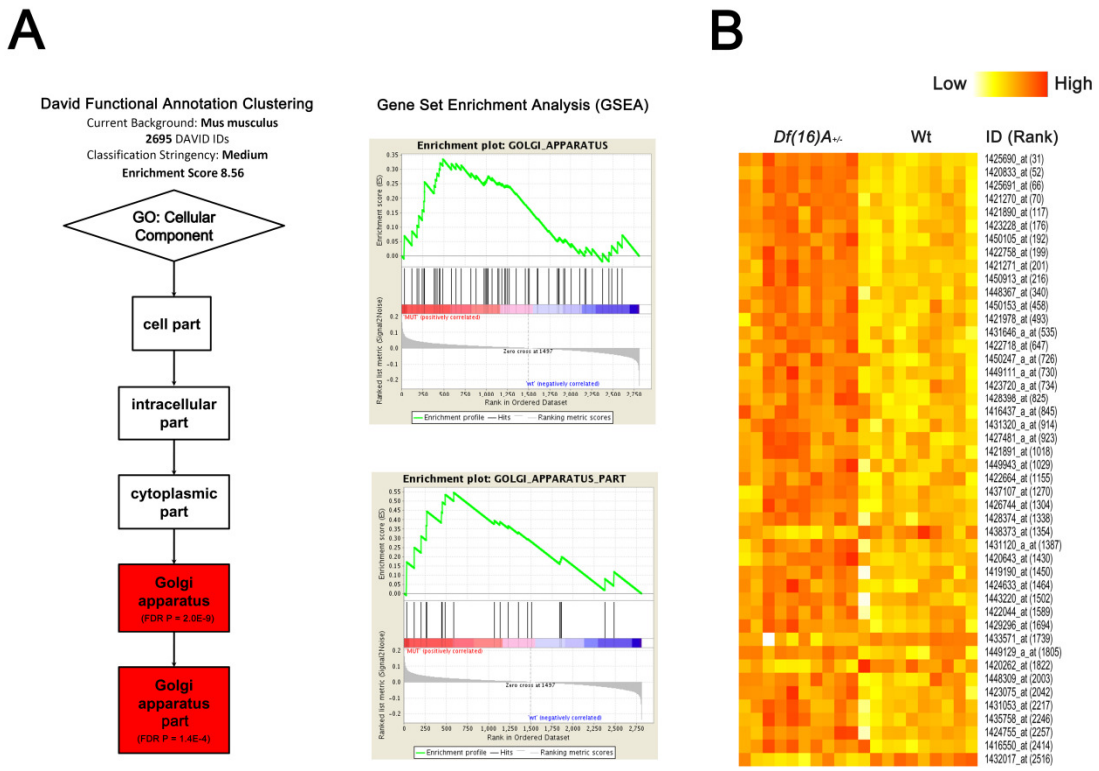

Figure 3.3 Coordinated Mild Dysregulation of Golgi-related Putative mir-185 Targets in *Df(16)A*$^{+/-}$ mice. (A) 2708 genes that were predicted to be miR-185 targets byTargetScan Mouse v5.2 were imported into the DAVID bioinformatics resources 6.7 (http://david.abcc.ncifcrf.gov) and 2695 genes have corresponding DAVID IDs. Functional annotation analysis using *Mus musculus* genes as background identified Gene Ontology (cellular component) term "Golgi apparatus" as the top enriched gene cluster (gene count = 159, Enrichment Score = 8.56, FDR-corrected $P = 2x10^{-9}$) and term "Golgi apparatus part" as the second best hit with FDR-corrected $P = 4x10^{-3}$ (left). The same gene list was also imported into Gene Set Enrichment Analysis (GSEA v2.0). The Gene Ontology (cellular component) terms "Golgi apparartus part" (NES = 1.35, $P = 0.1$) and "Golgi apparatus" (NES = 1.3, $P = 0.1$) were again among the top enriched gene sets (right). (B) Expression heatmap plot of the potential miR-185 targets that serve Golgi apparatus related functions (GO term) and are differentially expressed ($p < 0.005$) between adult hippocampus of *Df(16)A*$^{+/-}$ mice and Wt littermates. ID is Affymetrix ID (see Table 3.2) and Rank is the ranking position in the list of all differentially expressed genes according to significance level. Note that the majority (91%, 42 out of 46) of the genes are upregulated.

Mirta22 immunoreactivity was not detected in cultures stained with preimmune serum (Figure 3.2D) and was diminished by 64% in *Mirta22* shRNA-transfected neurons (RFP+ neuron, Figure 3.2E, lower panel), as compared to non-transfected neurons (RFP- neurons, marked by arrows in Figure 3.2E, lower panel) (Figure 3.2F).

3.2.3 Coordinated Mild Dysregulation of Golgi-related Genes due to miR-185 Reduction

Accumulating evidence suggests that miRNAs may target functionally connected genes, often in a developmental stage-specific manner (Tsang et al., 2010; Zhang et al., 2009). Consistent with this notion, functional annotation clustering analysis of 2708 predicted miR-185 targets (TargetScanMouse v5.2) included in the DAVID *Mus musculus* gene functional annotation database (http://david.abcc.ncifcrf.gov) identified as the top enriched gene cluster (gene count = 159, Enrichment Score = 8.56, FDR-corrected $P = 2x10^{-9}$) the Gene Ontology (cellular component) term "Golgi apparatus" (Figure 3.3A). Gene set enrichment analysis (GSEA) on the 2708 predicted miR-185 targets ranked based on the gene expression profile of *Df(16)A*$^{+/-}$ mice also indicated that the Gene Ontology terms "Golgi apparatus part" and "Golgi apparatus" were among the top 20 genesets in the adult hippocampus (HPC) (Figure 3.3A). A global perspective on the enrichment of this miR-185 target gene set among the differentially expressed genes in the *Df(16)A*$^{+/-}$ mice showed a significant enrichment in the adult HPC expression profile ($P = 5x10^{-4}$) where, as expected, most of top genes were upregulated (42 genes were upregulated and only 4 genes were downregulated at $P < 0.005$, Figure 3.3B and Table 3.3). A considerably more modest enrichment was suggested for the E17 ($P = 0.02$) and P6 HPC ($P = 0.016$) profiles (Figure 3.4). Interestingly, there was no significant enrichment within the prefrontal cortex (PFC) profiles in all three ages tested (E17: $P = 0.6311$; P6: $P = 0.1326$; Adult: $P = 0.244$). Expression changes were modest, with only 4 out of 159 Golgi-related probe sets included among the top 100 probe sets in the adult HPC. Overall, in addition to the robust and pervasive upregulation of *Mirta22*, reduction in miR-185 levels appears to affect in a milder, age and region-specific manner, expression of a group of Golgi apparatus-related genes.

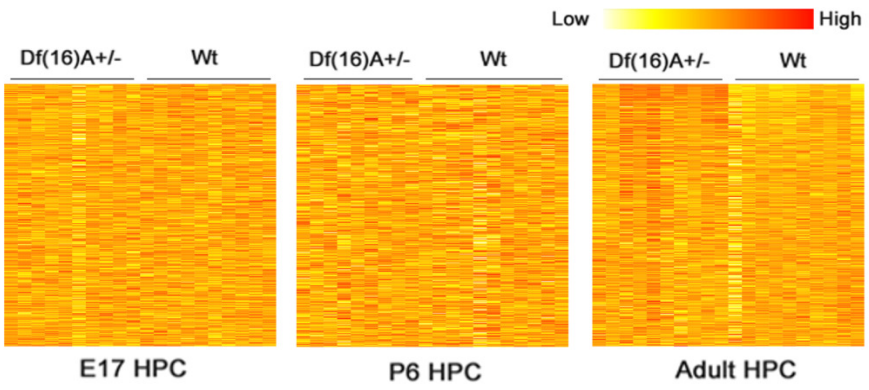

Figure 3.4. miR-185 Reduction Results in Coordinated Mild and Age-specific Dysregulation of Golgi-related Genes. Expression heatmap plot of all potential miR-185 targets that have Golgi apparatus related function in E17, P6 and adult (left, middle, right panel, respectively) hippocampus of *Df(16)A*$^{+/-}$ mice and Wt littermates.

3.2.4 Altered miR-185 Levels Contribute to Structural Alterations of Df(16)A$^{+/-}$ Neurons

We have previously shown that 22q11.2 microdeletion results in impaired formation of dendrites and spines in the brain. We have also shown that these deficits are faithfully recapitulated in primary neuronal cultures, affording the opportunity to study the underlying mechanisms in physiologically relevant cellular models. miRNAs have been shown to affect structural indices of neuronal connectivity, such as dendritic tree and dendritic spine development (Fiore et al., 2009; Schratt et al., 2006; Siegel et al., 2009; Stark et al., 2008), but impairment in these processes in *Df(16)A*$^{+/-}$ mice could only be partially accounted for by the 50% decrease in the levels of Dgcr8 (Fenelon et al., 2011; Stark et al., 2008). Localization of Mirta22 within the Golgi apparatus and dendritic shafts suggests that diminishment of the repressive influence of miR-185 on Mirta22 levels may also contribute to these deficits.

To test this hypothesis we first asked whether reduction of miR-185 levels results in deficits in dendritic and spine development similar to those observed in *Df(16)A*$^{+/-}$ neurons (Mukai et al., 2008). We introduced an anti-miR-185 and a scramble control LNA oligonucleotide into Wt primary hippocampal neurons and measured dendritic and spine morphology two days post-transfection at DIV9 and DIV19, respectively. As mentioned above, we confirmed that introduction of anti-miR-185 LNA oligonucleotide resulted in a significant increase of *Mirta22* mRNA levels when compared to anti-miR control transfected primary neurons (Figure 2.9C). Analysis of dendritic architecture indicated that reduction of miR-185 levels leads to deficits in dendritic complexity (Figure 3.5A), including a significant reduction in the number of primary dendrites (21%, $P < 0.05$; Figure 3.5B) and a significant reduction in total branch points in transfected neurons (16%, $P < 0.05$; Figure 3.5C). This finding was confirmed by a Sholl analysis, which compares branch point numbers at varying distances from the soma (Figure 3.6A). Moreover, reduction of miR-185 levels in DIV19 neurons results in decreased mushroom spine density (21%, $P < 0.05$; Figure 3.5D-E, 3.6B) and a significant reduction in their median width (15% decrease, $P < 0.001$, Kolmogorov-Smirnov test; Figure 3.5F). These structural deficits recapitulate those observed in *Df(16)A*$^{+/-}$ neurons. Thus the neuronal deficits in *Df(16)A*$^{+/-}$ mice are, at least in part, due to the aberrantly low level of miR-185. Consistently, introduction of pre-miR-185 mimic into Wt neurons increased the number of primary dendrites, the number of branch points, the density and head width of mushroom spines (Figure 3.6C, D).

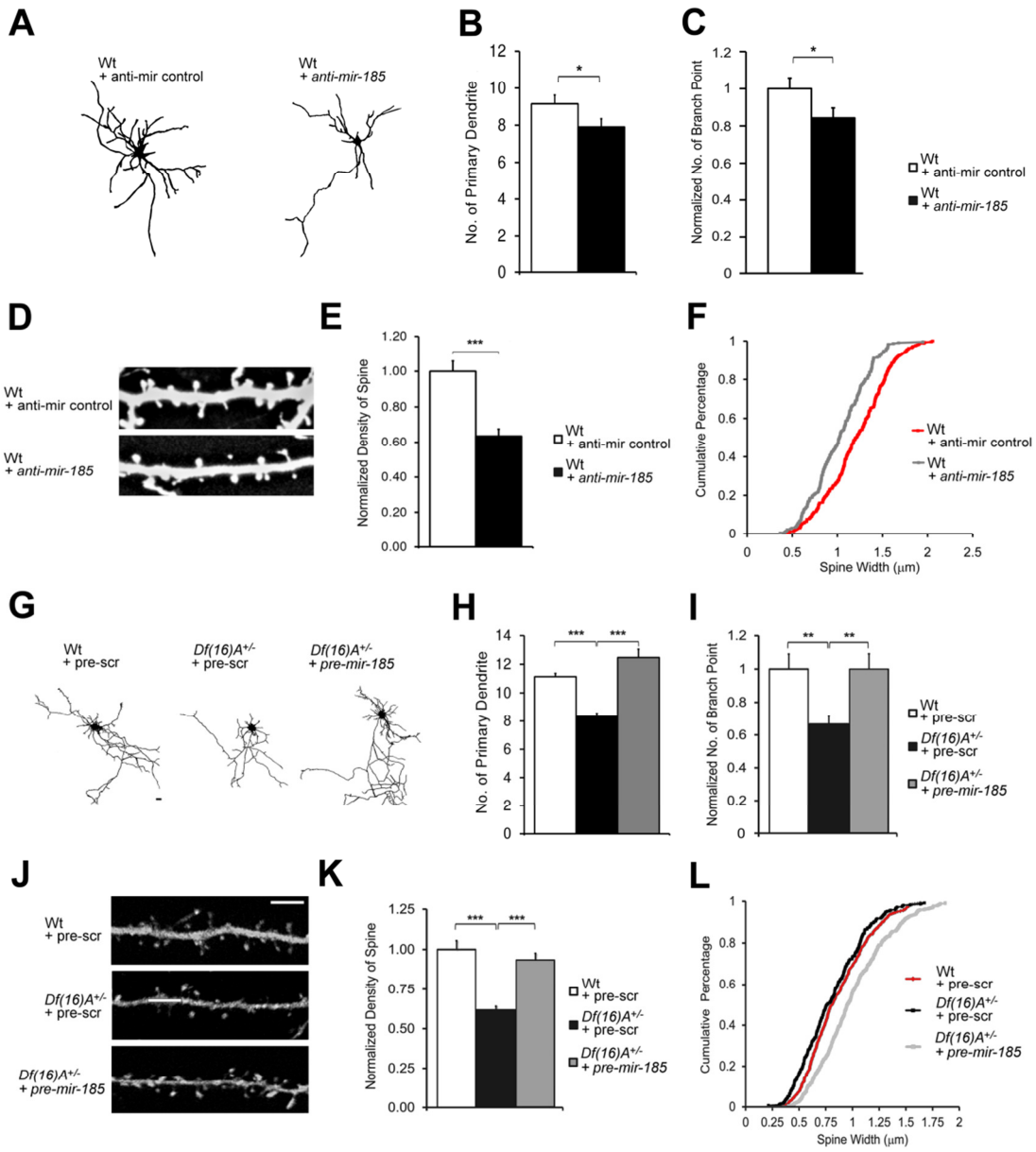

Figure 3.5 Reduced miR-185 Levels Contribute to Structural Alterations of *Df(16)A*$^{+/-}$ Neurons. (A) Representative images of Wt neurons at DIV9 transfected with anti-miR control or anti-miR-185 oligos. (B-C) Reduction in the number of primary dendrites (B) and branch points (C) in Wt neurons at DIV9, 2 days after transfected with anti-miR-185 relative to Wt neurons transfected with anti-miR control (n = 21 for Wt + anti-miR-185; n = 20 for Wt + anti-miR control). In (C), values of Wt + anti-miR-185 were normalized to Wt + anti-miR control. (D) Representative images of spines on Wt neurons at DIV19, transfected with anti-miR control or anti-miR-185 as well as enhanced GFP. (E) Reduction in the density of mushroom spines (quantified over 75 μm of dendritic length) in neurons transfected with anti-miR-185 relative to neurons transfected with anti-miR control (n = 20 for Wt + anti-miR-185; n = 20 for Wt + anti-miR control). Values of Wt + anti-miR-185 were normalized to Wt + anti-miR control. (F) Transfection of anti-miR-185 oligos significantly decreased the width of mushroom spines compared to that of the neurons transfected with anti-miR control at DIV19 (15%, $P < 0.001$, Kolmogorov-Smirnov test) (n = 232 for Wt + anti-miR-185; n = 293 for Wt + anti-miR control). (G) Representative *Df(16)A*$^{+/-}$ neurons at DIV9 transfected with pre-scramble or pre-miR-185 mimic and enhanced GFP for visualization. Scale

[Figure 3.5, continued from p88] Bar, 20 μm. (H-I) Reduction in the number of primary dendrites (H) and branch points (I) in *Df(16)A*$^{+/-}$ neurons at DIV9 relative to Wt neurons is reversed by the transfection of pre-miR-185, but not pre-scramble mimic (pre-scr) (n = 21 for Wt + pre-scr; n = 21 for *Df(16)A*$^{+/-}$ + pre-scr; n = 21 for *Df(16)A*$^{+/-}$ + pre-miR-185). In (I), values of *Df(16)A*$^{+/-}$ neurons were normalized to Wt + pre-scr. (J) Representative images of spines on *Df(16)A*$^{+/-}$ neurons at DIV19, transfected with pre-scramble or pre-miR-185 mimic as well as enhanced GFP. Scale Bar, 5 μm. (K) Reduction in the density of mushroom spines (quantified over 75 μm of dendritic length) in DIV19 *Df(16)A*$^{+/-}$ neurons relative to Wt control neurons is reversed by the transfection of pre-miR-185, but not pre-scramble mimic, into *Df(16)A*$^{+/-}$ neurons. (n = 23 for Wt + pre-scr; n = 21 for *Df(16)A*$^{+/-}$ + pre-scr; n = 23 for *Df(16)A*$^{+/-}$ + pre-miR-185). Values of *Df(16)A*$^{+/-}$ neurons were normalized to Wt + pre-scr. (L) Transfection of pre-miR-185 mimic, but not pre-scramble control, significantly increased the width of mushroom spines of *Df(16)A*$^{+/-}$ neurons at DIV19 (18%, $p < 0.001$, Kolmogorov-Smirnov test) (n = 568 for Wt + pre-scr; n = 339 for *Df(16)A*$^{+/-}$ + pre-scr; n = 527 for *Df(16)A*$^{+/-}$ + pre-miR-185). (B, C, E, H, I, K) Results are expressed as mean ± SEM. *$p < 0.05$, **$p < 0.01$ (Student's *t*-test).

We also examined whether elevation of miR-185 levels could, at least partially, reverse cytoarchitectural alterations observed in *Df(16)A*$^{+/-}$ neurons (Mukai et al., 2008). We transfected primary hippocampal neurons from *Df(16)A*$^{+/-}$ mice and their Wt littermates with a miRNA precursor mimic ("pre-miR-185") or a scramble precursor oligonucleotide ("pre-scramble"). A co-transfected GFP reporter plasmid allowed us to analyze the dendritic architecture (Figure 3.5G-I) and spine morphology (Figure 3.5J-L) of pyramidal neurons 2 days following transfection at DIV9 and DIV19, respectively. In control experiments we confirmed that introduction of pre-miR-185 resulted in significant decrease in the levels of *Mirta22* when compared to pre-scramble transfected neurons ($P < 0.01$; Figure 2.6B). Consistent with previous results (Mukai et al., 2008), compared to Wt neurons, *Df(16)A*$^{+/-}$ neurons transfected with pre-scramble showed reduced dendritic complexity as manifested by a decrease in the number of primary dendrites (25%, $P < 10^{-10}$; Figure 3.5H) and the number of dendritic branch points (38%, $P < 10^{-4}$; Figure 3.5I). They also showed reduced spine density (38%, $P < 10^{-6}$, Figure 3.5K) as well as a small, but statistically significant decrease in median head-width (8% decrease, $P < 0.01$; Figure 3.5L) of mushroom spines. Increase in miR-185 activity largely reversed the deficits in dendritic complexity (Figure 3.5H-I, 3.6E) and the reduction in spine density (Figure 3.5K, 3.6F) and significantly increased the spine head-width of mushroom spines in *Df(16)A*$^{+/-}$ hippocampal neurons (Figure 3.5L). Thus, introduction of pre-miR-185 into hippocampal neurons from *Df(16)A*$^{+/-}$ mice reversed some key deficits in the structural connections among neurons that emerge as a result of the microdeletion.

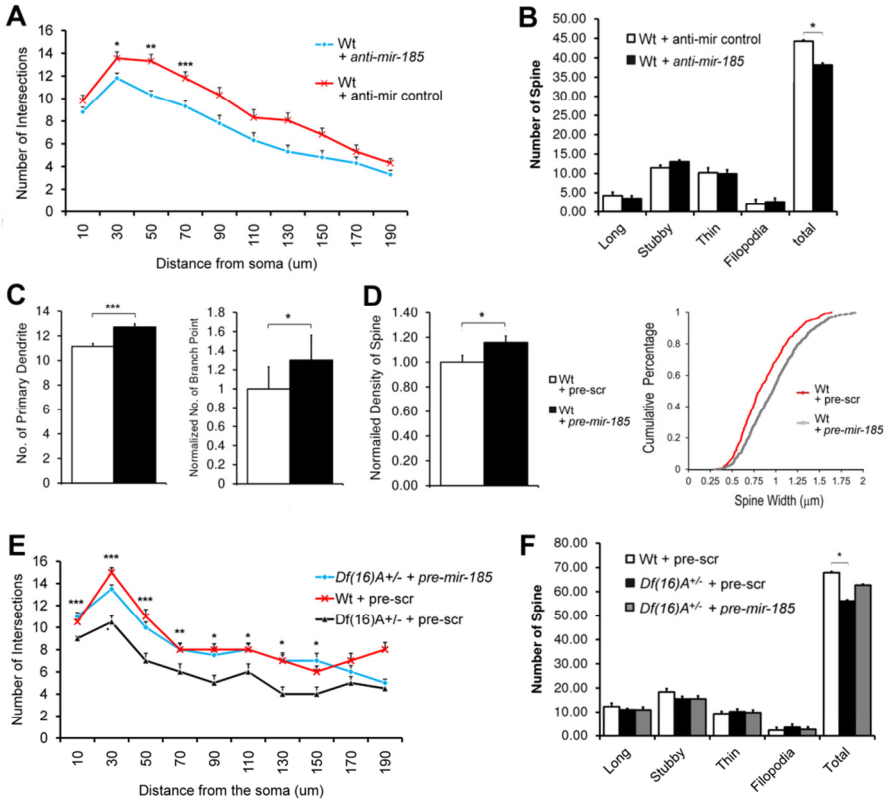

Figure 3.6 miR-185 Levels Affect Dendritic and Spine Development. (A) Wt neurons transfected with either anti-miR-185 (n = 21) or anti-miR control (n = 20) at DIV7 and fixed at DIV9. Increase in branching is prevalent in the vicinity of the most proximal dendrites. In (A) and (E), Sholl analysis of dendritic complexity using 10 μm concentric circles around the soma. (B) Distribution of spine morphotypes and total protrusions, in cultured Wt hippocampal neurons transfected with anti-miR-185 relative to neurons transfected with anti-miR control (n = 20 for Wt + anti-miRcontrol; n = 20 for Wt + anti-miR-185). In (B) and (F), spines other than mushroom spines are quantified over 75 μm of dendritic length from soma. (C) Increase in the number of primary dendrites and branch points in DIV9 (7+2) Wt neurons transfected with pre-miR-185 relative to Wt neurons transfected with pre-scramble mimic (pre-scr) (n = 21 for Wt+ pre-miR-185; n = 20 for Wt + pre-scr). (D) Left: Increase in the density of mushroom spines (quantified over 75 μm of dendritic length) in DIV19 Wt neurons transfected with pre-miR-185 relative to Wt neurons transfected with pre-scr (n = 23 for Wt + pre-scr; n = 23 for Wt+ pre-miR-185). Right: Transfection of pre-miR-185 mimic, but not pre-scramble control, significantly increased the width of mushroom spines on Wt neurons at DIV19 (18%, $P < 0.001$, Kolmogorov-Smirnov test) (n = 568 for Wt + pre-scr; n = 527 for Wt+ pre-miR-185). In (C and D right), values of Wt+ pre-miR-185 were normalized to Wt + pre-scr. (E) *Df(16)A*$^{+/-}$ neurons transfected with either pre-miR-185 mimic (n = 21) or or pre-scramble mimic (n = 21) at DIV7 and fixed at DIV9. (F) Distribution of spine morphotypes and total protrusions, in cultured DIV19 *Df(16)A*$^{+/-}$ hippocampal neurons transfected pre-miR-185 or pre-scramble mimic relative to Wt neurons transfected with pre-scramble mimic (n = 23 for Wt + pre-scr; n = 21 for *Df(16)A*$^{+/-}$ + pre-scr; n = 23 for *Df(16)A*$^{+/-}$ + pre-miR-185). Results are expressed as mean ± SEM. *p < 0.05, **p < 0.01, ***p < 0.001 (Student's *t*-test).

3.2.5 Elevation of Mirta22 Levels Inhibits Dendritic and Spine Development in Df(16)A$^{+/-}$ Neurons

We then considered the possibility that elevation of Mirta22 levels may contribute to at least some of the effects of the *miR-185* deficiency on the neuronal morphology in *Df(16)A*$^{+/-}$ mice. To this end, we first examined whether elevation of Mirta22 levels could partially phenocopy the structural alterations observed in *Df(16)A*$^{+/-}$ neurons (Mukai et al., 2008). We introduced a *Mirta22* cDNA into Wt primary hippocampal neurons and measured dendritic and spine morphology two days post-transfection at DIV9 and DIV19, respectively. Control experiments using qRT-PCR and Western blot confirmed that the

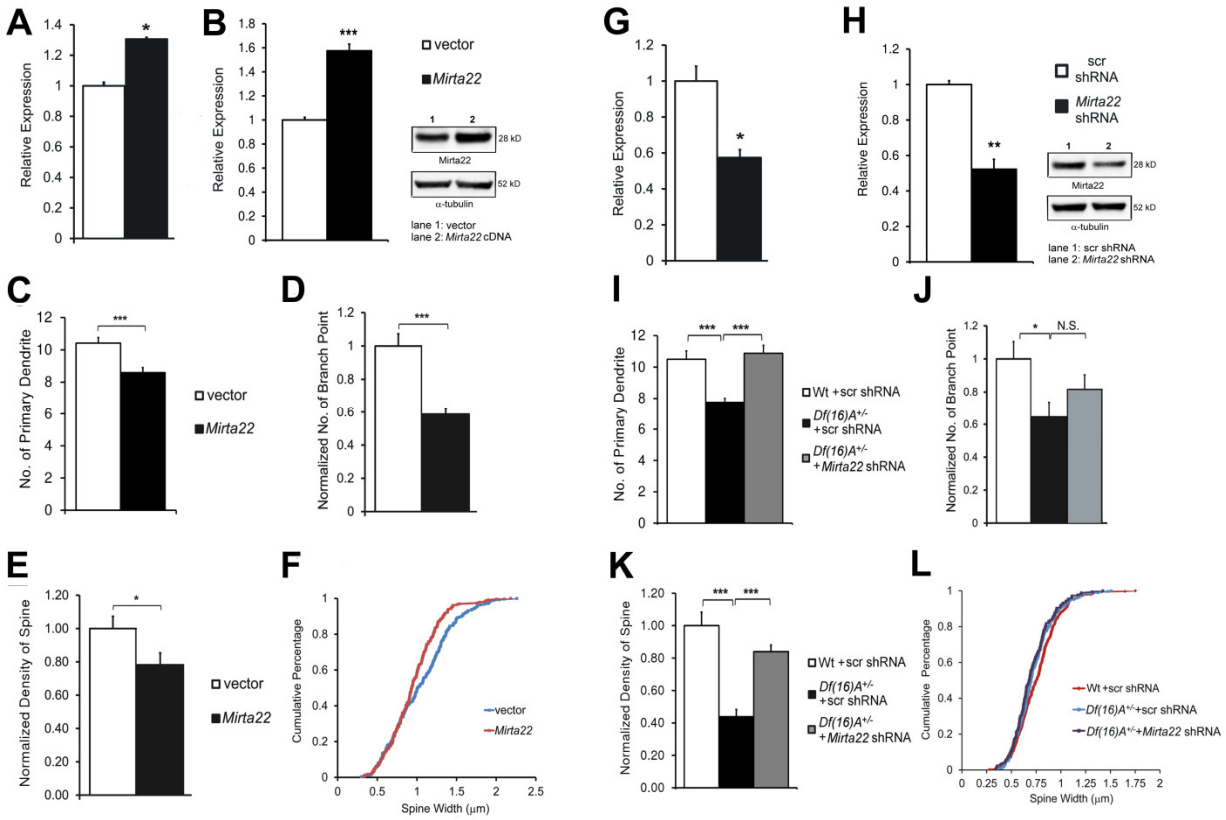

Figure 3.7 Elevated 2310044H10Rik (Mirta22) Levels Contribute to Structural Alterations of *Df(16)A*$^{+/-}$ Neurons. (A, B left) qRT-PCR and Western blot of *Mirta22* mRNA and protein levels in DIV12 hippocampal cultured neurons transfected with a full length *Mirta22* cDNA plasmid. Quantification of western blots showing a 58% increase ($p < 10^{-4}$; n = 4 each condition) in Mirta22 signal in *Mirta22* cDNA-transfected cells, compared to control cells. (B right) Representative blot of endogenous Mirta22 protein in neurons transfected with *Mirta22* cDNA (lane 2) or empty vector (lane 1). Alpha-tubulin is the loading control. (C-D) Transfection of a *Mirta22* expression construct into Wt neurons at DIV7 results in decrease in the number of primary dendrites (C) and branch points (D) at DIV9 (n = 24 for empty vector transfected and n = 27 for *Mirta22* transfected cells). In (D), values of *Mirta22* overexpressing neurons were normalized to empty vector-transfected neurons.(E-F) Introduction of *Mirta22* into Wt neurons at DIV17 results in decrease in the density of mushroom spines (E) and the width of those spines (F) ($P <$ 0.01, Kolmogorov-Smirnov test) at DIV19 [n = 16 for vector transfected and n = 17 for *Mirta22* transfected neurons (E); n = 278 for spines on vector transfected neurons and n = 231 for spines on *Mirta22* transfected neurons (F)]. Values of *Mirta22* overexpressing neurons were normalized to empty vector-transfected neurons. (G, H left) qRT-PCR and Western blot of *Mirta22* mRNA and protein levels in DIV12 hippocampal cultured neurons transfected with *Mirta22* shRNA. Quantification of western blots showing a 48% decrease ($p < 0.01$; n = 4 each condition) in Mirta22 levels in *Mirta22* shRNA-transfected cells, compared to control cells. (H right) Representative blot of the endogenous Mirta22 protein in neurons transfected with *Mirta22* shRNA (lane 2) or scramble shRNA (lane 1). Alpha-tubulin is the loading control. (I-J) Reduction in the number of primary dendrites (I), but not reduction in the number branch points (J), in *Df(16)A*$^{+/-}$ neurons at DIV9 relative to Wt neurons is reversed by the transfection of a construct that expresses *Mirta22* shRNA$^{+/-}$ (n = 24 for Wt + scr shRNA; n = 21 for *Df(16)A*$^{+/-}$ + scr shRNA; n = 25 for *Df(16)A*$^{+/-}$ + *Mirta22* shRNA). Scr shRNA: scramble shRNA. N.S.: not significant. In (J), values of *Df(16)A*$^{+/-}$ neurons were normalized to Wt + scr shRNA. (K) Reduction in the density of mushroom spines in *Df(16)A*$^{+/-}$ neurons at DIV19 relative to Wt neurons is reversed by the introduction of *Mirta22* shRNA, but not scramble shRNA (n = 22 for Wt + scr shRNA; n = 24 for *Df(16)A*$^{+/-}$ + scr shRNA; n = 15 for *Df(16)A*$^{+/-}$ + *Mirta22* shRNA). Values of *Df(16)A*$^{+/-}$

[Figure 3.7, continued from p90] neurons were normalized to Wt + scr shRNA. (L) Transfection of *Mirta22* shRNA does not affect the width of mushroom spines of *Df(16)A*$^{+/-}$ neurons at DIV19 ($p > 0.05$, Kolmogorov-Smirnov test). n = 342 for Wt + scr shRNA; n = 289 for *Df(16)A*$^{+/-}$ + scr shRNA, n = 177 for *Df(16)A*$^{+/-}$ + *Mirta22* shRNA. (A-E, G-K) Results are expressed as mean ± SEM. *$p < 0.05$, **$p < 0.01$ (Student's *t*-test).

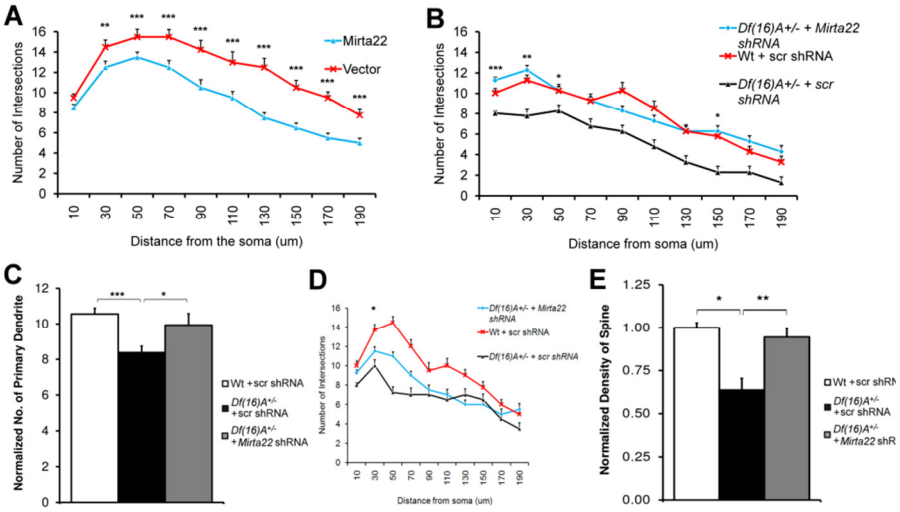

Figure 3.8 *2310044H10Rik (Mirta22)* Levels Affect Dendritic and Spine Development. In (A-B, D) Sholl analysis of dendritic complexity using 10-µm concentric circles around the soma was performed on neruons transfected on DIV7 and fixed at DIV9. (A) Dendritic complexity of Wt neurons transfected with a plasmid carrying either full length *Mirta22* (n = 25) or no insert (n = 24). (B) Dendritic complexity of *Df(16)A*$^{+/-}$ neurons transfected with either *Mirta22* shRNA (n = 29) or scramble shRNA (n = 26). (C) Reduction in the number of primary dendrites in *Df(16)A*$^{+/-}$ neurons at DIV9 relative to Wt neurons is reversed by the transfection of a construct that expresses an independent *Mirta22* shRNA (n = 16 for Wt + scr shRNA; n = 16 for *Df(16)A*$^{+/-}$ + scr shRNA; n = 16 for *Df(16)A*$^{+/-}$ + *Mirta22* shRNA). Scr shRNA: scramble shRNA. (D) Dendritic complexity of *Df(16)A*$^{+/-}$ neurons is partially reversed by *Mirta22* shRNA, especially in the vicinity of the most proximal dendrites. (E) Reduction in the density of mushroom spines (estimated over 75 µm of dendritic length) in *Df(16)A*$^{+/-}$ neurons at DIV19 relative to Wt neurons is reversed by the introduction of *2310044H10Rik (Mirta22)* shRNA, but not scramble shRNA (n = 12 for Wt + scr shRNA; n = 12 for *Df(16)A*$^{+/-}$ + scr shRNA; n = 12 for *Df(16)A*$^{+/-}$ + *Mirta22* shRNA). Values of *Df(16)A*$^{+/-}$ neurons were normalized to Wt + scr shRNA. Results are expressed as mean ± SEM. *$p < 0.05$, **$p < 0.01$, ***$p < 0.001$ (Student's *t*-test).

Mirta22-encoding plasmid drives increased expression of *Mirta22* at both mRNA and protein levels (Figure 3.7A, B). Analysis of dendritic architecture indicated that elevation of Mirta22 levels results in a significant reduction in the number of primary dendrites (18%, $P < 0.001$; Figure 3.7C) and total branch points in transfected neurons (41%, $P < 10^{-5}$; Figure 3.7D). This finding was confirmed by Sholl analysis (Figure 3.8A). Moreover, elevation of Mirta22 levels in DIV19 neurons results in decreased spine density (22%, $P < 0.05$; Figure 3.7E) and a small but significant reduction in the mushroom spine median width (8% decrease, $P < 0.001$, Kolmogorov-Smirnov test; Figure 3.7F). These structural deficits recapitulate those observed in *Df(16)A*$^{+/-}$ neurons, suggesting these deficits are, at least in part, due to the aberrantly high level of Mirta22.

We also asked whether reduction of *Mirta22* levels could, at least partially, reverse cytoarchitectural alterations observed in *Df(16)A*$^{+/-}$ neurons (Mukai et al., 2008). We transfected primary hippocampal neurons isolated from *Df(16)A*$^{+/-}$ embryos and their Wt littermates with constructs that coexpress turbo RFP (tRFP) and either an shRNA engineered to knock down expression of endogenous mouse Mirta22 or a scramble control shRNA (scr shRNA). We confirmed that the *Mirta22* shRNA can effectively knockdown the expression of *Mirta22* at both mRNA and protein levels (Figure 3.7G, H). We analyzed dendritic architecture and spine morphology two days following transfection, at DIV9 and DIV19 respectively. Introduction of *Mirta22* shRNA restored to Wt levels the number of primary dendrites of *Df(16)A*$^{+/-}$ neurons at DIV9 (*Mirta22* shRNA versus scr shRNA, 40% increase , $P < 10^{-5}$; Figure 3.7I). A trend toward an increase in the total number of branch points in *Df(16)A*$^{+/-}$ neurons was also observed (25%, $P = 0.16$; Figure 3.7J). Sholl analysis confirmed that introduction of *Mirta22* shRNA in *Df(16)A*$^{+/-}$ neurons increased branch point numbers mainly in the proximal dendritic segments from the soma (Figure 3.8B). Furthermore, while DIV19 *Df(16)A*$^{+/-}$ neurons transfected with the control shRNA had fewer and thinner mushroom spines than Wt neurons, introduction of *Mirta22* shRNA into *Df(16)A*$^{+/-}$ neurons reversed the deficit in density (*Mirta22* shRNA versus scr shRNA, 91% increase, $P < 10^{-6}$; Figure 3.7K) while it had no significant impact on spine width (Figure 3.7L). The observation that reduction of Mirta22 levels partially reverses the structural deficits observed in *Df(16)A*$^{+/-}$ mice was confirmed by using an independent *Mirta22* shRNA (Figures 3.8C-E) and strongly suggests that Mirta22 acts as an inhibitor mediating the effects of the structural mutation of dendritic and spine growth.

3.3 Discussion

3.3.1 What do We Know about Mirta22 Protein?

Through large scale sequencing efforts, draft sequences of the whole genomes of many mammals are available through various databases. However, expression and functional data of many putative genes are still missing. We identified a largely uncharacterized gene *Mirta22* (*2310044H10Rik*) as a major downstream effecter of miRNA dysregulation in *Df(16)A*$^{+/-}$ mice. *Mirta22* and its orthologues constitute a class of novel genes which are located in a conserved area of the genome and are evolutionarily conserved from mammals to plants (Junes-Gill et al., 2011). The mouse and human genes

have 7 constitutive exons and are predicted to encode proteins with a signal peptide and a transmembrane domain but no other known motif or domain. The human and mouse proteins have remarkably high homology (92.3% identity). It was reported that a secretable form of human Mirta22 orthologue (hHSS1 or C19orf63) is produced from a splice variant with the inclusion of an extra exon (Junes-Gill et al., 2011). The first 226 amino acids (aa) of the transmembrane form (hHSM1) and the secretable form (hHSS1) of human Mirta22 orthologue are encoded by the same first 6 exons. For mouse *Mirta22* gene, only transcripts encoding a transmembrane form of the protein are reported in GeneBank but a secratable form is likely to be produced. Since Mirta22 has no sequence homology to any known naturally occurring protein, there is little insight into the signaling pathways Mirta22 participates in or its interacting proteins. Therefore, what we knew previously about Mirta22 was from experimental results from a couple of reports.

Wang et al. cloned *hHSS1* (or termed *INM02* in this report) from a cDNA library of human insulinoma tissue in an attempt to identify glucose-responsive genes (Wang et al., 2009). *hHSS1* mRNA is expressed in testis, bladder, lung, kidney and brain, as well as islets of Langerhans in the pancreas. Immunohistochemistry showed that hHSS1 is exclusively expressed in islets of Langerhans and colocalized with insulin. hHSS1 is also detected in human serum and is induced by high but not low glucose from isolated islets of Langerhans. The authors speculated that hHSS1 is associated with functions of β-cells in response to glucose. Another group interested in novel therapeutic targets of tumors identified HSS1 gene from hematopoietic stem cells (Junes-Gill et al., 2011). They designated the protein products of *hHSS1* splice variants as hHSS1 (human Hematopoietic Signal peptide-containing Secreted 1) and hHSM1 (human Hematopoietic Signal peptide-containing Membrane domain-containing 1). hHSS1 suppresses proliferation and anchorage-independent growth when expressed in glioblastoma cells. Nude mice injected with hHSS1-expressing glioblastoma cells survive significantly longer than those injected with vector transfected cells, suggesting hHSS1 decreases malignancy of tumor cells. Interestingly, although hHSS1 has inhibitory effects on tumor growth, high levels of hHSS1 are only found in high-grade gliomas. Thus exactly how hHSS1 modulates tumorigenicity *in vivo* remains to be studied. In addition, from expression profiling data, *Mirta22* (*2310044H10Rik*) was found to be significantly upregulated in *MECP2*-Tg mice expressing a human transgene and endogenous genes (Chahrour et al., 2008) and significantly downregulated in *Neuropsin*$^{-/-}$ mice (Attwood et al., 2011). It is noteworthy that

these mouse strains have cognitive or behavioral abnormalities related to psychiatric symptoms, such as memory deficits and aberrant anxiety level. However, whether *Mirta22* dysregulation contributes to these abnormalities was not explored.

Here we show that Mirta22 is a neuronal morphogenesis inhibitor that suppressed dendritic and spine growth when overexpressed. Moreover, reducing Mirta22 expression by shRNA partially rescued the structural deficit of *Df(16)A*$^{+/-}$ neurons. It seems that Mirta22 plays diverse roles in different tissues and is possibly regulated by different signaling pathways. In the next sections, I will focus the discussion on the role of miR-185 and Mirta22 in regulating neuronal morphology.

3.3.2 A Neuronal Inhibitor Failed to be Repressed

The reduction in the levels of Mirta22 soon after birth, during periods of active neuronal maturation and synaptogenesis, suggests that repression of this gene may play an important role in promoting neural circuit formation, especially in the postnatal brain after embryonically generated neurons have migrated to their final destinations. Consistent with the notion that miRNAs function predominantly as fine-tuning regulators of the expression levels of their targets (Baek et al., 2008; Selbach et al., 2008), miR-185 and to a lesser extent other miRNAs affected by the 22q11.2 deletion appear to restrict and optimize *Mirta22* expression, presumably to avoid excessive inhibition during this critical stage of synapse formation. Accordingly, sustained derepression of the gene due to genomic loss at the 22q11.2 locus may have an impact on the formation of neural circuits in early development, as well on their maintenance during adulthood. Such structural changes may result in local and long-distance disruptions of neuronal communication that may contribute to the cognitive dysfunction, psychiatric phenotypes or both (Fenelon et al., 2011; Sigurdsson et al., 2010). In agreement with this prediction expression of the human orthologue of *Mirta22* (*C19orf63*) declines in infant brains (Colantuoni et al., 2011) and displays a spatio-temporal pattern that significantly overlaps with that of *Neuroligin-3*, consistent with participation in processes related to synapse and circuit formation and maturation (Kang et al., 2011). Moreover, it has been shown that during the transition between human fetal and early postnatal development a large number of the genes reverse their direction of expression from an increase *in utero* to a decrease in the months after birth and that ~40% of them are predicted miRNA targets (Colantuoni et al., 2011). In that respect, *Mirta22* is one of the first examples of a disease-related gene representative of this prominent

type of transcriptional trajectory. *Mirta22* is also indicative of a miRNA-imposed inhibitory control over postnatal brain development.

3.3.3 Role of miR-185, Mirta22 and Golgi Apparatus in Regulating Neuronal Morphology

miR-185 promotes dendritic and spine growth when overexpressed in both Wt and *Df(16)A*$^{+/-}$ neurons (Figure 3.5G-I, 3.6C). Importantly, fluctuation in miR-185 levels can bidirectionally control neuronal morphogenesis as mir-185 knockdown in Wt neurons phenocopies dendritic and spine deficits seen in *Df(16)A*$^{+/-}$ neurons (Figure 3.5A-F). Therefore miR-185 levels are likely to be tightly controlled during development and in adult brain. Alteration in miR-185 levels has a greater impact on spine development than dendritic development. Both spine density and spine width are dramatically altered by change of miR-185 levels (Figure 3.5D-F, 3.6D). Median spine width is increased by 19% and 25% when pre-miR-185 is applied to Wt and *Df(16)A*$^{+/-}$ neurons respectively, while median spine width is decreased by 15% when anti-miR-185 was applied in Wt neurons. Although miR-185 is not known to be enriched in synapse, it is an intriguing hypothesis that miR-185 has a role in activity-dependent synaptic plasticity in certain contexts, given its potent effects on spine development. Since Mirta22 is an inhibitor of neuronal morphogenesis and Mirta22 levels are strongly controlled by miR-185, it is likely that miR-185 exerts most of the effects on neuronal morphology through repressing Mirta22 expression. On the other hand, increasing miR-185 causes bigger changes of structural features of *Df(16)A*$^{+/-}$ neurons, as compared to decreasing abnormally high levels of Mirta22 in these neurons. Therefore, other targets downstream of miR-185 may contribute to structural deficits in *Df(16)A*$^{+/-}$ neurons, albeit to a lesser degree. In this context, it is noteworthy that RhoA and Cdc42, two members of the Rho GTPase family, are *bona fide* miR-185 targets (Liu et al., 2011). Although we did not detect changes of *RhoA* or *Cdc42* transcripts in microarrays, it is likely because miR-185 negatively regulates RhoA and Cdc42 primarily at the protein level. The Rho family of GTPases are important regulators of cytoskeletal dynamics and membrane trafficking (Benarroch, 2007; Govek et al., 2005), both of which are important determinants for structural modulations. Both RhoA and Cdc42 modulate exocytosis which is important for dendritic and spine growth (Ory and Gasman, 2011). RhoA and Cdc42 have largely opposing effects on actin polymerization and dendritic and spine growth (Benarroch, 2007; Tolias et al., 2011). Whereas RhoA acts through ROCK (Rho-kinase) to induce actomyosin contraction, Cdc42 activates WASP and PAK to promote actin

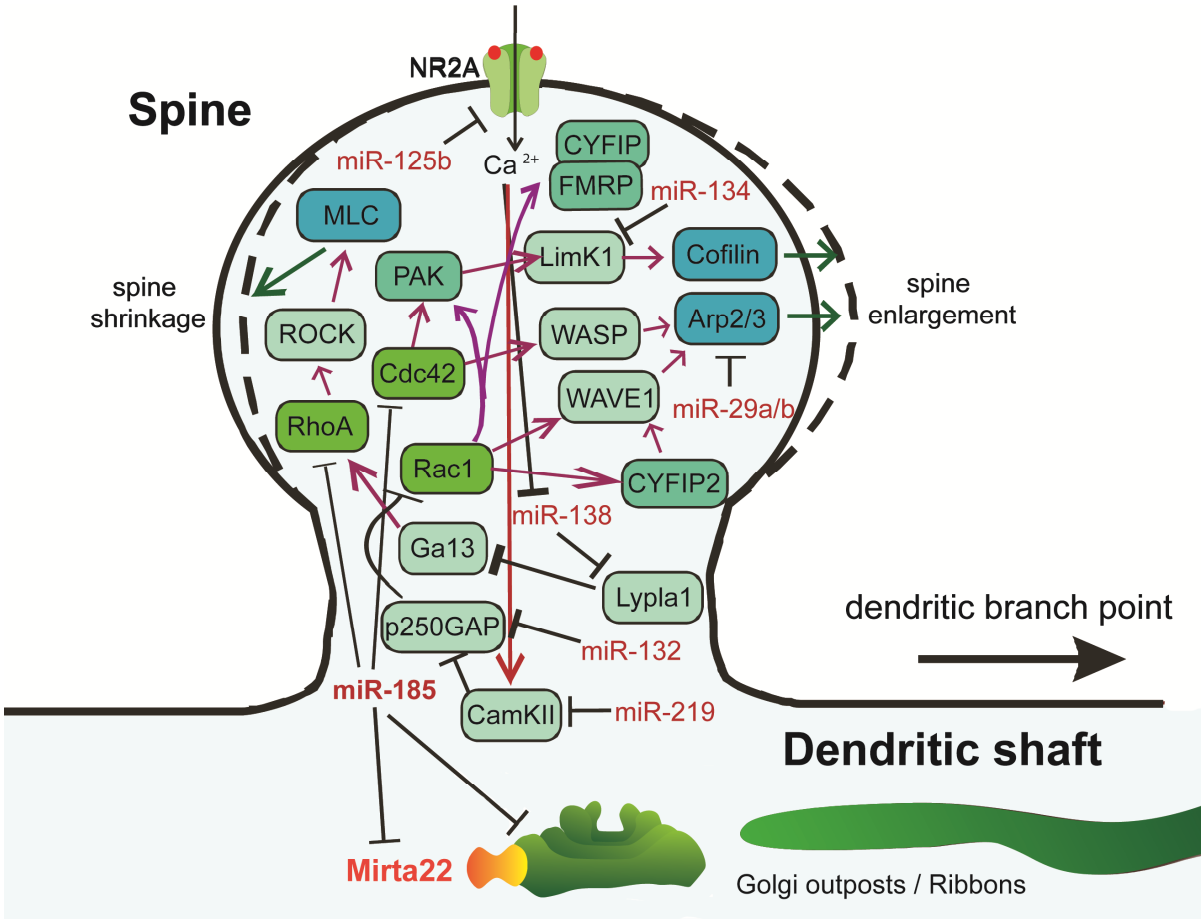

Figure 3.9 MicroRNAs Control Neuronal Morphogenesis through Cytoskeletal Regulations. Activation of Rho family GTPases Rac1 and Cdc42 results in actin polymerization through Arp2/3 and Cofilin, which in turn promotes spinogenesis and maturation. During neuronal activity, calcium influx through NMDA receptor also activates CamKII that inhibit p250GAP and further induce spine growth. By repressing the expression of NR2A, LimK1, Arp2/3 and CamKII respectively, miR-125b, miR-134, miR-29a/b and miR-219 inhibit actin remodeling and spine growth. miR-138 represses Lypla1 which leads to activation of RhoA that also inhibits spine maturation. On the contrary, miR-132 and miR-185 promote spine growth by inhibiting p250GAP and RhoA respectively. miR-185 also represses a novel neuronal morphogenesis inhibitor Mirta22 and a group of genes with Golgi-related function. Golgi outposts and extension of Golgi ribbons into dendrites are shown to regulates dendritic and spine morphogenesis, miR-185 may relieve the suppression of Golgi function by these genes. The exact molecular mechanism remains to be determined. Note that many of these miRNAs also affect dendritic growth through actin and microtubule remodeling (no shown here), for example, miR-132 and miR-185 promote dendritic arborization. The role of miR-134 in dendritic growth is complex and proper dendritic growth seems to require optimal range of miR-134 levels. See Chapter 3.1.1, 3.1.2, 3.3.3 and Table 3.1, 3.2 for details.

nucleation and filament assembly. As a result, RhoA generally inhibits dendritic and spine development, while Cdc42 promotes growth of dendrites and spines. How exactly miR-185 repression affects overall cytoskeletal dynamics remains to be carefully examined. Nevertheless, since multiple miRNAs control downstream targets that are important regulators of actin dynamics, such as Limk1, p250GAP, and Arpc3 (see Chapter 3.1), it is an emerging view that miR-185 and other miRNAs converge on cytoskeletal

regulation to control neuronal morphogenesis (Figure 3.9). Thus miRNAs provide an additional layer for integrating diverse signals downstream of morphogens, neurotrophins and synaptic activity.

Additional miR-185 targets which are only mildly affected by reduced miR-185 levels are likely present and contribute to morphological deficits in *Df(16)A*$^{+/-}$ mice. Indeed, in addition to *Mirta22*, there is hippocampus-specific modest dysregulation (mostly upregulation) of a group of miR-185 target genes with Golgi-related function in *Df(16)A*$^{+/-}$ mice (Figure 3.3). As discussed in Chapter 5.3, the concerted dysregulation of these Golgi-related genes can have a noticeable impact on Golgi function in the adult hippocampus. Furthermore, localization of Mirta22 in the Golgi apparatus and in vesicle and tubular-like extensions in dendrites is consistent with a role in membrane and protein trafficking and secretion, which is necessary for establishment and maintenance of neuronal connections (Horton et al., 2005). Golgi apparatus is found in both soma and dendritic compartment in neurons (Horton and Ehlers, 2004). As hippocampal pyramidal neurons mature, somatic Golgi is polarized toward and extended into the longest dendrite as ribbon-like structures in proximal dendrite (Horton et al., 2005). From proximal to distal dendrite, the Golgi ribbon becomes more fragmented and possibly gives rise to Golgi outposts which accumulate at dendritic branch points along the dendrites. In addition, Golgi membranes were shown to localize to dendritic spines and may regulate spine maintenance (Camera et al., 2008). This dendritic Golgi system mediates forward secretory tracking which is required for supplying proteins crucial for establishing as well as maintaining the proper dendritic morphology (Jan and Jan, 2010; Matsuki et al., 2010; Ramirez and Couve, 2011). Therefore it is conceivable that the elevated expression of neuronal morphology inhibitor Mirta22 coupled with the coordinated dysregulation of Golgi-related genes may affect the distribution of Golgi structures in dendrites. This hypothesis can be tested by future experiments examining the distribution of Golgi extensions and Golgi outposts in *Df(16)A*$^{+/-}$ and Wt neurons. It is suggested that the “non-canonical” route of protein tracking involving the dendritic Golgi system is especially important for some proteins crucial for forming new synapses, such as GluR2 (Horton et al., 2005; Ramirez and Couve, 2011). Thus the hypothesis that Golgi-dependent GluR2 trafficking is compromised in *Df(16)A*$^{+/-}$ neurons is consistent with the previous observation (see Chapter 3.1.3) that the number of GluR2 punta is decreased in these neurons. Certainly how elevated levels of Mirta22 and concerted dysregulation of Golgi-related genes in *Df(16)A*$^{+/-}$ neurons contribute to the morphological deficits of *Df(16)A*$^{+/-}$ neurons warrants further studies.

Mirta22 is also likely to act in concert with other genes within the 22q11.2 deletion (Karayiorgou et al., 2010), including the *Zdhhc8* palmitoyl-transferase, which is also located in the Golgi apparatus and has been shown to modulate dendritic and spine development (Mukai et al., 2008). A potential interaction between miRNA dysregulation and altered neuronal palmitoylation is supported by previous findings (Banerjee et al., 2009; Siegel et al., 2009) and contributions from more than one gene to the morphological phenotypes described in this study are consistent with an oligogenic basis for the psychiatric and cognitive symptoms associated with 22q11.2 microdeletions (Karayiorgou et al., 2010). Future challenges will be to design treatments that restore the genes lost in 22q11.2 microdeletions or to correct the dysregulation of molecular networks (e.g. miRNA regulatory networks) or functional pathways (e.g. Golgi-related function) (see Chapter 5.4).

3.3.4 Implication for Behavioral and Cognitive Impairments in 22q11.2DS

22q11.2DS patients exhibit a number of behavioral and cognitive abnormalities that are characteristic of schizophrenia patients in general (Drew et al., 2011a; Karayiorgou et al., 2010; Philip and Bassett, 2011). Besides psychosis, these abnormalities include attention deficits, anxiety, learning difficulties, memory impairment, and executive dysfunction. These behavioral and cognitive impairments indicate dysfunction in frontal cortical and hippocampal circuitry. It is known that the prefrontal cortex (PFC) is a key hub in the network that manages attention and executive function (Miller and Cohen, 2001), while the hippocampus (HPC) is crucial for learning and seems to be the storage place for short-term memory (Andersen, 2007). In addition, as most learning requires the proper allocation of attention and executive function involves the integration of goal and memory, the communication between the PFC and the HPC is important for proper cognitive function. Although a detailed comparison of neural circuitry in 22q11.2DS patients and normal individuals is lacking, the global cortical thinning and reduction of hippocampal volume likely underlie the cognitive dysfunction in 22q11.2DS (Drew et al., 2011a; Karayiorgou et al., 2010). In particular, reduced hippocampal volume suggests a reduction in neuron number or decreased dendrite arborization or soma size, all of which may lead to imbalance in the hippocampal circuit required for learning and memory.

Analysis of a 22q11.2DS model, *Df(16)A*$^{+/-}$ mice, revealed behavioral and cognitive deficits similar to some of the phenotypes of human patients, including memory impartment in fear conditioning

and working memory deficits in DNMTS task (Stark et al., 2008). In this context, our finding that Mira22 is a negative regulator of dendrite and spine suggests that excitatory transmission is likely attenuated in hippocampus of *Df(16)A*$^{+/-}$ mice and possibly 22q11.2DS patients. This can account for the decreased LTP in Schaffer collateral pathway under a particular stimulation protocol (Drew et al., 2011b). As LTP is thought to be the cellular correlate of learning and memory, decreased number of hippocampal synaptic contacts due to simplified dendritic trees and lower spine density *in vivo* likely limits the capacity for synaptic plasticity and thus compromises cognitive function in *Df(16)A*$^{+/-}$ mice. It remains unclear whether miR-185 and Mirta22 dysregulation affects neuronal morphology in other brain areas, and if so, how altered neuronal morphology in turn causes behavioral and cognitive impairments. As miR-185 reduction results in concerted dysregulation of Golgi-related genes in the hippocampus but not the prefrontal cortex, it is likely that neurons in different brain areas are influenced to a different degree by miR-185 and Mirta22 dysregulation in *Df(16)A*$^{+/-}$ mice. Detailed surveys of neurons in different brain areas in *mmu-mir-185* or *Mirta22* loss-of-function mice will help answer this question. Furthermore, experiments entailing normalization of Mirta22 levels in mice compound heterozygous for *Df(16)A* and *Mirta22* loss-of-function alleles should also establish which of the various behavioral (Stark et al., 2008), cognitive (Drew et al., 2011b; Stark et al., 2008) and circuit alterations (Fenelon et al., 2011; Sigurdsson et al., 2010) observed in *Df(16)A*$^{+/-}$ mice can be attributed to the inhibitory influence of Mirta22 upregulation.

3.4 Summary

We find that Mirta22 is a neuron-specific protein and localizes to the Golgi apparatus. In mature neurons, Mirta22, along with Golgi apparatus, is distributed in dendrites as vesicles and tubular-like clusters. Although Mirta22 represents a major downstream effector of miR-185 dysregulation, our finding of a coordinated miR-185 targeting of Golgi apparatus-related genes suggests that *Mirta22* upregulation may act in an age and brain region specific manner in concert with other modestly altered miR-185 targets to interfere with the Golgi-related processes required for neuronal maturation. miR-185 knockdown or Mirta22 overexpression in Wt neurons phenocopies *Df(16)A*$^{+/-}$ neurons. In contrast, elevation of miR-185 levels and reduction of Mirta22 levels reverse cytoarchitectural alterations of Wt neurons. We conclude that Mirta22 is a neuronal inhibitor of dendritic and spine development and its dysregulation may contribute to cognitive dysfunction. Thus, our findings highlight a link between the

Golgi apparatus and neuronal phenotypes associated with 22q11.2 microdeletions. The molecular mechanism of Mirta22 action in regulating neuronal morphogenesis remains obscure and needs to be deciphered.

Table 3.1 MicroRNA Regulation of Dendritic Complexity

Dendritic Phenotypes				
MicroRNA	**Manipulation**	**Target(s)**	**Morphological Phenotypes**	**Refs**
miR-132	Overexpression and inhibition	**p250GAP**	Expression promotes neurite sprouting from cultured cortical neurons	1
miR-132	Deletion in DG		Drastically decreased in dendritic arborization	2
miR-132	Overexpression and inhibition	**p250GAP**	Activity-induced dendritogenesis is blocked by miR-132 inhibition in cultured hippocampal neurons and organotypic hippocampal slices	3
miR-134	AAV-mediated OE in HPC		Mildly decreased in length and complexity of layer V cortical pyramidal neurons	4
miR-134	Overexpression	**Chrdl-1**	Mildly decreased dendritic complexity; increased complexity w/ BMP-4 in cultured cortical neurons	5
miR-134	Overepxression and inhibition	**Pumilio2**	Both overexpression and inhibition impairs activity-induced dendritogenesis in cultured hippocampal neurons	6
miR-381, miR-329 (miR-379–miR-410 cluster)	Inhibition		Impaired activity-induced dendritogenesis in cultured hippocampal neurons	6
miR-375	Lentivirus-mediated OE in HPC	**HuD**	Decreased dendritic complexity in DG granular cells	7
miR-124	Overexpression and inhibition	**Cdc42**	Expression increases the number of primary neuritis in cultured cortical neurons	8
let-7, miR-124, miR-125, miR-132	Inhibition		Decreased dendritic branching in cultured hippocampal neurons	9

DG: Dentate gyrus, HPC: hippocampus, OE: overexpression, AAV: adeno-associated virus.

References: 1. (Vo et al., 2005), 2. (Magill et al., 2010), 3. (Wayman et al., 2008), 4. (Christensen et al., 2010), 5. (Gaughwin et al., 2011), 6. (Fiore et al., 2009), 7. (Abdelmohsen et al., 2010), 8. (Yu et al., 2008), 9. (Edbauer et al., 2010), 10. (Schratt et al., 2006), 11. (Siegel et al., 2009), 12. (Impey et al., 2010), 13. (Luikart et al., 2011), 14. (Hansen et al., 2010), 15. (Mellios et al., 2011), 16. (Cohen et al., 2011), 17. (Lippi et al., 2011)

Table 3.2 MicroRNA Regulation of Spine Growth and Maturation

Spine Phenotypes				
MicroRNA	**Manipulation**	**Target(s)**	**Morphological Phenotypes**	**Refs**
miR-134	Overexpression and inhibition	**Limk1**	Expression decreases spine width in cultured hippocampal neurons	10
miR-138	Overexpression and inhibition	**Lypla1 (APT1)**	Expression increases spine volume in cultured hippocampal neurons	11
miR-125b	Overexpression and inhibition	**NR2A**	Overexpression increases spine length but decreases width; inhibition decreases spine width	9
miR-132	Overexpression and inhibition		Overexpression increases spine width; inhibition has no effect	9
miR-132	Overexpression and inhibition	**p250GAP**	Overexpression is sufficient to increase spine density; inhibition blocks activity-induced spinogenesis	12
miR-132	Retrovirus-mediated inhibition in HPC		Mildly decreased spine density in newborn DG neurons	13
miR-132	Transgenic miR-132 OE		Increased spine density in CA1 pyramidal neurons	14
miR-132	Lentivirus-mediated inhibition in visual cortex		A decrease in mushroom and stubby spines and an increase in thin spines and filopodia of layer V pyramidal neurons	15
let-7, miR-22, miR-124	Overexpression and inhibition		Overexpression has no effect; inhibition increases spine width (all) and length (let-7)	9
miR-485	Overexpression and inhibition	**SV2A**	Expression decreases spine density in hippocampal neurons	16
miR-29a/b	Overexpression	**Arpc3**	Decreased mushroom spine density and increased filopodia density in cultured hippocampal neurons	17

OE: overexpression, HPC: hippocampus.

References: 1. (Vo et al., 2005), 2. (Magill et al., 2010), 3. (Wayman et al., 2008), 4. (Christensen et al., 2010), 5. (Gaughwin et al., 2011), 6. (Fiore et al., 2009), 7. (Abdelmohsen et al., 2010), 8. (Yu et al., 2008), 9. (Edbauer et al., 2010), 10. (Schratt et al., 2006), 11. (Siegel et al., 2009), 12. (Impey et al., 2010), 13. (Luikart et al., 2011), 14. (Hansen et al., 2010), 15. (Mellios et al., 2011), 16. (Cohen et al., 2011), 17. (Lippi et al., 2011)

Table 3.3 Altered Expression of Predicted miR-185 Targets with Golgi-related Functions

Rank	AffyID	Gene Symbols	P.Value	logFC
31	1425690_at	B3gat1	3.94E-09	0.478
52	1420833_at	Vamp2	2.92E-07	0.607
66	1425691_at	B3gat1	6.47E-07	0.319
70	1421270_at	Sh3rf1	7.53E-07	0.391
117	1421890_at	St3gal2	3.97E-06	0.292
176	1423228_at	B4galt6	1.23E-05	0.286
192	1450105_at	Adam10	1.48E-05	0.28
199	1422758_at	Chst2	1.57E-05	0.296
201	1421271_at	Sh3rf1	1.58E-05	0.276
216	1450913_at	B4galt6	1.80E-05	0.291
340	1448367_at	Sdf4	5.34E-05	0.267
458	1450153_at	Gopc	9.82E-05	0.233
493	1421978_at	Gad2	1.16E-04	0.437
535	1431646_a_at	Stx6	1.42E-04	0.215
647	1422718_at	Ap3s2	2.27E-04	0.236
726	1450247_a_at	Scamp5	3.09E-04	0.255
730	1449111_a_at	Grb2	3.13E-04	0.217
734	1423720_a_at	Sar1a	3.16E-04	0.292
825	1428398_at	B3galt5	4.25E-04	0.224
845	1416437_a_at	Mapk8ip3	4.48E-04	0.238
914	1431320_a_at	Myo5a	5.23E-04	0.179
923	1427481_a_at	Atp1a3	5.33E-04	0.198
1018	1421891_at	St3gal2	6.61E-04	0.194
1029	1449943_at	Lfng	6.74E-04	0.312
1155	1422664_at	Rab10	8.79E-04	0.183
1270	1437107_at	Rab6b	1.08E-03	0.395
1304	1426744_at	Srebf2	1.14E-03	0.295
1338	1428374_at	Glce	1.20E-03	0.164
1354	1438373_at	App	1.22E-03	-0.21
1387	1431120_a_at	Golga1	1.28E-03	0.259
1430	1420643_at	Lfng	1.37E-03	0.283
1450	1419190_at	Vti1a	1.41E-03	0.217
1464	1424633_at	Camk1g	1.44E-03	0.161
1502	1443220_at	NA	1.50E-03	0.217
1589	1422044_at	Ndst1	1.68E-03	0.352
1694	1429296_at	Rab10	1.93E-03	0.166
1739	1433571_at	Serinc5	2.05E-03	-0.245
1805	1449129_a_at	Kcnip3	2.18E-03	0.161
1822	1420262_at	NA	2.25E-03	-0.203
2003	1448309_at	Ap3m1	2.74E-03	0.196
2042	1423075_at	Lman2	2.85E-03	0.17
2217	1431053_at	Mphosph9	3.37E-03	0.257
2246	1435758_at	B4galt6	3.45E-03	0.158
2257	1424755_at	Hip1	3.51E-03	0.264
2414	1416550_at	Slc35b4	4.08E-03	0.135
2516	1432017_at	Hip1	4.47E-03	-0.146
2712	1436321_at	B3gnt7	5.02E-03	-0.185
2740	1432054_at	Golga1	5.13E-03	0.244
2995	1451484_a_at	Syn1	6.13E-03	0.13
3025	1452174_at	Srebf2	6.30E-03	0.132
3093	1439853_at	B4galnt2	6.58E-03	-0.181
3148	1455924_at	Rab6b	6.85E-03	0.145
3281	1431066_at	Fut11	7.49E-03	0.187
3345	1450730_at	Hs2st1	7.76E-03	0.177
3358	1450104_at	Adam10	7.83E-03	0.144
3427	1457356_at	NA	8.17E-03	-0.17
3683	1416459_at	Arf2	9.41E-03	0.119
3710	1428397_at	B3galt5	9.58E-03	0.156
3722	1460191_at	Ykt6	9.65E-03	0.144
3788	1436155_at	Nmnat2	1.01E-02	0.145
3822	1457045_at	Galnt13	1.03E-02	0.251
3826	1423743_at	Arcn1	1.03E-02	0.148
3969	1448477_at	Chst12	1.10E-02	0.113
3986	1415670_at	Copg	1.11E-02	0.124
3998	1419754_at	Myo5a	1.12E-02	0.134
4049	1444943_at	NA	1.14E-02	-0.184
4089	1423358_at	Ece2	1.16E-02	-0.207
4101	1444413_at	Ap3s2	1.17E-02	0.255
4459	1436525_at	Ap3s2	1.39E-02	0.135
4584	1455986_at	Zdhhc17	1.48E-02	0.245
4608	1423229_at	Inpp5e	1.49E-02	0.119
4656	1436193_at	Man1c1	1.52E-02	0.099
4708	1435762_at	Pacs1	1.55E-02	0.153
4795	1453095_at	Rab10	1.60E-02	0.094

Rank	AffyID	Gene Symbols	P.Value	logFC
4866	1434945_at	Lpcat2	1.66E-02	-0.1
4905	1443398_at	NA	1.68E-02	0.308
5038	1426575_at	Sgms1	1.77E-02	0.185
5075	1449063_at	Sec22b	1.80E-02	0.125
5154	1440684_at	Lpcat2	1.85E-02	-0.121
5157	1460329_at	B4galt6	1.85E-02	0.086
5225	1443842_at	Arfgef2	1.90E-02	0.133
5582	1430966_at	Cml3	2.16E-02	-0.158
5633	1460070_at	NA	2.20E-02	0.13
5663	1455735_at	Ap1s3	2.22E-02	0.129
5664	1418508_a_at	Grb2	2.22E-02	0.101
5671	1425363_at	B4galnt1	2.22E-02	-0.122
5681	1422468_at	Ppt1	2.23E-02	0.133
5811	1416549_at	Slc35b4	2.33E-02	0.107
5837	1422129_at	Apc2	2.36E-02	0.114
5882	1425539_a_at	Rtn3	2.40E-02	0.108
6004	1447834_at	NA	2.51E-02	-0.162
6169	1423167_at	Mobkl3	2.63E-02	0.117
6247	1445103_at	NA	2.70E-02	-0.101
6461	1454865_at	Slc9a8	2.88E-02	0.11
6526	1424112_at	Igf2r	2.94E-02	0.126
6637	1451837_at	Ap3b2	3.04E-02	-0.111
6756	1459801_at	B3galt5	3.16E-02	-0.185
6868	1457316_at	Mtap6	3.24E-02	0.133
6882	1428150_at	Coro7	3.26E-02	0.105
6950	1426704_at	Gak	3.33E-02	-0.118
6971	1426576_at	Sgms1	3.35E-02	0.113
7015	1426274_at	Slc9a8	3.39E-02	0.194
7049	1453221_at	Gopc	3.42E-02	0.095
7088	1450729_at	Hs2st1	3.45E-02	0.116
7283	1458363_at	Zdhhc17	3.61E-02	0.114
7303	1423152_at	Vapb	3.63E-02	0.314
7426	1429661_at	Rhobtb3	3.74E-02	0.173
7435	1431136_at	Rab36	3.75E-02	0.141
7450	1447012_at	Gm10791	3.76E-02	-0.127
7669	1459144_at	NA	3.97E-02	-0.093
7928	1426703_at	Gak	4.23E-02	0.092
7956	1418582_at	Cbfa2t3	4.26E-02	0.102
8007	1458501_at	Vapb	4.31E-02	0.169

Rank	AffyID	Gene Symbols	P.Value	logFC
8158	1428149_at	Coro7	4.48E-02	0.162
8286	1460322_at	Chst3	4.60E-02	-0.114
8611	1448308_at	Ap3m1	4.93E-02	0.094
8746	1419189_at	Vti1a	5.07E-02	0.079
8831	1450384_at	Bace1	5.15E-02	0.086
8939	1423038_at	Stx6	5.28E-02	0.078
8968	1442028_at	B4galnt2	5.30E-02	-0.138
9185	1458189_at	Emid2	5.57E-02	-0.111
9251	1448464_at	Ykt6	5.63E-02	0.087
9285	1439610_at	Rab27b	5.68E-02	0.128
9324	1441216_at	St3gal1	5.73E-02	-0.124
9331	1421825_at	Bace1	5.74E-02	0.116
9491	1425876_a_at	Glce	5.92E-02	0.174
9552	1424856_at	Atp1a3	5.98E-02	-0.098
9608	1442234_at	Chst2	6.05E-02	0.127
9850	1416548_at	Slc35b4	6.36E-02	0.098
9907	1435718_at	Ap3s2	6.42E-02	0.069
9932	1416375_at	Ap3m1	6.45E-02	0.163
10029	1421892_at	St3gal2	6.58E-02	0.117
10410	1424708_at	Tmed10	7.12E-02	0.159
10733	1416374_at	Ap3m1	7.55E-02	0.087
10817	1450509_at	Chst11	7.66E-02	0.126
10868	1454821_at	B3gat1	7.75E-02	0.077
10928	1436676_at	Mapk8ip3	7.84E-02	-0.092
11304	1435199_at	Apc2	8.31E-02	0.182
11552	1415958_at	Slc2a4	8.65E-02	-0.131
11608	1452471_at	Il17rd	8.73E-02	-0.13
11746	1443857_at	Hook3	8.90E-02	0.138
11832	1436471_at	Rab36	9.03E-02	-0.073
11896	1445688_at	NA	9.12E-02	-0.093
11919	1419909_at	Mphosph9	9.17E-02	-0.094
12475	1433630_at	Map6d1	9.98E-02	0.068
12508	1428044_at	Ap3s2	1.00E-01	-0.102
12518	1428902_at	Chst11	1.00E-01	0.084
12643	1417215_at	Rab27b	1.02E-01	0.104
12745	1460083_at	Adam10	1.04E-01	-0.073
12789	1423759_a_at	Tmco1	1.04E-01	0.078
12811	1435801_at	Fktn	1.05E-01	0.101
12906	1427020_at	Scara3	1.06E-01	0.125

Rank	AffyID	Gene Symbols	P.Value	logFC
12922	1430549_at	Bet1l	1.07E-01	0.107
13027	1425316_at	B3gat1	1.08E-01	-0.106
13056	1446049_at	NA	1.09E-01	-0.096
13109	1418946_at	St3gal1	1.09E-01	0.091
13608	1453227_at	Rhobtb3	1.17E-01	0.105
13625	1437748_at	Fut11	1.17E-01	0.103
13687	1418929_at	Ift57	1.18E-01	0.084
13889	1419186_a_at	St8sia4	1.22E-01	-0.075
13935	1447656_at	Zdhhc17	1.22E-01	-0.109
13967	1418655_at	B4galnt1	1.23E-01	0.106
13968	1423647_a_at	Zdhhc3	1.23E-01	0.063
14000	1448404_at	Scamp2	1.23E-01	0.139
14073	1438008_at	Gga3	1.25E-01	0.094
14264	1440011_at	NA	1.27E-01	-0.176
14265	1445374_at	NA	1.28E-01	-0.07
14657	1451036_at	Spg21	1.34E-01	0.105
14708	1420928_at	St6gal1	1.35E-01	0.093
14715	1428367_at	Ndst1	1.35E-01	0.092
14960	1439094_at	Cltc	1.39E-01	-0.116
15016	1450528_at	B3galt5	1.40E-01	0.129
15062	1451017_at	Ergic3	1.40E-01	-0.064
15117	1421853_at	Psen1	1.41E-01	0.072
15173	1450844_at	Stx6	1.43E-01	0.06
15267	1452657_at	Ap1s2	1.44E-01	0.054
15301	1438063_at	Mphosph9	1.45E-01	0.107
15413	1458296_at	NA	1.47E-01	-0.147
15447	1443881_at	Pofut1	1.48E-01	0.064
15609	1442463_at	NA	1.50E-01	0.101
15617	1456655_at	NA	1.50E-01	-0.09
15685	1424111_at	Igf2r	1.52E-01	0.062
15742	1442904_at	Chst2	1.53E-01	-0.144
16001	1415766_at	Sec22b	1.57E-01	0.075
16220	1439922_at	Prrc1	1.61E-01	0.117
16277	1421155_at	B3galt6	1.62E-01	0.067
16372	1424707_at	Tmed10	1.64E-01	0.063
16416	1435679_at	Optn	1.65E-01	-0.075
16561	1418544_at	Kcnip3	1.67E-01	0.055
16664	1447347_at	NA	1.69E-01	-0.117
16694	1454982_at	Arfgef2	1.69E-01	0.064
16773	1435982_at	Stx12	1.71E-01	-0.065
17109	1434123_at	Fut11	1.77E-01	-0.052
17199	1440585_at	Stx6	1.78E-01	-0.086
17742	1429778_at	Optn	1.90E-01	0.114
18074	1420621_a_at	App	1.96E-01	0.054
18150	1417327_at	Cav2	1.97E-01	0.093
18184	1440014_at	NA	1.98E-01	-0.102
18225	1455368_at	Zdhhc3	1.99E-01	0.074
18374	1440979_at	Igf2r	2.02E-01	-0.047
18470	1446737_a_at	Hook3	2.04E-01	0.095
18685	1436051_at	Myo5a	2.08E-01	0.057
18823	1442079_at	Sgms1	2.11E-01	-0.058
18878	1416086_at	Tpst2	2.12E-01	0.059
19009	1423168_at	Mobkl3	2.14E-01	0.046
19055	1425549_at	Psen1	2.15E-01	0.07
19058	1420832_at	Qsox1	2.15E-01	-0.061
19193	1448936_at	Stx12	2.19E-01	0.054
19621	1440963_at	Cbfa2t3	2.28E-01	-0.069
19946	1445009_at	NA	2.34E-01	-0.072
20048	1420016_at	Ppt1	2.37E-01	-0.063
20091	1426393_a_at	Sdf4	2.37E-01	0.066
20302	1426886_at	Cln5	2.42E-01	-0.072
20382	1440915_at	Mphosph9	2.44E-01	0.108
20406	1422467_at	Ppt1	2.44E-01	0.057
20483	1438566_at	St8sia6	2.46E-01	-0.08
20589	1427442_a_at	App	2.49E-01	0.041
20638	1431325_at	Cml3	2.50E-01	0.083
20681	1420112_at	NA	2.51E-01	-0.054
20768	1444275_at	NA	2.52E-01	-0.07
21064	1452515_a_at	Xylt2	2.60E-01	-0.063
21300	1420927_at	St6gal1	2.65E-01	0.075
21507	1446617_at	NA	2.70E-01	-0.066
21565	1460436_at	Ndst1	2.72E-01	0.05
21605	1458920_at	NA	2.73E-01	0.116
21742	1415696_at	Sar1a	2.76E-01	0.057
21867	1418129_at	Dhcr24	2.80E-01	0.137
21870	1455584_at	Sdf4	2.80E-01	0.053
22017	1432230_at	Hip1	2.83E-01	-0.069
22036	1446696_at	Ift57	2.84E-01	-0.123

Rank	AffyID	Gene Symbols	P.Value	logFC
22131	1434397_at	Zdhhc17	2.86E-01	0.051
22165	1455741_a_at	Ece1	2.87E-01	0.05
22331	1436192_at	Arfgef2	2.91E-01	0.058
22341	1460431_at	Gcnt1	2.91E-01	0.095
22363	1440905_at	Hs2st1	2.91E-01	-0.077
22645	1436664_a_at	Slc35a2	2.98E-01	0.042
22797	1425031_at	Fktn	3.02E-01	0.051
22906	1451215_at	Prrc1	3.05E-01	0.048
23037	1451089_a_at	Arcn1	3.08E-01	0.035
23265	1439876_at	Vti1a	3.14E-01	-0.061
23269	1430904_at	Arfgap3	3.14E-01	-0.075
23324	1436062_at	Arcn1	3.15E-01	0.045
23558	1436956_at	NA	3.22E-01	-0.053
23566	1436101_at	NA	3.22E-01	0.044
23601	1453858_at	Slc35a2	3.23E-01	-0.044
23760	1424746_at	Kif1c	3.27E-01	0.069
23774	1439877_at	NA	3.27E-01	-0.098
23978	1449538_a_at	Gcnt1	3.32E-01	-0.06
24169	1458524_at	Fndc3a	3.37E-01	-0.073
24233	1457968_at	NA	3.38E-01	0.064
24321	1440457_at	NA	3.41E-01	-0.056
24330	1450137_at	Pofut1	3.41E-01	0.054
24445	1421609_a_at	Cml3	3.44E-01	0.048
24546	1422687_at	Nras	3.47E-01	0.041
24588	1418774_a_at	Atp7a	3.48E-01	-0.077
24690	1435157_at	Hook3	3.51E-01	0.034
24721	1432631_at	Prrc1	3.51E-01	-0.06
24887	1434316_at	NA	3.56E-01	-0.055
24932	1420821_at	Sgpp1	3.57E-01	-0.1
24999	1440340_at	B3galt6	3.59E-01	-0.062
25088	1434557_at	Hip1	3.61E-01	0.055
25240	1425128_at	B3gnt8	3.65E-01	-0.075
25460	1439433_a_at	Slc35a2	3.71E-01	0.074
25610	1422622_at	Nos3	3.75E-01	0.076
25660	1458342_at	Tmem90a	3.76E-01	0.078
25735	1443863_at	Fndc3a	3.78E-01	-0.039
25921	1424747_at	Kif1c	3.82E-01	-0.043
25932	1426903_at	Fndc3a	3.83E-01	0.038
26127	1455826_a_at	Bace1	3.88E-01	0.055
26230	1446314_at	Gcnt7	3.92E-01	-0.053
26239	1450399_at	Psen1	3.92E-01	0.035
26692	1423074_at	Lman2	4.05E-01	0.036
26788	1453393_a_at	Chst4	4.07E-01	-0.037
26884	1417730_at	Ext1	4.10E-01	0.046
27080	1425955_at	Cav2	4.15E-01	-0.053
27188	1434914_at	Rab6b	4.18E-01	0.033
27310	1424894_at	Rab13	4.20E-01	0.037
27493	1444873_at	NA	4.25E-01	-0.048
27548	1439899_at	Galnt13	4.27E-01	-0.06
27767	1458608_at	NA	4.33E-01	-0.046
27770	1423230_at	Inpp5e	4.33E-01	0.055
27794	1444705_at	NA	4.34E-01	-0.071
28091	1439417_at	Qsox1	4.43E-01	0.051
28164	1416828_at	Snap25	4.45E-01	-0.035
28323	1440386_at	Glce	4.50E-01	-0.038
28342	1459654_at	NA	4.50E-01	0.043
28620	1444563_at	NA	4.58E-01	-0.045
28728	1431761_at	Entpd4	4.61E-01	-0.048
28771	1441423_at	Ece1	4.62E-01	-0.048
28825	1426372_a_at	Bet1l	4.64E-01	0.026
29026	1451224_at	Scamp5	4.70E-01	0.031
29052	1444361_at	Ap1s2	4.71E-01	0.05
29079	1428147_at	Coro7	4.71E-01	0.038
29100	1420902_at	St6galnac3	4.72E-01	0.065
29292	1422550_a_at	Mtap6	4.78E-01	0.033
29339	1438661_a_at	Arf2	4.79E-01	0.054
29538	1439196_at	Hook3	4.85E-01	0.045
29727	1454626_at	Cltc	4.91E-01	0.025
29739	1458084_at	Zdhhc17	4.91E-01	-0.029
30054	1454077_at	Vti1a	5.00E-01	-0.03
30521	1418195_at	Galnt10	5.12E-01	0.056
30636	1458897_at	Ust	5.16E-01	0.036
30681	1422980_a_at	Bet1l	5.18E-01	0.038
31145	1459097_at	NA	5.32E-01	0.038
31455	1427617_at	Fut10	5.41E-01	-0.032
31508	1435027_at	Golga1	5.43E-01	0.022
31615	1459707_at	NA	5.46E-01	-0.027
31807	1426325_at	Kif1c	5.51E-01	0.034

Rank	AffyID	Gene Symbols	P.Value	logFC
32077	1444102_at	NA	5.60E-01	0.033
32304	1438355_at	Tmem90a	5.67E-01	0.029
32464	1446624_at	Fktn	5.72E-01	-0.037
32703	1421522_at	B4galnt2	5.79E-01	-0.038
32779	1439218_at	NA	5.81E-01	-0.049
32833	1415959_at	Slc2a4	5.83E-01	-0.038
32882	1437388_at	Fut10	5.84E-01	0.035
32946	1416591_at	Rab34	5.86E-01	-0.028
32960	1416590_a_at	Rab34	5.87E-01	-0.024
33007	1416760_at	Galntl1	5.88E-01	0.023
33138	1432819_at	Prrc1	5.93E-01	-0.032
33158	1416611_at	Scamp2	5.94E-01	0.022
33175	1447235_at	NA	5.94E-01	0.033
33517	1455149_at	Sh3rf1	6.04E-01	0.035
33813	1432818_at	Prrc1	6.14E-01	0.029
34235	1421824_at	Bace1	6.27E-01	0.018
34412	1445505_at	Ndst1	6.32E-01	0.023
34607	1436865_at	Slc26a11	6.39E-01	-0.032
34680	1431549_at	NA	6.41E-01	-0.038
34744	1416017_at	Copg	6.44E-01	0.022
34779	1436499_at	Sgms1	6.45E-01	0.026
34819	1452365_at	Csgalnact1	6.47E-01	0.027
34832	1454924_at	Fut10	6.47E-01	0.027
34887	1451825_a_at	Copz1	6.49E-01	-0.017
35005	1441133_at	NA	6.52E-01	-0.023
35022	1429589_at	Gad2	6.52E-01	-0.019
35229	1429652_at	Prrc1	6.59E-01	0.026
35272	1430391_a_at	St8sia4	6.60E-01	0.029
35397	1453032_at	Mobkl3	6.64E-01	0.019
35670	1420333_at	Txndc8	6.74E-01	0.028
35685	1441993_at	Ap3s2	6.75E-01	-0.019
35814	1458616_at	NA	6.80E-01	0.019
35954	1416199_at	Kifc3	6.84E-01	-0.021
36001	1444884_at	Ppt1	6.86E-01	0.019
36267	1445966_at	NA	6.95E-01	-0.029
36278	1418014_a_at	B4galt1	6.95E-01	0.022
36301	1421967_at	B4galt5	6.96E-01	0.025
36355	1441148_at	NA	6.98E-01	0.027
36408	1459970_at	NA	7.00E-01	-0.021
36487	1437998_at	Ap1s2	7.03E-01	-0.02
36607	1458773_at	NA	7.07E-01	-0.021
36699	1453929_at	Rnf24	7.10E-01	0.032
36742	1438252_at	Qsox1	7.12E-01	-0.014
36795	1425310_a_at	Emid2	7.13E-01	-0.021
36894	1417214_at	Rab27b	7.16E-01	0.022
37011	1454060_a_at	Nras	7.20E-01	0.022
37023	1445178_at	Sh3rf1	7.20E-01	0.05
37039	1451895_a_at	Dhcr24	7.21E-01	-0.015
37096	1420261_at	Psen1	7.23E-01	-0.015
37194	1422739_at	Hs2st1	7.26E-01	0.022
37503	1420831_at	Qsox1	7.35E-01	-0.026
37522	1427923_at	Zmpste24	7.36E-01	0.018
37524	1419910_at	Mphosph9	7.36E-01	-0.019
37638	1424058_at	Prrc1	7.41E-01	-0.021
37757	1458054_at	Ext1	7.45E-01	-0.022
37768	1456147_at	St8sia6	7.45E-01	0.035
37836	1429893_at	Il17rd	7.47E-01	0.019
38090	1446739_at	NA	7.56E-01	0.023
38187	1458258_at	NA	7.60E-01	0.012
38215	1447763_at	NA	7.61E-01	-0.017
38284	1436797_a_at	Surf4	7.63E-01	0.016
38293	1440493_at	Galnt10	7.63E-01	-0.02
38312	1460036_at	Ap1s2	7.64E-01	-0.052
38364	1440092_at	NA	7.66E-01	-0.028
38429	1444411_at	NA	7.68E-01	-0.025
38435	1419320_at	Chst5	7.69E-01	-0.02
38548	1418130_at	Dhcr24	7.73E-01	-0.015
38586	1436224_at	Kif1c	7.74E-01	0.019
38629	1423646_at	Zdhhc3	7.76E-01	-0.011
38767	1438705_at	Cbfa2t3	7.80E-01	0.017
38795	1442365_at	NA	7.81E-01	-0.019
38806	1440121_at	NA	7.82E-01	0.032
38913	1421517_at	St6galnac1	7.85E-01	-0.011
39243	1426927_at	Ap3b2	7.98E-01	-0.011
39548	1424561_at	Ece2	8.08E-01	-0.014
39772	1418101_a_at	Rtn3	8.15E-01	-0.008
40008	1424979_at	Aph1a	8.24E-01	0.014
40539	1423609_a_at	Mgat1	8.42E-01	0.007

Rank	AffyID	Gene Symbols	P.Value	logFC
40735	1415672_at	Golga7	8.48E-01	-0.008
40782	1456323_at	Pofut1	8.50E-01	-0.012
40839	1443082_at	NA	8.52E-01	-0.01
41035	1434862_at	Fut2	8.58E-01	-0.009
41074	1428103_at	Adam10	8.59E-01	-0.01
41243	1457009_at	Rhobtb3	8.65E-01	0.014
41365	1432533_a_at	Slc35a2	8.70E-01	0.009
41408	1436921_at	Atp7a	8.71E-01	0.016
41588	1446365_at	Vti1a	8.77E-01	-0.014
41613	1420834_at	Vamp2	8.78E-01	0.007
41628	1451853_at	Fktn	8.79E-01	0.007
41685	1452366_at	Csgalnact1	8.81E-01	0.008
41705	1435252_at	B3galt6	8.81E-01	0.008
41726	1438897_at	Zdhhc3	8.82E-01	-0.009
41824	1457583_at	NA	8.86E-01	-0.012
42111	1425975_a_at	Mapk8ip3	8.96E-01	-0.006
42167	1450246_at	Fut2	8.97E-01	0.006
42229	1448255_a_at	Surf4	9.00E-01	0.006
42245	1449432_a_at	Mmel1	9.00E-01	-0.006
42495	1443141_at	NA	9.08E-01	0.005

Rank	AffyID	Gene Symbols	P.Value	logFC
42617	1450497_at	Apc2	9.13E-01	-0.008
42710	1434177_at	Ece1	9.16E-01	-0.006
42987	1445466_at	Map6d1	9.26E-01	-0.007
43014	1445838_at	NA	9.26E-01	0.004
43082	1431941_at	Slc35b4	9.29E-01	0.005
43387	1431205_at	Slc9a8	9.40E-01	0.004
43455	1430932_at	Slc9a8	9.43E-01	0.004
43457	1416458_at	Arf2	9.43E-01	0.004
43643	1418194_at	Galnt10	9.50E-01	0.003
43797	1458179_at	NA	9.55E-01	0.003
43822	1422688_a_at	NA	9.56E-01	0.003
44117	1442402_at	Sh3rf1	9.66E-01	-0.003
44298	1455064_at	Rab36	9.72E-01	-0.002
44305	1445224_at	NA	9.73E-01	0.002
44314	1420903_at	St6galnac3	9.73E-01	-0.002
44475	1451554_a_at	Aph1a	9.78E-01	-0.004
44677	1424756_at	Hip1	9.85E-01	-0.001
44797	1449737_at	NA	9.89E-01	0.001
44798	1458525_at	NA	9.89E-01	-0.001
44883	1443581_at	St6gal1	9.92E-01	-0.001

3.5 Methods

3.5.1 Generation of Mirta22 Antibody

A 20 amino acid peptide ([C]- CEQAQKAKNPQEQKSFFAKY -[N]) was designed, synthesized and conjugated to KLH (Keyhole Limpet Hemocyanin) and then injected into rabbits using Covance custom antibody production service (Covance). Antibody serum was then purified using Melon Gel IgG purification Kit (Thermo Scientific) and the purified antibody was tested by Western blot (1:50), immunohistochemistry and immunocytochemistry assays (1:25).

In western blot assays of 293T cell lysates, the purified antibody specifically recognized overexpressed full length Mirta22 tagged with C-terminal FLAG (~28 kD), which was independently verified using both polyclonal and monoclonal anti-FLAG antibodies (Figure 3.2A). The specificity of the antibody was tested in western blot assays of protein extracts from N18 cells transfected with a *2310044H10Rik* shRNA or a full length *2310044H10Rik* cDNA plasmid. The intensity of the band at ~28 kD, changed as predicted for each manipulation (Figure 3.2B,C). Finally, when used to stain cultured neurons the antibody generated a specific staining pattern whereas the pre-immune serum failed to show signal (Figure 3.2D).

3.5.2 Western Blot

Hippocampus (HPC) or prefrontal cortex (PFC) from 8-wk old mice were isolated and homogenized in ice-old modified RIPA buffer containing 1% Triton X-100, 0.1% SDS, 0.5% Sodium Deoxycholate, 150 mM NaCl and 50 mM Tris pH 8.0 and Proteinase inhibitor cocktail (Roche). Homogenates were centrifuged at 12,000 x g at 4℃ for 30 min. The supernatant was saved and the protein concentration in each sample was determined by DC Protein Assay (Bio-Rad). An aliquot of the supernatant equivalent to 20 µg protein was resolved on 4–12% polyacrylamide gel (Bio-Rad) and then transferred onto an ECF plus membrane (Amersham Biosciences) or Immobilon-FL membrane (Millipore). The membrane was first blocked by 5% nonfat dry milk in PBS buffer containing 0.5% Tween-20 for 1 h at room temperature. The membrane was then washed three times with the same buffer and then treated with 1:50 dilution of purified Mirta22. The membrane was washed again with the same buffer three times, treated with 1:5000 dilution of horseradish peroxidase conjugated secondary antibody for 1 h at room

temperature and then washed thoroughly. The washed membrane was incubated with HRP substrate (Western Lightning Chemiluminescence Reagent, PerkinElmer Life Sciences) for 1 min, and chemiluminescence images were obtained using Alpha imaging system. The membrane was then stripped by Restore Western Blot Stripping Buffer (Thermo Scientific) and re-probed with 1: 5000 dilution of α-tubulin antibody (T5168, Simga-Aldrich) as a loading control, using the same procedure described above. Protein bands were subjected to densitometric analysis with NIH Image J.

3.5.3 Neuronal Culture and Transfection

Dissociated hippocampal neurons were isolated from E17 mouse embryos and plated at 2 x 10^5 cells/ml in 6-well plates containing glass coverslips coated with poly-D-lysine. Neurons were cultured for 9 – 19 days, depending on the experiments. Two independent pRFP-C-2310044H10Rik shRNAs (FI587489 and FI587487) and pRFP-C-scramble shRNA control (Origene), *2310044H10Rik* (*Mirta22*) cDNA clone (Origene), as well as pre-miR-185 mimic and pre-scramble control (Ambion) were used for high efficiency calcium-phosphate mediated transfections as described previously (Jiang and Chen, 2006). For all experiments, 5 µg of total plasmids and/or 100 pmol of pre-miRNA mimics were used per well. Images of basal dendrites and dendritic spines were acquired as described previously (Mukai et al., 2008; Stark et al., 2008). Detailed procedures of neuronal morphological analysis can be found in Chapter 3.5.7, Chapter 3.5.8 below.

3.5.4 Immunohistochemistry Assays

Immunohistochemistry assays were described previously (Schneider Gasser et al., 2006). Briefly, fresh brains were dissected and immediately frozen in OCT. Brains were then sliced at a thickness of 15–20 µm and brain sections were dried at room temperature and then fixed. Sections were incubated overnight with one or two primary antibodies and subsequently incubated for 1 hr with secondary antibody coupled to the Alexa Fluor fluorochromes (1:1,000, Invitrogen). Images were examined under a fluorescence microscope (Nikon).

3.5.5 Immunocytochemistry Assays

Neurons were cultured on coverslips, fixed, permeabilized, and then exposed to primary antibodies and secondary antibodies as described previously (Mukai et al., 2008). Images were examined under a fluorescence microscope (Nikon). For quantification of Mirta22 signals, images were acquired as described previously (Mukai et al., 2008). The raw LSM images were projected and exported using ImageJ. Mirta22 immunocytochemical signal from cell body of each individual neuron was calculated as total integrated density minus background of the cell body area.

3.5.6 Functional and Geneset Enrichment Analysis (GSEA) of Predicted miR-185 Targets

miR-185 target predictions were obtained using TargetScan Mouse v5.2. The gene list was imported into DAVID gene functional annotation database. 92% (2708 out of 2932) predicted targets genes were mapped into the DAVID database. Functional annotation was conducted using the program's functional annotation clustering analysis with default settings. The gene list from the top cluster ("Golgi apparatus") was converted into Affymetrix IDs using the DAVID ID conversion tool and further mapped to the corresponding IDs of the Affymetrix mouse 430 2.0 chip. This final probeset list was used as a user-defined geneset for downstream analysis. Geneset enrichment analysis was conducted using the ErmineJ software (Lee et al., 2005). Analysis was conducted using the receiver operator characteristic (ROC) analysis based on *P* value rankings.

3.5.7 Analysis of Dendritic Complexity

An experimenter blind to the genotype performed imaging and analysis. The number of primary dendrites and total branch points for each treatment condition were calculated by L-measure [version 4.0] (Scorcioni et al., 2008). The basal dendrite branches were semi-automatically traced from the somata of neurons using NeuronStudio (Wearne et al., 2005). The output .swc files were imported into L-measure (Scorcioni et al., 2008). The number of primary dendrites and total branch points for each treatment condition were calculated by L-measure (version 4.0). Statistical analysis was conducted using the Student's *t*-test as implemented in L-measure. Sholl analysis was conducted in ImageJ (http://rsbweb.nih.gov/ij/) using the "Sholl analysis" plugin (http://biology.ucsd.edu/labs/ghosh/software/ShollAnalysis.pdf). The results were combined in the MS-Excel and a Student's *t*-test was conducted to

determine the intersection number and significance at each step size between the experimental group and the controls.

3.5.8 Analysis of Spine Morphology

For each experiment, images across all genotypes were acquired with similar optimal settings for laser power, detector gain, and amplifier offset. An experimenter blind to the genotype performed all imaging and analysis. The raw LSM images were projected and exported using ImageJ. Quantification of mushroom spine density, length, and width was first performed using automatic tracing implemented in NeuronStudio (Rodriguez et al., 2008) and followed by manual adjustment. All spines on a basal dendrite, each at least 75 μm in length from the soma, were analyzed per neuron. We analyzed at least 4 neurons from each animal. The mushroom spine width was measured as the length of a straight line drawn across the widest part of the spine head and the mushroom spine length was measured as the length of the shortest line drawn from the tip of the spine head to the shaft of the dendrite. All measurements were determined by NeuronStudio. The results of spine analysis were exported, combined in MS-Excel and classified according to genotype or treatment information. The spine type was defined according to Chakravarthy et al (Chakravarthy et al., 2006). Changes in mushroom spine density were assessed by Student's *t*-test. The distribution of width of mushroom spines was compared using the Kolmogorov-Smirnov test.

3.6 References

Abdelmohsen, K., Hutchison, E.R., Lee, E.K., Kuwano, Y., Kim, M.M., Masuda, K., Srikantan, S., Subaran, S.S., Marasa, B.S., Mattson, M.P.*, et al.* (2010). miR-375 inhibits differentiation of neurites by lowering HuD levels. Molecular and cellular biology *30*, 4197-4210.

Agostini, M., Tucci, P., Steinert, J.R., Shalom-Feuerstein, R., Rouleau, M., Aberdam, D., Forsythe, I.D., Young, K.W., Ventura, A., Concepcion, C.P.*, et al.* (2011). microRNA-34a regulates neurite outgrowth, spinal morphology, and function. Proceedings of the National Academy of Sciences of the United States of America *108*, 21099-21104.

Andersen, P.A.M., R.G.M. AND Amaral, D.G. AND Bliss, T.V.P. AND O'Keefe, J. (2007). The Hippocampus Book (London: Oxford University Press).

Ashraf, S.I., McLoon, A.L., Sclarsic, S.M., and Kunes, S. (2006). Synaptic protein synthesis associated with memory is regulated by the RISC pathway in Drosophila. Cell *124*, 191-205.

Attwood, B.K., Bourgognon, J.M., Patel, S., Mucha, M., Schiavon, E., Skrzypiec, A.E., Young, K.W., Shiosaka, S., Korostynski, M., Piechota, M.*, et al.* (2011). Neuropsin cleaves EphB2 in the amygdala to control anxiety. Nature *473*, 372-375.

Baek, D., Villen, J., Shin, C., Camargo, F.D., Gygi, S.P., and Bartel, D.P. (2008). The impact of microRNAs on protein output. Nature *455*, 64-71.

Banerjee, S., Neveu, P., and Kosik, K.S. (2009). A coordinated local translational control point at the synapse involving relief from silencing and MOV10 degradation. Neuron *64*, 871-884.

Benarroch, E.E. (2007). Rho GTPases: role in dendrite and axonal growth, mental retardation, and axonal regeneration. Neurology *68*, 1315-1318.

Camera, P., Schubert, V., Pellegrino, M., Berto, G., Vercelli, A., Muzzi, P., Hirsch, E., Altruda, F., Dotti, C.G., and Di Cunto, F. (2008). The RhoA-associated protein Citron-N controls dendritic spine maintenance by interacting with spine-associated Golgi compartments. EMBO reports *9*, 384-392.

Campbell, L.E., Daly, E., Toal, F., Stevens, A., Azuma, R., Catani, M., Ng, V., van Amelsvoort, T., Chitnis, X., Cutter, W.*, et al.* (2006). Brain and behaviour in children with 22q11.2 deletion syndrome: a volumetric and voxel-based morphometry MRI study. Brain : a journal of neurology *129*, 1218-1228.

Chahrour, M., Jung, S.Y., Shaw, C., Zhou, X., Wong, S.T., Qin, J., and Zoghbi, H.Y. (2008). MeCP2, a key contributor to neurological disease, activates and represses transcription. Science (New York, NY *320*, 1224-1229.

Chakravarthy, S., Saiepour, M.H., Bence, M., Perry, S., Hartman, R., Couey, J.J., Mansvelder, H.D., and Levelt, C.N. (2006). Postsynaptic TrkB signaling has distinct roles in spine maintenance in adult visual cortex and hippocampus. Proc Natl Acad Sci U S A *103*, 1071-1076.

Chow, E.W., Zipursky, R.B., Mikulis, D.J., and Bassett, A.S. (2002). Structural brain abnormalities in patients with schizophrenia and 22q11 deletion syndrome. Biol Psychiatry *51*, 208-215.

Christensen, M., Larsen, L.A., Kauppinen, S., and Schratt, G. (2010). Recombinant Adeno-Associated Virus-Mediated microRNA Delivery into the Postnatal Mouse Brain Reveals a Role for miR-134 in Dendritogenesis in Vivo. Frontiers in neural circuits *3*, 16.

Cohen, J.E., Lee, P.R., Chen, S., Li, W., and Fields, R.D. (2011). MicroRNA regulation of homeostatic synaptic plasticity. Proceedings of the National Academy of Sciences of the United States of America *108*, 11650-11655.

Colantuoni, C., Lipska, B.K., Ye, T., Hyde, T.M., Tao, R., Leek, J.T., Colantuoni, E.A., Elkahloun, A.G., Herman, M.M., Weinberger, D.R.*, et al.* (2011). Temporal dynamics and genetic control of transcription in the human prefrontal cortex. Nature *478*, 519-523.

Drew, L.J., Crabtree, G.W., Markx, S., Stark, K.L., Chaverneff, F., Xu, B., Mukai, J., Fenelon, K., Hsu, P.K., Gogos, J.A.*, et al.* (2011a). The 22q11.2 microdeletion: fifteen years of insights into the genetic and neural complexity of psychiatric disorders. International journal of developmental neuroscience : the official journal of the International Society for Developmental Neuroscience *29*, 259-281.

Drew, L.J., Stark, K.L., Fenelon, K., Karayiorgou, M., Macdermott, A.B., and Gogos, J.A. (2011b). Evidence for altered hippocampal function in a mouse model of the human 22q11.2 microdeletion. Molecular and cellular neurosciences *47*, 293-305.

Edbauer, D., Neilson, J.R., Foster, K.A., Wang, C.F., Seeburg, D.P., Batterton, M.N., Tada, T., Dolan, B.M., Sharp, P.A., and Sheng, M. (2010). Regulation of synaptic structure and function by FMRP-associated microRNAs miR-125b and miR-132. Neuron *65*, 373-384.

Eliez, S., Schmitt, J.E., White, C.D., and Reiss, A.L. (2000). Children and adolescents with velocardiofacial syndrome: a volumetric MRI study. Am J Psychiatry *157*, 409-415.

Fenelon, K., Mukai, J., Xu, B., Hsu, P.K., Drew, L.J., Karayiorgou, M., Fischbach, G.D., Macdermott, A.B., and Gogos, J.A. (2011). Deficiency of Dgcr8, a gene disrupted by the 22q11.2 microdeletion, results in altered short-term plasticity in the prefrontal cortex. Proceedings of the National Academy of Sciences of the United States of America *108*, 4447-4452.

Fiore, R., Khudayberdiev, S., Christensen, M., Siegel, G., Flavell, S.W., Kim, T.K., Greenberg, M.E., and Schratt, G. (2009). Mef2-mediated transcription of the miR379-410 cluster regulates activity-dependent dendritogenesis by fine-tuning Pumilio2 protein levels. EMBO J *28*, 697-710.

Fonseca, R., Vabulas, R.M., Hartl, F.U., Bonhoeffer, T., and Nagerl, U.V. (2006). A balance of protein synthesis and proteasome-dependent degradation determines the maintenance of LTP. Neuron *52*, 239-245.

Garcia-Lopez, P., Garcia-Marin, V., and Freire, M. (2007). The discovery of dendritic spines by Cajal in 1888 and its relevance in the present neuroscience. Progress in neurobiology *83*, 110-130.

Gaughwin, P., Ciesla, M., Yang, H., Lim, B., and Brundin, P. (2011). Stage-specific modulation of cortical neuronal development by Mmu-miR-134. Cerebral cortex (New York, NY : 1991) *21*, 1857-1869.

Govek, E.E., Newey, S.E., and Van Aelst, L. (2005). The role of the Rho GTPases in neuronal development. Genes & development *19*, 1-49.

Hansen, K.F., Sakamoto, K., Wayman, G.A., Impey, S., and Obrietan, K. (2010). Transgenic miR132 alters neuronal spine density and impairs novel object recognition memory. PLoS ONE *5*, e15497.

Henny, P., Brown, M.T., Northrop, A., Faunes, M., Ungless, M.A., Magill, P.J., and Bolam, J.P. (2012). Structural correlates of heterogeneous in vivo activity of midbrain dopaminergic neurons. Nature neuroscience.

Horton, A.C., and Ehlers, M.D. (2004). Secretory trafficking in neuronal dendrites. Nat Cell Biol *6*, 585-591.

Horton, A.C., Racz, B., Monson, E.E., Lin, A.L., Weinberg, R.J., and Ehlers, M.D. (2005). Polarized secretory trafficking directs cargo for asymmetric dendrite growth and morphogenesis. Neuron *48*, 757-771.

Impey, S., Davare, M., Lasiek, A., Fortin, D., Ando, H., Varlamova, O., Obrietan, K., Soderling, T.R., Goodman, R.H., and Wayman, G.A. (2010). An activity-induced microRNA controls dendritic spine formation by regulating Rac1-PAK signaling. Molecular and cellular neurosciences *43*, 146-156.

Jan, Y.N., and Jan, L.Y. (2010). Branching out: mechanisms of dendritic arborization. Nat Rev Neurosci *11*, 316-328.

Jiang, M., and Chen, G. (2006). High Ca2+-phosphate transfection efficiency in low-density neuronal cultures. Nat Protoc *1*, 695-700.

Junes-Gill, K.S., Gallaher, T.K., Gluzman-Poltorak, Z., Miller, J.D., Wheeler, C.J., Fan, X., and Basile, L.A. (2011). hHSS1: a novel secreted factor and suppressor of glioma growth located at chromosome 19q13.33. J Neurooncol *102*, 197-211.

Kang, H.J., Kawasawa, Y.I., Cheng, F., Zhu, Y., Xu, X., Li, M., Sousa, A.M., Pletikos, M., Meyer, K.A., Sedmak, G.*, et al.* (2011). Spatio-temporal transcriptome of the human brain. Nature *478*, 483-489.

Karayiorgou, M., Simon, T.J., and Gogos, J.A. (2010). 22q11.2 microdeletions: linking DNA structural variation to brain dysfunction and schizophrenia. Nat Rev Neurosci *11*, 402-416.

Kasai, H., Fukuda, M., Watanabe, S., Hayashi-Takagi, A., and Noguchi, J. (2010). Structural dynamics of dendritic spines in memory and cognition. Trends in neurosciences *33*, 121-129.

Kim, S., Guzman, S.J., Hu, H., and Jonas, P. (2012). Active dendrites support efficient initiation of dendritic spikes in hippocampal CA3 pyramidal neurons. Nature neuroscience.

Lee, H.K., Braynen, W., Keshav, K., and Pavlidis, P. (2005). ErmineJ: tool for functional analysis of gene expression data sets. BMC Bioinformatics *6*, 269.

Lippi, G., Steinert, J.R., Marczylo, E.L., D'Oro, S., Fiore, R., Forsythe, I.D., Schratt, G., Zoli, M., Nicotera, P., and Young, K.W. (2011). Targeting of the Arpc3 actin nucleation factor by miR-29a/b regulates dendritic spine morphology. The Journal of cell biology *194*, 889-904.

Liu-Yesucevitz, L., Bassell, G.J., Gitler, A.D., Hart, A.C., Klann, E., Richter, J.D., Warren, S.T., and Wolozin, B. (2011). Local RNA translation at the synapse and in disease. J Neurosci *31*, 16086-16093.

Liu, M., Lang, N., Chen, X., Tang, Q., Liu, S., Huang, J., Zheng, Y., and Bi, F. (2011). miR-185 targets RhoA and Cdc42 expression and inhibits the proliferation potential of human colorectal cells. Cancer letters *301*, 151-160.

Lugli, G., Torvik, V.I., Larson, J., and Smalheiser, N.R. (2008). Expression of microRNAs and their precursors in synaptic fractions of adult mouse forebrain. J Neurochem *106*, 650-661.

Luikart, B.W., Bensen, A.L., Washburn, E.K., Perederiy, J.V., Su, K.G., Li, Y., Kernie, S.G., Parada, L.F., and Westbrook, G.L. (2011). miR-132 mediates the integration of newborn neurons into the adult dentate gyrus. PLoS ONE *6*, e19077.

Machado, A.M., Simon, T.J., Nguyen, V., McDonald-McGinn, D.M., Zackai, E.H., and Gee, J.C. (2007). Corpus callosum morphology and ventricular size in chromosome 22q11.2 deletion syndrome. Brain research *1131*, 197-210.

Magee, J.C. (2000). Dendritic integration of excitatory synaptic input. Nat Rev Neurosci *1*, 181-190.

Magill, S.T., Cambronne, X.A., Luikart, B.W., Lioy, D.T., Leighton, B.H., Westbrook, G.L., Mandel, G., and Goodman, R.H. (2010). microRNA-132 regulates dendritic growth and arborization of newborn neurons in the adult hippocampus. Proceedings of the National Academy of Sciences of the United States of America *107*, 20382-20387.

Mainen, Z.F., and Sejnowski, T.J. (1996). Influence of dendritic structure on firing pattern in model neocortical neurons. Nature *382*, 363-366.

Matsuki, T., Matthews, R.T., Cooper, J.A., van der Brug, M.P., Cookson, M.R., Hardy, J.A., Olson, E.C., and Howell, B.W. (2010). Reelin and stk25 have opposing roles in neuronal polarization and dendritic Golgi deployment. Cell *143*, 826-836.

Mellios, N., Sugihara, H., Castro, J., Banerjee, A., Le, C., Kumar, A., Crawford, B., Strathmann, J., Tropea, D., Levine, S.S.*, et al.* (2011). miR-132, an experience-dependent microRNA, is essential for visual cortex plasticity. Nature neuroscience *14*, 1240-1242.

Miller, E.K., and Cohen, J.D. (2001). An integrative theory of prefrontal cortex function. Annual review of neuroscience *24*, 167-202.

Mukai, J., Dhilla, A., Drew, L.J., Stark, K.L., Cao, L., MacDermott, A.B., Karayiorgou, M., and Gogos, J.A. (2008). Palmitoylation-dependent neurodevelopmental deficits in a mouse model of 22q11 microdeletion. Nature neuroscience *11*, 1302-1310.

Nakamura, N., Rabouille, C., Watson, R., Nilsson, T., Hui, N., Slusarewicz, P., Kreis, T.E., and Warren, G. (1995). Characterization of a cis-Golgi matrix protein, GM130. J Cell Biol *131*, 1715-1726.

Ory, S., and Gasman, S. (2011). Rho GTPases and exocytosis: what are the molecular links? Seminars in cell & developmental biology *22*, 27-32.

Philip, N., and Bassett, A. (2011). Cognitive, behavioural and psychiatric phenotype in 22q11.2 deletion syndrome. Behavior genetics *41*, 403-412.

Piskorowski, R.A., and Chevaleyre, V. (2012). Synaptic integration by different dendritic compartments of hippocampal CA1 and CA2 pyramidal neurons. Cellular and molecular life sciences : CMLS *69*, 75-88.

Ramirez, O.A., and Couve, A. (2011). The endoplasmic reticulum and protein trafficking in dendrites and axons. Trends in cell biology *21*, 219-227.

Rodriguez, A., Ehlenberger, D.B., Dickstein, D.L., Hof, P.R., and Wearne, S.L. (2008). Automated three-dimensional detection and shape classification of dendritic spines from fluorescence microscopy images. PLoS ONE *3*, e1997.

Schneider Gasser, E.M., Straub, C.J., Panzanelli, P., Weinmann, O., Sassoe-Pognetto, M., and Fritschy, J.M. (2006). Immunofluorescence in brain sections: simultaneous detection of presynaptic and postsynaptic proteins in identified neurons. Nat Protoc *1*, 1887-1897.

Schratt, G.M., Tuebing, F., Nigh, E.A., Kane, C.G., Sabatini, M.E., Kiebler, M., and Greenberg, M.E. (2006). A brain-specific microRNA regulates dendritic spine development. Nature *439*, 283-289.

Scorcioni, R., Polavaram, S., and Ascoli, G.A. (2008). L-Measure: a web-accessible tool for the analysis, comparison and search of digital reconstructions of neuronal morphologies. Nat Protoc *3*, 866-876.

Segal, M. (2002). Dendritic spines: elementary structural units of neuronal plasticity. Progress in brain research *138*, 53-59.

Selbach, M., Schwanhausser, B., Thierfelder, N., Fang, Z., Khanin, R., and Rajewsky, N. (2008). Widespread changes in protein synthesis induced by microRNAs. Nature *455*, 58-63.

Siegel, G., Obernosterer, G., Fiore, R., Oehmen, M., Bicker, S., Christensen, M., Khudayberdiev, S., Leuschner, P.F., Busch, C.J., Kane, C.*, et al.* (2009). A functional screen implicates microRNA-138-dependent regulation of the depalmitoylation enzyme APT1 in dendritic spine morphogenesis. Nat Cell Biol *11*, 705-716.

Sigurdsson, T., Stark, K.L., Karayiorgou, M., Gogos, J.A., and Gordon, J.A. (2010). Impaired hippocampal-prefrontal synchrony in a genetic mouse model of schizophrenia. Nature *464*, 763-767.

Simon, T.J., Ding, L., Bish, J.P., McDonald-McGinn, D.M., Zackai, E.H., and Gee, J. (2005). Volumetric, connective, and morphologic changes in the brains of children with chromosome 22q11.2 deletion syndrome: an integrative study. NeuroImage *25*, 169-180.

Stark, K.L., Xu, B., Bagchi, A., Lai, W.S., Liu, H., Hsu, R., Wan, X., Pavlidis, P., Mills, A.A., Karayiorgou, M.*, et al.* (2008). Altered brain microRNA biogenesis contributes to phenotypic deficits in a 22q11-deletion mouse model. Nat Genet *40*, 751-760.

Swanger, S.A., and Bassell, G.J. (2011). Making and breaking synapses through local mRNA regulation. Current opinion in genetics & development *21*, 414-421.

Tay, Y., Zhang, J., Thomson, A.M., Lim, B., and Rigoutsos, I. (2008). MicroRNAs to Nanog, Oct4 and Sox2 coding regions modulate embryonic stem cell differentiation. Nature *455*, 1124-1128.

Tierling, S., Dalbert, S., Schoppenhorst, S., Tsai, C.E., Oliger, S., Ferguson-Smith, A.C., Paulsen, M., and Walter, J. (2006). High-resolution map and imprinting analysis of the Gtl2-Dnchc1 domain on mouse chromosome 12. Genomics *87*, 225-235.

Tolias, K.F., Duman, J.G., and Um, K. (2011). Control of synapse development and plasticity by Rho GTPase regulatory proteins. Progress in neurobiology *94*, 133-148.

Tsang, J.S., Ebert, M.S., and van Oudenaarden, A. (2010). Genome-wide dissection of microRNA functions and cotargeting networks using gene set signatures. Mol Cell *38*, 140-153.

van Amelsvoort, T., Daly, E., Robertson, D., Suckling, J., Ng, V., Critchley, H., Owen, M.J., Henry, J., Murphy, K.C., and Murphy, D.G. (2001). Structural brain abnormalities associated with deletion at chromosome 22q11: quantitative neuroimaging study of adults with velo-cardio-facial syndrome.[see comment]. British Journal of Psychiatry *178*, 412-419.

van Spronsen, M., and Hoogenraad, C.C. (2010). Synapse pathology in psychiatric and neurologic disease. Current neurology and neuroscience reports *10*, 207-214.

Vo, N., Klein, M.E., Varlamova, O., Keller, D.M., Yamamoto, T., Goodman, R.H., and Impey, S. (2005). A cAMP-response element binding protein-induced microRNA regulates neuronal morphogenesis. Proceedings of the National Academy of Sciences of the United States of America *102*, 16426-16431.

Wang, X., Gong, W., Liu, Y., Yang, Z., Zhou, W., Wang, M., Yang, Z., Wen, J., and Hu, R. (2009). Molecular cloning of a novel secreted peptide, INM02, and regulation of its expression by glucose. The Journal of endocrinology *202*, 355-364.

Wayman, G.A., Davare, M., Ando, H., Fortin, D., Varlamova, O., Cheng, H.Y., Marks, D., Obrietan, K., Soderling, T.R., Goodman, R.H.*, et al.* (2008). An activity-regulated microRNA controls dendritic plasticity by down-regulating p250GAP. Proceedings of the National Academy of Sciences of the United States of America *105*, 9093-9098.

Wearne, S.L., Rodriguez, A., Ehlenberger, D.B., Rocher, A.B., Henderson, S.C., and Hof, P.R. (2005). New techniques for imaging, digitization and analysis of three-dimensional neural morphology on multiple scales. Neuroscience *136*, 661-680.

Yu, J.Y., Chung, K.H., Deo, M., Thompson, R.C., and Turner, D.L. (2008). MicroRNA miR-124 regulates neurite outgrowth during neuronal differentiation. Exp Cell Res *314*, 2618-2633.

Yuste, R., and Tank, D.W. (1996). Dendritic integration in mammalian neurons, a century after Cajal. Neuron *16*, 701-716.

Zhang, L., Hammell, M., Kudlow, B.A., Ambros, V., and Han, M. (2009). Systematic analysis of dynamic miRNA-target interactions during C. elegans development. Development *136*, 3043-3055.

Chapter IV

MicroRNA and Target Dysregulation in a Mouse Model of *BDNF Val66Met* SNP

4.1 Introduction

Discovered in 1982 (Barde et al., 1982), brain-derived neurotrophic factor (BDNF) is a polypeptide growth factor of the neurotrophin family that regulate the development and function of nervous system. BDNF is synthesized as a 247 amino acid (32 kD) pre-pro-BDNF in the endoplasmic reticulum (ER) (Lu, 2003). Pro-BDNFs form homodimers and are packed into dense-core vesicles that are transported to terminals for constitutive secretion or activity-dependent release (Lessmann et al., 2003). Upon release, Pro-BDNF dimers can either bind to p75 receptors or are proteolytically cleaved by extracellular proteases, such as plasmin or MMP7, giving rise to mature BDNF (Lessmann et al., 2003; Seidah et al., 1996). Mature BDNF binds to tropomyosin-related kinase receptor type B (TrkB) which in turns activates PI3K-Akt, PLCγ, and Ras-MAPK signaling pathways (Martinowich and Lu, 2008; Minichiello, 2009). Although there is continuous debate about the differential functional outcomes and relative importance of TrkB versus p75 signaling pathways in different scenarios (Lu et al., 2005), it is now believed that mature BDNF signaling through widely expressed TrkB receptors is of predominant physiological relevance in the mature brain (Matsumoto et al., 2008; Rauskolb et al., 2010).

BDNF is the most intensively studied member of the neurotrophin family due to its high expression in diverse brain regions and its involvement in neuronal survival, neurogenesis, neuronal morphogenesis and synaptic plasticity (Binder and Scharfman, 2004). Given the important role of BDNF in brain function, it has been hypothesized that the genetic variants of Bdnf can predispose carriers to cognitive dysfunction or even psychiatric disorders (Buckley et al., 2011; Frielingsdorf et al., 2010; Martinowich and Lu, 2008). As discussed below, many association studies have been performed aiming to investigate this hypothesis and most of them focused on a single nucleotide polymorphism (SNP), *Val66Met*.

4.1.1 BDNF Val66Met Single Nucleotide Polymorphism

There are so far 891 single nucleotide polymorphisms (SNPs) within human *BDNF* gene in the dbSNP database to date, of which 41 have been studied and 2 of them, including rs6265, are reported as probable-pathogenic. The common single SNP at nucleotide 196 (G/A) (dbSNP number rs6265) is particularly interesting as it results in a Valine to Methionine substitution (missense mutation) at codon 66 located in the pro-domain. This SNP is only found in human and its allele frequency is ethnically variable and stratified from near 0% in a population in Kenya, Africa to 60% in a population in Japan, Asia (http://www.ncbi.nlm.nih.gov/projects/SNP/snp_ref.cgi?rs=6265). It is estimated about 30% (Caucasians) to 50% (Asians) of world population are *Met* carriers (Shimizu et al., 2004), while about only 4% (Caucasians) and 20% (Asians) of individuals are homozygous for the *Met* allele (Petryshen et al., 2010).

Although it is usually difficult to comprehend how most SNPs affect the expression or function of its host genes, *Val66Met* is a notable exception. Studies in cell culture systems using overexpressed protein showed that *Val66Met* mutation reduces the expression of BDNF at neuronal terminals by disrupting the transportation of both the mRNA and protein that contain this mutation (Chen et al., 2004; Egan et al., 2003). The Met form of BDNF ($BDNF_{Met}$) fails to interact with sortilin and to be correctly sorted into secretory granules for activity-dependent release at the dendrites (Chen et al., 2005). Furthermore, the observation that sorting of $BDNF_{Met}$– $BDNF_{Val}$ heterodimers into secretory granules was also impaired suggested that $BDNF_{Met}$ may act in a dominant negative fashion to affect release of $BDNF_{Val}$ molecules (Chen et al., 2004). Besides these well-documented protein sorting/trafficking deficits, *Val66Met* mutation also blocks the translin-mediated dendritic trafficking of *BDNF* mRNA (Chiaruttini et al., 2009). As the majority of BDNF is released in response to activity through regulated secretory pathways, these results suggest there is a significant reduction in BDNF levels in regions with high neuronal activities, such as a learning-strengthened hippocampal circuit.

4.1.2 BDNF Val66Met SNP and Mood Disorders

BDNF plays diverse and important roles in the development and function of the brain (Cohen-Cory et al., 2010; Yoshii and Constantine-Paton, 2010). Moreover, BDNF is also shown to be a crucial modulator for a variety of cognitive functions and emotion. It is therefore not surprising that multiple

groups have hypothesized the involvement of altered BDNF expression and function in pathophysiology of psychiatric disorders, especially mood or affective disorders. Indeed, expression levels of BDNF and its receptor TrkB are reduced in the CNS, especially hippocampus, of patients with depression (Karege et al., 2005; Marvanova et al., 2001). Furthermore, most effective antidepressant treatment and antidepressants, including serotonin reuptake inhibitors (SSRIs), induce the expression of BDNF in hippocampus (Alme et al., 2007; Chen et al., 2001; Duman and Monteggia, 2006) and in serum (Sen et al., 2008; Shimizu et al., 2003). BDNF expression in plasma and neurons is also increased by lithium (de Sousa et al., 2011; Yasuda et al., 2009), an effective treatment for bipolar disorders. Thus, there has been considerable interests in revealing the possible association or the lack of it between of *BDNF Val66Met* and psychiatric disorders in the past decade.

Association of the *Met* allele with depression was found in several case-control studies of both Asian (Hwang et al., 2006; Su et al., 2011) and Caucasian (Borroni et al., 2009; Lavebratt et al., 2010) populations. A meta-analysis also revealed significant effects of the *Met* allele or the *Met/Met* genotype on risk of major depression disorder in men (Verhagen et al., 2010). It is worth noting that in some reports, interaction of the *Met* allele with early life stress leads to a higher risk of depression (Carver et al., 2011; Lavebratt et al., 2010). The *Met* allele is also associated with higher anxiety level (Montag et al., 2010) and smaller hippocampus (Frodl et al., 2007; Montag et al., 2009) and amygdala (Montag et al., 2009) volumes, all of which are potent risk factors for depression. However, a number of studies found no association of *Val66Met* with depression (Figueira et al., 2010; Jessen et al., 2009; Sun et al., 2011; Zou et al., 2010) or reported *Val/Val* to be associated with depression diagnosis (Ribeiro et al., 2007) or symptoms (Duncan et al., 2009).

There are continuous debates of the association of *Val66Met* with anxiety disorders (Frustaci et al., 2008; Jiang et al., 2005; Kobayashi et al., 2005; Tocchetto et al., 2011). In addition, the involvement of *Val66Met* in bipolar disorder is equally controversial, with most population case-control studies showing no association (Green et al., 2006; Nakata et al., 2003; Neves-Pereira et al., 2005; Oswald et al., 2004; Schumacher et al., 2005; Skibinska et al., 2004; Tang et al., 2008; Wellcome Trust Case Control, 2007), while one case-control (Lohoff et al., 2005) and several family-based studies (Geller et al., 2004;

Kremeyer et al., 2006; Muller et al., 2006; Sklar et al., 2002) conducted in US reported higher risk of *Val* allele (odds ratio ranging from 1.22-2.33) (Petryshen et al., 2010).

In summary, evidence suggests (but not unequivocally confirms) the possible association of the *Met* allele with depression disorders and anxiety level (whereas the *Val* allele may be associated with psychosis, as described below at Chapter 4.1.3). The study of a mouse model of *BDNF Val66Met* later provides supporting evidence for the deleterious effects of the Met allele in development of depression and anxiety traits (see Chapter 4.1.5) (Chen et al., 2006b).

4.1.3 BDNF Val66Met SNP and Schizophrenia

Whether *BDNF Val66Met* SNP modulates the risk of schizophrenia is also under intensive scrutiny. In schizophrenia patients (as in depression patients), expression levels of BDNF and its receptor TrkB are reduced in the brain, especially in the hippocampus (Durany et al., 2001; Iritani et al., 2003). Intriguingly, some studies indicated a protective effect for the *Met* allele. A study examining a large Scottish schizophrenia sample found a significant excess of *Val* in schizophrenia patients (Neves-Pereira et al., 2005). In a Spanish family-based study, the transmission disequilibrium test (TDT) showed a preferential transmission of *Val* allele from heterozygous parents to the affected schizophrenic offspring (Rosa et al., 2006). The association of the *Val* allele with schizophrenia was later replicated in a Russian male sample (Golimbet et al., 2008). On the contrary, there was no association of *Val66Met* or other *BDNF* SNPs (rs3750934, ro. 000001, *G-172A*, *C270T*) with schizophrenia in Han Chinese samples (Chen et al., 2006a; Sun et al., 2011; Wang et al., 2010; Yi et al., 2011). In addition, several case-control studies and meta-analysis of a Japanese population found no association of *Val66Met* with schizophrenia (Kawashima et al., 2009; Naoe et al., 2007; Tochigi et al., 2006). Considering ethnicity as a factor in those studies, *Val66Met* may differentially affect schizophrenia susceptibility in different races. As there is substantial linkage disequilibrium between *BDNF* SNPs (Petryshen et al., 2010), it is an intriguing possibility that the ethnic differences in haplotype (combination of alleles) frequency can explain more variability in schizophrenia susceptibility among different races than *Val66Met* allele alone.

Although the *Met* allele was linked to schizophrenia in an Armenian sample (Zakharyan et al., 2011), most studies that reported a positive association with schizophrenia pointed to a higher odds ratio

of the *Val* allele. This could represent a result of evolutionary trade-off that a recent mutation (*Val66Met*) persists due to the balance between the advantages (protection from schizophrenia or schizoaffective disorders) and disadvantages it offers (vulnerability to depression; memory deficits, as discussed in Chapter 4.1.2 and 4.1.4).

The contribution of *Val66Met* to the risk of schizoaffective disorders is most likely very small. Nevertheless, *Val66Met* may establish background liability, together with other common variants with small effect sizes, that is then modified by rare genetic variants and environmental factors.

Although the results regarding association of *Val66Met* and psychiatric disorders is inconsistent, it seems highly likely that *Val66Met* is associated with more intermediate phenotypes or endophenotypes, such as memory and executive function. Moreover, the discrepancy of human association studies may be due to confounding factors like small sample size, genetic heterogeneity and population stratification. To get around these problems, mouse models of the *Val66Met* SNP were used to study the association of *Val66Met* with behavioral measures of depression or anxiety and offer opportunity to analyze the mechanism of any altered behaviors.

4.1.4 BDNF Val66Met SNP and Cognitive Function

BDNF, like other neurotropins, appears relatively late in evolution and is not found in invertebrate species. In addition, phylogenetic analysis showed that *BDNF* genes are under even more selective pressure in mammals (Tettamanti et al., 2010). These results suggest that BDNF plays specialized roles in the development and function of more complex nervous systems and is an important modulator of highly specific cognitive function in mammalian brains.

Seminal work by Daniel Weinberger et al. showed that individuals with *Val/Met* genotype have worse episodic memory than *Val/Val* individuals, as assessed with the Wechsler Memory Scale (WMS) (Egan et al., 2003; Hariri et al., 2003). In these studies, *Met* carriers (predominantly *Val/Met*) performed worse on tasks that rely on hippocampal activity, such as recalling places and events, but not on tasks that are less hippocampal dependent, such as word learning and planning (Egan et al., 2003; Hariri et al., 2003). In addition, the interaction between the *Val66Met* genotype and the hippocampal response during encoding accounted for 25% of the total variation in memory performance (Hariri et al., 2003). Deficits in

hippocampal dependent task are correlated with diminished hippocampal activation during encoding and retrieval processes (Hariri et al., 2003) and with lower hippocampal n-acetyl aspartate (NAA) (Egan et al., 2003). The effect of *Val66Met* on episodic memory was later replicated in healthy (Cathomas et al., 2010) and schizophrenia patients (Tan et al., 2005).

Besides hippocampal activation deficits, schizophrenia patients carrying the *Met* allele also performed worse in prefrontal cortex (PFC)-dependent N-back tasks (Rybakowski et al., 2006a), implying that PFC-dependent working memory is also affected by the *Val66Met* SNP. Furthermore, bipolar patients with at least one *Met* allele made more perseverative errors (Rybakowski et al., 2006a; Rybakowski et al., 2006b), indicating compromised attention, which is also PFC-dependent. As behavioral flexibility relies on error detection that requires attention as well as effective communication of error-responding neural networks (Holroyd and Coles, 2002), it is noteworthy that the *Met* allele also compromised the post-error phase locking, indicative of reduced synchronization between the basal ganglia and anterior cingulate cortex (ACC) (Beste et al., 2010). Unlike the association with psychiatric disorders, the literature regarding the association of *Val66Met* SNP with cognitive dysfunction is largely consistent in pointing to detrimental effects of the *Met* allele.

One possible cause of the functional deficits in hippocampus and frontal cortex in *Met* carriers is the anomaly in brain structures due to impaired neuronal survival during development. Consistent with this idea, the *Met* allele is associated with decreased volume of various brain regions, including the hippocampus (Pezawas et al., 2004; Szeszko et al., 2005), and the dorsolateral prefrontal cortex (Gerritsen et al., 2011; Pezawas et al., 2004). On the other hand, as *Val66Met* results in deficient synaptic plasticity as discussed in Chapter 4.1.5, difficulties in achieving or maintaining the activation of relevant circuits likely contribute significantly to the cognitive dysfunction in *Met* allele-carrying individuals. Thus there are several possible mechanisms via which the Met allele could impair cognitive function.

4.1.5 Mouse Models of BDNF Val66Met SNP

This *Val66Met* SNP is only found in human as *BDNF* orthologues in non-primate animals encode Valine at codon 66 (Tettamanti et al., 2010). To study the functional consequences of *Val66Met* in a homogeneous genetic background, Francis Lee's group in Cornell and our group have generated

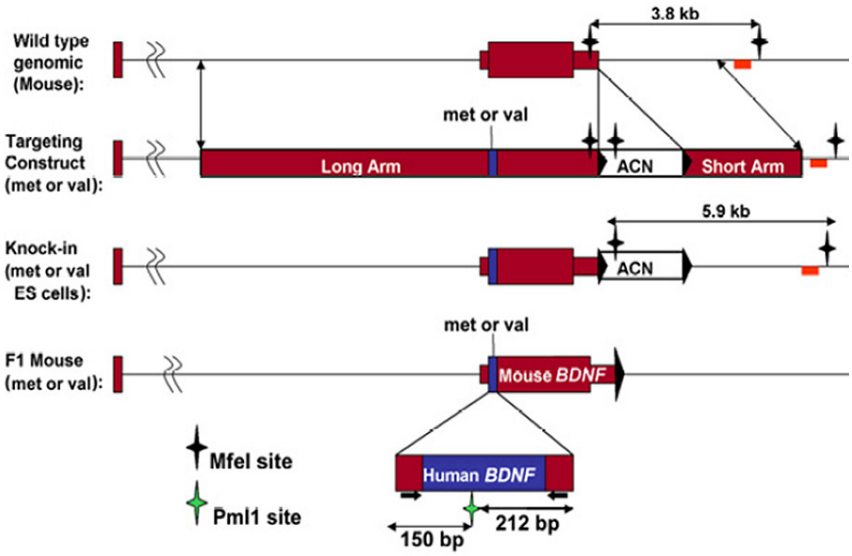

Figure 4.1 Generation of A Mouse Model of *BDNF Val66Met* SNP. Targeting constructs carrying human BDNF gene (*Val* or *Met* allele) and upstream (Long Arm) and downstream (Short Arm) flanking sequence were introduced into mouse ES cells and replace endogensou mouse *Bdnf* gene. The knock-in lines thus generated express human $BDNF^{met}$ or $BDNF^{val}$ allele transcriptionally controlled by endogenous mouse regulatory elements. See text and Method for details.

independent knock-in mice expressing *Met* alleles. While the Lee group made a G196A substitution in the mouse *Bdnf* coding sequence ($Bdnf^{Met}$ allele) (Chen et al., 2006b), our lab generated two "humanized" *BDNF* knock-in mouse lines by replacing the mouse *Bdnf* coding sequence with human *BDNF* sequence carrying either *Met* ($BDNF^{met}$) or *Val* ($BDNF^{val}$) allele (Cao et al., 2007) (Figure 4.1).

With our mouse lines, our group has demonstrated that BDNF is involved in activity-dependent axonal competition within the olfactory bulb and that *Met* homozygotes have axonal competition deficits and the resulting impaired pruning of silent arbors (Cao et al., 2007). Through a series of experiments, Francis Lee and collaborators showed a variety of morphological and functional abnormalities associated with the *Val66Met* SNP. They confirmed that the activity-dependent release of endogenous $BDNF_{Met}$ is impaired from *Met/Met* and *+/Met* cultured cortical neurons (Chen et al., 2006b) and from ventral tegmental area (VTA) dopaminergic neuron terminals ending at the nucleus accumbens (NAc) (Krishnan et al., 2007). They also showed reduced dendritic complexity in dentate gyrus (DG) neurons (Chen et al., 2006b), layer II/III (Yu et al., 2009) and layer V (Liu et al., 2011) vmPFC pyramidal neurons, as well as decreased survival of migrating olfactory neuroblasts (Bath et al., 2008) and newly-born DG cells (Bath et al., 2012) in the $Bdnf^{Met/Met}$ mice. In addition, NMDA receptor-dependent long-term potentiation (LTP) and long-term depression (LTD) of hippocampal CA3-CA1 synapses (Ninan et al., 2010) and LTP of medial perforant path (MPP)-DG synapses (Bath et al., 2012) were significantly reduced. Spine density and size in layer V cortical neurons were also decreased at basal state and under ketamine stimulation, correlating

to reduced frequency and amplitude of serotonin (5-HT) and hypocretin (Hcrt)-induced EPSC under these conditions (Liu et al., 2011). The converging evidence indicated that *Met* allele carriers (mice and possibly humans) have synaptic plasticity-related deficits in certain neural circuits due to impaired activity-dependent released of BDNF.

The *Bdnf*^{Met} knock-in mouse line displayed several anxiety phenotypes that suggest *Val66Met* may predispose individuals to anxiety and depression disorders. *Met/Met* mice showed increased anxiety in open field, elevated plus maze and novelty-induced hypophagia test. These mice were not responsive to the SSRI fluoxetine, a common anxiety treatment (Chen et al., 2006b). Even under chronic fluoxetine treatment (28 days), *Met/Met* mice still had decreased hippocampal BDNF protein level and impaired survival of newly born cells as well as LTP in the dentate gyrus (Bath et al., 2012). These results implicate the involvement of *Val66Met* in a treatment-resistant form of affective disorders. *Met/Met* mice also displayed abnormalities in fear-related behaviors, with deficits in contextual but not cue-dependent fear conditioning (Chen et al., 2006b) and impairment in extinction learning (Soliman et al., 2010; Yu et al., 2009). Importantly, those findings paralleled human behavioral studies which showed that *Met/Met* individuals have deficits in fear learning (Hajcak et al., 2009) and extinction (Montag et al., 2010), and demonstrated the face validity of this *Bdnf*^{Met} mouse model in anxiety-related measures.

The adverse effects of the *Met* allele on cognitive function (see Chapter 4.1.4) are also validated in the *Bdnf*^{Met} knock-in mouse line. There was a dosage-dependent deficit of the *Met* allele in contextual fear memory (Chen et al., 2006b). Additionally, *Met/Met* mice showed impaired extinction learning in cue-dependent fear conditioning (Soliman et al., 2010) and worse performance in object recognition (OR) and object placement (OP) tests (Spencer et al., 2010). These data point to an anomaly in hippocampus-connected neural circuits that underlie these forms of learning.

4.1.6 BDNF and MicroRNAs

Accumulating data suggests miRNAs play an integral part in BDNF-mediated synaptic plasticity underlying learning and memory. miRNA dysregulation due to altered BDNF expression may also play an important role in development of addiction or psychiatric disorders, such as Rett Syndrome (de Leon-Guerrero et al., 2011).

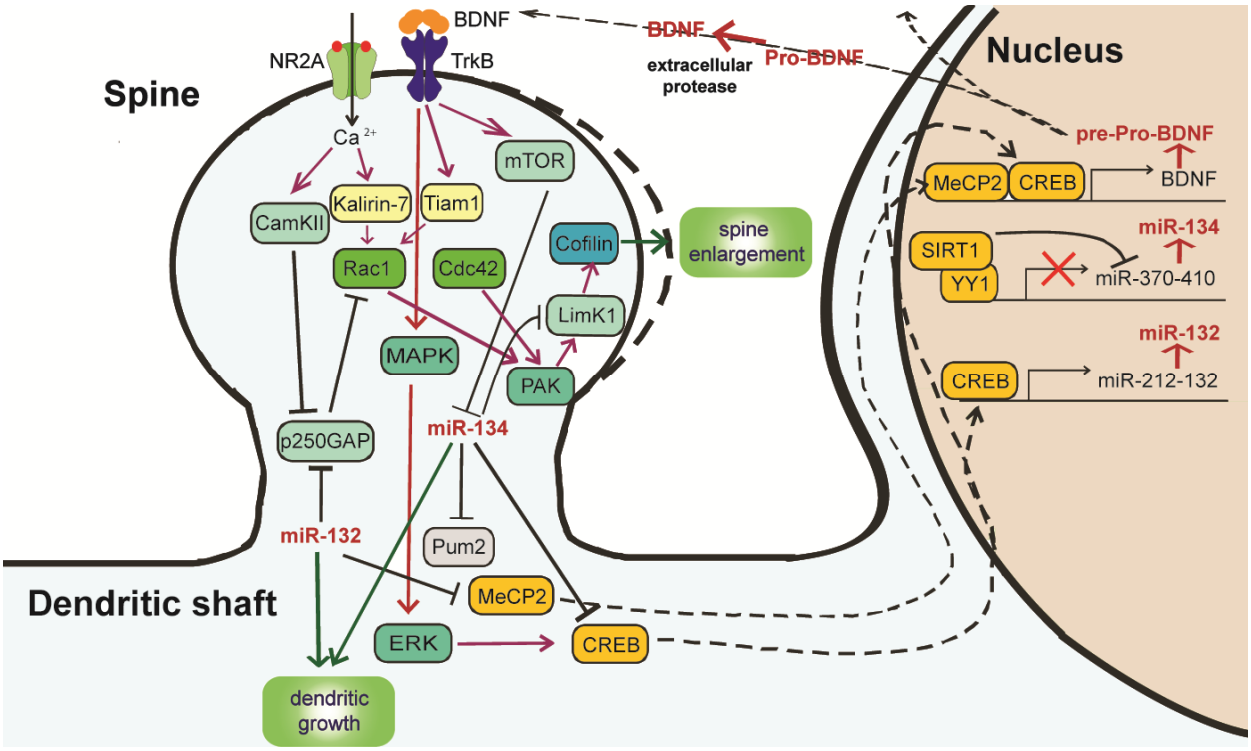

Figure 4.2 BDNF-induced MicroRNA Regulation in Neurons. Through activation of TrkB receptors, BDNF leads to spine and dendritic growth through activation of Rac1 and actin polymerization. This is partly via repression of p250GAP by miR-132 and derepression of Limk1 from miR-134. In the nucleus, BDNF also induces expression of miR-132 and miR-134 from *mir-212–mir-132* and *mir-370–mir-410* respectively, through MAPK signaling and CREB activation. It is hypothesized that transcriptionally-expressed miR-134 represses translational repressor Pum2 and promote dendritic growth, along with other miRNAs encoded in *mir-370–mir-410* locus on a longer time frame. The transcriptional expression of *BDNF* is homeostastically regulated by CREB, MeCP2, miR-134 and miR-132, while *mir-370–mir-410* is also controlled by SIRT1 and YY1 repressors and Mef2. Note that BDNF is secreted mostly as pro form and processed by extracellular proteases. See text for details.

BDNF induces a rapid change in spine structures and synaptic protein expression after synaptic transmission. As discussed in Chapter 1.3.2 and Chapter 3.1.2, miR-134, the first individual miRNA identified to function locally at dendrites, is acutely inactivated after BDNF release during synaptic activity. This leads to the derepression of Limk1 and an increase of spine size through the mTOR pathway downstream of TrkB (Figure 4.2) (Schratt et al., 2006). BDNF is also involved in long-term activity-induced synaptic changes. Synaptic activity, including glutaminergic and BDNF transmission (Vo et al., 2005), activates CREB which induces the transcription of *mir-132–mir-212* cluster (Vo et al., 2005) and *Bdnf* itself (Hong et al., 2008), along with other synaptic proteins. miR-132 enhances dendritic growth through inhibition of Rho GTPase-activating protein p250GAP (Magill et al., 2010; Vo et al., 2005) and increases spine width which correlates with elevated mEPSC amplitude (Edbauer et al., 2010). Since MeCP2

induces BDNF expression (Chahrour et al., 2008; Klein et al., 2007; Zhou et al., 2006) while miR-132 repress MeCP2 levels (Klein et al., 2007), these molecules form a negative feedback loop that mediates homeostatic control over the levels of activation and of MeCP2 expression (Figure 4.2). It has been shown that both loss and gain of MeCP2 can lead to Rett syndrome (Chahrour et al., 2008), and the fine control represented by this feedback loop appears to be important in regulating synaptic function. Furthermore, the expression of BDNF is under the control of miRNAs transcriptionally and post-transcriptionally. By translationally repressing CREB, miR-134 limits the extent of CREB-mediated *Bdnf* transcription. miR-134 is itself restricted by SIRT1-YY1 repressor complex and brain-specific knockouts of SIRT1 had increased miR-134 levels and impaired memory and synaptic plasticity (Gao et al., 2010) (Figure 4.2). On the other hand, BDNF mRNA is targeted by many miRNAs including miR-181a (Chandrasekar and Dreyer, 2011), miR-124 (Chandrasekar and Dreyer, 2009), miR-30a (Mellios et al., 2008), miR-206 (Miura et al., 2012) and miR-26 (Caputo et al., 2011) (check also TargetScanMouse, version 6.0). Two SNPs (rs11030100 and rs11030099) in the *BDNF* 3'UTR abrogate miR-26a and miR-26b targeting, and interestingly, *Val66Met* is in high linkage disequilibrium with these SNPs (Caputo et al., 2011). However, it remains to be tested if these two SNPs are associated with cognitive dysfunction or psychiatric disorders. More importantly, whether a common SNP *Val66Met* in *BDNF* results in miRNA alteration was never investigated.

4.1.7 In this Chapter

While I have so far discussed the impact of miRNA dysregulation due to the rare 22q11.2 microdeletion, it is conceivable that common variants also induce changes in expression of miRNAs and their targets. Although these changes in protein expression levels are generally mild perturbations to a robust system, the combination of several common or rare variants can lead to a more profound alteration in gene expression and functional pathways in the brain that predispose the affected individual to cognitive dysfunction or psychiatric disorders. In this regard, I investigated the miRNA expression profile of a mouse line that carries a common human SNP, *BDNF Val66Met* (rs6265), and described the alteration in expression levels of targets of the dysregulated miR-146b.

4.2 Results

4.2.1 miRNA Expression Profile of BDNF^{Val} and BDNF^{Met} Mouse Lines

We speculated that BDNF *Val66Met* SNP could change the expression of miRNA and wanted to find out the scope and amplitude of the possible miRNA dysregulation. Using a miRNA microarray, we compared the expression of 559 miRNAs (miRBaser Release 10.1) in the hippocampus (HPC) of adult *Val/Val* and *Met/Met* animals. 325 miRNAs that showed positive signals above mean background for all replicated spots on the array were further analyzed. We identified 24 miRNAs with significantly altered expression in *Met/Met* animals versus *Val/Val* animals (FDR-corrected *P*-value < 0.05) (Figure 4.3A and

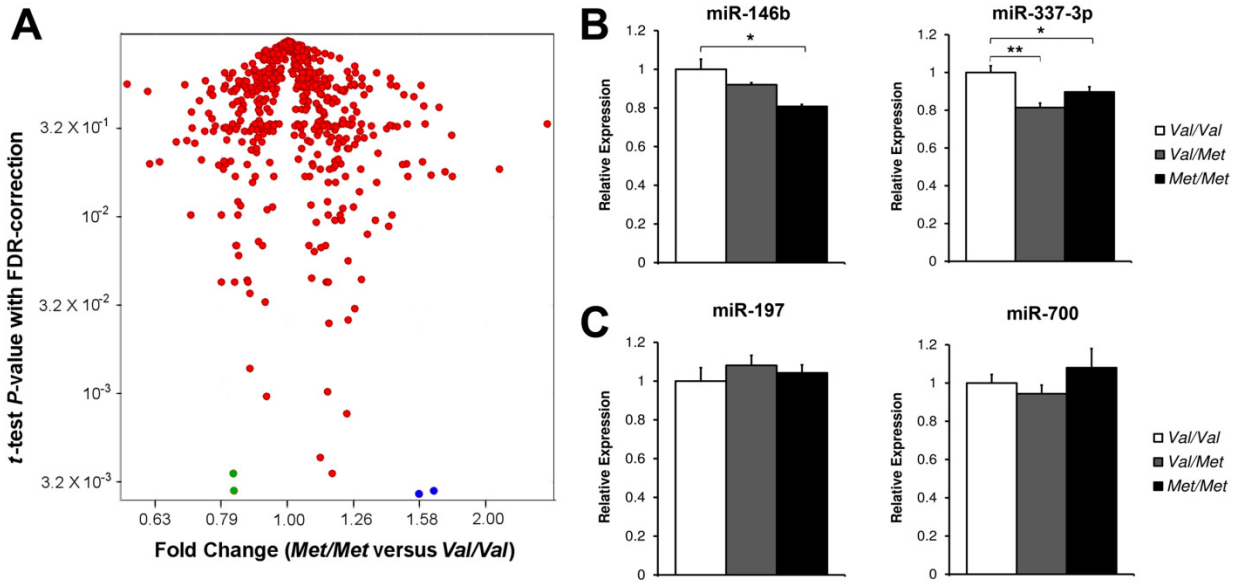

Figure 4.3 MicroRNA Alterations in the Hippocampus of *BDNF$^{Met/Met}$* versus *BDNF$^{Val/Val}$* Mice. (A) Volcano plot showing miRNA expression profile in hippocampus (HPC) of *Met/Met* animals versus *Val/Val* animals (n = 6 each genotype). For each miRNA, the FDR-corrected *P*-value and corresponding relative expression (shown as fold change) are indicated by the location of a dot. Green dots, miR-146b and miR-337-3p; blue dots, miR-197 and miR-700. (B-C) Expression levels of miR-146b, miR-337-3p (B) and miR-197, miR-700 (C) in HPC of *Val/Val*, *Val/Met* and *Met/Met* mice (n = 6 each genotype), as measured by qRT-PCR. The expression levels in *Val/Met* and *Met/Met* mice were normalized to *Val/Val* animals. Results are expressed as mean ± SEM. **P* < 0.05, ***P* < 0.01 (Student's *t*-test)

Table 4.1). Fourteen of these miRNAs were significantly upregulated, while 10 of them were significantly down-regulated. As expected, the expression changes were relatively modest, with fold change (FC) ranging from 1.29 to 0.79, except for miR-197 (FC = 1.58) and miR-700 (FC = 1.66). Mild expression changes found in expression microarray can be due to sample variation or stochastic factors and may not be genuine and robust finding. Furthermore, these changes with small magnitude are generally difficult to

verify by qRT-PCR due to the requirement for large sample sizes. Therefore, we then focused our studies on 4 miRNAs (miR-197, miR-146b, miR-700 and miR-337-3p) with absolute fold change > 1.2 and FDR-corrected *P*-value < 0.005. miR-132 and miR-212, which are located in the same cluster that is transcriptionally up-regulated by BDNF through CREB transcription factor (Vo et al., 2005) were downregulated in *Met/Met* mice, with FC of 0.90 ($P = 0.35$; uncorrected $P = 0.12$) and 0.95 ($P = 0.31$; uncorrected $P = 0.07$) respectively. Although these changes were not significant, it is consistent with the idea that BDNF levels are decreased in *Met/Met* animals and suggests that at least some of the changes we found in the miRNA expression profiling could be due to the direct effect of the *BDNF Val66Met* SNP.

4.2.2 miR-146b and miR-337-3p are Downregulated in Met/Met Mice

We were able to verify the miRNA expression change by quantitative real-time PCR (qRT-PCR) in adult hippocampus (HPC) of the 2 down-regulated miRNAs (miR-146b and miR-337-3p) out of 4 miRNAs with absolute fold change > 1.2 and FDR-corrected *P*-value < 0.005. As compared with levels in *Val/Val* animals, miR-146b was decreased by 8% ($P = 0.20$) and 19% ($P < 0.05$) in *Val/Met* and *Met/Met* animals respectively, and miR-337-3p was decreased by 19% ($P < 0.01$) and 10% ($P < 0.05$) in *Val/Met* and *Met/Met* animals respectively (Figure 4.3B). Interestingly, both miR-146 and miR-337 are reported to be among the top 20 most enriched miRNAs in synaptic compartments of adult mouse forebrain, suggesting they have synaptic-related function (Lugli et al., 2008).

Unfortunately, we were not able to replicate the up-regulation of miR-197 (FC = 1.04, $P = 0.64$, *Met/Met* versus *Val/Val*) and miR-700 (FC = 1.08, $P = 0.48$, *Met/Met* versus *Val/Val*) in *Met/Met* animals (Figure 4.3C). The expression levels of miR-197 and miR-700 were low in HPC and their signals could be detected above background after more than 35 cycles of amplification in qRT-PCR. Therefore there were probably more variations in qRT-PCR assays of miR-197 and miR-700 due to their low signal-to-noise ratio. mmu-mir-197 was later removed from miRBASE because only two clones supported the presence of miR-197 in mouse (Landgraf et al., 2007) and the sequence does not map in a stem-loop region of the genomic sequence or any known mouse transcript sequence. Since miR-700 is expressed at very low levels in HPC and it demonstrated a relatively flat FC due to *Val66Met* SNP, it seems that gene expression changes in *Met/Met* mice due to altered miR-700 levels, if any, were likely to be minor.

4.2.3 BDNF Acutely Induces miR-146b and miR-337-3p Expression in Met/Met Mice

We speculated that reduced expression levels of miR-146b and miR-337-3p were due to lower BDNF levels in these animals and increasing BDNF levels would induce the expression of these 2 miRNAs. To test this hypothesis, we apply physiological levels of BDNF to acute hippocampal slice preparations from Wt animals and monitored expression levels of miR-146b and miR-337 after 2 hours of stimulation. We found that acute BDNF stimulation increased the levels of miR-146b and miR-337-3p by 22% ($P < 0.05$) and 21% ($P = 0.11$) respectively (Figure 4.4A, B). As these experiments demonstrated that expression of miR-146b was significantly changed due to *BDNF Val66Met* SNP and in response to BDNF treatment, we therefore sought the targets of mir-146b that are in turn altered due to *Val66Met* SNP.

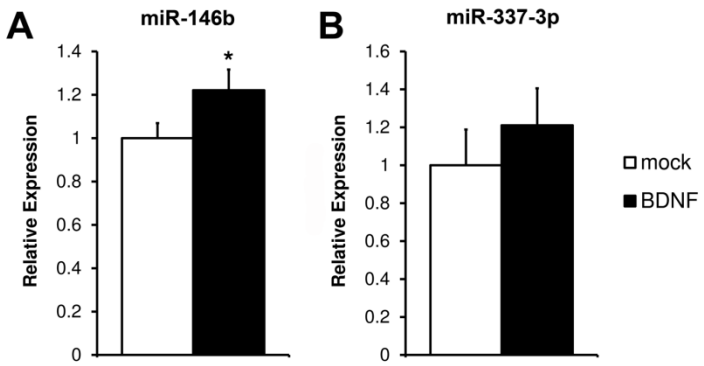

Figure 4.4 BDNF-induced Expression of miR-146b in Hippocampal Slices. (A-B) miR-146 (A) and miR-337-3p (B) expression levels in acute hippocampal slices (n = 9, from 3 animals, each treatment) treated with BDNF for 2 hours, as measured by qRT-PCR. Expression levels in BDNF treatments were normalized to mock treatment control. Results are expressed as mean ± SEM. *$P < 0.05$ (Student's *t*-test).

4.2.4 Search for miR-146 Targets in Hippocampus

We used miRNA target site prediction programs, TargetScan Mammal v.4.2 (http://www.targetscan.org/vert_42/) and PicTar (updated March 2007, http://pictar.mdc-berlin.de/) and found 39 genes that were predicted by both programs. Among them, 12 target candidates (*Irak1*, *Traf6*, *Per1*, *Stx3*, *Syt1*, *Cask*, *Robo1*, *Kctd15*, *Dlgap1*, *Gria3*, *Npas4*, *Lin28A*) were initially selected for further analysis due to their roles in neural development and/or plasticity (Table 4.2). Since *Sort1* encodes sortilin that is required for intracellular BDNF trafficking and activity-regulated release and has a miR-146b seed sequence in the 3'UTR of its mRNA, we also included *Sort1* for candidate target testing in a luciferase assay. It is worth noting that almost all of these targets were later found to be predicted by a more updated version of TargetScanMouse (v6.0, http://www.targetscan.org/mmu_60/) and miRanda (released:

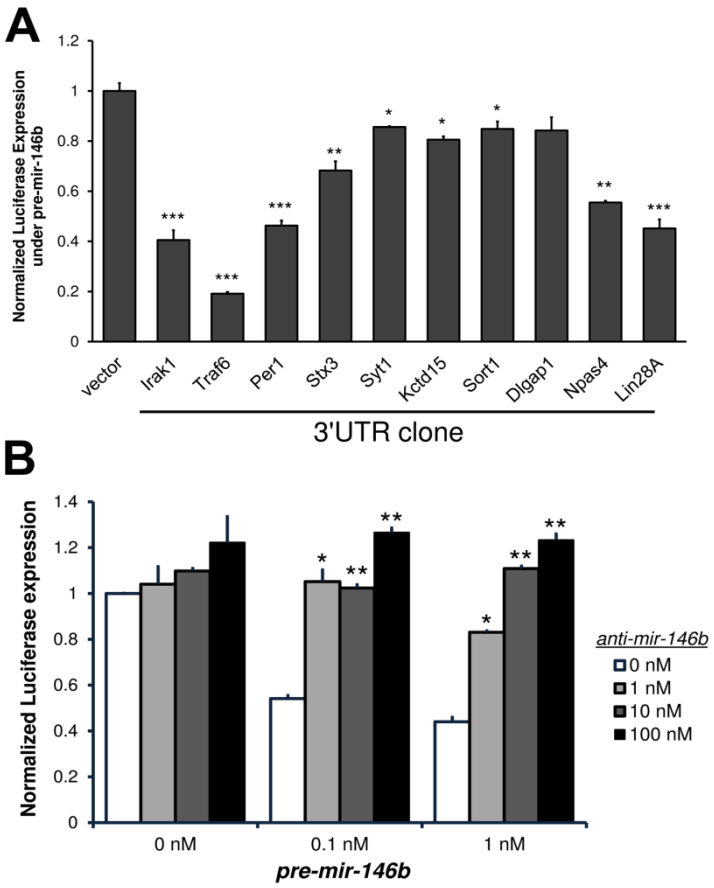

Figure 4.5 Identification of miR-146b Targets using Luciferase Assays. (A) Effects of pre-miR-146b application on 3'UTR luciferase reporters of a group of putative targets were examined by a luciferase reporter assay performed in N18. neuroblastoma cell line (n = 3 for each reporter). Normalized expression values of each reporter to no 3'UTR control (vector). (B). Pre-miR-146b significantly decreases the *Per1 3'*UTR reporter expression over a concentration range of 1 nM to 0.1 nM. The repression effect of pre-miR-146b can be completely neutralized by anti-miR-146b transfection (n = 3 for each condition) at a concentration ratio of around 10:1. Results are expressed as mean ± SEM. *p < 0.05, **p < 0.01, ***p < 0.001 (Student's *t*-test).

August 2010, updated: Nov 2010) and by additional programs – mirDB (Wang, 2008) (updated: January 2012, http://mirdb.org/miRDB/index.html) and microT (Maragkakis et al., 2011) (v4.0, http://diana.cslab.ece.ntua.gr/DianaTools/ index.php?r=microtv4/index). In fact, all candidates originally predicted by both TargetScan Mammal v.4.2 and PicTar except Per1 are predicted by 3 or more of these 5 programs (TargetScanMouse v6.0, microT v4.0, PicTar, miRanda 08/2010, mirDB 01/2012), indicating that we have tested the expression of a group of highly probable miR-146b target candidates in $BDNF^{Val}$ and $BDNF^{Met}$ knock-in mice.

We were able to clone the 3'UTR of 10 of these candidates from adult mouse HPC cDNA and tested the expression of the 3'UTR-fused luciferase reporter constructs under "pre-miR-146b" mimic or a scramble precursor ("pre-scramble") in N18 cells. Luciferase expression from 3'UTR constructs of *Irak1*, *Traf6*, *Per1*, *Stx3*, *Syt1*, *Kctd15*, *Sort1*, *Npas4* and *Lin28A* were significant down-regulated ($P < 0.05$) by pre-miR-146b cotransfection as normalized expression under pre-scramble application. The repression of luciferase expression by pre-miR-146b is especially salient on 3'UTR of *Irak1* (59%, $P < 0.001$), *Traf6*

(81%, $P < 0.001$), *Per1* (54%, $P < 0.001$), *Lin28A* (55%, $P < 0.001$), *Npas4* (44%, $P < 0.01$) and *Stx3* (32%, $P < 0.01$), while constructs with 3'UTR of *Syt1* (14%, $P < 0.05$), *Kctd15* (19%, $P < 0.05$) and *Sort1* (15%, $P < 0.05$) were modestly repressed (Figure 4.5A). To demonstrate the specificity of the effects of pre-miR-146b on luciferase reporters on target 3'UTR clones, we tested the ability of anti-miR-146b LNA oligonucleotides to antagonize the impact of pre-miR-146b mimics on *Per1* 3'UTR construct. Addition of 0.1 nM and 1 nM of pre-mir-146b resulted in 46% ($P < 0.05$) and 56% ($P < 0.05$) repression in luciferase expression as compared to the pre-scramble control. On the other hand, when increasing concentration of anti-miR-146b oligonucleotides were cotransfected with pre-miR-146b mimics, there were corresponding increases in luciferase expression from the *Per1* 3'UTR reporter clone transfected with pre-miR-146b (Figure 4.5B). Anti-miR-146b LNA oligonucleotides were less efficient and only fully antagonized pre-miR-146b mimics at a stoichiometric ratio of around 10:1. Nevertheless, the observation that anti-miR-146 antagonizes the impact of pre-miR-146b on *Per1* 3'UTR-controled luciferase expression suggested that the luciferase assay screen for miR-146b targets was specific and miR-146b can repress expression of these predicted targets, except Dlgap1, through their 3'UTR sequences.

4.2.5 Per1 and Npas4 are Regulated by miR-146b

As mammalian miRNAs inhibit target expression predominantly through decreasing mRNA levels rather than translational repression (Guo et al., 2010), we hypothesized that most of the physiologically relevant target genes *in vivo* are upregulated at the transcript levels in *Met/Met* animals which have lower levels of mir-146b, as compared to *Val/Val* animals. Therefore, we measured and compared the expression levels of the predicted candidates in *Val/Val*, *Val/Met* and *Met/Met* animals by qRT-PCR. Expression of 3 additional targets predicted by miRanda (Betel et al., 2008) (*Akt3*, *Srrd*, *Bsn*, see Table 4.2) with important function in transmitter production (*Srrd*), postsynaptic density (*Bsn*) and TrkB signaling (*Akt3*) were also analyzed. Expression levels of only *Per1* and *Npas4* were upregulated in *Val/Met* (24% for *Per1* and 27% for *Npas4*) and *Met/Met* mice (28% for *Per1* and 79% for *Npas4*) as compared to *Val/Val* mice and were significant influenced by genotype as analyzed by one-way ANOVA ($P < 0.01$ for *Per1*; $P < 0.05$ for *Npas4*) (Table 4.3, left panel and Figure 4.6A and 4.6B). There was no genotype effect on expression levels for other predicted targets, except for *Kctd15* which is drastically down-regulated in

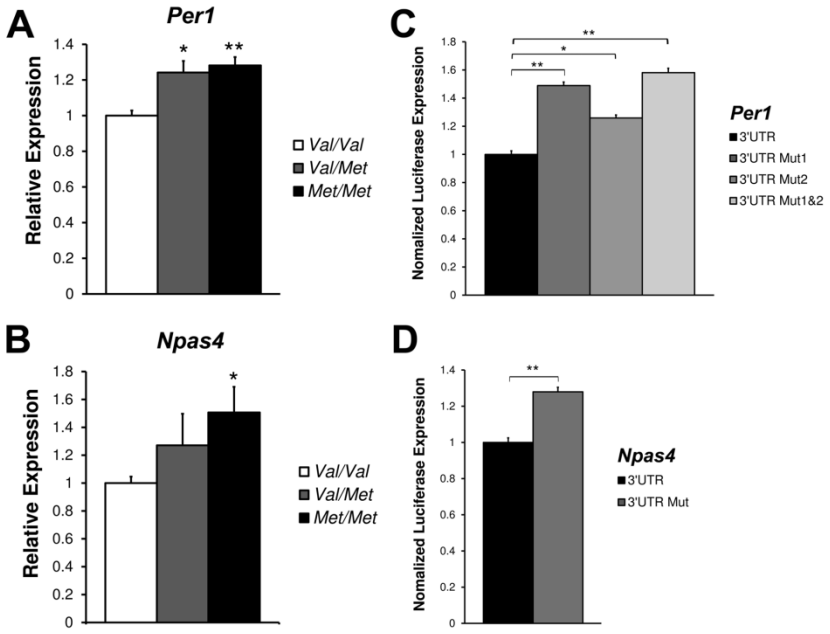

Figure 4.6 *Per1* and *Npas4* Expression is Regulated by miR-146b. (A-B) Expression levels of *Per1* (A) and *Npas4* (B) in hippocampus (HPC) of *Val/Val*, *Val/Met* and *Met/Met* mice (n = 6 each genotype), as measured by qRT-PCR. The expression levels in *Val/Met* and *Met/Met* mice were normalized to *Val/Val* animals. (C-D) *Per1* 3′UTR luciferase reporters with mutations at Site 1 (Mut1) or Site 2 (Mut2) or both sites (Mut1&2) (C) and Npas4 3'UTR report with a mutation at the binding site (D) were analyzed in luciferase assay conducted in N18 cells (n = 3 for each reporter). Mutated *Per1* and *Npas4* 3′UTR reporters express significantly higher luciferase activities than Wt *Per1* 3′UTR reporters. Normalized expression values of each reporter to Wt 3'UTR reporters. Results are expressed as mean ± SEM. *p < 0.05, **p < 0.01, ***p < 0.001 (Student's *t*-test).

Val/Met but not *Met/Met* mice. This result is hard to explain and may be due to technical issues of PCR probe design or low and fluctuated levels of *Kctd15* in the HPC. None of the genes without a miR-146b seed sequence showed significantly elevated expression in *Val/Met* and *Met/Met* mice (Table 4.3, right panel). Fisher's Exact Test showed a $P = 0.24$ for equal distribution of significantly upregulated genes in target group and non-target group. Since we showed that luciferase reporter fused with either the *Per1* or *Npas4* 3'UTRs were downregulated by pre-miR-146b application (Figure 4.5A), an increase in *Per1* and *Npas4* levels in *Val/Met* and *Met/Met* mice were likely due to reduced endogenous miR-146b levels in these mice.

To investigate if miR-146-mediated repression is specific and operates directly via the target sites predicted by TargetScan (Table 4.2), we engineered luciferase reporters carrying mutated versions of *Per1* and *Npas4* 3′UTR with miR-146 binding sites mutated. *Per1* 3'UTR contains two cognate miR-146b binding sites at position 190-197 (an 8-mer site) and position 505-511 (a 7mer-1A site), so for *Per1*, 3 different 3'UTR mutants were generated (Mut1: Site 1 mutant; Mut2: Site 2 mutant; Mut1&2: Site 1 and 2 mutants; see Methods). A mutant *Npas4* 3'UTR (Mut) with the 7mer-m8 site at position 315-321 was also generated. Under pre-miR-146b mimic transfection in N18 cells, Mut1, Mut2 and Mut1&2 in *Per1* 3'UTR

increased the luciferase activity by 49% ($P < 0.01$), 26% ($P < 0.05$), and 58% ($P < 0.01$) respectively, while Mut in *Npas4* 3'UTR increased the luciferase activity by 29% ($P < 0.01$) (Figure 4.6C, D). Thus both miR-146b binding sites in *Per1* 3'UTR control miR-146b-mediated regulation on *Per1* expression, although the 8mer site seems to have a larger impact. The miR-146b binding site in *Npas4* 3'UTR similarly controls the miR-146b-mediated repression of *Npas4* expression. Taken together, we have identified *Per1* and *Npas4* as genuine targets of mir-146b *in vivo*. miR-146b likely represses *Per1* and *Npas4* expression by mRNA degradation. Therefore lower miR-146b levels in *Val/Met* and *Met/Met* animals results in the corresponding rise in *Per1* and *Npas4* transcript levels.

4.2.6 Irak1 is a Translationally Repressed Target of miR-146

We noticed 2 other target genes (*Traf6*, *Irak1*) for which luciferase clones were strongly affected by miR-146b (Figure 4.5A) but lacking upregulated expression in *Met/Met* mice compared to *Val/Val* mice (Table 4.2). More intriguingly, these 2 genes have been shown to be verified targets of miR-146 in human monocytes (Taganov et al., 2006) and are important in mediating the signaling downstream of Toll-like receptors (TLRs). It is likely that these targets are repressed by miR-146b translationally without any changes in their transcript levels and thus no expression change was identified by qRT-PCR assays of hippocampus (HPC) (Table 4.3). Therefore, we performed Western blotting to determine whether *Traf6* and *Irak1* are translationally repressed targets altered by *Val66Met* SNP *in vivo*.

Western blot assays of protein extracts from the HPC of $BDNF^{Val}$ and $BDNF^{Met}$ knock-in mice showed increases of Irak1 in *Val/Met* (19%, $P = 0.39$) and *Met/Met* animals (56%, $P < 0.05$) as compared

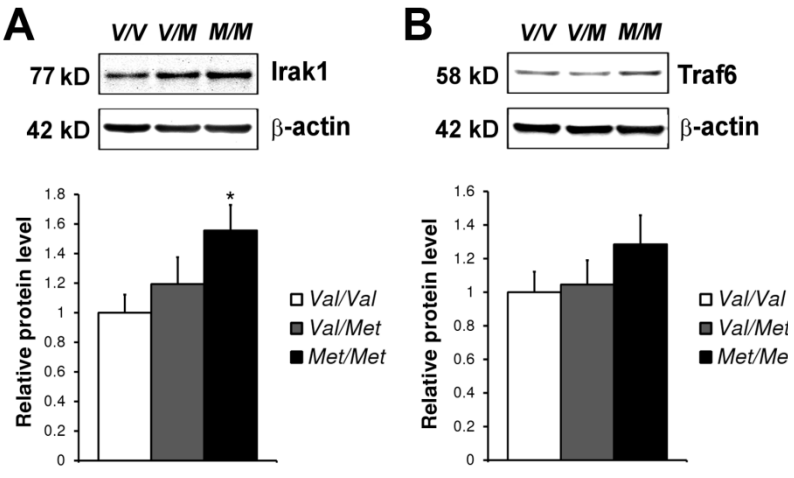

Figure 4.7 Elevation of Irak1 Protein Levels in $BDNF^{Met/Met}$ Mice. (A-B) Western blots in hippocampus (HPC) lysates of Irak1 (A) and Traf6 (B) protein in *Val/Val*, *Val/Met* and *Met/Met* mice (n = 7 each genotype). *Upper:* Representative western blot assays of Irak1 (A) and Tarf6 (B). Beta-actin was used as loading control. *Lower:* Quantification of Irak1 and Traf6 protein levels. Expression levels in *Val/Met* and *Met/Met* mice were normalized to *Val/Val* littermates. Results are expressed as mean ± SEM. **p < 0.01 (Student's *t*-test).

to *Val/Val* animals (Figure 4.7A). There is a trend toward increased Traf6 levels in *Met/Met* animals (28%, $P = 0.18$), but not in *Val/Met* animals (5%, $P = 0.81$) (Figure 4.7B). Thus, although we did not find altered mRNA levels of *Irak1* in *Val/Met* and *Met/Met* mice, Irak1 protein levels were significantly elevated in *Met/Met* mice likely due to decreased miR-146b levels and reduced miR-146b-mediated translational repression in these mice.

4.3 Discussion

By generating knock-in mouse lines with human *BDNF Val* or *Met* allele, we generated "*BDNF*-humanized" mice to study the this common human SNP (rs6265) (Cao et al., 2007). We investigated the impact of *BDNF Val66Met* on the expression profile of miRNAs in the hippocampus (HPC) and identified miR-146b and miR-337-3p to be significantly downregulated by the *Val66Met* SNP. In *Met/Met* mice, the decrease in miR-146b levels is likely due to the lower overall levels of BDNF released either constitutively or during activities, as exogenously applied BDNF acutely elevated miR-146b expression in HPC slices. In a series of experiments, we then identified *Per1*, *Npas4* and *Irak1* as physiological targets affected by altered miR-146b levels in HPC of *Val66Met* mice (Figure 4.8). Importantly, miR-146b binds to target sites in the 3'UTR of *Per1* and *Npas4* and results in degradation of the mRNA, whereas miR-146b represses the translation of Irak1 protein without changing its mRNA levels. As a whole, these data suggested a

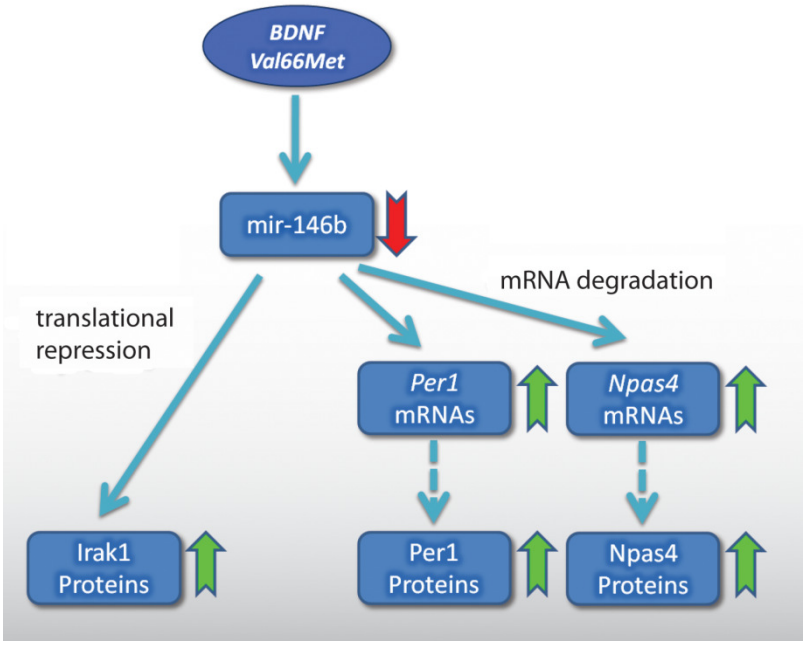

Figure 4.8 Dysregulation of miR-146b and Its Targets due to *BDNF Val66Met* SNP. Carrying *BDNF Met* allele results in the downregulation of miR-146b in *Met/Met* animals. This in turn leads to derepression of translationally repressed target Irak1 ofmiR-146b. Per1 and Npas4 mRNA levels are increased in *Met/Met* animals due to a reduction in miR-146b-mediated mRNA degradation.

common human SNP *BDNF Val66Met* results in specific miRNA alteration that is modest in magnitude but can possibly lead to physiological changes of expression levels and functions of certain targets.

4.3.1 BDNF-mediated Regulation of miRNAs

BDNF has been shown to induce the expression of genes (e.g. *Arc*) involved in synaptic plasticity (Lyons and West, 2011). This is mediated through activation of MAPK pathway and Akt1/2 downstream of TrkB which in turn leads to activation of CREB, MEF2 and NF-κB transcription factors(Huang and Reichardt, 2003; Shalizi and Bonni, 2005; Yoshii and Constantine-Paton, 2010). *mir-212–mir-132* cluster (Vo et al., 2005) and *mir-379–mir-410* cluster (Fiore et al., 2009) are among many activity-independent transcriptional targets induced by BDNF. The nature of the induction has been characterized. CRE motifs are found upstream of mir-212 (two CRE motifs) and mir-132 (one CRE motif) and were shown to be bound by CREB (Vo et al., 2005). Likewise, MEF2 binds to a site found in the promoter region of the *mir-379–mir-410* cluster (Fiore et al., 2009). During activity, BDNF-dependent activation of CREB and MEF2 thus induces the expression of these miRNAs. miR-132 and at least 3 individual miRNAs of the *mir-379–mir-410* cluster (miR-134, miR-381 and miR-329) are required for activity-dependent dendritic outgrowth. In addition, miR-134 also regulates spine size in a BDNF-controlled fashion (Schratt et al., 2006). Recently it was also shown that BDNF rapidly activates Dicer and induces GW182-containing RNA processing bodies, leading to a general increase in mature miRNA levels in hippocampal neurons. 89.4% of significantly altered miRNAs from hippocampal neurons treated with BDNF for 30 min were increased by more than two-fold. However, BDNF-induced expression of Lin28 specifically downregulates Lin28-associated miRNAs (e.g. let-7). Expression of a Lin28-resistant let-7 precursor prevented BDNF-dependent dendritic arborization (Huang et al., 2012). This evidence points to the importance of BDNF-induced miRNA expression in neuronal morphogenesis and function. Nevertheless, we should be cautious in interpreting these results in a physiological context as these experiments were all done in cultured hippocampal neurons with exogenously applied BDNF. Questions remain regarding whether these miRNA are regulated by BDNF *in vivo* during activity and regarding the magnitude of the BDNF-induced miRNA alteration. It is also not known whether genetic variations that affect BDNF expression or

function alter the expression of BDNF-regulated miRNAs. Thus, we want to study a miRNA alteration due to the common *BDNF* SNP *Val66Met* in knock-in mice harboring the human *BDNF Val* or *Met* alleles.

4.3.2 BDNF SNP and miRNA Expression

Since *BDNF Val66Met* has been shown to impair the constitutive and activity-induced dendritic targeting of BDNF mRNA (Chiaruttini et al., 2009) and protein (Chen et al., 2005), it is conceivable that *BDNF* knock-in mice carrying the *Met* allele have reduced BDNF release from terminals at both basal and activated states. Therefore, we predicted to see downregulation of BDNF-induced miRNAs, especially miR-132 and miR-134. From the miRNA array, miR-132 and miR-212 were both downregulated in *Met/Met* animals as compared to *Val/Val* animals, with FC of 0.90 (P = 0.35) and 0.95 (P = 0.31) respectively. Although the changes were not significant, probably partly due to the small number of mice compared and the modest downregulation, it suggested a baseline reduction of expression from the *mir-212–mir-132* cluster in *Met/Met* animals due to lower BDNF levels. Of the 49 miRNAs in the array from the *mir-379–mir-410* cluster, we found 28 were upregulated and 21 were downregulated, with no miRNA passing a FDR-corrected P-value < 0.12. It is of note that the BDNF-dependent induction of the *mir-379–mir-410* cluster peaked at 2 hours after treatment and went back to basal levels before 5 hours (Fiore et al., 2009). It is likely the expression of the *mir-379–mir-410* cluster is under BDNF control only at a specific temporal window during activity and thus any BDNF-dependent expression alteration would not be detected in our experimental design which monitors the basal expression of miRNAs in hippocampus.

In general, our miRNA expression profiling showed that the miRNA alteration due to *Val66Met* is very restricted and modest, with expression of only 24 miRNAs significantly changed (0.79< FC < 1.6, FDR-corrected P-value < 0.05). Only 4 of these miRNAs were changed by more than 25%. Focusing on 4 miRNAs with highly significant FDR-corrected P-value (P < 0.005) and absolute fold change > 1.2, we verified miR-146b, which was shown to be synaptically enriched (Lugli et al., 2008), to be significant changed due to *BDNF Val66Met* SNP, and in response to BDNF treatment. It was shown that the transcriptional induction of miR-146a and miR-146b downstream of TLR activation is mediated through NF-κB and JNK-1/2 (*mir-146a*) and MEK-1/2 and JNK-1/2 (*mir-146b*) (Perry et al., 2009; Taganov et al., 2006), but how exactly *mmu-mir-146b* expression is regulated by transcription factors is still unknown.

4.3.3 Is miR-146b Transcriptionally Activated by BDNF?

We speculate that the miR-146b can be transcriptionally activated by transcription factors downstream of BDNF, such as CREB or MEF2, which are important in transcriptional activation of *mir-132* (Vo et al., 2005) and the *mir-379–mir-410* cluster (Fiore et al., 2009) respectively. We thus searched for putative transcription factor binding sites within the promoter region predicted according to the H3K4me3 landscape (Marson et al., 2008), about 2.5 kb upstream of the transcription start site (TSS) of *Tmem180* which contains *mmu-mir-146b* within its first intron , using web-based prediction program TFSEARCH v.1.3 (http://www.cbrc.jp/research/db/TFSEARCH.html) and ConSite (http://asp.ii.uib.no:8090/cgi-bin/CONSITE/consite). There is a *CRE* sequence (CREB binding site) and a CRE-BP binding site at -149 from TSS and a MEF2 at -32 from TSS. There are additional MEF2 sites at -1694, -860 and +560 from TSS and 2 potential CREB sites at -1186 and +87. Additionally, 8 NF-κB binding sites are found at -2239, -1725, -1566, -1507, -1093, -341, -170 and +260 from TSS. It remains to be proved whether BDNF signaling can induce *mir-146b* through transcription factors binding to these sites. Nevertheless, it is an intriguing idea that reduced binding of CREB or MEF2 to the *mir-146b* promoter due to lower BDNF signaling in *Val/Met* and *Met/Met* animals leads to the decreased expression of miR-146b in these animals. Since MeCP2 transcriptionally activates *BDNF*, it is noteworthy that miR-146b is downregulated in an *Mecp2*-null (KO) mouse model of Rett syndrome (Urdinguio et al., 2010). Furthermore, quantitative chromosome immunoprecipitation (ChIP) assays reveal the occupancy of MeCP2 to 5'-end CpG islands in the *mmu-mir-146b* genomic locus and suggest that MeCP2 directly transcriptionally activates *mir-146b* expression by binding to its promoter. Although the exact mechanism by which miR-146b is altered by *Val66Met* SNP remains to be examined, it is conceivable that dysregulation of miR-146b caused by *Val66Met* could possibly lead to some functional alteration or phenotypic variation in *Met* allele carriers.

4.3.4 Functional Implication of miRNA-146b Dysregulation due to Val66Met SNP

There was extensive research indicating important roles of miR-146b and miR-146a in regulation of immune responses and inflammation (Hou et al., 2009; Taganov et al., 2006), cancer metastasis (Bhaumik et al., 2008; Li et al., 2010) and tumor development (Jazdzewski et al., 2009; Jazdzewski et al.,

2008). miR-146a has the same seed sequence as miR-146b and likely shares largely overlapping targets with miR-146b. Multiple reports showed that both miR-146a and miR-146b were upregulated after TLR and NF-κB activation and repressed Traf6 and Irak1 to control the extent of TLR and cytokine signaling (Lu et al., 2010; Perry et al., 2009; Taganov et al., 2006). This negative regulatory loop is critical to suppress widespread immune responses which lead to inflammation and likely rheumatoid arthritis (Stanczyk et al., 2008), osteoarthritis (Yamasaki et al., 2009) and systemic lupus erythematosus (Luo et al., 2011). Besides a role in immune regulation, miR-146b was cloned and identified from the hippocampus (He et al., 2007) and was found to be the 72nd most abundant miRNA in mouse hippocampus by counts of sequencing reads in one report (Zovoilis et al., 2011) (in comparison, brain-specific miR-134 was the 99th most abundant in that study). Here we showed that Irak1 was a translationally repressed target of miR-146b and was upregulated in *Met/Met* animals. Traf6 protein levels also increased though not significantly in *Met/Met* animals and its 3'UTR is under pre-miR-146b control in a luciferase assay. Interestingly, in a microarray study, *Irak1* is shown be upregulated in *Mecp2*-null mice (Chahrour et al., 2008). Since *Bdnf* is downregulated in *Mecp2*-null mice, this result is consistent with our identification of *Irak1* as a physiological target upregulated in *Met/Met* animals. Irak1 upregulation in *Met/Met* mice enhances NF-κB signaling and results in pro-inflammatory responses in hippocampus. Recently, the role of a miR-146a-mediated inflammatory circuit in Alzheimer Disease and in stressed human brain cells was proposed (Cui et al., 2010; Li et al., 2011; Lukiw et al., 2008; Pogue et al., 2009). Since miR-146a and miR-146b share similar targets and can be induced by NF-κB, it is possible that there can be an association of *Val66Met* is with Alzheimer Disease.

In addition, *Per1* and *Npas4* were also miR-146b targets because mRNA levels were upregulated in *Met/Met* animals. Per1 is a transcriptional repressor with a PAS domain which is transcriptionally activated by master regulator Clock–Bmal1 complex. Accumulation of Per1 which peaks at Zeitgeber Time (ZT) 10-14 (around lights off) leads to increased inhibition of Clock–Bmal1 transcriptional activity and thus reduced expression of Per1 itself. This feedback cycle of the core loop provides a nearly 24 hour circadian cycle and drives rhythmic expression of many other clock modulated genes. It will be interesting to test whether *BDNF Val66Met* knock-in animals have any circadian rhythm anomaly.

Interestingly, another transcriptional factor with a PAS domain, Npas4 (neuronal period aryl hydrocarbon receptor nuclear translocator single-minded domain protein 4) is also a miR-146b target. Npas4 is a membrane depolarization-activated transcription factor that upregulates expression of BDNF, c-Fos, Zif268 and Arc (Lin et al., 2008; Ramamoorthi et al., 2011) while downregulating other membrane depolarization-regulated genes (Lin et al., 2008) and is required for inhibitory synapse development in hippocampus. In addition, Npas4 expression in the hippocampus and the lateral nucleus of amygdala (LA) is required for formation and reactivation of fear memories. Activation of the Npas4-regulated transcriptional program in CA3 is required for contextual learning (Ramamoorthi et al., 2011). Npas4 activation in LA is required for formation and retention of a reactivated auditory cue-associated fear memory (Ploski et al., 2011). BDNF or other neurotrophic factors are not able to induce Npas4 expression (Ramamoorthi et al., 2011), so Npas4 expression after membrane depolarization and Ca^{2+} influx appears to precede BDNF upregulation. We showed here that BDNF-induced miR-146b limits the expression level of Npas4 and its transcriptional targets therefore controlling the extent of neuronal activity. Similar negative regulatory loops MeCP2–BDNF–miR-132 and CREB–BDNF–miR-134 were previously described (Fiore et al., 2009; Gao et al., 2010; Klein et al., 2007; Zhou et al., 2006), and these transcription factor–BDNF–miRNA loops may represent a general mechanism that neuronal activity-dependent transcriptional programs can be finely controlled. These negative feedback loops may also be important for the homeostasis of activity within neural circuits in hippocampus and other brain areas. Therefore, alteration of Npas4-regulated transcriptional program in *Met* allele carrying animals may underlie the impaired cognitive function that relies on hippocampal circuits.

4.4 Summary

We performed a microRNA expression profiling in hippocampus of humanized *BNDF* knock-in mice and find that a BDNF-induced miRNA, miR-146b, is downregulated in *Met/Met* animals. Moreover, the reduced levels of miR-146b in turn lead to the increased *Per1* and *Npas4* mRNA levels and increased Irak1 protein but not mRNA levels in *Met/Met* mice (Figure 4.8). These findings highlight molecular alterations downstream of a modest miRNA dysregulation caused by a common human SNP in the *BDNF* gene. The resulting changes in proteins with roles in immune regulation, circadian rhythm and activity-

dependent transcription regulation may have functional impacts in cognitive functions which are compromised due to *Val66Met* variant.

Table 4.1 Significantly Altered MicroRNAs in the Hippocampus of *BDNF*$^{Met/Met}$ Mice

mmu-miR	FDR *P*–value	regulation	Fold Change	Stem-loop Accession	Chr	Chr_start	Chr_end	Strand	Note
197	**2.73E-03**	**up**	**1.58**	MI0005485					a
146b	**2.83E-03**	**down**	**0.83**	MI0004665	19	46417252	46417360	+	
700	**2.83E-03**	**up**	**1.66**	MI0004684	4	134972470	134972548	-	
337-3p	**3.54E-03**	**down**	**0.83**	MI0000615	12	110823999	110824095	+	
130b	3.54E-03	up	1.17	MI0000408	16	17124154	17124235	-	
127-5p	4.38E-03	up	1.12	MI0000154	12	110831056	110831125	+	b
328	7.71E-03	up	1.23	MI0000603	8	107832264	107832360	-	
291a-5p	9.73E-03	down	0.93	MI0000389	7	3218920	3219001	+	
10a	1.03E-02	up	1.15	MI0000685	11	96178479	96178588	+	
20b	1.40E-02	down	0.88	MI0003536	X	50095290	50095369	-	
337-5p	2.51E-02	up	1.15	MI0000615	12	110823999	110824095	+	
532-5p	2.61E-02	up	1.23	MI0003206	X	6825528	6825623	-	
674	3.05E-02	up	1.26	MI0004611	2	117010863	117010962	+	
27b	3.30E-02	down	0.92	MI0000142	13	63402020	63402092	+	
874	3.70E-02	down	0.88	MI0005479	13	58124486	58124561	-	
804	4.29E-02	up	1.15	MI0005203	11	50171287	50171381	-	
7a-1-3p	4.29E-02	down	0.83	MI0000728	13	58494140	58494247	-	c
485-3p	4.29E-02	up	1.14	MI0003492	12	110973112	110973184	+	d
491	4.29E-02	up	1.15	MI0004680	4	87767944	87768029	+	
721	4.29E-02	down	0.79	MI0004708	5	136851586	136851673	-	
688	4.29E-02	down	0.87	MI0004653	15	102502223	102502297	-	
342-3p	4.40E-02	down	0.87	MI0000627	12	109896830	109896928	+	
378	4.45E-02	up	1.29	MI0000795	18	61557489	61557554	-	
185	4.51E-02	up	1.09	MI0000227	16	18327494	18327558	-	

a: removed from miRBase, b: previously mmu-miR-127*, c: previously mmu-miR-7a*, d: previously mmu-miR-485*

Table 4.2 Candidate miR-146b Targets Selected for Validation

	TargetScanMouse version 6.0, 11/2011									microT version 4	PicTar 03/2007	miRanda 08/2010	mirDB 01/2012	
		Conserved sites				Poorly conserved sites								
Target	total context+ score	total	8mer	7mer-m8	7mer-1A	total	8mer	7mer-m8	7mer-1A	miTG score	PicTar score	mirSVR score	target score	Note
Irak1	**-0.77**	2	2	0	0	1	0	0	1	**0.68**	**8.79**	**-1.65**	**94**	
Traf6	**-0.53**	3	3	0	0	0	0	0	0	**0.86**	**6.28**	**-0.72**	**95**	
Per1	**-0.31**	0	0	0	0	2	1	0	1		**2.52**	**-0.66**		a
Stx3	**-0.25**	1	1	0	0	0	0	0	0	**0.41**	**1.06**	**-0.46**		
Syt1	**-0.22**	1	1	0	0	1	0	0	1	**0.50**	**4.44**	**-1.15**		
Cask	**-0.21**	1	0	1	0	1	0	0	1	**0.57**	**1.02**	**-0.48**	**65**	
Robo1	**-0.19**	1	0	0	1	0	0	0	0	**0.51**	**1.30**	**-0.52**		
Kctd15	**-0.17**	1	1	0	0	0	0	0	0	**0.39**	**5.00**	**-0.20**		
Sort1	**-0.13**	1	1	0	0	0	0	0	0			**-0.22**	**50**	
Dlgap1	**-0.09**	0	0	0	0	1	0	1	0	**0.51**	**0.75**	**-0.18**		b
Srrd	**-0.08**	0	0	0	0	1	0	1	0		**1.56**	**-0.03**		c
Bsn	**-0.07**	0	0	0	0	1	0	0	1			**>-0.01**		c
Gria3	**-0.03**	0	0	0	0	1	1	0	0	**0.43**	**0.83**	**>-0.01**		a
Npas4	**-0.02**	1	0	1	0	0	0	0	0	**0.43**	**2.02**	**-0.02**		
Lin28A	**-0.01**	0	0	0	0	1	0	0	1	**0.44**	**2.53**	**-0.01**		b
Akt3	**-0.01**	0	0	0	0	1	0	0	1			**-0.31**		

Note:

[a] Predicted in TargetScan v4.2 but not v5.0Mouse or v5.0Human due to low site conservation score

[b] Predicted in TargetScan v4.2 and v5.0Human but not v5.0Mouse due to low site conservation score

[c] Not Predicted in TargetScan v4.2Vertebrate due to low site conservation score

Table 4.3 Expression Levels of Candidate miR-146b Targets and Non-Targets in The HPC of *BDNF*$^{Met/Met}$ Mice

Genes with miR-146b Binding Site(s)			
	V/M	M/M	ANOVA
gene	fold change	fold change	*P*-value
Kctd15	0.25	1.05	<1.0E-4
Per1	1.24	1.28	1.1E-3
Npas4	1.27	1.79	0.02
Robo1	1.10	1.04	0.06
Akt3	1.10	1.10	0.14
Traf6	1.03	0.94	0.19
Syt1	1.13	1.05	0.29
Irak1	1.02	0.96	0.30
Sort1	1.10	1.03	0.33
Cask	1.01	0.88	0.36
Gria3	0.99	1.11	0.40
Stx3	0.91	1.01	0.41
Srr	1.09	1.00	0.53
Bsn	1.03	1.05	0.55

Genes without miR-146b Binding Site(s)			
	V/M	M/M	ANOVA
gene	fold change	fold change	*P*-value
Cpeb4	1.01	0.93	0.03
B3gat1	0.91	0.97	0.09
Kif5c	1.13	1.06	0.10
Cdk5r1	1.07	1.09	0.12
Ldb2	1.02	0.95	0.18
Cpeb2	1.07	1.01	0.31
GSK3b	1.03	0.97	0.37
Cdk5r2	1.05	1.15	0.39
vGlut1	0.99	0.95	0.49
Agxt2l1	1.10	1.24	0.64
Nptx2	0.97	1.05	0.67
Hspa8	0.98	0.94	0.71
Clec16a	1.01	1.01	0.97
Mef2C	0.99	0.99	0.98

4.5 Methods

4.5.1 Generation of BDNF^{Val} and BDNF^{Met} Knock-in Allele

A 370 bp fragment, located 5′ of the mouse *Bdnf* coding region, was amplified from genomic mouse DNA with the following primers: 5′-ACAGATGTAGTAAAACGTTGGAG-3′ and 5′-TTACTGATCCACTCCAGCTGC-3′. This fragment was subcloned into pGEMT (Promega) with T-A cloning and was used as a probe against a 129 Sv/Ev BAC library. One of the identified BAC clones was expanded for use in the generation of targeting constructs. Flanking sequence 11 kb upstream (long arm) and 3 kb downstream (short arm) of the *Bdnf* gene was PCR-ed from the BAC clone using the following sets of primers: 5′-GCGGCCGCCAGGCTCTATTTGATTATAAAATAG-3′, 5′-GGCCGGCCATGTGCACT GAATTTCAGTTCAG-3′ and 5′-ACGCGTCGACTGACTGCCTGCGACAAACTT-3′, 5′-GGCGCGCCTC AGCCCTGGTTCATGGATCCTG-3′.

Additionally, 274 bp of sequence including the 5′ UTR and a portion of the coding sequence was amplified from human DNA extracted from a *Val/Val* or a *Met/Met* individual with the following primers: 5′-ACCAGGTGAGAAGAG TGATGACCATCCTTTTCCTTAC-3′ and 5′-CACCCGGGA CGTGTACAAGTC-3′. The long arm was further modified into the long arm^{Val} and the long arm^{Met} fragments by excision of the mouse sequence located between unique *Xma*I and *SexA*I sites, aligned with the human 274 base pair fragment, and replacement with sequence from the *Val/Val* or the *Met/Met* individuals. Finally, the *BDNF^{Met}* and *BDNF^{Val}* knockin constructs were assembled, by cloning the corresponding long arms into the *Asc*I site of the pACNIII targeting construct (5′ of a self-excisable neo cassette) and the short arm into the *Not*I and *Fse*I sites, located at the 3′ of this cassette. All PCR reactions related to the generation of this construct were conducted with the Expand High Fidelity kit (Roche), and subcloning steps involved the use of the Rapid Ligation Kit (Roche) or the Infusion Kit (BD Biosciences). A total of 70 µg of each plasmid (*BDNF^{Met}* and *BDNF^{Val}*) was electroporated into 129 Sv/Ev embryonic stem cells. Twenty-four hours after electroporation, neomycin selection was applied and approximately 400 clones were picked for each construct after 5 days of selection. These clones were analyzed with a PCR approach, expanded, and confirmed with Southern blot analysis. The restriction enzyme *Mfe*I was used to digest ES cell DNA, and a probe located outside the targeting construct (at the 3′ end) generated a 5.9 kb targeted band and a 3.8 kb wild-type band in correctly targeted clones. Both constructs recombined at a rate of ~1%. Upon

germline transmission, DNA extracted from tail-biopsy samples of both lines of mice was genotyped with the human primers described above, and this was followed by a diagnostic restriction-enzyme analysis with either *Pml*I ($BDNF^{Val}$) or *BmgB*I ($BDNF^{Met}$).

4.5.2 miRNA Microarray

6 pairs of 8-week-old male homozygous $BDNF^{Val}$ and $BDNF^{Met}$ knock-in mice (6 pairs of *Val/Val* and *Met/Met*) are used for global miRNA expression profiling. We isolated 25-35 mg of total RNA from HPC of these mice using mirVana miRNA isolation kit (Ambion). Quality of RNA samples were verified by BioAnalyzer (Agilent) and all RNAs had a RIN > 7.0. Small RNAs (<300 nt) were then isolated and processed for microarray analysis (LC Sciences). Purified small RNAs were labeled with Cy3 (*Val/Val*) or Cy5 (*Met/Met*) fluorescent dyes and hybridized to dual-channel microarray mParaFlo microfluidics chips (LC Sciences) containing 569 miRNA probes to mouse mature miRNA. The miRNA probe sequences used were from miRBase Sequence database version 10.1 (microrna.sanger.ac.uk). Hybridization images were collected using GenePix 4000B laser scanner (Molecular Devices) and digitalized using Array-Pro image analysis software (Media Cybernetics). Raw data were imported into ArrayAssist 5.0 (Stratagene). The microarray data were corrected by removing spots with intensity equal to or below median background and then normalized with the LOWESS (locally weighted regression) method implemented in ArrayAssist software. Differentiation analysis was conducted to determine the FDR *P*-value of each miRNA gene.

4.5.3 Quantitative RT-PCR

Total RNA samples were extracted from 8-wk old male mice using using mirVana miRNA Isolation Kit (Ambion) according to manufacturer's protocol. We treated 3 µg of total RNA from each sample with DNA-free kit (Ambion/Applied Biosystems). For qRT-PCR of mature miRNA, 100 ng of treatment RNA each sample was reverse transcribed. A *glyceraldehyde-3-phosphate dehydrogenase (GAPDH)* gene-specific RT primer was also included RT reaction. For qRT-PCR of other genes, the remaining DNase-treated RNA each sample was reverse transcribed using random primers and SuperScript II Reverse Transcriptase (Invirtogen). qPCR was performed in a 7900 Sequence Detection System (Applied Biosystems) and the qPCR and quantification procedures are described in Chapter 2.

All PCR primers and probes were designed at Primer3 web site (http://frodo.wi.mit.edu/) and purchased from Sigma Genosys (Sigma-Aldrich) and the sequences can be found in Appendix 1, except for *Nptx2* (Mm00479438_m1, Applied Biosystems) and *Clec16a* (Mm00624340_m1, Applied Biosystems). All target gene probes were 5' FAM and 3' BHQ™-1 Dual labeled. Mouse *GAPDH* mRNA was used as the endogenous control. The *GAPDH* gene probe was 5' JOE™ and 3' BHQ™-1 dual labeled.

4.5.4 BDNF-treatment of Hippocampal Slices

8-wk old Wt C57Bl/6J mice were anesthetized with isoflourane and then decapitated. The brain was removed and chilled in ice-cold dissection solution (in mM: sucrose 195, NaCl 10, KCl 2.5, NaH_2PO_4 1, $NaHCO_3$ 25, glucose 10, $MgCl_2$ 5, $MgSO_4$ 1, $CaCl_2$ 0.5). The cerebellum and the anterior portion of the brain were removed and horizontal brain sections cut on a vibratome (Leica VT1200S). About 10 slices of 250 µm slices were cut and then immediately transferred to an interface chamber and allowed to recover for 1 h at 31–32 ℃. Slices were then transferred to another chamber and incubated for 2 hours with pre-oxygenated artificial cerebrospinal fluid (aCSF) (bubbled with 5% CO2/95% O2) that had the following composition (in mM): NaCl 124, KCl 2.5, NaH2PO4 1, NaHCO3 25, Glucose 10, MgSO4 1, CaCl2 2. In the BDNF treatment group, the aCSF also contained 50 ng/ml of BDNF (#B3795, Sigma-Aldrich). Slices were removed immediately after 2 hour incubation and total RNAs from the BDNF or sham treated slices were extracted using Trizol (Invitrogen).

4.5.5 Luciferase Assay

The longest 3′UTRs of predicted miR-146b targets (*Irak1*, *Tarf6*, *Per1*, *Stx3*, *Syt1*, *Kctd15*, *Sort1*, *Dlgap1*, *Npas4*, *Lin28A*) were cloned into *Xho*I and *Not*I sites psiCHECK2 luciferase reporter construct (Promega). Mir-146b binding site mutant clones of *Per1* and *Npas4* were generated by PCR-based mutagenesis. *Per1* 3'UTR mutant clone: Site Mut1 sequence (starting from position 186 in 3′UTR): TccAAGTTCagA (lower case letters denote altered nucleotide). Site Mut2 sequence (starting from position 495): GctCCCAGGTGTTacaA. *Npas4* 3'UTR mutant clone: Site Mut sequence (starting from position 309 in 3′UTR): TccGCCAGTTaca. All the clones were verified by Sanger sequencing. Mutations are predicted by RNAhybrid (Rehmsmeier et al., 2004) to disrupt the binding of *miR-146b* at the seeds and secondary binding sites.

N18 neuroblastoma cells were transfected with various psiCHECK2 reporter constructs (100 ng per well of a 24-well plate) together with pre-miR-146b mimic or pre-scramble control (1 nM, unless mentioned otherwise). In the antagonizing experiments, anti-miR-146b was also co-transfected along with pre-miR-146b and *Per1* 3'UTR reporter constructs. Luciferase assays were performed using the Promega Dual-Luciferase Reporter Assay System 24 hours after transcfection and all experiments were performed at least 2 times and all data presented is the average of 3 technical repeats.

4.5.6 Western Blot

General Western blot procedures are described in Chapter 2, with the following modification: (1) ice-old lysis buffer containing 1% Triton X-100, 0.2 mM EDTA, 100 mM KCl and 20 mM Tris pH 8.0 and Proteinase inhibitor cocktail (Roche) was used instead of modified RIPA buffer. (2) Primary anitbody used were Traf6 (#597, MBL), 1:1000 dilution and Irak1 (D51G7, Cell Signaling), 1:1000 dilution. (3) Membranes were re-probed with 1:10000 dilution of β-actin antibody (A5441, Sigma-Aldrich) as loading control. (4) ImageQuant (Molecular Dynamics) was used for densitometric analysis of protein bands.

4.6 References

Alme, M.N., Wibrand, K., Dagestad, G., and Bramham, C.R. (2007). Chronic fluoxetine treatment induces brain region-specific upregulation of genes associated with BDNF-induced long-term potentiation. Neural plasticity *2007*, 26496.

Barde, Y.A., Edgar, D., and Thoenen, H. (1982). Purification of a new neurotrophic factor from mammalian brain. EMBO J *1*, 549-553.

Bath, K.G., Jing, D.Q., Dincheva, I., Neeb, C.C., Pattwell, S.S., Chao, M.V., Lee, F.S., and Ninan, I. (2012). BDNF Val66Met Impairs Fluoxetine-Induced Enhancement of Adult Hippocampus Plasticity. Neuropsychopharmacology.

Bath, K.G., Mandairon, N., Jing, D., Rajagopal, R., Kapoor, R., Chen, Z.Y., Khan, T., Proenca, C.C., Kraemer, R., Cleland, T.A.*, et al.* (2008). Variant brain-derived neurotrophic factor (Val66Met) alters adult olfactory bulb neurogenesis and spontaneous olfactory discrimination. J Neurosci *28*, 2383-2393.

Beste, C., Kolev, V., Yordanova, J., Domschke, K., Falkenstein, M., Baune, B.T., and Konrad, C. (2010). The role of the BDNF Val66Met polymorphism for the synchronization of error-specific neural networks. J Neurosci *30*, 10727-10733.

Betel, D., Wilson, M., Gabow, A., Marks, D.S., and Sander, C. (2008). The microRNA.org resource: targets and expression. Nucleic acids research *36*, D149-153.

Bhaumik, D., Scott, G.K., Schokrpur, S., Patil, C.K., Campisi, J., and Benz, C.C. (2008). Expression of microRNA-146 suppresses NF-kappaB activity with reduction of metastatic potential in breast cancer cells. Oncogene *27*, 5643-5647.

Binder, D.K., and Scharfman, H.E. (2004). Brain-derived neurotrophic factor. Growth factors *22*, 123-131.

Borroni, B., Archetti, S., Costanzi, C., Grassi, M., Ferrari, M., Radeghieri, A., Caimi, L., Caltagirone, C., Di Luca, M., Padovani, A.*, et al.* (2009). Role of BDNF Val66Met functional polymorphism in Alzheimer's disease-related depression. Neurobiology of aging *30*, 1406-1412.

Buckley, P.F., Pillai, A., and Howell, K.R. (2011). Brain-derived neurotrophic factor: findings in schizophrenia. Current opinion in psychiatry *24*, 122-127.

Cao, L., Dhilla, A., Mukai, J., Blazeski, R., Lodovichi, C., Mason, C.A., and Gogos, J.A. (2007). Genetic modulation of BDNF signaling affects the outcome of axonal competition in vivo. Curr Biol *17*, 911-921.

Caputo, V., Sinibaldi, L., Fiorentino, A., Parisi, C., Catalanotto, C., Pasini, A., Cogoni, C., and Pizzuti, A. (2011). Brain derived neurotrophic factor (BDNF) expression is regulated by microRNAs miR-26a and miR-26b allele-specific binding. PLoS One *6*, e28656.

Carver, C.S., Johnson, S.L., Joormann, J., Lemoult, J., and Cuccaro, M.L. (2011). Childhood adversity interacts separately with 5-HTTLPR and BDNF to predict lifetime depression diagnosis. Journal of affective disorders *132*, 89-93.

Cathomas, F., Vogler, C., Euler-Sigmund, J.C., de Quervain, D.J., and Papassotiropoulos, A. (2010). Fine-mapping of the brain-derived neurotrophic factor (BDNF) gene supports an association of the Val66Met polymorphism with episodic memory. The international journal of neuropsychopharmacology / official scientific journal of the Collegium Internationale Neuropsychopharmacologicum *13*, 975-980.

Chahrour, M., Jung, S.Y., Shaw, C., Zhou, X., Wong, S.T., Qin, J., and Zoghbi, H.Y. (2008). MeCP2, a key contributor to neurological disease, activates and represses transcription. Science (New York, NY *320*, 1224-1229.

Chandrasekar, V., and Dreyer, J.L. (2009). microRNAs miR-124, let-7d and miR-181a regulate cocaine-induced plasticity. Molecular and cellular neurosciences *42*, 350-362.

Chandrasekar, V., and Dreyer, J.L. (2011). Regulation of MiR-124, Let-7d, and MiR-181a in the accumbens affects the expression, extinction, and reinstatement of cocaine-induced conditioned place preference. Neuropsychopharmacology *36*, 1149-1164.

Chen, B., Dowlatshahi, D., MacQueen, G.M., Wang, J.F., and Young, L.T. (2001). Increased hippocampal BDNF immunoreactivity in subjects treated with antidepressant medication. Biol Psychiatry *50*, 260-265.

Chen, Q.Y., Chen, Q., Feng, G.Y., Wan, C.L., Lindpaintner, K., Wang, L.J., Chen, Z.X., Gao, Z.S., Tang, J.S., Li, X.W.*, et al.* (2006a). Association between the brain-derived neurotrophic factor (BDNF) gene and schizophrenia in the Chinese population. Neuroscience letters *397*, 285-290.

Chen, Z.Y., Ieraci, A., Teng, H., Dall, H., Meng, C.X., Herrera, D.G., Nykjaer, A., Hempstead, B.L., and Lee, F.S. (2005). Sortilin controls intracellular sorting of brain-derived neurotrophic factor to the regulated secretory pathway. J Neurosci *25*, 6156-6166.

Chen, Z.Y., Jing, D., Bath, K.G., Ieraci, A., Khan, T., Siao, C.J., Herrera, D.G., Toth, M., Yang, C., McEwen, B.S.*, et al.* (2006b). Genetic variant BDNF (Val66Met) polymorphism alters anxiety-related behavior. Science (New York, NY *314*, 140-143.

Chen, Z.Y., Patel, P.D., Sant, G., Meng, C.X., Teng, K.K., Hempstead, B.L., and Lee, F.S. (2004). Variant brain-derived neurotrophic factor (BDNF) (Met66) alters the intracellular trafficking and activity-dependent secretion of wild-type BDNF in neurosecretory cells and cortical neurons. J Neurosci *24*, 4401-4411.

Chiaruttini, C., Vicario, A., Li, Z., Baj, G., Braiuca, P., Wu, Y., Lee, F.S., Gardossi, L., Baraban, J.M., and Tongiorgi, E. (2009). Dendritic trafficking of BDNF mRNA is mediated by translin and blocked by the G196A (Val66Met) mutation. Proceedings of the National Academy of Sciences of the United States of America *106*, 16481-16486.

Cohen-Cory, S., Kidane, A.H., Shirkey, N.J., and Marshak, S. (2010). Brain-derived neurotrophic factor and the development of structural neuronal connectivity. Developmental neurobiology *70*, 271-288.

Cui, J.G., Li, Y.Y., Zhao, Y., Bhattacharjee, S., and Lukiw, W.J. (2010). Differential regulation of interleukin-1 receptor-associated kinase-1 (IRAK-1) and IRAK-2 by microRNA-146a and NF-kappaB in stressed human astroglial cells and in Alzheimer disease. J Biol Chem *285*, 38951-38960.

de Leon-Guerrero, S.D., Pedraza-Alva, G., and Perez-Martinez, L. (2011). In sickness and in health: the role of methyl-CpG binding protein 2 in the central nervous system. The European journal of neuroscience *33*, 1563-1574.

de Sousa, R.T., van de Bilt, M.T., Diniz, B.S., Ladeira, R.B., Portela, L.V., Souza, D.O., Forlenza, O.V., Gattaz, W.F., and Machado-Vieira, R. (2011). Lithium increases plasma brain-derived neurotrophic factor in acute bipolar mania: a preliminary 4-week study. Neuroscience letters *494*, 54-56.

Duman, R.S., and Monteggia, L.M. (2006). A neurotrophic model for stress-related mood disorders. Biol Psychiatry *59*, 1116-1127.

Duncan, L.E., Hutchison, K.E., Carey, G., and Craighead, W.E. (2009). Variation in brain-derived neurotrophic factor (BDNF) gene is associated with symptoms of depression. Journal of affective disorders *115*, 215-219.

Durany, N., Michel, T., Zochling, R., Boissl, K.W., Cruz-Sanchez, F.F., Riederer, P., and Thome, J. (2001). Brain-derived neurotrophic factor and neurotrophin 3 in schizophrenic psychoses. Schizophrenia research *52*, 79-86.

Edbauer, D., Neilson, J.R., Foster, K.A., Wang, C.F., Seeburg, D.P., Batterton, M.N., Tada, T., Dolan, B.M., Sharp, P.A., and Sheng, M. (2010). Regulation of synaptic structure and function by FMRP-associated microRNAs miR-125b and miR-132. Neuron *65*, 373-384.

Egan, M.F., Kojima, M., Callicott, J.H., Goldberg, T.E., Kolachana, B.S., Bertolino, A., Zaitsev, E., Gold, B., Goldman, D., Dean, M.*, et al.* (2003). The BDNF val66met polymorphism affects activity-dependent secretion of BDNF and human memory and hippocampal function. Cell *112*, 257-269.

Figueira, P., Malloy-Diniz, L., Campos, S.B., Miranda, D.M., Romano-Silva, M.A., De Marco, L., Neves, F.S., and Correa, H. (2010). An association study between the Val66Met polymorphism of the BDNF gene and postpartum depression. Archives of women's mental health *13*, 285-289.

Fiore, R., Khudayberdiev, S., Christensen, M., Siegel, G., Flavell, S.W., Kim, T.K., Greenberg, M.E., and Schratt, G. (2009). Mef2-mediated transcription of the miR379-410 cluster regulates activity-dependent dendritogenesis by fine-tuning Pumilio2 protein levels. EMBO J *28*, 697-710.

Frielingsdorf, H., Bath, K.G., Soliman, F., Difede, J., Casey, B.J., and Lee, F.S. (2010). Variant brain-derived neurotrophic factor Val66Met endophenotypes: implications for posttraumatic stress disorder. Annals of the New York Academy of Sciences *1208*, 150-157.

Frodl, T., Schule, C., Schmitt, G., Born, C., Baghai, T., Zill, P., Bottlender, R., Rupprecht, R., Bondy, B., Reiser, M.*, et al.* (2007). Association of the brain-derived neurotrophic factor Val66Met polymorphism with reduced hippocampal volumes in major depression. Arch Gen Psychiatry *64*, 410-416.

Frustaci, A., Pozzi, G., Gianfagna, F., Manzoli, L., and Boccia, S. (2008). Meta-analysis of the brain-derived neurotrophic factor gene (BDNF) Val66Met polymorphism in anxiety disorders and anxiety-related personality traits. Neuropsychobiology *58*, 163-170.

Gao, J., Wang, W.Y., Mao, Y.W., Graff, J., Guan, J.S., Pan, L., Mak, G., Kim, D., Su, S.C., and Tsai, L.H. (2010). A novel pathway regulates memory and plasticity via SIRT1 and miR-134. Nature *466*, 1105-1109.

Geller, B., Badner, J.A., Tillman, R., Christian, S.L., Bolhofner, K., and Cook, E.H., Jr. (2004). Linkage disequilibrium of the brain-derived neurotrophic factor Val66Met polymorphism in children with a prepubertal and early adolescent bipolar disorder phenotype. The American journal of psychiatry *161*, 1698-1700.

Gerritsen, L., Tendolkar, I., Franke, B., Vasquez, A.A., Kooijman, S., Buitelaar, J., Fernandez, G., and Rijpkema, M. (2011). BDNF Val66Met genotype modulates the effect of childhood adversity on subgenual anterior cingulate cortex volume in healthy subjects. Molecular psychiatry.

Golimbet, V.E., Korovaitseva, G.I., Abramova, L.I., Kasparov, S.V., and Uvarova, L.G. (2008). [Association between the Val66Met polymorphism of brain-derived neurotrophic factor gene and schizophrenia in Russians]. Molekuliarnaia biologiia *42*, 599-603.

Green, E.K., Raybould, R., Macgregor, S., Hyde, S., Young, A.H., O'Donovan, M.C., Owen, M.J., Kirov, G., Jones, L., Jones, I.*, et al.* (2006). Genetic variation of brain-derived neurotrophic factor (BDNF) in bipolar disorder: case-control study of over 3000 individuals from the UK. The British journal of psychiatry : the journal of mental science *188*, 21-25.

Guo, H., Ingolia, N.T., Weissman, J.S., and Bartel, D.P. (2010). Mammalian microRNAs predominantly act to decrease target mRNA levels. Nature *466*, 835-840.

Hajcak, G., Castille, C., Olvet, D.M., Dunning, J.P., Roohi, J., and Hatchwell, E. (2009). Genetic variation in brain-derived neurotrophic factor and human fear conditioning. Genes, brain, and behavior *8*, 80-85.

Hariri, A.R., Goldberg, T.E., Mattay, V.S., Kolachana, B.S., Callicott, J.H., Egan, M.F., and Weinberger, D.R. (2003). Brain-derived neurotrophic factor val66met polymorphism affects human memory-related hippocampal activity and predicts memory performance. J Neurosci *23*, 6690-6694.

He, X., Zhang, Q., Liu, Y., and Pan, X. (2007). Cloning and identification of novel microRNAs from rat hippocampus. Acta biochimica et biophysica Sinica *39*, 708-714.

Holroyd, C.B., and Coles, M.G. (2002). The neural basis of human error processing: reinforcement learning, dopamine, and the error-related negativity. Psychological review *109*, 679-709.

Hong, E.J., McCord, A.E., and Greenberg, M.E. (2008). A biological function for the neuronal activity-dependent component of Bdnf transcription in the development of cortical inhibition. Neuron *60*, 610-624.

Hou, J., Wang, P., Lin, L., Liu, X., Ma, F., An, H., Wang, Z., and Cao, X. (2009). MicroRNA-146a feedback inhibits RIG-I-dependent Type I IFN production in macrophages by targeting TRAF6, IRAK1, and IRAK2. Journal of immunology *183*, 2150-2158.

Huang, E.J., and Reichardt, L.F. (2003). Trk receptors: roles in neuronal signal transduction. Annual review of biochemistry *72*, 609-642.

Huang, Y.W., Ruiz, C.R., Eyler, E.C., Lin, K., and Meffert, M.K. (2012). Dual Regulation of miRNA Biogenesis Generates Target Specificity in Neurotrophin-Induced Protein Synthesis. Cell *148*, 933-946.

Hwang, J.P., Tsai, S.J., Hong, C.J., Yang, C.H., Lirng, J.F., and Yang, Y.M. (2006). The Val66Met polymorphism of the brain-derived neurotrophic-factor gene is associated with geriatric depression. Neurobiology of aging *27*, 1834-1837.

Iritani, S., Niizato, K., Nawa, H., Ikeda, K., and Emson, P.C. (2003). Immunohistochemical study of brain-derived neurotrophic factor and its receptor, TrkB, in the hippocampal formation of schizophrenic brains. Progress in neuro-psychopharmacology & biological psychiatry *27*, 801-807.

Jazdzewski, K., Liyanarachchi, S., Swierniak, M., Pachucki, J., Ringel, M.D., Jarzab, B., and de la Chapelle, A. (2009). Polymorphic mature microRNAs from passenger strand of pre-miR-146a contribute to thyroid cancer. Proceedings of the National Academy of Sciences of the United States of America *106*, 1502-1505.

Jazdzewski, K., Murray, E.L., Franssila, K., Jarzab, B., Schoenberg, D.R., and de la Chapelle, A. (2008). Common SNP in pre-miR-146a decreases mature miR expression and predisposes to papillary thyroid carcinoma. Proceedings of the National Academy of Sciences of the United States of America *105*, 7269-7274.

Jessen, F., Schuhmacher, A., von Widdern, O., Guttenthaler, V., Hofels, S., Suliman, H., Scheef, L., Block, W., Urbach, H., Maier, W.*, et al.* (2009). No association of the Val66Met polymorphism of the brain-derived neurotrophic factor with hippocampal volume in major depression. Psychiatric genetics *19*, 99-101.

Jiang, X., Xu, K., Hoberman, J., Tian, F., Marko, A.J., Waheed, J.F., Harris, C.R., Marini, A.M., Enoch, M.A., and Lipsky, R.H. (2005). BDNF variation and mood disorders: a novel functional promoter

polymorphism and Val66Met are associated with anxiety but have opposing effects. Neuropsychopharmacology *30*, 1353-1361.

Karege, F., Vaudan, G., Schwald, M., Perroud, N., and La Harpe, R. (2005). Neurotrophin levels in postmortem brains of suicide victims and the effects of antemortem diagnosis and psychotropic drugs. Brain research Molecular brain research *136*, 29-37.

Kawashima, K., Ikeda, M., Kishi, T., Kitajima, T., Yamanouchi, Y., Kinoshita, Y., Okochi, T., Aleksic, B., Tomita, M., Okada, T.*, et al.* (2009). BDNF is not associated with schizophrenia: data from a Japanese population study and meta-analysis. Schizophrenia research *112*, 72-79.

Klein, M.E., Lioy, D.T., Ma, L., Impey, S., Mandel, G., and Goodman, R.H. (2007). Homeostatic regulation of MeCP2 expression by a CREB-induced microRNA. Nature neuroscience *10*, 1513-1514.

Kobayashi, K., Shimizu, E., Hashimoto, K., Mitsumori, M., Koike, K., Okamura, N., Koizumi, H., Ohgake, S., Matsuzawa, D., Zhang, L.*, et al.* (2005). Serum brain-derived neurotrophic factor (BDNF) levels in patients with panic disorder: as a biological predictor of response to group cognitive behavioral therapy. Progress in neuro-psychopharmacology & biological psychiatry *29*, 658-663.

Kremeyer, B., Herzberg, I., Garcia, J., Kerr, E., Duque, C., Parra, V., Vega, J., Lopez, C., Palacio, C., Bedoya, G.*, et al.* (2006). Transmission distortion of BDNF variants to bipolar disorder type I patients from a South American population isolate. Am J Med Genet B Neuropsychiatr Genet *141B*, 435-439.

Krishnan, V., Han, M.H., Graham, D.L., Berton, O., Renthal, W., Russo, S.J., Laplant, Q., Graham, A., Lutter, M., Lagace, D.C.*, et al.* (2007). Molecular adaptations underlying susceptibility and resistance to social defeat in brain reward regions. Cell *131*, 391-404.

Landgraf, P., Rusu, M., Sheridan, R., Sewer, A., Iovino, N., Aravin, A., Pfeffer, S., Rice, A., Kamphorst, A.O., Landthaler, M.*, et al.* (2007). A mammalian microRNA expression atlas based on small RNA library sequencing. Cell *129*, 1401-1414.

Lavebratt, C., Aberg, E., Sjoholm, L.K., and Forsell, Y. (2010). Variations in FKBP5 and BDNF genes are suggestively associated with depression in a Swedish population-based cohort. Journal of affective disorders *125*, 249-255.

Lessmann, V., Gottmann, K., and Malcangio, M. (2003). Neurotrophin secretion: current facts and future prospects. Progress in neurobiology *69*, 341-374.

Li, Y., Vandenboom, T.G., 2nd, Wang, Z., Kong, D., Ali, S., Philip, P.A., and Sarkar, F.H. (2010). miR-146a suppresses invasion of pancreatic cancer cells. Cancer research *70*, 1486-1495.

Li, Y.Y., Cui, J.G., Dua, P., Pogue, A.I., Bhattacharjee, S., and Lukiw, W.J. (2011). Differential expression of miRNA-146a-regulated inflammatory genes in human primary neural, astroglial and microglial cells. Neuroscience letters *499*, 109-113.

Lin, Y., Bloodgood, B.L., Hauser, J.L., Lapan, A.D., Koon, A.C., Kim, T.K., Hu, L.S., Malik, A.N., and Greenberg, M.E. (2008). Activity-dependent regulation of inhibitory synapse development by Npas4. Nature *455*, 1198-1204.

Liu, R.J., Lee, F.S., Li, X.Y., Bambico, F., Duman, R.S., and Aghajanian, G.K. (2011). Brain-Derived Neurotrophic Factor Val66Met Allele Impairs Basal and Ketamine-Stimulated Synaptogenesis in Prefrontal Cortex. Biol Psychiatry.

Lohoff, F.W., Sander, T., Ferraro, T.N., Dahl, J.P., Gallinat, J., and Berrettini, W.H. (2005). Confirmation of association between the Val66Met polymorphism in the brain-derived neurotrophic factor (BDNF) gene and bipolar I disorder. Am J Med Genet B Neuropsychiatr Genet *139B*, 51-53.

Lu, B. (2003). Pro-region of neurotrophins: role in synaptic modulation. Neuron *39*, 735-738.

Lu, B., Pang, P.T., and Woo, N.H. (2005). The yin and yang of neurotrophin action. Nat Rev Neurosci *6*, 603-614.

Lu, L.F., Boldin, M.P., Chaudhry, A., Lin, L.L., Taganov, K.D., Hanada, T., Yoshimura, A., Baltimore, D., and Rudensky, A.Y. (2010). Function of miR-146a in controlling Treg cell-mediated regulation of Th1 responses. Cell *142*, 914-929.

Lugli, G., Torvik, V.I., Larson, J., and Smalheiser, N.R. (2008). Expression of microRNAs and their precursors in synaptic fractions of adult mouse forebrain. J Neurochem *106*, 650-661.

Lukiw, W.J., Zhao, Y., and Cui, J.G. (2008). An NF-kappaB-sensitive micro RNA-146a-mediated inflammatory circuit in Alzheimer disease and in stressed human brain cells. J Biol Chem *283*, 31315-31322.

Luo, X., Yang, W., Ye, D.Q., Cui, H., Zhang, Y., Hirankarn, N., Qian, X., Tang, Y., Lau, Y.L., de Vries, N.*, et al.* (2011). A functional variant in microRNA-146a promoter modulates its expression and confers disease risk for systemic lupus erythematosus. PLoS genetics *7*, e1002128.

Lyons, M.R., and West, A.E. (2011). Mechanisms of specificity in neuronal activity-regulated gene transcription. Progress in neurobiology *94*, 259-295.

Magill, S.T., Cambronne, X.A., Luikart, B.W., Lioy, D.T., Leighton, B.H., Westbrook, G.L., Mandel, G., and Goodman, R.H. (2010). microRNA-132 regulates dendritic growth and arborization of newborn neurons in the adult hippocampus. Proceedings of the National Academy of Sciences of the United States of America *107*, 20382-20387.

Maragkakis, M., Vergoulis, T., Alexiou, P., Reczko, M., Plomaritou, K., Gousis, M., Kourtis, K., Koziris, N., Dalamagas, T., and Hatzigeorgiou, A.G. (2011). DIANA-microT Web server upgrade supports Fly and Worm miRNA target prediction and bibliographic miRNA to disease association. Nucleic acids research *39*, W145-148.

Marson, A., Levine, S.S., Cole, M.F., Frampton, G.M., Brambrink, T., Johnstone, S., Guenther, M.G., Johnston, W.K., Wernig, M., Newman, J.*, et al.* (2008). Connecting microRNA genes to the core transcriptional regulatory circuitry of embryonic stem cells. Cell *134*, 521-533.

Martinowich, K., and Lu, B. (2008). Interaction between BDNF and serotonin: role in mood disorders. Neuropsychopharmacology *33*, 73-83.

Marvanova, M., Lakso, M., Pirhonen, J., Nawa, H., Wong, G., and Castren, E. (2001). The neuroprotective agent memantine induces brain-derived neurotrophic factor and trkB receptor expression in rat brain. Molecular and cellular neurosciences *18*, 247-258.

Matsumoto, T., Rauskolb, S., Polack, M., Klose, J., Kolbeck, R., Korte, M., and Barde, Y.A. (2008). Biosynthesis and processing of endogenous BDNF: CNS neurons store and secrete BDNF, not pro-BDNF. Nature neuroscience *11*, 131-133.

Mellios, N., Huang, H.S., Grigorenko, A., Rogaev, E., and Akbarian, S. (2008). A set of differentially expressed miRNAs, including miR-30a-5p, act as post-transcriptional inhibitors of BDNF in prefrontal cortex. Hum Mol Genet *17*, 3030-3042.

Minichiello, L. (2009). TrkB signalling pathways in LTP and learning. Nat Rev Neurosci *10*, 850-860.

Miura, P., Amirouche, A., Clow, C., Belanger, G., and Jasmin, B.J. (2012). Brain-derived neurotrophic factor expression is repressed during myogenic differentiation by miR-206. J Neurochem *120*, 230-238.

Montag, C., Basten, U., Stelzel, C., Fiebach, C.J., and Reuter, M. (2010). The BDNF Val66Met polymorphism and anxiety: support for animal knock-in studies from a genetic association study in humans. Psychiatry research *179*, 86-90.

Montag, C., Weber, B., Fliessbach, K., Elger, C., and Reuter, M. (2009). The BDNF Val66Met polymorphism impacts parahippocampal and amygdala volume in healthy humans: incremental support for a genetic risk factor for depression. Psychological medicine *39*, 1831-1839.

Muller, D.J., de Luca, V., Sicard, T., King, N., Strauss, J., and Kennedy, J.L. (2006). Brain-derived neurotrophic factor (BDNF) gene and rapid-cycling bipolar disorder: family-based association study. The British journal of psychiatry : the journal of mental science *189*, 317-323.

Nakata, K., Ujike, H., Tanaka, Y., Takaki, M., Sakai, A., Nomura, A., Katsu, T., Uchida, N., Imamura, T., Fujiwara, Y.*, et al.* (2003). No association between the dihydropyrimidinase-related protein 2 (DRP-2) gene and bipolar disorder in humans. Neuroscience letters *349*, 171-174.

Naoe, Y., Shinkai, T., Hori, H., Fukunaka, Y., Utsunomiya, K., Sakata, S., Matsumoto, C., Shimizu, K., Hwang, R., Ohmori, O.*, et al.* (2007). No association between the brain-derived neurotrophic factor (BDNF) Val66Met polymorphism and schizophrenia in Asian populations: Evidence from a case-control study and meta-analysis. Neuroscience letters *415*, 108-112.

Neves-Pereira, M., Cheung, J.K., Pasdar, A., Zhang, F., Breen, G., Yates, P., Sinclair, M., Crombie, C., Walker, N., and St Clair, D.M. (2005). BDNF gene is a risk factor for schizophrenia in a Scottish population. Molecular psychiatry *10*, 208-212.

Ninan, I., Bath, K.G., Dagar, K., Perez-Castro, R., Plummer, M.R., Lee, F.S., and Chao, M.V. (2010). The BDNF Val66Met polymorphism impairs NMDA receptor-dependent synaptic plasticity in the hippocampus. J Neurosci *30*, 8866-8870.

Oswald, P., Del-Favero, J., Massat, I., Souery, D., Claes, S., Van Broeckhoven, C., and Mendlewicz, J. (2004). Non-replication of the brain-derived neurotrophic factor (BDNF) association in bipolar affective disorder: a Belgian patient-control study. Am J Med Genet B Neuropsychiatr Genet *129B*, 34-35.

Perry, M.M., Williams, A.E., Tsitsiou, E., Larner-Svensson, H.M., and Lindsay, M.A. (2009). Divergent intracellular pathways regulate interleukin-1beta-induced miR-146a and miR-146b expression and chemokine release in human alveolar epithelial cells. FEBS letters *583*, 3349-3355.

Petryshen, T.L., Sabeti, P.C., Aldinger, K.A., Fry, B., Fan, J.B., Schaffner, S.F., Waggoner, S.G., Tahl, A.R., and Sklar, P. (2010). Population genetic study of the brain-derived neurotrophic factor (BDNF) gene. Molecular psychiatry *15*, 810-815.

Pezawas, L., Verchinski, B.A., Mattay, V.S., Callicott, J.H., Kolachana, B.S., Straub, R.E., Egan, M.F., Meyer-Lindenberg, A., and Weinberger, D.R. (2004). The brain-derived neurotrophic factor val66met polymorphism and variation in human cortical morphology. J Neurosci *24*, 10099-10102.

Ploski, J.E., Monsey, M.S., Nguyen, T., DiLeone, R.J., and Schafe, G.E. (2011). The neuronal PAS domain protein 4 (Npas4) is required for new and reactivated fear memories. PLoS One *6*, e23760.

Pogue, A.I., Li, Y.Y., Cui, J.G., Zhao, Y., Kruck, T.P., Percy, M.E., Tarr, M.A., and Lukiw, W.J. (2009). Characterization of an NF-kappaB-regulated, miRNA-146a-mediated down-regulation of complement factor H (CFH) in metal-sulfate-stressed human brain cells. Journal of inorganic biochemistry *103*, 1591-1595.

Ramamoorthi, K., Fropf, R., Belfort, G.M., Fitzmaurice, H.L., McKinney, R.M., Neve, R.L., Otto, T., and Lin, Y. (2011). Npas4 regulates a transcriptional program in CA3 required for contextual memory formation. Science (New York, NY *334*, 1669-1675.

Rauskolb, S., Zagrebelsky, M., Dreznjak, A., Deogracias, R., Matsumoto, T., Wiese, S., Erne, B., Sendtner, M., Schaeren-Wiemers, N., Korte, M.*, et al.* (2010). Global deprivation of brain-derived neurotrophic factor in the CNS reveals an area-specific requirement for dendritic growth. J Neurosci *30*, 1739-1749.

Rehmsmeier, M., Steffen, P., Hochsmann, M., and Giegerich, R. (2004). Fast and effective prediction of microRNA/target duplexes. RNA *10*, 1507-1517.

Ribeiro, L., Busnello, J.V., Cantor, R.M., Whelan, F., Whittaker, P., Deloukas, P., Wong, M.L., and Licinio, J. (2007). The brain-derived neurotrophic factor rs6265 (Val66Met) polymorphism and depression in Mexican-Americans. Neuroreport *18*, 1291-1293.

Rosa, A., Cuesta, M.J., Fatjo-Vilas, M., Peralta, V., Zarzuela, A., and Fananas, L. (2006). The Val66Met polymorphism of the brain-derived neurotrophic factor gene is associated with risk for psychosis: evidence from a family-based association study. Am J Med Genet B Neuropsychiatr Genet *141B*, 135-138.

Rybakowski, J.K., Borkowska, A., Skibinska, M., and Hauser, J. (2006a). Illness-specific association of val66met BDNF polymorphism with performance on Wisconsin Card Sorting Test in bipolar mood disorder. Molecular psychiatry *11*, 122-124.

Rybakowski, J.K., Borkowska, A., Skibinska, M., Szczepankiewicz, A., Kapelski, P., Leszczynska-Rodziewicz, A., Czerski, P.M., and Hauser, J. (2006b). Prefrontal cognition in schizophrenia and bipolar illness in relation to Val66Met polymorphism of the brain-derived neurotrophic factor gene. Psychiatry and clinical neurosciences *60*, 70-76.

Schratt, G.M., Tuebing, F., Nigh, E.A., Kane, C.G., Sabatini, M.E., Kiebler, M., and Greenberg, M.E. (2006). A brain-specific microRNA regulates dendritic spine development. Nature *439*, 283-289.

Schumacher, J., Kaneva, R., Jamra, R.A., Diaz, G.O., Ohlraun, S., Milanova, V., Lee, Y.A., Rivas, F., Mayoral, F., Fuerst, R.*, et al.* (2005). Genomewide scan and fine-mapping linkage studies in four European samples with bipolar affective disorder suggest a new susceptibility locus on chromosome 1p35-p36 and provides further evidence of loci on chromosome 4q31 and 6q24. Am J Hum Genet *77*, 1102-1111.

Seidah, N.G., Benjannet, S., Pareek, S., Chretien, M., and Murphy, R.A. (1996). Cellular processing of the neurotrophin precursors of NT3 and BDNF by the mammalian proprotein convertases. FEBS letters *379*, 247-250.

Sen, S., Duman, R., and Sanacora, G. (2008). Serum brain-derived neurotrophic factor, depression, and antidepressant medications: meta-analyses and implications. Biol Psychiatry *64*, 527-532.

Shalizi, A.K., and Bonni, A. (2005). brawn for brains: the role of MEF2 proteins in the developing nervous system. Current topics in developmental biology *69*, 239-266.

Shimizu, E., Hashimoto, K., and Iyo, M. (2004). Ethnic difference of the BDNF 196G/A (val66met) polymorphism frequencies: the possibility to explain ethnic mental traits. Am J Med Genet B Neuropsychiatr Genet *126B*, 122-123.

Shimizu, E., Hashimoto, K., Okamura, N., Koike, K., Komatsu, N., Kumakiri, C., Nakazato, M., Watanabe, H., Shinoda, N., Okada, S.*, et al.* (2003). Alterations of serum levels of brain-derived neurotrophic factor (BDNF) in depressed patients with or without antidepressants. Biol Psychiatry *54*, 70-75.

Skibinska, M., Hauser, J., Czerski, P.M., Leszczynska-Rodziewicz, A., Kosmowska, M., Kapelski, P., Slopien, A., Zakrzewska, M., and Rybakowski, J.K. (2004). Association analysis of brain-derived neurotrophic factor (BDNF) gene Val66Met polymorphism in schizophrenia and bipolar affective disorder. World J Biol Psychiatry *5*, 215-220.

Sklar, P., Gabriel, S.B., McInnis, M.G., Bennett, P., Lim, Y.M., Tsan, G., Schaffner, S., Kirov, G., Jones, I., Owen, M.*, et al.* (2002). Family-based association study of 76 candidate genes in bipolar disorder: BDNF is a potential risk locus. Brain-derived neutrophic factor. Molecular psychiatry *7*, 579-593.

Soliman, F., Glatt, C.E., Bath, K.G., Levita, L., Jones, R.M., Pattwell, S.S., Jing, D., Tottenham, N., Amso, D., Somerville, L.H.*, et al.* (2010). A genetic variant BDNF polymorphism alters extinction learning in both mouse and human. Science (New York, NY *327*, 863-866.

Spencer, J.L., Waters, E.M., Milner, T.A., Lee, F.S., and McEwen, B.S. (2010). BDNF variant Val66Met interacts with estrous cycle in the control of hippocampal function. Proceedings of the National Academy of Sciences of the United States of America *107*, 4395-4400.

Stanczyk, J., Pedrioli, D.M., Brentano, F., Sanchez-Pernaute, O., Kolling, C., Gay, R.E., Detmar, M., Gay, S., and Kyburz, D. (2008). Altered expression of MicroRNA in synovial fibroblasts and synovial tissue in rheumatoid arthritis. Arthritis and rheumatism *58*, 1001-1009.

Su, N., Zhang, L., Fei, F., Hu, H., Wang, K., Hui, H., Jiang, X.F., Li, X., Zhen, H.N., Li, J.*, et al.* (2011). The brain-derived neurotrophic factor is associated with alcohol dependence-related depression and antidepressant response. Brain research *1415*, 119-126.

Sun, R.F., Zhu, Y.S., Kuang, W.J., Liu, Y., and Li, S.B. (2011). The G-712A polymorphism of brain-derived neurotrophic factor is associated with major depression but not schizophrenia. Neuroscience letters *489*, 34-37.

Szeszko, P.R., Lipsky, R., Mentschel, C., Robinson, D., Gunduz-Bruce, H., Sevy, S., Ashtari, M., Napolitano, B., Bilder, R.M., Kane, J.M.*, et al.* (2005). Brain-derived neurotrophic factor val66met polymorphism and volume of the hippocampal formation. Molecular psychiatry *10*, 631-636.

Taganov, K.D., Boldin, M.P., Chang, K.J., and Baltimore, D. (2006). NF-kappaB-dependent induction of microRNA miR-146, an inhibitor targeted to signaling proteins of innate immune responses. Proceedings of the National Academy of Sciences of the United States of America *103*, 12481-12486.

Tan, Y.L., Zhou, D.F., Cao, L.Y., Zou, Y.Z., Wu, G.Y., and Zhang, X.Y. (2005). Effect of the BDNF Val66Met genotype on episodic memory in schizophrenia. Schizophrenia research *77*, 355-356.

Tang, J., Xiao, L., Shu, C., Wang, G., Liu, Z., Wang, X., Wang, H., and Bai, X. (2008). Association of the brain-derived neurotrophic factor gene and bipolar disorder with early age of onset in mainland China. Neuroscience letters *433*, 98-102.

Tettamanti, G., Cattaneo, A.G., Gornati, R., de Eguileor, M., Bernardini, G., and Binelli, G. (2010). Phylogenesis of brain-derived neurotrophic factor (BDNF) in vertebrates. Gene *450*, 85-93.

Tocchetto, A., Salum, G.A., Blaya, C., Teche, S., Isolan, L., Bortoluzzi, A., Rebelo, E.S.R., Becker, J.A., Bianchin, M.M., Rohde, L.A.*, et al.* (2011). Evidence of association between Val66Met polymorphism at BDNF gene and anxiety disorders in a community sample of children and adolescents. Neuroscience letters *502*, 197-200.

Tochigi, M., Otowa, T., Suga, M., Rogers, M., Minato, T., Yamasue, H., Kasai, K., Kato, N., and Sasaki, T. (2006). No evidence for an association between the BDNF Val66Met polymorphism and schizophrenia or personality traits. Schizophrenia research *87*, 45-47.

Urdinguio, R.G., Fernandez, A.F., Lopez-Nieva, P., Rossi, S., Huertas, D., Kulis, M., Liu, C.G., Croce, C.M., Calin, G.A., and Esteller, M. (2010). Disrupted microRNA expression caused by Mecp2 loss in a mouse model of Rett syndrome. Epigenetics : official journal of the DNA Methylation Society *5*, 656-663.

Verhagen, M., van der Meij, A., van Deurzen, P.A., Janzing, J.G., Arias-Vasquez, A., Buitelaar, J.K., and Franke, B. (2010). Meta-analysis of the BDNF Val66Met polymorphism in major depressive disorder: effects of gender and ethnicity. Molecular psychiatry *15*, 260-271.

Vo, N., Klein, M.E., Varlamova, O., Keller, D.M., Yamamoto, T., Goodman, R.H., and Impey, S. (2005). A cAMP-response element binding protein-induced microRNA regulates neuronal morphogenesis. Proceedings of the National Academy of Sciences of the United States of America *102*, 16426-16431.

Wang, X. (2008). miRDB: a microRNA target prediction and functional annotation database with a wiki interface. RNA (New York, NY *14*, 1012-1017.

Wang, Y., Wang, J.D., Wu, H.R., Zhang, B.S., Fang, H., Ma, Q.M., Liu, H., Chen da, C., Xiu, M.H., Hail, C.N.*, et al.* (2010). The Val66Met polymorphism of the brain-derived neurotrophic factor gene is not associated with risk for schizophrenia and tardive dyskinesia in Han Chinese population. Schizophrenia research *120*, 240-242.

Wellcome Trust Case Control, C. (2007). Genome-wide association study of 14,000 cases of seven common diseases and 3,000 shared controls. Nature *447*, 661-678.

Yamasaki, K., Nakasa, T., Miyaki, S., Ishikawa, M., Deie, M., Adachi, N., Yasunaga, Y., Asahara, H., and Ochi, M. (2009). Expression of MicroRNA-146a in osteoarthritis cartilage. Arthritis and rheumatism *60*, 1035-1041.

Yasuda, S., Liang, M.H., Marinova, Z., Yahyavi, A., and Chuang, D.M. (2009). The mood stabilizers lithium and valproate selectively activate the promoter IV of brain-derived neurotrophic factor in neurons. Molecular psychiatry *14*, 51-59.

Yi, Z., Zhang, C., Wu, Z., Hong, W., Li, Z., Fang, Y., and Yu, S. (2011). Lack of effect of brain derived neurotrophic factor (BDNF) Val66Met polymorphism on early onset schizophrenia in Chinese Han population. Brain research *1417*, 146-150.

Yoshii, A., and Constantine-Paton, M. (2010). Postsynaptic BDNF-TrkB signaling in synapse maturation, plasticity, and disease. Developmental neurobiology *70*, 304-322.

Yu, H., Wang, Y., Pattwell, S., Jing, D., Liu, T., Zhang, Y., Bath, K.G., Lee, F.S., and Chen, Z.Y. (2009). Variant BDNF Val66Met polymorphism affects extinction of conditioned aversive memory. J Neurosci *29*, 4056-4064.

Zakharyan, R., Boyajyan, A., Arakelyan, A., Gevorgyan, A., Mrazek, F., and Petrek, M. (2011). Functional variants of the genes involved in neurodevelopment and susceptibility to schizophrenia in an Armenian population. Human immunology *72*, 746-748.

Zhou, Z., Hong, E.J., Cohen, S., Zhao, W.N., Ho, H.Y., Schmidt, L., Chen, W.G., Lin, Y., Savner, E., Griffith, E.C.*, et al.* (2006). Brain-specific phosphorylation of MeCP2 regulates activity-dependent Bdnf transcription, dendritic growth, and spine maturation. Neuron *52*, 255-269.

Zou, Y.F., Wang, Y., Liu, P., Feng, X.L., Wang, B.Y., Zang, T.H., Yu, X., Wei, J., Liu, Z.C., Liu, Y.*, et al.* (2010). Association of BDNF Val66Met polymorphism with both baseline HRQOL scores and improvement in HRQOL scores in Chinese major depressive patients treated with fluoxetine. Human psychopharmacology *25*, 145-152.

Zovoilis, A., Agbemenyah, H.Y., Agis-Balboa, R.C., Stilling, R.M., Edbauer, D., Rao, P., Farinelli, L., Delalle, I., Schmitt, A., Falkai, P.*, et al.* (2011). microRNA-34c is a novel target to treat dementias. EMBO J *30*, 4299-4308.

Chapter V

General Discussion

5.1 Summary of results

5.1.1 Elucidation of MicroRNA-Target Dysregulation in a Pathogenic CNV – 22q11.2 Microdeletions

Elucidation of the biological processes affected by pathogenic CNVs may offer novel insights into the pathogenesis of psychiatric disorders as well as disorders of cognitive development (Karayiorgou et al., 2010). However, the transcriptional networks and signaling cascades that mediate the effects of CNVs on neuronal structure and function remain, to a large extent, uncharacterized. Our study in a mouse model of 22q11.2DS was designed to identify such downstream targets and processes disrupted by a *bona fide* pathogenic mutation that predisposes an individual to schizophrenia and cognitive dysfunction. By applying an array of morphological, molecular and cellular assays to a mouse model of this mutation, we provide a number of novel mechanistic insights to the pathogenesis.

5.1.2 miR-185 Downregulation is an Important Component of MicroRNA Dysregulation due to Gene X Gene Interaction

First, taken together with previous results on the effects of *Dgcr8* hemizygosity (Fenelon et al., 2011; Stark et al., 2008), we provide a comprehensive view of the pattern of miRNA dysregulation emerging due to 22q11.2 deletions, which is shaped by the combined (synergistic and additive) effect of *miR-185* and *Dgcr8* hemizygosity (Figure 5.1). Our findings show how a genuine gene X gene interaction within a pathogenic CNV can result in a considerably greater reduction of the expression of a resident gene than expected by the 50% decrease in gene dosage. These results indicate that mechanisms other than simple haploinsufficiency could represent an important and previously unappreciated component of CNV pathogenicity. Along these lines, our results also raise the more general and intriguing possibility that 22q11.2 microdeletions, by partially disabling the miRNA machinery, create a sensitized genetic background, which promotes the effects of deleterious mutations that affect the expression or activity of a subset of miRNAs (Brenner et al., 2010).

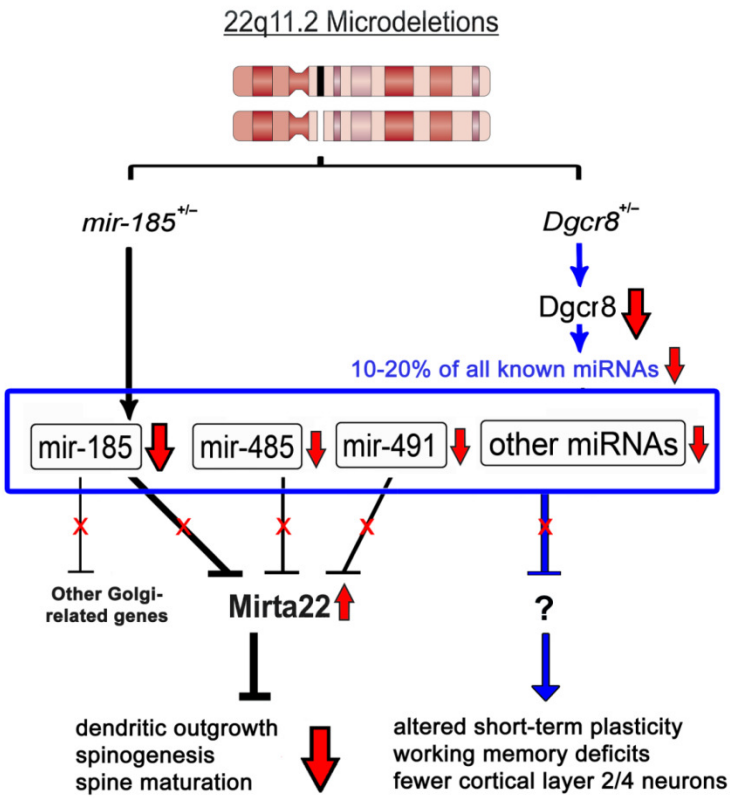

Figure 5.1 The Pattern of MicroRNA Dysregulation Emerging due to 22q11.2 Deletions. miR-185 (due to a combined effect of hemizygosity and impaired maturation of the pri-miR-185 transcript produced from the remaining copy) results in derepression and protracted elevation of the expression levels of 2310044H10Rik (Mirta22) and other Golgi-related miR-185 target genes. Increased Mirta22 levels may, in turn, impair the growth of dendrites and spines and affect formation and maintenance of neural circuits. *Dgcr8* hemizygosity, on its own, results in modest downregulation of a specific subset of mature miRNAs (10-20% of all miRNAs, including a modest 20% decrease in the levels of miR-185) and results in a number of cellular, synaptic and behavioral alterations found in *Dgcr8*$^{+/-}$ mice. Most notable among them are deficits in cortical short-term plasticity and related deficits in working-memory dependent cognitive assays. *Dgcr8* hemizygosity also results in modest and layer-specific changes in neuronal density in the cortex as well as modest alterations in dendritic spine size and dendritic tree formation. Downstream targets that mediate these effects and the extent that 2310044H10Rik (Mirta22) contributes to these phenotypes remain unknown.

5.1.3 Mirta22 is a Major Downstream Effector of 22q11.2-associated MicroRNA Dysregulation

By comparing gene expression profiles over three developmental stages and variable levels of genomic dosage at the 22q11.2 locus, we identified elevated levels of a previously uncharacterized gene, *Mirta22* as the most robust change in gene expression resulting from the 22q11.2 microdeletion. This alteration occurred in addition to the major downstream transcriptional effects of the 22q11.2- associated miRNA dysregulation.

5.1.4 Mirta22 is a Novel MicroRNA-regulated Inhibitor of Neuronal Morphogenesis

Furthermore, using physiologically relevant cellular models, we provide unequivocal evidence that *Mirta22* as well as its primary miRNA regulator miR-185 mediate, at least in part, the effects of the 22q11.2 microdeletions on dendrite and spine formation. Although results from acute manipulations of gene expression via transient transfections of primary neurons should not be over-interpreted

quantitatively, the observed convergence and remarkable consistency of data from a multitude of experimental manipulations and approaches convincingly identified *Mirta22* as a novel miRNA-regulated inhibitory factor of neuronal maturation.

5.1.5 MicroRNA Dysregulation due to BDNF Val66Met SNP

Besides characterizing the miRNA-related dysregulation in a mouse model of rare variants, we delineate the miRNA dysregulation due to a common genetic variant *BDNF Val66Met.* Although miRNA dysregulation is generally mild in *BDNF Val66Met* mice, we uncovered a reduction of mir-146b levels that occur as a result of lower BDNF levels. The reduction results in a failure of mir-146b to repress the transcript or protein levels of a few targets, which may in turn lead to functional consequences.

5.1.6 MicroRNA Dysregulation as an Integral Part of Pathophysiology of Psychiatric Disorders

Altogether, our identification and functional characterization of an important component of miRNA dysregulation in a mouse model of 22q11.2DS represents an important first step toward a comprehensive elucidation of the pathophysiological involvement of non-coding RNA in these devastating disorders. Furthermore, the study of the miRNA dysregulation due to *BDNF Val66Met* SNP demonstrates the potential impact of a common variant on the miRNA-dependent molecular network. Our results presented in this thesis thus echo the multiple threads of evidence presented in Chapter 1, which suggest that miRNAs play an important role in the pathogenesis of psychiatric and neurodevelopmental disorders (Kvajo et al., 2011) and cognitive dysfunction. Moreover, the identification of physiologically relevant targets of miRNA dysregulation offers valuable leads to further unwrap the hidden pathophysiology mechanisms that underlie these conditions.

5.2 MicroRNA Dysregulation due to Rare and Common Genetic Variants

5.2.1 Models of Genetic Architecture of Neuropsychiatric Disorders

Neuropsychiatric disorders are genetically complex in nature with heterogeneous genetic etiologies. Therefore, the genetic architecture of psychiatric disorders such as schizophrenia is under continuous debate (Gibson, 2011). Considering the frequency and effect size (odds ratio) of risk alleles,

there have been two main hypotheses that take conceptually different perspectives on the etiology of psychiatric disorders. The common disease-common allele (CDCA) hypothesis purports the cooperation of a core set of common variants in every affected individual (Goldstein, 2009). Since the risk variants are common within the population, the effect size of these alleles is unlikely to be high. Only through the combined effect of many common risk alleles will the disease start to emerge. The alternative hypothesis, the common disease-rare allele (CDRA) hypothesis, emphasizes the contribution of a few, or even a single, rare variants that each has high penetrance. Since the variants that predispose the disease are rare, each affected individual may have different genetic profile of rare variants. Additionally, this hypothesis implies that in order to sustain the prevalence of disease, highly penetrant *de novo* mutations need to be continuously generated in the population, because they are strongly selected against (Crow, 2000).

Empirical data from both the traditional genome-wide association studies (GWASs) and studies employing new techniques such as copy number scan and high-throughput sequencing unequivocally reveal the contribution from both common and rare variants in psychiatric disorders (Gibson, 2011; Rodriguez-Murillo et al., 2012). Although the proportion of susceptibility conferred by common versus rare variants has not been precisely determined, recently it is estimated that common SNPs collectively account for 23% of variation in liability to schizophrenia (Lee et al., 2012). It is likely that most of the remaining variation in liability (77%) is attributed to rare variants, suggesting the rare variants like CNVs are the principal determinants of disease risk. The accumulating data from human genetic studies leads to the proposal of new compound models integrating the aspects of CDCA and CDRA (Gibson, 2011; Rodriguez-Murillo et al., 2012). According to new models, the development of clinical manifestations of primary disease-causing CNVs (or other rare variants) is modulated by a constellation of common variants, environmental factors and stochastic factors. Comprehensive analysis of the location of human genetic variants showed that many of these variants, including CNVs and SNPs, overlap with genomic loci of pre-miRNAs or miRNA-processing genes (Duan et al., 2009). In fact, more than 10% (170 out of 1527) of human pre-miRNA genes overlap with known genetic variants and since the pool of annotated variants keeps increasing, this figure is probably an underestimation. However, much less is known about the impact of the genetic variants on the miRNA-mediated regulation. In this context, the results in this

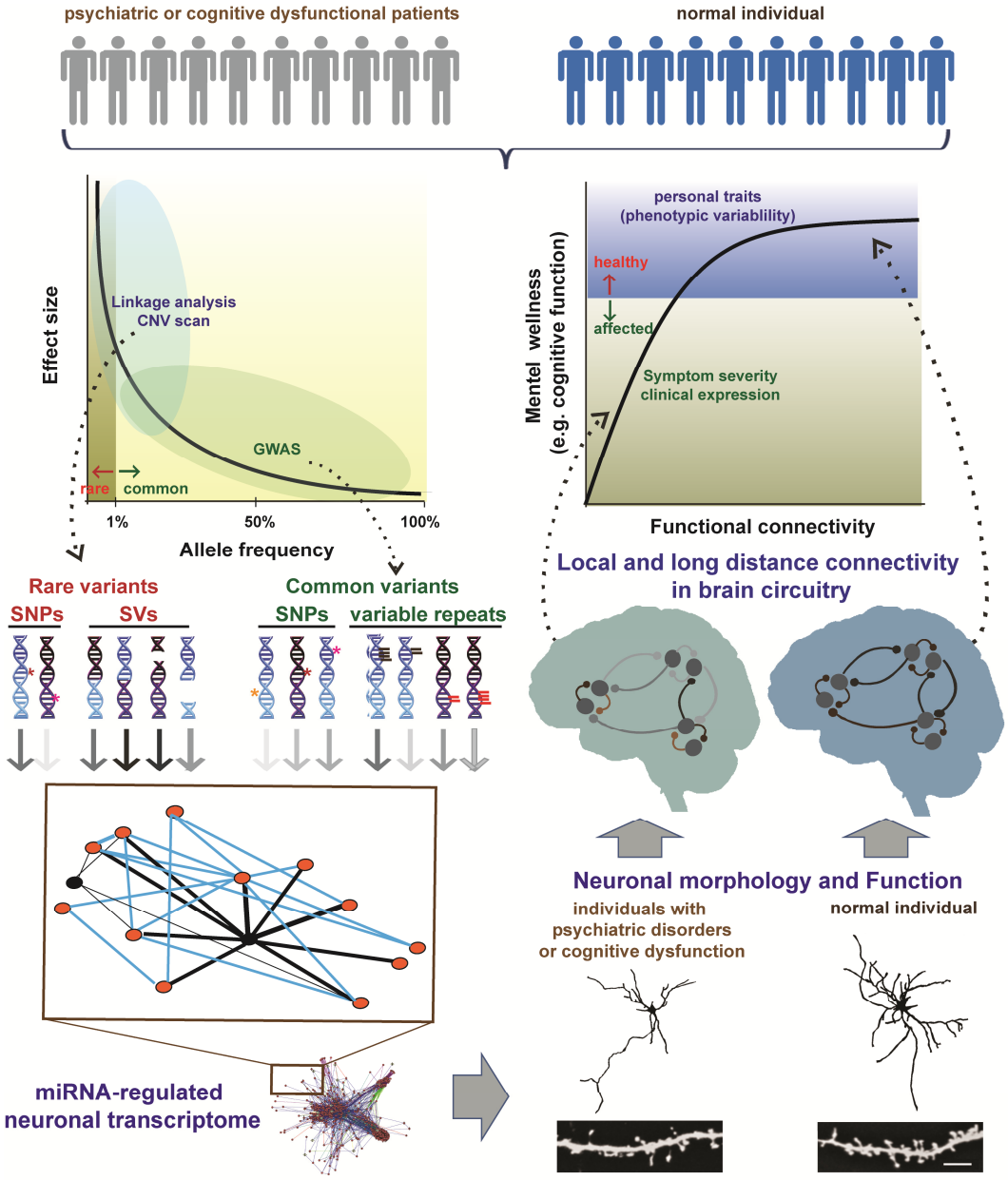

Figure 5.2 MicroRNA Dysregulation as Liability Imposed by Genetic Variants. Human genetic studies have identified multiple common or rare genetic variants that predispose individuals to psychiatric disorders and cognitive dysfunction. The distribution of these genetics variants on allele frequency –effect size graph indicates an inverse relationship between allele frequency and effect size, as most common variants (consisting mostly of SNP and variable length of repeats) fall in the green area that is targeted by GWAS, while most rare variants (frequency < 1%) falls in blue area that is the detection zone of linkage analysis and sequencing scan of structure variant (SV), such as CNV and chromosomal translocation. These genetics variants have varying degree of impact on transcriptome of a neuron, partly through the effects on miRNA expression (as shown by arrows with varying degree of darkness). Altered miRNAs (shown as black nodes in the transcriptomeic network; other genes are shown as red nodes) can have a widespread and profound impact depending on the degree expression change. Thick and thin black edges in transcriptomeic network denote enhanced and reduced repression of miRNAs on target genes, respectively. Evidence here and elsewhere suggests that common variants generally have mild or limited impact on miRNA-mediated network, while some rare variants may have

[Figure 5.2, continued from p156] strong impact. It is import to note that genetic variants affect other nodes (genes), besides miRNAs, directly in the molecular network. The effects of genetic variants on different components of the transcriptomic network likely have to be deciphered case-by-case. The altered molecular network leads to variation in neuronal morphology and function, such as changes in spine density and dendritic complexity. These neuronal characteristics in turn reflect on the connectivity of local and distant brain circuitries (strength of a connection shown by lines of varying darkness in between brain areas). The ultimate functional output is determined by the degree of functional connectivity that is required for proper brain function, such as sensory and cognitive processes. The functional connectivity–"mental wellness" curve indicates continuous phenotypic variation that spans zones of "healthy" and "affected" defined by clinical criteria (the horizontal line denotes clinical criteria or threshold). In the "healthy" zone, phenotypic variance is manifested as personality traits, cognitive capability, etc., and in "affected" zone, it is expressed as symptom severity. In summary, genetic variants have a range of impact on molecular network, neuronal properties, functional circuitry and ultimately on phenotypic variance. In every level, effect of different genetic variants may interact, further modulating the variance positively or negatively.

thesis demonstrate that the miRNA dysregulation appears to be an important component of the total liability imposed by disease-related rare and common variants (Figure 5.2).

We studied mouse models of 2 genetic variants, a rare variant – 22q11.2 microdeletions and a common variant – *BDNF Val66Met*. 22q11.2 microdeletion is a recurrent *de novo* CNV that occurs at a frequency of 1/4000 and has strong penetrance for schizophrenia or schizoaffective disorders, while *BDNF Val66Met* is a SNP that has variable allele frequency (0-50%) across different ethnic groups and is associated with cognitive dysfunction, though the effect size is only moderate. Since disease penetrance of a genetic variant largely depends on the degree of perturbation in biological systems induced by the variant, it seems plausible that variants with high effect size generally cause more profound miRNA dysregulation. It is thus not surprising the miRNA-related dysregulation is much larger in both scope and amplitude in *Df(16)A*$^{+/-}$ mice, a model of a rare variant, 22q11.2 microdeletion, as compared to dysregulation in *BDNF Val66Met* mice.

5.2.2 MicroRNA Alterations due to Common Variants are Generally Modest

Evolutionary theory argues that the disease-promoting variants are actively selected against (Pritchard and Cox, 2002). This prediction is supported by empirical population genetic data indicating that deleterious variants are rare (Kryukov et al., 2007; Zhu et al., 2011). This distribution of fitness-reducing variants reflects the dynamics between *de novo* mutagenesis and active purifying selection. In order to put things into perspective, it should be noted that *BDNF Val66Met* is a primate-specific allele

that appeared late in evolution and its frequency is possibly modulated by evolutionary forces *hic et nunc*. In addition, *BDNF Val66Met* seems to have a protective effect against psychotic disorders but compromise the cognitive dysfunction (see Chapter 4.1.3 and 4.1.4). Therefore, it is plausible that *BDNF Val66Met* results in mild miRNA alteration that modulates certain brain functions together with miRNA and transcript alterations imposed by other variants. The combined mild miRNA alteration induced by common variants can positively or negatively modulate the anomalous molecular network caused by rare variants (see below, Chapter 5.3.2) to affect the development and expression of psychiatric disorders and cognitive dysfunction. Since the miRNA-related alterations due to common variants are modest in nature, challenges remain to functionally elucidate the impact of these changes on the molecular network that are ultimately reflected as variance of behaviors or cognitive function.

5.2.3 MicroRNA Dysregulation due to Rare Variants can be Pervasive and Drastic

On the other hand, in several cases, psychiatric disorders can be largely attributed to rare alleles of large effect (Brandon and Sawa, 2011; Drew et al., 2011; Levy et al., 2012; Malhotra and Sebat, 2012; Rodriguez-Murillo et al., 2012). In addition, it is calculated that for a disease with 2% prevalence, one or two risk variants of high effect size (e.g. odds ratio = 5) and very low frequency (e.g. 0.1%) are able to significantly increase the probability of disease (Gibson, 2011). This is likely the case for many psychiatric disorders, as these parameters are relevant: schizophrenia affects ~1% of the general population while 22q11.2 microdeletions has a frequency of 0.025% and odds ratio of 30. It is conceivable that many of the rare variants that confer high risk may result in pronounced and possibly widespread miRNA dysregulation. This view is supported by the fact that some human CNVs encompass loci of miRNAs or miRNA-processing genes (Duan et al., 2009; Levy et al., 2012), though the scope and magnitude of ensuing miRNA dysregulation have not been determined. Thus, our analysis provides a proof-of-concept that rare variants may lead to pervasive and drastic miRNA dysregulation that can be directly linked to functional abnormalities. However, it should be emphasized that not all rare variants have big effect size while high-risk rare variants do not necessarily result in profound miRNA-related dysregulation. Although there is likely a core group of miRNAs affected in the pathogenesis of certain psychiatric disorders (see Chapter 2.3.2), individual disease-predisposing variants may affect the molecular network in a variety of

manners that results in the similar functional consequences. Hence miRNA dysregulation due to rare variants need to be examined on a case-by-case basis.

New systemic approaches for surveying the human genome have revealed numerous common or rare genetic variants associated with psychiatric disorders and revolutionized our conception of the genetic architecture of these disorders. The delineation of the impact of individual variants on miRNA-mediated molecular network will further advance our understanding of the pathophysiology of psychiatric disorders (see Chapter 5.3) and provide important insights for diagonosis and the development of personalized therapies (see Chapter 5.4)

5.3 Concerted Regulation of Functionally-related Genes by MicroRNAs

5.3.1 Concurrent Regulation Manages the Output of a Signaling Pathway

We show that as a result of 22q11.2 microdeletion the drastic decrease in miR-185 concurrently results in the upregulation of Mirta22, a major downstream effector, and a group of Golgi-related genes. As these genes and *Mirta22* appears to converge on specific functional pathways, the genetic interactions between these miR-185 targets couple and augment the detrimental effects of miR-185 dysregulation on Golgi-related functions. Furthermore, Irak1 and Traf6 are also important component of TLR signaling and are targets of miR-146b which levels are altered by *BDNF Val66Met* SNP. Thus it seems common and rare variants alike may lead to aberrant levels of miRNAs that simultaneously target functionally related genes.

Multiple studies have demonstrated that individual miRNAs or related miRNAs (e.g. from a same family) are able to concurrently target genes in the same signaling pathways, especially the hub genes (Allantaz et al., 2012; Davalos et al., 2011; Jiang et al., 2012; Ooi et al., 2011; Sarachana et al., 2010; Sun et al., 2012; Xiao et al., 2012). For example, several members of BMP signaling pathway are upregulated in the *Drosophila mir-124* mutant and were proved to be genuine miR-124 targets (Sun et al., 2012). The overexpression of two of these targets in flies results in structural and functional defects which phenocopy the defects observed in *mir-124* mutants. Likewise, miR-33 represses multiple targets in fatty acid metabolism and insulin signaling pathways (Davalos et al., 2011). Moreover, there is a tendency for signaling pathways to concertedly regulate multiple independent miRNAs that in turn target overlapping

signaling pathways (Boot et al., 2011; Herranz and Cohen, 2010; Schlesinger et al., 2011; Xiao et al., 2012; Zhang et al., 2010), resulting in a variety of complex regulatory motifs, such as feedback loops. In a positive feedback loop, miRNA can suppress the inhibitors so that the signals through certain pathway can be selectively amplified and generate strong stimulation-dependent responses (Herranz and Cohen, 2010). This is likely the case during development when establishing an “all-or-none” decision is necessary. In neurons, rigorous activity is often accompanied by corresponding change in processes such as gene expression. Therefore, miRNA-mediated feedback mechanisms can help maintain long-term plasticity. On the other hand, in a negative feedback loop, a miRNA can act as a homeostasis regulator of a pathway or as a part of a bistable switch. Given the conceivably pivotal roles of miRNA in signaling pathways altered in psychiatric disorders, initial attempts have been made to delineate the transcriptomic network involving miRNAs and other transcripts, in the context of functional modules or pathways.

5.3.2 Study of MicroRNA-regulated Transcriptomic Network may Pinpoint Molecular Pathology

First, it is relevant to note that several groups have identified functional coexpression modules in human brains using weighted gene co-expression network analysis (WGCNA) which analyzes expression profiles across normal and affected individuals (Ben-David and Shifman, 2012; Oldham et al., 2008; Voineagu et al., 2011). Importantly, these modules are highly enriched in genes with similar function and expressed in specific neuronal subgroups in specific brain regions (Ben-David and Shifman, 2012; Voineagu et al., 2011), implying they likely function in interrelating pathways. Although the functional modules in the brain of control and autistic patients are largely the same, a few differentially expressed modules are enriched in genes important for structural and functional plasticity. Therefore, these analyses provide proof-of-principle that the network analyses of transcriptomic datasets can uncover convergent molecular pathophysiology of psychiatric disorders. Although miRNAs altered in psychiatric disorders likely contribute significantly to the molecular pathophysiology, to date, an effort to map the empirical (not predicted) miRNA-mediated repression onto these functional transcriptomic networks has yet to be reported.

An alternative approach to determine and compare the involvement of miRNA in functional networks in normal and disease state was demonstrated recently (Ooi et al., 2011). Tan et al. made the

assumption that correlating gene expression patterns denote functional connections and constructed a microRNA–pathway network based on expression signatures in tumor samples. This network reveals the interconnecting nature of miRNAs and oncogenic pathways and provides further proof that miRNAs are able to concertedly regulate functionally related targets. The application of this strategy to psychiatric disorder gene expression datasets could uncover formerly unappreciated roles of miRNAs in disease pathways as well as help define the nature of molecular pathogenic alterations within the transcriptomic network.

5.3.3 A Mechanism for Synchronous Changes in Expression of Functionally Related Targets

The recent discovery of reciprocal regulation of miRNA and target mRNAs reveals an additional layer of complexity in miRNA-mediated regulation of transcriptomic networks (Rubio-Somoza et al., 2011; Salmena et al., 2011). As exemplified by studies of the scope and impact of interaction between miRNAs and their corresponding set of competitive endogenous RNAs (ceRNAs) in tumors, there is extensive crosstalk between miRNA–RNA interaction when multiple RNA targets bearing common miRNA recognition elements (MREs) compete to bind their cognate miRNAs (Karreth et al., 2011; Sumazin et al., 2011). In this scenario, it is predicted that if a miRNA is stoichiometrically limited, the upregulation of one or a few of its target mRNAs will lead to a concomitant increase of other target mRNAs with the same MRE. Thus functionally related genes with the same MREs are likely to be synchronously up- or down-regulated. This effect can be magnified when levels of the cognate miRNAs are decreased, such as the drastic decrease of miR-185 that occurs in *Df(16)A*$^{+/-}$ mice.

5.3.4 Delineation of specific functional pathways controlled by genuine targets

The discovery that miRNAs tend to regulate functionally-related genes in cell-specific manner provides a new perspective on our understanding of miRNA-mediated pathophysiological mechanisms. Although individual miRNAs have numerous potential targets, empirical data indicate that not every potential target is regulated in a given physiological context. Our ultimate goal is to determine the specific functional pathways affected by genuine targets dysregulated by disease-associated miRNAs. In this respect, our finding of concerted upregulation of Golgi-related genes due to reduced miR-185 levels in a

22q11.2DS model presents a functional pathological mechanism due to miRNA dysregulation in a psychiatric disorder.

5.4 Clinical Implications for Diagnosis and Treatment

5.4.1 MicroRNA-related Signatures as Diagnostic Biomarkers

We show that a drastic decrease of miR-185expression and a concomitant upregulation of Mirta22 are prominent components of miRNA-related dysregulation in hippocampus and prefrontal cortex of *Df(16)A*$^{+/-}$ mice. These molecular signatures are likely conserved in 22q11.2 microdeletions carriers and can be considered as diagnostic biomarkers for screening 22q11.2 microdeletions. Moreover, these pathophysiologically relevant molecular signatures may also help predict the disease state and the trajectory of future progression. However, since biopsy of neural tissue is not feasible for routine screening, it has to be determined whether these molecular signatures also exist in the peripheral tissues such as skin, blood, or saliva. One possible confounding factor is the tissue-specific expression of miRNA and their targets. In this regard, it is of note that a group of miRNAs, many of which are synaptically enriched and located within an imprinted *DLK1-DIO3* locus, are downregulated in peripheral blood mononuclear cells of schizophrenia patients (Gardiner et al., 2011) (see Chapter 2.3.2). As many of these miRNAs were also shown to be downregulated in postmortem brains (Moreau et al., 2011) and in brains of *Df(16)A*$^{+/-}$ mice (Stark et al., 2008) (Figure 2.11), it seems likely there is a core group of miRNAs that are prone to be affected during schizophrenia pathogenesis in both brain and peripheral tissues. If verified, these molecular signatures will lead to the development of low-cost diagnostic tests for schizophrenia that will greatly help early diagnosis and treatment. It is plausible that other pathophysiologically relevant miRNA-related signatures exist for other diseases or aging-related processes, as exemplified by the identification of mir-34c as a target for diagnosing and treating dementias (Zovoilis et al., 2011).

Recently, comprehensive analysis of personal omics profiling that combines genomic, transcriptomic, proteomic, metabolomics and other medical profiles has been conceptualized (Chen et al., 2012). Initial testing suggests that an integrative personal omics profile (iPOP) may offer longitudinal information of fluctuation of molecular components where signatures of dynamic biological processes can

be extracted over healthy and diseased states. Undoubtedly, the integration of our understanding of disease-relevant alterations in miRNA profile with signatures in other omics profiles will offer an unprecedented opportunity to accurately assess disease risk, monitor disease progression and evaluate the effectiveness of treatment.

5.4.2 Normalization of MicroRNA Expression using Recombinant Adeno-associated Virus (AAV)

Besides early diagnosis, our understanding of miRNA-related dysregulation and its contribution to pathophysiology holds promise for the development of novel drugs or therapies that help ameliorate associated cognitive and psychiatric symptoms. As the elevation of miR-185 levels and reduction of Mirta22 levels each reverses the deficits in neuronal morphology due to loss of 22q11.2 syntenic region, miR-185 and Mirta22 represent attractive therapeutic targets. Since inhibition of Mirta22 function is predicted to promote formation of neuronal connections in 22q11.2 deletion carriers, drugs that target this protein may enhance excitatory connections in the brain. On the other hand, phenotypic comparison of *Dgcr8*$^{+/-}$ and *Df(16)A*$^{+/-}$ mice suggests that miRNA dysregulation contributes significantly to the structural and functional impairments associated with schizophrenia symptoms in 22q11.2DS patients (Stark et al., 2008). Therefore, gene therapy that delivers *mir-185* or *Dgcr8* gene back to affected brain regions can be considered as a means to restore miRNA levels in 22q11.2DS patients.

One available option for *in vivo* gene deilvery is the recombinant adeno-associated virus (AAV) (McCarty, 2008; Wang et al., 2003). Unlike recombinant retrovirus, AAV does not integrate into the genome, so it is non-mutagenic. Engineered miRNA-carrying AAV with specific serotype was shown to achieve highly efficient transduction (close to 100%) of selective tissues such as liver (Kota et al., 2009). In addition, as described in Chapter 3.1.2, AAV-mediated miR-134 delivery was demonstrated to successfully increase mir-134 levels in adult mouse hippocampus (Christensen et al., 2010). Nevertheless, the delivery involved injection of virus into the brain so the efficiency and durability of AAV-based therapies need to be carefully assessed given the inherent risk.

5.4.3 Systemic Application of MicroRNA Mimics or Antagonists

None-invasive therapies utilizing mir-185 synthetic mimics, such as that used in our experiments, is another viable alternative. Antisense oligonucleotides like locked nucleic acid (LNA) or antagomirs can

be exploited to treat diseases or conditions that are associated with aberrant upregulation of miRNAs. The most notable success thus far in miRNA therapeutic is the use of anti-miR-122 LNA to treat hepatitis C in non-human primates (Elmen et al., 2008; Lanford et al., 2010). The replication of hepatitis C virus is significantly hampered by the downregulation of miR-122. Similarly, a Phase II clinical trial is currently underway to test the effectiveness of SPC3649, a miR-122 antagonist, in inhibiting hepatitis C viral production. A main concern for the systemic adminstration of miRNA mimics or antagonists is whether the effective concentration in target cells is achieved. Passage of these oligonucleotides across the cell membrane can be enhanced by packaging these oligonucleotides into lipid nanoparticles (Pramanik et al., 2011; Trang et al., 2011). Successful delivery of tumor-suppressing miRNAs into malignant cells of several mouse tumor models has demonstrated the feasibility of this approach. Nevertheless, the possible side-effects of miRNA alteration in other tissues should be monitored and whether systemically applied miRNA mimics or antagonists are able to reach CNS neurons remains to be seen.

5.4.4 Discovering Small Molecules that Neutralize MicroRNA-related Dysregulation

In addition to synthetic oligonucleotides as therapeutic agents, the small molecule reserve is a possible gold mine for future drug discovery. The rigorous exploration of chemical space for biologically active molecules promises to reveals small molecules with the capability to neutralize miRNA-related dysregulation (Crews, 2010; Lipinski and Hopkins, 2004). Agents that boost miRNA biogenesis or RISC activity may help confine the extent of miRNA dysregulation and limit its impact on brain structure and function. Interesting, recently it was discovered that natural compounds resveratrol and its analogue pterostilbene promote Ago2 activity and the upregulation of a number of tumor-suppressive miRNAs, including has-miR-185 (2.75 fold by 25 µM resveratrol) in adenocarcinoma cells (Hagiwara et al., 2012). It will be interesting to test if stilbene derivatives alleviate the cognitive and behavioral deficits of *Df(16)A*$^{+/-}$ mice.

5.4.5 Induced Pluripotent Stem Cell (iPSC) as a Therapeutic Means

Recently, the development of induced pluripotent stem cell (iPSC) technology has revealed a brand new avenue for studying and, down the road, treating psychiatric disorders (Cherry and Daley, 2012; Robinton and Daley, 2012). Patient-derived iPSCs can be differentiated into a variety of cell types

to allow the observation of cellular phenotypes. Since the genetic composition is preserved in iPSCs (exceptions exist, see below), iPSC technology allows the analysis of the impact of the complete genetic background on cellular phenotypes. More importantly, iPSC-derived cultures can be used for drug screening that help design personalized treatment. Furthermore, in the cases where the primary genetic lesion is known (e.g. 22q11.2DS), patient-derived iPSCs can be genetically repaired and differentiated into either the affected cell types or progenitors of the affected cells. These immune-compatible progenitors or mature cells are then implanted back to the same patient. A seminal work by Jaenisch et al. demonstrated that iPSC-derived dopaminergic neurons can integrate into existing circuits and improve the symptoms after being engrafted into a rat model of Parkinson Disease (Wernig et al., 2008). More recently, human iPSC-derived neural stem cells have been shown to differentiate into neurons after implantation into the CNS of rodent models of stroke and spinal cord injury (Fujimoto et al., 2012; Jensen et al., 2011). The engrafted stem cells form synaptic connections, integrate into neural circuits and contribute to the restored motor function (Fujimoto et al., 2012). Furthermore, human iPSC-derived cortical stem cells are able to recapitulate *in vivo* cortical neurogenesis and give rise to all classes of cortical projection neurons that show mature electrical properties and form synapses (Shi et al., 2012). These studies demonstrate the practicability of using genetically repaired iPSCs in cell-replacement therapy in the brain.

Since schizophrenia is neurodevelopmental disorder, it is plausible that early intervention of the disease progression can greatly help alleviate or even prevent the manifestation of certain symptoms. In principle, 22q11.2DS patient-derived iPSCs corrected for miRNA dysregulation can be differentiated into neuron progenitors and then transplanted back to hippocampus or prefrontal cortex of the affected patients. However, several concerns and hurdles need to be resolved before this approach achieves clinical use for psychiatric disorders. First, we need to have a more comprehensive understanding of the specific anomalies in the neural circuits that underlie the disease phenotypes. The responsible cell types and the specific cellular abnormalities need to be determined in order to design iPSC-based therapy. Second, the morphology and function of the iPSC-derived cells should be carefully compared to cells in normal individuals and patients. Since even modest alteration in cells could be the origin of the disease symptoms, it is essential for clinical success that the iPSC-derived cells are functionally equivalent to

normal cells and can be integrated properly into the affected neural circuits. Third, iPSC reprogramming seems to alter DNA methylation pattern that affect mRNA and miRNA expression (Deng et al., 2009; Stadtfeld et al., 2010; Wilson et al., 2009). The comparison of iPSCs and embryonic stem cells (ESCs) uncovered an aberrant silencing of the imprinted *Dlk1–Dio3* locus that contains a large miRNA cluster (Stadtfeld et al., 2010) (see Chapter 2.3.2 and 3.1.1). The *Dlk1–Dio3* locus encodes many miRNAs that are required for neural function and are associated with psychiatric disorders. Furthermore, the inactivation of *Dlk1–Dio3* locus is associated with poor contribution to chimeras and failure to generate all-iPSC mice. This is a great obstacle for iPSC therapies, especially for those designed to correct disease-associated miRNA dysregulation. Recently, ascorbic acid is shown to prevent loss of *Dlk1–Dio3* imprinting and increase expression of several transcripts of genes in this locus, including *Mirg* (Stadtfeld et al., 2012). Whether ascorbic acid restores expression of miRNAs from maternal alleles is not examined. In addition, it is also reported that reprogramming of human iPSC introduces many *de novo* CNVs in the genome which conferred selective disadvantage (Hussein et al., 2011; Laurent et al., 2011). Therefore, technical improvement is necessary to generate iPSCs and iPSC-derived cells with the genetic and epigenetic composition more faithfully resembling normal primary cells.

5.4.6 Identification of Genuine Targets for Constructing Specific Therapies

In light of the increasing opportunities offered by the aforementioned treatments designed to reverse the miRNA-related dysregulation in diseases, our studies on miRNA-related dysregulation caused by 22q11.2 microdeletions reveal genuine targets for constructing specific therapies for intervening the disease processes. Treatments that normalize the expression levels of miR-185 or Mirta22 may help to alleviate symptoms and disease progression.

5.5 Conclusion

Accumulating evidence suggests that miRNAs play an important role in the pathogenesis and pathophysiology of psychiatric disorders and cognitive dysfunction (Moreau et al., 2011; Xu et al., 2010). Therefore we aimed to study the miRNA-related dysregulation in mouse models of rare and common variants. First, we analyzed schizophrenia-associated miRNA dysregulation and revealed a possible core group of miRNAs that are concertedly downregulated in disease conditions. Although additive or

synergistic miRNA dysregulation can result in a more profound impact on proteome, we identified an important component of miRNA dysregulation due to 22q11.2 microdeletion. This component, a drastic decrease in miR-185 levels, was a consequence of the genetic interaction within the pathogenic CNV. Furthermore, our work represents one of the first examples where a major downstream target of a disease-related miRNA dysregulation has been unequivocally identified and its function has been characterized. The major downstream effector of miRNA dysregulation, Mirta22, is a neuronal morphogenesis inhibitor with Golgi-related function. Knockdown of Mirta22 levels corrects the dendritic and spine deficits in mutant neurons. Second, we delineated the dysregulation of mir-146b and its targets due to the *BDNF Val66met* SNP. Altogether, our studies exemplified alterations in miRNA-regulated network that may exist downstream of other rare or common genetic variants. Future experiments will help understand the impact of Mirta22 upregulation on neuronal functions, the integrity of neural circuits, and behavior and cognitive performance. Ultimately, by integrating results from these studies, we hope to have a comprehensive understanding of the disease mechanism. Moreover, advancement in gene therapy, chemical biology and iPSC techniques will undoubtedly further our arsenal to correct miRNA dysregulation underlying psychiatric disorders and eventually translate our knowledge to effective remedies.

5.6 References

Allantaz, F., Cheng, D.T., Bergauer, T., Ravindran, P., Rossier, M.F., Ebeling, M., Badi, L., Reis, B., Bitter, H., D'Asaro, M*., et al.* (2012). Expression profiling of human immune cell subsets identifies miRNA-mRNA regulatory relationships correlated with cell type specific expression. PLoS ONE *7*, e29979.

Ben-David, E., and Shifman, S. (2012). Networks of neuronal genes affected by common and rare variants in autism spectrum disorders. PLoS genetics *8*, e1002556.

Boot, E., Booij, J., Abeling, N., Meijer, J., da Silva Alves, F., Zinkstok, J., Baas, F., Linszen, D., and van Amelsvoort, T. (2011). Dopamine metabolism in adults with 22q11 deletion syndrome, with and without schizophrenia--relationship with COMT Val(1)/(1)Met polymorphism, gender and symptomatology. Journal of psychopharmacology *25*, 888-895.

Brandon, N.J., and Sawa, A. (2011). Linking neurodevelopmental and synaptic theories of mental illness through DISC1. Nat Rev Neurosci *12*, 707-722.

Brenner, J.L., Jasiewicz, K.L., Fahley, A.F., Kemp, B.J., and Abbott, A.L. (2010). Loss of individual microRNAs causes mutant phenotypes in sensitized genetic backgrounds in C. elegans. Curr Biol *20*, 1321-1325.

Chen, R., Mias, G.I., Li-Pook-Than, J., Jiang, L., Lam, H.Y., Chen, R., Miriami, E., Karczewski, K.J., Hariharan, M., Dewey, F.E*., et al.* (2012). Personal omics profiling reveals dynamic molecular and medical phenotypes. Cell *148*, 1293-1307.

Cherry, A.B., and Daley, G.Q. (2012). Reprogramming Cellular Identity for Regenerative Medicine. Cell *148*, 1110-1122.

Christensen, M., Larsen, L.A., Kauppinen, S., and Schratt, G. (2010). Recombinant Adeno-Associated Virus-Mediated microRNA Delivery into the Postnatal Mouse Brain Reveals a Role for miR-134 in Dendritogenesis in Vivo. Frontiers in neural circuits *3*, 16.

Crews, C.M. (2010). Targeting the undruggable proteome: the small molecules of my dreams. Chemistry & biology *17*, 551-555.

Crow, J.F. (2000). The origins, patterns and implications of human spontaneous mutation. Nat Rev Genet *1*, 40-47.

Davalos, A., Goedeke, L., Smibert, P., Ramirez, C.M., Warrier, N.P., Andreo, U., Cirera-Salinas, D., Rayner, K., Suresh, U., Pastor-Pareja, J.C*., et al.* (2011). miR-33a/b contribute to the regulation of fatty acid metabolism and insulin signaling. Proceedings of the National Academy of Sciences of the United States of America *108*, 9232-9237.

Deng, J., Shoemaker, R., Xie, B., Gore, A., LeProust, E.M., Antosiewicz-Bourget, J., Egli, D., Maherali, N., Park, I.H., Yu, J.*, et al.* (2009). Targeted bisulfite sequencing reveals changes in DNA methylation associated with nuclear reprogramming. Nature biotechnology *27*, 353-360.

Drew, L.J., Crabtree, G.W., Markx, S., Stark, K.L., Chaverneff, F., Xu, B., Mukai, J., Fenelon, K., Hsu, P.K., Gogos, J.A.*, et al.* (2011). The 22q11.2 microdeletion: fifteen years of insights into the genetic and neural complexity of psychiatric disorders. International journal of developmental neuroscience : the official journal of the International Society for Developmental Neuroscience *29*, 259-281.

Duan, S., Mi, S., Zhang, W., and Dolan, M.E. (2009). Comprehensive analysis of the impact of SNPs and CNVs on human microRNAs and their regulatory genes. RNA biology *6*, 412-425.

Elmen, J., Lindow, M., Schutz, S., Lawrence, M., Petri, A., Obad, S., Lindholm, M., Hedtjarn, M., Hansen, H.F., Berger, U.*, et al.* (2008). LNA-mediated microRNA silencing in non-human primates. Nature *452*, 896-899.

Fenelon, K., Mukai, J., Xu, B., Hsu, P.K., Drew, L.J., Karayiorgou, M., Fischbach, G.D., Macdermott, A.B., and Gogos, J.A. (2011). Deficiency of Dgcr8, a gene disrupted by the 22q11.2 microdeletion, results in altered short-term plasticity in the prefrontal cortex. Proceedings of the National Academy of Sciences of the United States of America *108*, 4447-4452.

Fujimoto, Y., Abematsu, M., Falk, A., Tsujimura, K., Sanosaka, T., Juliandi, B., Semi, K., Namihira, M., Komiya, S., Smith, A.*, et al.* (2012). Treatment of a Mouse Model of Spinal Cord Injury by Transplantation of Human iPS Cell-derived Long-term Self-renewing Neuroepithelial-like Stem Cells. Stem cells (Dayton, Ohio).

Gardiner, E., Beveridge, N.J., Wu, J.Q., Carr, V., Scott, R.J., Tooney, P.A., and Cairns, M.J. (2011). Imprinted DLK1-DIO3 region of 14q32 defines a schizophrenia-associated miRNA signature in peripheral blood mononuclear cells. Molecular psychiatry.

Gibson, G. (2011). Rare and common variants: twenty arguments. Nat Rev Genet *13*, 135-145.

Goldstein, D.B. (2009). Common genetic variation and human traits. The New England journal of medicine *360*, 1696-1698.

Hagiwara, K., Kosaka, N., Yoshioka, Y., Takahashi, R.U., Takeshita, F., and Ochiya, T. (2012). Stilbene derivatives promote Ago2-dependent tumour-suppressive microRNA activity. Scientific reports *2*, 314.

Herranz, H., and Cohen, S.M. (2010). MicroRNAs and gene regulatory networks: managing the impact of noise in biological systems. Genes & development *24*, 1339-1344.

Hussein, S.M., Batada, N.N., Vuoristo, S., Ching, R.W., Autio, R., Narva, E., Ng, S., Sourour, M., Hamalainen, R., Olsson, C.*, et al.* (2011). Copy number variation and selection during reprogramming to pluripotency. Nature *471*, 58-62.

Jensen, M.B., Yan, H., Krishnaney-Davison, R., Al Sawaf, A., and Zhang, S.C. (2011). Survival and Differentiation of Transplanted Neural Stem Cells Derived from Human Induced Pluripotent Stem Cells in A Rat Stroke Model. Journal of stroke and cerebrovascular diseases : the official journal of National Stroke Association.

Jiang, W., Chen, X., Liao, M., Li, W., Lian, B., Wang, L., Meng, F., Liu, X., Chen, X., Jin, Y.*, et al.* (2012). Identification of links between small molecules and miRNAs in human cancers based on transcriptional responses. Scientific reports *2*, 282.

Karayiorgou, M., Simon, T.J., and Gogos, J.A. (2010). 22q11.2 microdeletions: linking DNA structural variation to brain dysfunction and schizophrenia. Nat Rev Neurosci *11*, 402-416.

Karreth, F.A., Tay, Y., Perna, D., Ala, U., Tan, S.M., Rust, A.G., DeNicola, G., Webster, K.A., Weiss, D., Perez-Mancera, P.A.*, et al.* (2011). In vivo identification of tumor- suppressive PTEN ceRNAs in an oncogenic BRAF-induced mouse model of melanoma. Cell *147*, 382-395.

Kota, J., Chivukula, R.R., O'Donnell, K.A., Wentzel, E.A., Montgomery, C.L., Hwang, H.W., Chang, T.C., Vivekanandan, P., Torbenson, M., Clark, K.R.*, et al.* (2009). Therapeutic microRNA delivery suppresses tumorigenesis in a murine liver cancer model. Cell *137*, 1005-1017.

Kryukov, G.V., Pennacchio, L.A., and Sunyaev, S.R. (2007). Most rare missense alleles are deleterious in humans: implications for complex disease and association studies. Am J Hum Genet *80*, 727-739.

Kvajo, M., McKellar, H., and Gogos, J.A. (2011). Avoiding mouse traps in schizophrenia genetics: lessons and promises from current and emerging mouse models. Neuroscience.

Lanford, R.E., Hildebrandt-Eriksen, E.S., Petri, A., Persson, R., Lindow, M., Munk, M.E., Kauppinen, S., and Orum, H. (2010). Therapeutic silencing of microRNA-122 in primates with chronic hepatitis C virus infection. Science (New York, NY *327*, 198-201.

Laurent, L.C., Ulitsky, I., Slavin, I., Tran, H., Schork, A., Morey, R., Lynch, C., Harness, J.V., Lee, S., Barrero, M.J.*, et al.* (2011). Dynamic changes in the copy number of pluripotency and cell proliferation genes in human ESCs and iPSCs during reprogramming and time in culture. Cell stem cell *8*, 106-118.

Lee, S.H., Decandia, T.R., Ripke, S., Yang, J., The Schizophrenia Psychiatric Genome-Wide Association Study, C., The International Schizophrenia, C., The Molecular Genetics of Schizophrenia, C., Sullivan, P.F., Goddard, M.E., Keller, M.C.*, et al.* (2012). Estimating the proportion of variation in susceptibility to schizophrenia captured by common SNPs. Nat Genet *44*, 247-250.

Levy, R.J., Xu, B., Gogos, J.A., and Karayiorgou, M. (2012). Copy number variation and psychiatric disease risk. Methods in molecular biology *838*, 97-113.

Lipinski, C., and Hopkins, A. (2004). Navigating chemical space for biology and medicine. Nature *432*, 855-861.

Malhotra, D., and Sebat, J. (2012). CNVs: Harbingers of a Rare Variant Revolution in Psychiatric Genetics. Cell *148*, 1223-1241.

McCarty, D.M. (2008). Self-complementary AAV vectors; advances and applications. Molecular therapy : the journal of the American Society of Gene Therapy *16*, 1648-1656.

Moreau, M.P., Bruse, S.E., David-Rus, R., Buyske, S., and Brzustowicz, L.M. (2011). Altered microRNA expression profiles in postmortem brain samples from individuals with schizophrenia and bipolar disorder. Biol Psychiatry *69*, 188-193.

Oldham, M.C., Konopka, G., Iwamoto, K., Langfelder, P., Kato, T., Horvath, S., and Geschwind, D.H. (2008). Functional organization of the transcriptome in human brain. Nature neuroscience *11*, 1271-1282.

Ooi, C.H., Oh, H.K., Wang, H.Z., Tan, A.L., Wu, J., Lee, M., Rha, S.Y., Chung, H.C., Virshup, D.M., and Tan, P. (2011). A densely interconnected genome-wide network of microRNAs and oncogenic pathways revealed using gene expression signatures. PLoS genetics *7*, e1002415.

Pramanik, D., Campbell, N.R., Karikari, C., Chivukula, R., Kent, O.A., Mendell, J.T., and Maitra, A. (2011). Restitution of tumor suppressor microRNAs using a systemic nanovector inhibits pancreatic cancer growth in mice. Molecular cancer therapeutics *10*, 1470-1480.

Pritchard, J.K., and Cox, N.J. (2002). The allelic architecture of human disease genes: common disease-common variant...or not? Hum Mol Genet *11*, 2417-2423.

Robinton, D.A., and Daley, G.Q. (2012). The promise of induced pluripotent stem cells in research and therapy. Nature *481*, 295-305.

Rodriguez-Murillo, L., Gogos, J.A., and Karayiorgou, M. (2012). The genetic architecture of schizophrenia: new mutations and emerging paradigms. Annual review of medicine *63*, 63-80.

Rubio-Somoza, I., Weigel, D., Franco-Zorilla, J.M., Garcia, J.A., and Paz-Ares, J. (2011). ceRNAs: miRNA target mimic mimics. Cell *147*, 1431-1432.

Salmena, L., Poliseno, L., Tay, Y., Kats, L., and Pandolfi, P.P. (2011). A ceRNA hypothesis: the Rosetta Stone of a hidden RNA language? Cell *146*, 353-358.

Sarachana, T., Zhou, R., Chen, G., Manji, H.K., and Hu, V.W. (2010). Investigation of post-transcriptional gene regulatory networks associated with autism spectrum disorders by microRNA expression profiling of lymphoblastoid cell lines. Genome medicine *2*, 23.

Schlesinger, J., Schueler, M., Grunert, M., Fischer, J.J., Zhang, Q., Krueger, T., Lange, M., Tonjes, M., Dunkel, I., and Sperling, S.R. (2011). The cardiac transcription network modulated by Gata4, Mef2a, Nkx2.5, Srf, histone modifications, and microRNAs. PLoS genetics *7*, e1001313.

Shi, Y., Kirwan, P., Smith, J., Robinson, H.P., and Livesey, F.J. (2012). Human cerebral cortex development from pluripotent stem cells to functional excitatory synapses. Nature neuroscience *15*, 477-486.

Stadtfeld, M., Apostolou, E., Akutsu, H., Fukuda, A., Follett, P., Natesan, S., Kono, T., Shioda, T., and Hochedlinger, K. (2010). Aberrant silencing of imprinted genes on chromosome 12qF1 in mouse induced pluripotent stem cells. Nature *465*, 175-181.

Stark, K.L., Xu, B., Bagchi, A., Lai, W.S., Liu, H., Hsu, R., Wan, X., Pavlidis, P., Mills, A.A., Karayiorgou, M.*, et al.* (2008). Altered brain microRNA biogenesis contributes to phenotypic deficits in a 22q11-deletion mouse model. Nat Genet *40*, 751-760.

Sumazin, P., Yang, X., Chiu, H.S., Chung, W.J., Iyer, A., Llobet-Navas, D., Rajbhandari, P., Bansal, M., Guarnieri, P., Silva, J.*, et al.* (2011). An extensive microRNA-mediated network of RNA-RNA interactions regulates established oncogenic pathways in glioblastoma. Cell *147*, 370-381.

Sun, K., Westholm, J.O., Tsurudome, K., Hagen, J.W., Lu, Y., Kohwi, M., Betel, D., Gao, F.B., Haghighi, A.P., Doe, C.Q.*, et al.* (2012). Neurophysiological Defects and Neuronal Gene Deregulation in Drosophila mir-124 Mutants. PLoS genetics *8*, e1002515.

Trang, P., Wiggins, J.F., Daige, C.L., Cho, C., Omotola, M., Brown, D., Weidhaas, J.B., Bader, A.G., and Slack, F.J. (2011). Systemic delivery of tumor suppressor microRNA mimics using a neutral lipid emulsion inhibits lung tumors in mice. Molecular therapy : the journal of the American Society of Gene Therapy *19*, 1116-1122.

Voineagu, I., Wang, X., Johnston, P., Lowe, J.K., Tian, Y., Horvath, S., Mill, J., Cantor, R.M., Blencowe, B.J., and Geschwind, D.H. (2011). Transcriptomic analysis of autistic brain reveals convergent molecular pathology. Nature *474*, 380-384.

Wang, Z., Ma, H.I., Li, J., Sun, L., Zhang, J., and Xiao, X. (2003). Rapid and highly efficient transduction by double-stranded adeno-associated virus vectors in vitro and in vivo. Gene therapy *10*, 2105-2111.

Wernig, M., Zhao, J.P., Pruszak, J., Hedlund, E., Fu, D., Soldner, F., Broccoli, V., Constantine-Paton, M., Isacson, O., and Jaenisch, R. (2008). Neurons derived from reprogrammed fibroblasts functionally integrate into the fetal brain and improve symptoms of rats with Parkinson's disease. Proceedings of the National Academy of Sciences of the United States of America *105*, 5856-5861.

Wilson, K.D., Venkatasubrahmanyam, S., Jia, F., Sun, N., Butte, A.J., and Wu, J.C. (2009). MicroRNA profiling of human-induced pluripotent stem cells. Stem cells and development *18*, 749-758.

Xiao, Y., Xu, C., Guan, J., Ping, Y., Fan, H., Li, Y., Zhao, H., and Li, X. (2012). Discovering Dysfunction of Multiple MicroRNAs Cooperation in Disease by a Conserved MicroRNA Co-Expression Network. PLoS ONE *7*, e32201.

Xu, B., Karayiorgou, M., and Gogos, J.A. (2010). MicroRNAs in psychiatric and neurodevelopmental disorders. Brain Res *1338*, 78-88.

Zhang, H., Li, Y., and Lai, M. (2010). The microRNA network and tumor metastasis. Oncogene *29*, 937-948.

Zhu, Q., Ge, D., Maia, J.M., Zhu, M., Petrovski, S., Dickson, S.P., Heinzen, E.L., Shianna, K.V., and Goldstein, D.B. (2011). A genome-wide comparison of the functional properties of rare and common genetic variants in humans. Am J Hum Genet *88*, 458-468.

Zovoilis, A., Agbemenyah, H.Y., Agis-Balboa, R.C., Stilling, R.M., Edbauer, D., Rao, P., Farinelli, L., Delalle, I., Schmitt, A., Falkai, P.*, et al.* (2011). microRNA-34c is a novel target to treat dementias. EMBO J *30*, 4299-4308.

Appendix 1. Sequence of primers and probes used in qRT-PCR

Name	Sequence	
Kctd15	L:	ATGGAAGCCTAGATGCCTCAC
	P:	GGTCCTCGCTTAACGCACACGG
	R:	GAGTGACAGCCGGGACATATT
Per1	L:	TCTCAGCGGAGTTCTCATAGTTC
	P:	GCTCTGCTGGAGACCACTGAGAGCA
	R:	ACTCAGGAGGCTGTAGGCAAT
Npas4	L:	TACGATATCATTGACCCTGCT
	P:	CTGATCGCCTTTTCCGTTGTCGATT
	R:	AATAAGCACCAGTTTGTTTCCTG
Robo1	L:	CAGCAACCTGACAACCTACAGTC
	P:	CAAACAAATCTGATGCTCCCTGAGTCA
	R:	AAGGTCCACATCACCATAAACAG
Akt3	L:	TTTCAGGGCTCTTGATAAAGGAT
	P:	CCAAATAAACGCCTTGGTGGAGGG
	R:	ACATCTTGCCAGTTTACTCCAGA
Traf6	L:	GAGCAAGTATGAGTGTCCCATCT
	P:	AGGTTCTGCAAAGCCTGCATCATCA
	R:	TCCAGCAGTATTTCATTGTCAAC
Syt1	L:	AAACCCTCAATCCAGTCTTCAAT
	P:	GGTGCCATACTCGGAATTAGGTGGC
	R:	GAGAAGCGGTCAAAATCATACAC
Irak1	L:	CCTGAGGAGTACATCAAGACAGG
	P:	ACTGGAGACCCTTGCTGGTCAGAGG
	R:	AAATACTTGGTCTTTGCACCTTG
Sort1	L:	AGATGATGTACAGCCCTCAGAAT
	P:	GGGTGTCCAAGAATTTTGGGGAAA
	R:	CCAAACATACTGCTTTGTGGATT
Cask	L:	GTAGCCAAGTTCACATCAAGTCC
	P:	GCGGGAAGCCAGTATCTGTCATATGC
	R:	CTCCAACAGCTCTACAATGTGTG
Gria3	L:	CTTTCCTGACTGTGGAGAGGAT
	P:	ATTGCATACGGGACCCTGGACTCTG
	R:	TTTCTCATACACAGCAATTTTGG
Stx3	L:	ATGAAGGACCGGCTGGAG
	P:	GGATGATGACACGGACGAGGTTGAG
	R:	CAGAGAAGAACTCGTCCATGAAG
Srr	L:	ATGTGAGCTCTTCCAGAAAACTG
	P:	ATTCGAGGTGCCCTTAATGCCATCA
	R:	CTGCTGTGAGTAACTACGGCTTT

Bsn	L:	AATATGCAAGACCTCGGACCT
	P:	ACACCTGCACCCAGTGTCACAACAA
	R:	TGACAGTTCAAACAGAGCCACT
Cpeb4	L:	GCTATCAGTGCCCGCTTT
	P:	CCCGTTTATCTATCTCTCCATGCTGCA
	R:	ACACAGCTGGTCATCCAAGA
B3gat1	L2:	CTGGTCAATGAGGGGAAGAAG
	P2:	GGCCTGCCATCCTCTCCCAT
	R2:	GGAAGCCCTCGGAATACATAA
Kif5c	L2:	GAGGTGGCTCTTCAAACTCTACTC
	P2:	TGACTCCACGTAGCATGAAAAGGAC
	R2:	GCAAGTGTAAAAAGAAACGGA
Cdk5r1	L:	CTGGCTCAAGGATTCCACTT
	P:	TGTCTAGCAGAGCCACCAAGGGC
	R:	AGGAAAGAACGTGGGAAGAG
Ldb2	L:	AAAAATATCACCAGGATGGGTCT
	P:	TGTGTGTAATACTGGAGCCAATGCAGG
	R:	GGACTGAGGTTGTAGGTTTTGTG
Cpeb2	L2:	AGCTACATTGCTGCCATCAG
	P2:	TGTTCAGCTTCAGCACGGTGACA
	R2:	GCACTCGTCACACATCTGGT
GSK3b	L:	GCACTCTTCAACTTTACCACTCAA
	P:	CACCATCCTTATCCCTCCACATGCT
	R:	GGTCTCCAGCATTAGTATCTGAGG
Cdk5r2	L:	ATCGTGCAGGCGTCTACC
	P:	CTGCTACCGCCTCAAGGAGCTGAG
	R:	GAACCAGCCCACCAGCTC
vGlut1	L:	ACACTGTCTGGGATGGTGTG
	P:	GAGGAGTGGCAGTACGTGTTCCTCA
	R:	GAAGCAAAGACCCCATAGAAGAT
Agxt2l1	L:	CGAGGTGAAGAAGATCATTGAAGAG
	P:	TGAATCCATGCAGAGTTGTGGTGGA
	R:	GTAGCCTGCTGGAGGAATAATTT
Mef2C	L:	CCTGACTCCTCTTATGCACTCAC
	P:	AAATTCCTGCTGTTCCACCTC
	R:	ATGGTAACTGGCATCTCAAAGC
Hspa8	L:	GCAAGATCAATGATGAGGACAA
	P:	TCATCAGCTGGCTGGATAAGAACCA
	R:	GGTTGCAGACTTTCTCCAGTTC
Lpcat3	L:	CGAGGATCTGAGCCTTAACAAGT
	P:	CGGCTCATCTTCTCCATCTTCCTGG
	R:	AAGGTAATGCCGGTAAAACAGAG

Coro2b	L:	GTACATGACAACCACTTCTGTGC
	P:	TGGCCATAGTCACTGAGAGCGCAG
	R:	TGGCCATAGTCACTGAGAGCGCAG
Epb4.1l1	L:	CCCAAGATTCTCAAGATCTCCT
	P:	TTCAAGCTCCCTAACCACCGCTCA
	R:	GATGCAGACCTTCCACAACC
Begain	L:	CTAAGGTGACCATTGACAAGCTG
	P:	CTGCTGCAGTGCAGCCAGACCTAC
	R:	AGCTCGGACACCTTATGGAC
Mirta22 (2310044H10Rik)	L:	CTGCTGTCAATGGCCTCTAC
	P:	CATGGCCGCCAGCTTCTGA
	R:	GTCCGAAAGGTGCGACTC
Gapdh	L:	CAGGTTGTCTCCTGCGACTT
	P:	GGCTGGCATTGCTCTCAATGACA
	R:	CCTGTTGCTGTAGCCGTATTC